



# **Tesis Doctoral**

## **Eco-cements containing Belite, Alite and Ye'elite. Hydration and mechanical properties**

**Diana Londoño Zuluaga**

Universidad de Málaga

Facultad de Ciencias

Departamento de Química Inorgánica, Mineralogía y Cristalografía

Málaga, España


2018





UNIVERSIDAD  
DE MÁLAGA

AUTOR: Diana Londoño Zuluaga

 <http://orcid.org/0000-0002-6842-8754>

EDITA: Publicaciones y Divulgación Científica. Universidad de Málaga



Esta obra está bajo una licencia de Creative Commons Reconocimiento-NoComercial-SinObraDerivada 4.0 Internacional:

<http://creativecommons.org/licenses/by-nc-nd/4.0/legalcode>

Cualquier parte de esta obra se puede reproducir sin autorización pero con el reconocimiento y atribución de los autores.

No se puede hacer uso comercial de la obra y no se puede alterar, transformar o hacer obras derivadas.

Esta Tesis Doctoral está depositada en el Repositorio Institucional de la Universidad de Málaga (RIUMA): [riuma.uma.es](http://riuma.uma.es)



# **Eco-cements containing Belite, Alite and Ye'elimite. Hydration and mechanical properties**

**Diana Londoño Zuluaga**

Tesis doctoral presentada como requisito para optar al título de:  
**Doctora en Química y Tecnologías Químicas. Materiales y Nanotecnología**  
**“Mención Internacional”**

Directores:

Dra. María de los Ángeles Gómez de la Torre

PhD Jorge Iván Tobón

Dra. María Isabel Santacruz Cruz

Universidad de Málaga

Facultad de Ciencias

Departamento de Química Inorgánica, Mineralogía y Cristalografía

Málaga, España

2018





UNIVERSIDAD  
DE MÁLAGA

Science is not only a disciple of reason, but, also, one of romance and passion.

*Stephen Hawking, PARADE Magazine (2010)*





UNIVERSIDAD  
DE MÁLAGA

# Acknowledgement

Now, when I have finished this 4-year adventure abroad, called PhD studies, it is time to thank everyone who made this dream come true.

First at all, I would like to give my deepest appreciation to my supervisors, PhD. Maria Angeles Gomez de la Torre and PhD. Maria Isabel Santacruz, for their guidance, support and encourage during my doctoral study. Their kindly suggestion and trust were very important to me. As well as, to PhD. Jorge Ivan Tobon, whose adopt me since 2010 as his “scientific daughter”. He, through the distance, gave me his advice, total confidence and constant support; who allowed me the freedom to grow as a researcher. I would also like to thank to Prof. Miguel Angel Garcia Aranda for giving me the opportunity to work with him and his research group in 2012. Work with him permitted to me obtaining valuable ideas and insights. Thanks to that experience, I took the decision to start my PhD here in Malaga.

I am grateful to people in the Department of Inorganic Chemistry, Crystallography and Mineralogy at the University of Malaga. During my four years here, I had the privilege to meet, share knowledge and work with technicians, PhD students and academic staff, whom I would like to acknowledge for their help and great moments. In particular, Jesus and Ana Cuesta, my cement colleagues, for the stimulating scientific and friendly atmosphere in and out the lab. To Laura, Estefania, Maria Dolores, Goyo, Toñi and Ana Lucena, for their help and hospitality during my regular visits for “urgent” measurements. Montse, Rosi and “mommy” Merce deserve my most deep-felt thanks for help me, feed me, be my friends and the pleasant moments that we spent together. I am going to miss you

girls!!! To Ines, Lucy, Mari Jose and Jose, I want to say thank you for not only our lunch times talks, but also to be excellent officemates. Everybody here made sure I had fun both at and outside of my thesis research.

I would like to acknowledge to “Doctorados en el exterior” – Colciencias 646 program, and “Doctorado en el exterior” – Enlaza mundos 2013 and Colfuturo 2013 programs for awarding me with my PhD grant that allowed me to put full efforts into research and study.

Finally, quiero agradecer a mis padres, Luz Alba y Fabio, a mi hermano Pi, por su constante amor e ilimitado apoyo en la distancia. I also want to sincerely thank my new Family, “Los Compañía”, for their support and affection, and for enduring my absence to family meetings the last several months. Special thanks go to my “Cari” Jose Compañía, for his love, patience, understanding, encouragement, trust and infinite support during all these 6 years together.



# Table of Contents

<b>List of Figures</b> .....	<b>XI</b>
<b>List of Tables</b> .....	<b>XV</b>
<b>Notation</b> .....	<b>XVII</b>
<b>Abstract</b> .....	<b>XXI</b>
<b>Resumen</b> .....	<b>XXXIII</b>
<b>Introduction</b> .....	<b>1</b>
<b>Objectives</b> .....	<b>17</b>
<b>1. Materials and Methods</b> .....	<b>19</b>
1.1. Materials .....	19
1.1.1. Belite-Alite-Ye'elimite (BAY) clinkers and cements .....	19
1.1.2. Alite-Ye'elimite-Anhydrite mixture .....	20
1.1.3. "Commercial binder", B83 .....	21
1.1.4. Polycarboxylate-based material as superplasticizer (SP) .....	22
1.2. Samples preparation.....	23
1.2.1. Clinker preparation .....	23
1.2.2. Paste preparation.....	23
1.2.3. Stopping hydration of pastes.....	25
1.2.4. Mortar preparation.....	25
1.3. Analytical Methods.....	25
1.3.1. Laboratory X-ray Powder Diffraction (LXRPD) .....	25
1.3.2. Synchrotron X-ray Powder Diffraction (SXRPD) .....	26
1.3.3. Rietveld methodology and ACn quantification .....	27
1.3.4. Scanning electron microscopy (SEM) and Field emission scanning electron microscopy (FE-SEM) .....	28
1.3.5. Specific surface measurement.....	28
1.3.6. Particle size distribution (PSD).....	29
1.3.7. Isothermal calorimetry.....	29

<b>2. Clinkering and scaled-up of BAY .....</b>	<b>33</b>
2.1. BAY clinkering optimization .....	33
2.1.1. Dosage optimization .....	33
2.1.2. Mineralizer optimization .....	38
2.2. BAY clinker scaled-up .....	39
2.3. BAY cement preparation .....	44
2.4. Summary .....	45
<b>3. BAY cement hydration and mechanical behavior .....</b>	<b>47</b>
3.1. Early-age behavior of fresh pastes .....	47
3.2. Mineralogical behavior of BAY pastes .....	51
3.3. Compressive strength development of BAY mortars .....	57
3.4. Summary .....	58
<b>4. Pure phase hydration study .....</b>	<b>61</b>
4.1. <i>In-Situ</i> SXRPD hydration study .....	62
4.2. <i>Ex-Situ</i> hydration study .....	75
4.3. Summary .....	81
<b>5. Influence of Fly Ash addition on BAY cement hydration and properties .....</b>	<b>83</b>
5.1. Rheological behavior .....	84
5.2. Isothermal calorimetric studies .....	88
5.2.1. Effect of superplasticizer on FA0BAY early-age hydration .....	88
5.2.2. Effect of FA substitution on heat released .....	90
5.3. Hydration studies of FA#BAY binders .....	92
5.4. Mechanical behavior of FA#BAY binders .....	102
5.5. Summary .....	104
<b>6. “Commercial binder” study associated with BAY cement .....</b>	<b>107</b>
6.1. Optimization of the superplasticizer content .....	107
6.2. Isothermal calorimetric behavior .....	110
6.3. Hydration mechanism in B83 .....	112
6.4. Compressive strength of B83 mortars .....	115
6.5. Summary .....	116
<b>Conclusions and Perspectives .....</b>	<b>119</b>
Conclusions .....	119
Perspectives .....	124
<b>Annex I: .....</b>	<b>127</b>
<b>Annex II: .....</b>	<b>139</b>
<b>Annex III: .....</b>	<b>151</b>
<b>References .....</b>	<b>155</b>

## List of Figures

	Pág.
<b>Figure Int.1.</b> Patents in the system $C_4A_3S-C_2S$ -others. ....	6
<b>Figure Int.2.</b> Compressive strength of BYF compared to OPC at $w/c = 0.55$ at 20 °C. ....	8
<b>Figure 2.3.</b> LXRPD patterns for BAY clinkers with monochromatic $CuK\alpha_1(\lambda=1.5406\text{\AA})$ . ....	35
<b>Figure 2.4.</b> Rietveld plot of scBAY_4 (~90 g of sample) at 1300 °C for 15 min and excess of sulfate, measured by XRPD with monochromatic $CuK\alpha_1$ radiation .....	41
<b>Figure 2.5.</b> SEM micrographs of fresh fracture surface of scBAY_4 clinker . ....	42
<b>Figure 2.6.</b> Backscatter electron (BSE) image of scBAY4 clinker (FE-SEM). ....	43
<b>Figure 2.7.</b> Particle size distribution of BAY cement. ....	45
<b>Figure 3.8.</b> Flow curves of BAY pastes prepared at water/cement ratios of 0.4 (with 0.1wt% superplasticizer) and 0.5 (without superplasticizer).....	48
<b>Figure 3.9.</b> Flow curves of BAY pastes at $w/c = 0.4$ and different superplasticizer contents.....	49
<b>Figure 3.10.</b> Deflocculation curve of BAY pastes with $w/c$ ratio of 0.4 and different SP content at the shear rate of $100\text{ s}^{-1}$ .....	51
<b>Figure 3.11.</b> LXRPD patterns of BAY pastes at a $w/c$ ratio of 0.4. ....	53
<b>Figure 3.12.</b> Thermogravimetric plots of BAY cement pastes after 1, 7 and 28 days of hydration. (a) $w/c=0.4$ and (b) $w/c=0.5$ .....	56
<b>Figure 3.13.</b> Compressive strengths of BAY cements as a function of $w/c$ ratio. ....	58
<b>Figure 4.14.</b> Particle size distribution of $C_4A_3S$ (pseudocubic and orthorhombic), Cs and $C_3S$ powders.....	63
<b>Figure 4.15.</b> <i>In-situ</i> SXRPD hydration evolution of c137_132. ....	63
<b>Figure 4.16.</b> Rietveld plots of (a) c137_132 and (b) o137_132 at 24 hours of hydration. ....	64
<b>Figure 4.17.</b> Heat flow and mineralogical in-situ hydration evolution of (a and c) c137 and (b and d) o137.....	66

<b>Figure 4.18.</b> Heat flow and mineralogical in-situ hydration evolution of (a and c) c274 and (b and d) o274. ....	67
<b>Figure 4.19.</b> a) Total heat (cumulative) and b) heat flow curves of c137 and o137. ....	69
<b>Figure 4.20.</b> Comparison between measured and calculated results of heat for c137 and o137 mixtures at different water/solid ratios. ....	70
<b>Figure 4.21.</b> a) Total heat (cumulative) and b) heat flow curves of c274 and o274. ....	72
<b>Figure 4.22.</b> TG-DTG of c137_132 and o137_132 at 7 curing days. ....	77
<b>Figure 4.23.</b> <sup>27</sup> Si HPDEC and <sup>29</sup> Al One pulse MAS-NMR spectra of stopped-pastes of c137_132 and o137_132 at 7 curing days. ....	78
<b>Figure 4.24.</b> Deconvolution of <sup>27</sup> Si and <sup>29</sup> Al MAS-NMR spectra of (a) c137_132 and (b) o137_132 at 7 days of hydration. ....	79
<b>Figure 5.25.</b> Particle size distribution of FA#BAY powders. ....	84
<b>Figure 5.26.</b> Flow curves of (a) FA0BAY, (b) FA15BAY and (c) FA30BAY pastes at w/c = 0.4 and different superplasticizer contents. ....	86
<b>Figure 5.27.</b> Deflocculation curves of FA15BAY and FA30BAY pastes at the shear rate of 100 s <sup>-1</sup> . ....	87
<b>Figure 5.28.</b> Phase evolution and heat flow of FA0BAY paste prepared (w/c=0.40) (a) without superplasticizer and (b) with 0.5 wt% of superplasticizer. ....	89
<b>Figure 5.29.</b> Cumulative heat released by FA0BAY prepared without and with superplasticizer. ....	90
<b>Figure 5.30.</b> Normalized heat flow (a) and cumulative heat (b) per gram of solid for FA#BAY pastes prepared at a constant w/c of 0.4 and 0.5 wt% SP. ....	91
<b>Figure 5.31.</b> Thermogravimetric and differential thermogravimetric analyses (TG-DTG) of (a) FA0BAY, (b) FA15BAY and (c) FA30BAY pastes, with w/c=0.4 prepared with 0.5 wt% of superplasticizer. ....	96
<b>Figure 5.32.</b> <sup>27</sup> Al and <sup>29</sup> Si MAS-NMR of FA#BAY pastes at a) 7 days, b) 90 days and c) 180 days. ....	98
<b>Figure 5.33.</b> Deconvolution of <sup>29</sup> Al MAS-NMR spectra of FA0BAY at 180 days. ....	99
<b>Figure 5.34.</b> Deconvolution of <sup>27</sup> Si MAS-NMR spectra of (a) FA0BAY, (b) FA15BAY and (c) FA30BAY at 180 days. ....	101
<b>Figure 5.35.</b> Compressive strength of FA#BAY. ....	103
<b>Figure 5.36.</b> Pore size distribution of FA#BAY pastes at 180 hydration days. ....	103
<b>Figure 6.37.</b> Flow curves of B83 pastes with different superplasticizer contents (water/cement ratio of 0.4). ....	109

---

<b>Figure 6.38.</b> Deflocculation curve of B83 pastes prepared at a w/c ratio of 0.4 and different SP contents at the shear rate of $100 \text{ s}^{-1}$ .....	109
<b>Figure 6.39.</b> Heat flow (a) and total heat (b) of B83 and FA0BAY .....	111
<b>Figure 6.40.</b> LXRPD patterns of B83 anhydrous and hydrated at selected times with peaks due to a given phase labelled.....	114
<b>Figure 6.41.</b> Thermogravimetric and differential thermogravimetric analyses (TG-DTG) of B83 pastes.....	114
<b>Figure 6.42.</b> Compressive strength of FA0BAY (w/c=0.4 and 0.5 wt% SP) and B83 (w/c=0.4) with 0.3 and 0.4 wt% of SP .....	116



UNIVERSIDAD  
DE MÁLAGA

## List of Tables

	Pág.
<b>Table 1.1.</b> Elemental composition of raw materials determined by XRF (in oxide wt%) .....	20
<b>Table 1.2.</b> Chemical and mineralogical composition for the two clinkers (belite and CSA) determinate by XRF and Rietveld quantitative phase analysis (RQPA) quantification respectively. ....	22
<b>Table 2.3.</b> Targeted mineralogical phase assemblage (in wt%) of BAY clinkers, nominal elemental composition of raw mixtures (expressed as oxides) excluding H <sub>2</sub> O and CO <sub>2</sub> and raw materials dosages (wt%). ....	34
<b>Table 2.4.</b> Direct RQPA (wt%) for BAY clinkers. ....	36
<b>Table 2.5.</b> Raw materials dosages (wt%) and nominal elemental composition of raw mixtures (expressed as oxides) for BAY_3 attempts. ....	38
<b>Table 2.6.</b> Direct RQPA (wt%) for BAY_3 clinkers synthesized with different amounts of CaF <sub>2</sub> . ....	39
<b>Table 2.7.</b> Mineralogical composition (RQPA in wt%) for scBAY_4 clinker with 0.9 wt% CaF <sub>2</sub> at different thermal treatments. ....	40
<b>Table 2.8.</b> Average atomic ratio obtained by EDS in sc-BAY4 clinker.....	44
<b>Table 3.9.</b> Rheological properties of the fresh BYA paste prepared at w/c=0.4 and different SP contents. ....	50
<b>Table 3.10.</b> RQPA (wt%) for BAY pastes at w/c 0.4 (with SP) and w/c 0.5.....	52
<b>Table 4.11.</b> Pure phase mixture compositions, in weight percentages (wt%). ....	62
<b>Table 4.12.</b> Degree of reaction of ye'elinite in all the samples calculated from calorimetric data at 25 minutes (0.4 hours).....	66
<b>Table 4.13.</b> Degree of reaction (%) of ye'elinite in each mixture at selected times calculated from RQPA.....	68
<b>Table 4.14.</b> Mineralogical composition in weight (wt%) at 7 days (168 hours) of <i>in-situ</i> SXRPD hydration study.....	73
<b>Table 4.15.</b> Hydration degree of alite at 24, 48 hours, and 7 days from RPQA.....	74

<b>Table 4.16.</b> Comparative mineralogical composition of c137_132 and o137_132 at 0 and 7 days.....	76
<b>Table 4.17.</b> Relative area percentages (%) from deconvolution of <sup>29</sup> Si and <sup>27</sup> Al MAS-NMR spectra of c137_132 and o137_132 pastes .....	79
<b>Table 5.18.</b> Proportion of cement, fly ash and water used in pastes. ....	85
<b>Table 5.19.</b> RQPA results (wt%) on cement pastes, as a function of hydration time obtained from LXRPD for FA#BAY pastes (w/c=0.4 and 0.5 wt% SP), including ACn and free water (FW) contents. ....	95
<b>Table 5.20.</b> RQPA comparative results (wt%) on cement pastes of FA0BAY and FA30BAY prepared at w/c of 0.57, as a function of hydration time obtained from LXRPD. . ....	97
<b>Table 5.21.</b> Comparative content (wt%) of katoite and stratlingite on FA0BAY at 28 days, as a function of w/c ratio used. ....	97
<b>Table 5.22.</b> Increase of the strength (in percentage) referred to FA0BAY-mortar at the same ages. ....	102
<b>Table 6.23.</b> RQPA (wt%) for B83 pastes. ....	113



## Notation

### Cement notation of oxide compounds

C : CaO	A : Al <sub>2</sub> O <sub>3</sub>	S : SiO <sub>2</sub>	F : Fe <sub>2</sub> O <sub>3</sub>
H : H <sub>2</sub> O	s : SO <sub>3</sub>	T : TiO <sub>2</sub>	M : MgO

This leads to the following abbreviations for anhydrous and hydrates phases:

C <sub>3</sub> S	3CaO.SiO <sub>2</sub>	alite, tricalcium silicate
C <sub>2</sub> S	2CaO.SiO <sub>2</sub>	belite, dicalcium silicate
C <sub>4</sub> AF	4CaO.Al <sub>2</sub> O <sub>3</sub> .Fe <sub>2</sub> O <sub>3</sub>	ferrite
C <sub>3</sub> A	3CaO. Al <sub>2</sub> O <sub>3</sub>	tricalcium aluminate
C <sub>12</sub> A <sub>7</sub>	12CaO.7Al <sub>2</sub> O <sub>3</sub>	mayenite
C <sub>4</sub> A <sub>3</sub> S	3CaO.3Al <sub>2</sub> O <sub>3</sub> .CaSO <sub>4</sub>	ye'elimite, calcium sulfoaluminate
CsH <sub>2</sub>	CaSO <sub>4</sub> .2H <sub>2</sub> O	gypsum
Cs	CaSO <sub>4</sub>	anhydrite
CT	CaO.TiO <sub>2</sub>	perovskite
CA	CaO.Al <sub>2</sub> O <sub>3</sub>	calcium aluminate
C <sub>2</sub> AS	2CaO.Al <sub>2</sub> O <sub>3</sub> .SiO <sub>2</sub>	gehlenite
C <sub>5</sub> S <sub>2</sub> S	4CaO.2SiO <sub>2</sub> .CaSO <sub>4</sub>	ternesite, calcium sulfospurrite
C <sub>free</sub>	CaO	free lime
M	MgO	periclase
CH	Ca(OH) <sub>2</sub>	portlandite, calcium hydroxide
C-S-H	(CaO) <sub>x</sub> (SiO <sub>2</sub> ) <sub>y</sub> (H <sub>2</sub> O) <sub>z</sub>	calcium silicate hydrate gel
AFt (C <sub>6</sub> As <sub>3</sub> H <sub>32</sub> )	3CaO.Al <sub>2</sub> O <sub>3</sub> .3CaSO <sub>4</sub> .32H <sub>2</sub> O	ettringite, calcium trisulfoaluminate
AFm (C <sub>4</sub> AsH <sub>12</sub> )	3CaO.Al <sub>2</sub> O <sub>3</sub> .CaSO <sub>4</sub> .12H <sub>2</sub> O	calcium monosulfoaluminate

$C_2ASH_8$	$2CaO \cdot Al_2O_3 \cdot SiO_2 \cdot 8H_2O$	stratlingite
$AH_3$	$Al_2O_3 \cdot 3H_2O$	gibbsite
$C_3ASH_4$	$3CaO \cdot Al_2O_3 \cdot SiO_2 \cdot 4H_2O$	Katoite, silicious hydrogarnet

## Some materials notation

BAY:	belite-alite-ye'elimite cement
BYF:	belite-ye'elimite-ferrite cement
BYT:	belite-ye'elimite-ternesite cement
CSA:	calcium sulfoaluminate cement
FA:	Fly Ash
HBC:	High Belite Cement
OPC:	Ordinary Portland Cement
SCMs:	Supplementary Cementitious Materials
SP:	Superplasticizer

## Techniques acronyms

BET:	Brunauer–Emmett–Teller (specific surface area)
BSE:	Backscattering electron
EDS:	Energy Dispersive X-ray Spectroscopy
FE-SEM:	Field Emission – Scanning Electron Microscopy
LXRPD:	Laboratory X-Ray Powder Diffraction
MAS-NMR:	Magic Angle Spinning - Nuclear Magnetic Resonance
MIP:	Mercury Intrusion Porosimetry
PSD:	Particle Size Distribution
RQPA:	Rietveld Quantitative Phase Analysis
SEM:	Scanning Electron Microscopy
SXRPD:	Synchrotron X-Ray Powder Diffraction
TG-DTG:	Thermogravimetric Analysis – Derivative Thermogravimetric
XRF:	X-Ray Fluorescence

XRPD: X-ray Powder Diffraction

## Other acronyms

ACn: Amorphous and Crystalline non-quantified  
D<sub>v50</sub>: The median size for a volume particle distribution  
D<sub>v90</sub>: 90 percent of the particle distribution lies below that size.  
Eq.: Equation  
LoI: Loss of Ignition  
mol%: Mol percent  
vol%: Volume percent  
w/c: Water to cement ratio  
w/s: Water to solid ratio  
wt%: Weight percent



UNIVERSIDAD  
DE MÁLAGA

## Abstract

Climate change mitigation usually involves seeking for the reduction of greenhouse gases emissions in general and of carbon dioxide (CO<sub>2</sub>) in particular. Concrete is considered the most manufactured product in the world as it is the main component of the construction industry. Cement industry is one of the major contributors of greenhouse gases (GHG) emissions, releasing about one ton of carbon dioxide (0.97 tons) per ton of ordinary portland cement (OPC) fabricated. Thus, it is responsible for up to 10% of the total man-made CO<sub>2</sub> emissions, just behind the power industries. The development of world economies will cause a five-fold increase of the global cement production by 2050 compared to 1990, reaching 5 billion tons produced all over the world; in spite of significant improvements in efficiency, cement related emissions are expected to increase by 260% throughout the 1990 - 2050 period. Consequently, the challenge lies on the transformation of the traditional way of producing cement into a sustainable business model, and on the reduction of emissions from the cement sector in a timely way.

Due to these environmental issues the cement industry is under increasing scrutiny to reduce the energy used in production of Portland cement and mainly associated carbon dioxide emissions. In addition, Portland cement is not the ideal binder for all construction applications, as it suffers durability problems in particularly aggressive environments. For these reasons, there is a growing interest in the development, characterization, and implementation of alternatives binders to Portland cement which present similar mechanical performances than OPC.

OPC clinker is mainly composed by four crystalline phases: ~65 wt% alite ( $\text{Ca}_3\text{SiO}_5$ ;  $3\text{CaO} \cdot \text{SiO}_2$ ;  $\text{C}_3\text{S}$ ); ~15 wt% belite ( $\text{Ca}_2\text{SiO}_4$ ;  $2\text{CaO} \cdot \text{SiO}_2$ ;  $\text{C}_2\text{S}$ ); ~15 wt% ferrite ( $\text{Ca}_4\text{Al}_2\text{Fe}_2\text{O}_{10}$ ;  $4\text{CaO} \cdot \text{Al}_2\text{O}_3 \cdot \text{Fe}_2\text{O}_3$ ;  $\text{C}_4\text{AF}$ ) and ~5 wt% tricalcium aluminate or celite ( $\text{Ca}_3\text{Al}_2\text{O}_6$ ;  $3\text{CaO} \cdot \text{Al}_2\text{O}_3$ ;  $\text{C}_3\text{A}$ ). Its main phase is a high calcite demanding phase, thus releases high  $\text{CO}_2$  contents from the decarbonation of calcite, the main calcium source (i.e.  $0.58 \text{ t CO}_2/\text{t C}_3\text{S}$ ). Additionally, the formation temperature required is around  $1450 \text{ }^\circ\text{C}$ , needing high calorific fuel. OPC is produced by mixing clinker with a setting time regulator, commonly gypsum.

The hydration of OPC basically consists of two different reactions that happen at the same time. These are the silicate reaction and the aluminate reaction. The silicate reaction consists of alite dissolution in water, followed by precipitation of calcium silicate hydrate (C-S-H) gel/nanocrystalline phase and crystalline calcium hydroxide (known as portlandite, CH). The aluminate reaction consists on tricalcium aluminate hydration in presence of a calcium sulfate source (usually gypsum or hemihydrates), to give ettringite (AFt;  $\text{C}_6\text{As}_3\text{H}_{32}$ ). These hydrated phases (C-S-H and AFt) are responsible for the development of mechanical strengths with time. The increment on mechanical properties after 28 days is due to slow hydration of belite which also produces C-S-H gel and portlandite.

In addition, a new kind of binder, an “alternative eco-friendly cement”, may well be an alternative to OPC. The term “alternative eco-friendly cement” refers to a man-made mineral material that, when ground to a fine powder, reacts with water or  $\text{CO}_2$  quickly enough to produce a hardened mass which can be used as binder in concrete or mortar. This is the case of ye'elimite-rich cements and belite-rich cements.

Ye'elimite ( $\text{Ca}_4\text{Al}_6\text{SO}_{16}$ ;  $3\text{CaO} \cdot 3\text{Al}_2\text{O}_3 \cdot \text{CaSO}_4$ ;  $\text{C}_4\text{A}_3\text{S}$ ) rich cements (calcium sulfoaluminate; CSA) are known since Alexander Klein patented an expansive cement in 1963, with the objective of reducing the retraction of OPC. The classic CSA cements with ye'elimite as main phase (around 40 – 70 wt%) have been produced and used under the name of “Third Cement Series” in China since the

1970s. These ones are considered as environmentally eco-friendly cements for several reasons, including the low amount of limestone required to achieve the desired composition (mainly ye'elimite and belite), jointly with a low clinkering temperature, about 1200 – 1300 °C (~ 200 °C less than OPC). The properties and applications of this type of binder are strongly influenced by many factors: i) chemical and mineralogical composition of the clinker (mainly due to the presence of minor phases such as CA, CA<sub>2</sub>, C<sub>12</sub>A<sub>7</sub>, C<sub>4</sub>AF, CT, or C<sub>2</sub>AS); ii) sulfate source added (amount and type); iii) water to cement ratio (w/c); or iv) blending with other binders, such as supplementary cementitious materials (SCMs) or even OPC. The properties can be summarized in rapid setting, high early strength, high durability, and self-leveling and/or shrinkage compensation. However, due to the high levels of aluminum in these CSA cements (30–40 wt%) and the very expensive bauxite needed as raw material, these cements are not competitive from an economic point of view.

Moreover, recent studies and developments are focused on belite-calcium sulfoaluminate-ferrite cements (BYF) with belite as main phase and ye'elimite as second phase in percentage. These BYF contain up to 17% less aluminum than CSA, and consequently more iron sources are used, producing larger amounts of C<sub>4</sub>AF. These BYF cements usually contain 40 - 50 wt% of β-C<sub>2</sub>S and 20 - 30 wt% of C<sub>4</sub>A<sub>3</sub>s. Its clinkering temperature is similar than classical CSA, being around 1250 - 1300 °C (~200 °C lower than OPC clinkering temperature). The main problem of these belite-rich cements is the space between the extremely fast reaction of ye'elimite (during the first 24 hours of hydration), and the slow reaction of β-polymorphs of belite, after 28 hydration days. Trying to solve this problem, a number of ideas have been developed and partially implemented in recent years.

A possible solution is the activation of BYF clinkers by stabilizing high temperature polymorphs of belite, such as α-C<sub>2</sub>S and α'-C<sub>2</sub>S. That activation can be carried out by the addition of minor elements, such as B<sub>2</sub>O<sub>3</sub>, Na<sub>2</sub>O or P<sub>2</sub>O<sub>5</sub>. Technically, this concept has been implemented and patented by Lafarge as part

of a large-scale project named AETHER™. Thus, active-BYF cements are considered, currently, as one of the most promising alternatives to OPC. This is supported by both environmental benefits (lower CO<sub>2</sub> emissions) and industrial interest. However, it is needed to evaluate the cost/beneficial matrix prior to the implantation around the world since the raw materials for their production are more expensive than those of OPC.

A different approach, recently investigated, is the so-called belite calcium sulfoaluminate-ternesite (BYT) cement, where ternesite ( $\text{Ca}_5\text{Si}_2\text{SO}_{12}$ ;  $4\text{CaO} \cdot 2\text{SiO}_2 \cdot \text{CaSO}_4$ ;  $\text{C}_5\text{S}_2\text{S}$ ) is the main phase, jointly with belite and ye'elimite. Ternesite (as sulfospurrite) has been long time considered as hydraulically inactive. However, recent studies show that in the presence of reactive aluminum-bearing phases (such as  $\text{C}_4\text{A}_3\text{S}$ ,  $\text{C}_{12}\text{A}_7$ , CA, and  $\text{CA}_2$ ) ternesite is highly reactive forming C-S-H and ettringite, the main hydration phases of OPC and CSA respectively, which are responsible of their properties. However, further research is needed to evaluate the long-term performance of them, such as that related to strength development, dimensional stability and durability.

A step forward in the activation of BYF is the production of cements that jointly content alite and ye'elimite, known as **belite – alite – ye'elimite (BAY)** cements. Their production releases up to 18% less CO<sub>2</sub> than OPC, depending on their composition. Alite is the main component of OPC and is responsible for early mechanical strengths. For that reason, the reaction of alite and ye'elimite with water could yield cements with high mechanical strengths at early curing time, while belite should contribute to later ages. However, the production of such cement represents an important challenge, due to the differences between the formation/decomposition temperatures of the main phases. For the alite formation at least ~1350 °C are needed, while ye'elimite decomposes above that temperature. Recent research focused on obtaining alite – calcium sulfoaluminate cement (known as ACSA), where the main phases are  $\text{C}_3\text{S}$  (30 – 50 wt%),  $\text{C}_2\text{S}$  (30 – 40 wt%) and  $\text{C}_4\text{A}_3\text{S}$  (5 – 20 wt%) phases demonstrated the



coexistence of both phases. In those investigations the formation temperature of the alite was reduced to a range between 1230 - 1300 °C by using mineralizers, such as calcium fluoride plus copper oxide, magnesium oxide, titanium oxide or zinc oxide; or stabilized the ye'elimite by adding barium or strontium, as a suitable approach to prevent the decomposition at high temperatures. Despite of those results on ACSA cements mineralogy, **it has not been found evidences, papers or reports focused on the synthesis of BAY cements**, where the alite content could mitigate the space between ye'elimite and  $\beta$ -belite. For this reason, further investigation on their synthesis, actual mineralogy, hydration mechanisms and properties performance compared to non-active BYF cement is needed.

According to the last statement, this PhD thesis is focused on the design, synthesis, processing and characterization of a BAY cement, with and without fly ash addition (as supplementary cementitious material); as well as the deep understanding of the joint hydration mechanism of alite with ye'elimite. In addition, for the sake of comparison, a blended of two commercial cements (belite and calcium sulfoaluminate) was prepared, which final mineralogy was similar to the synthesized BAY.

One of the main objectives of this thesis has been to obtain a BAY clinker with higher jointly content of alite and ye'elimite from natural raw materials (such as kaolin, limestone, gypsum and sand). This study was carried out in two scales. Firstly, at laboratory scale ("small" size), where ~ 7 g of clinker with different targeted phase compositions, prepared with 0.9 wt% of fluorite ( $\text{CaF}_2$ ), were synthesized. The optimized clinkering process consisted on heating at 900 °C during 30 min at a heating rate of 5 °C/min, followed by further heating to 1300 °C during 15 min, at the same rate. Later, the clinker was rapidly quenched by forced air flow. This initial study showed that dosage presented an important influence on the mineralogical composition, where high amounts of  $\text{Fe}_2\text{O}_3$  significantly affected the formation of the ye'elimite ( $\text{C}_4\text{A}_3\text{S}$ ), favoring its decomposition into mayenite ( $\text{C}_{12}\text{A}_7$ ). In addition, the quantity of  $\text{C}_3\text{S}$  and  $\text{C}_4\text{A}_3\text{S}$

increased by decreasing the amount of iron oxide and increasing the amount of  $\text{SO}_3$  (added as gypsum). Finally, the maximum obtained percentages of alite jointly with ye'elimite were 16.0 and 12.1 wt% respectively, presenting an alite/ye'elimite ratio of  $\sim 1.3$ . These phases were associated with 60.3 wt%  $\text{C}_2\text{S}$ , 2.3 wt%  $\text{C}_{12}\text{A}_7$ , 7.0 wt%  $\text{C}_4\text{AF}$  and 2.3 wt%  $\text{C}_3\text{A}$  in the clinker.

Secondly, 2 kg of clinker ("medium" scale, named as "scaled-up clinker") were synthesized. To do that, the thermal conditions and raw meal dosage were optimized again. The best results were achieved when an excess of gypsum (up to 4.3 wt%  $\text{SO}_3$  as total content in the dosage) was added and the raw mixture was heated at 1300 °C for 15 min. The scaled-up BAY clinker was characterized through LXRPD and SEM-EDS; it showed a final composition of 60.9(2) wt%  $\text{C}_2\text{S}$ , 6.9(2) wt%  $\text{C}_4\text{AF}$ , 0.6(1) wt% Cs, 10.4(1) wt%  $\text{C}_4\text{A}_3\text{S}$ , 13.5(2) wt%  $\text{C}_3\text{S}$ , 2.6(1) wt% Fluorellestadite ( $\text{C}_7\text{S}_3\text{S}_3\text{F}$ ;  $6\text{CaO} \cdot 3\text{SiO}_2 \cdot 3\text{CaSO}_4 \cdot \text{CaF}_2$ ;  $\text{Ca}_{10}(\text{SiO}_4)_3(\text{SO}_4)_3\text{F}_2$ ) and 5.1(1) wt%  $\text{C}_{12}\text{A}_7$ . As it can be seen, it also presented an alite/ye'elimite ratio of  $\sim 1.3$ . Moreover, the morphologic characterization by SEM-EDS of the scaled-up BAY clinker revealed that the average particle sizes of ye'elimite (with rhombic shaped particles), alite (with prismatic shape particles) and belite (with typical spherical shape) were near to 5  $\mu\text{m}$ . As a final step, this scaled-up clinker was blended with 12 wt% of anhydrite (its stoichiometric amount of calcium sulfate taking into account ye'elimite and calcium aluminate contents) to fulfill reaction of ettringite formation. The rest of the characterization was performed using this scaled-up cement.

It is important to highlight that the quantitative phase analysis of BAY clinker and its hydration products is an essential part of this thesis. X-ray powder diffraction (XRPD) combined with Rietveld methodology allows direct quantification of the crystalline phases in the samples. This technique was widely used to understand the anhydrous mineralogy of the samples, as well as the hydration mechanism in BAY and alite-ye'elimite systems. Thus, this allowed correlating the mineralogy with the mechanical properties development.

The application of RQPA to characterize clinkers/anhydrous cements/pastes is not an easy task due to the presence of appreciable amounts of amorphous and/or non-crystalline phases (ACn). Amorphous content, determined indirectly by RQPA, is constituted by all amorphous phases without long range periodic order, but also misfitting problems of the analyzed crystalline phases (due to its own internal disordered) and any crystalline phase non-included in the Rietveld control file. Therefore, the quantification of ACn phases is a very important issue to understand hydration mechanisms, especially when important hydrated products can be part of them.

The hydration studies have been performed using LXRPD with the internal standard methodology to determine the full phase assemblage, including ACn contents. This method was applied to stopped-hydration samples; consequently, it enables to obtain only ACn contents. The free water (FW) content was determined by the comparison of TGA-DTG mass losses up to 600 °C of stopped-hydration samples and the total added water.

Another important objective of this thesis has been to understand the water-to-cement (w/c) ratio effect, the superplasticizer content and the addition of fly ash - FA as supplementary cementitious material (SCMs) in the hydration mechanism and mechanical properties (i.e. compressive strength) of BAY cement pastes and mortars. These studies were made through the analysis of the hydration process in the cement pastes, as well as the mechanical properties of the corresponding mortars.

In a first step, the effect of different w/c ratios (0.4, 0.5 and 0.57) was studied on the crystalline mineralogy of BAY. In all cases the hydrated phases, independently of w/c used, were ettringite (AFt) and AFm-type phases (such as monosulfoaluminate, stratlingite and/or katoite); and in a minor amount low-crystalline C-S-H and amorphous aluminum hydroxide were identified by TG-DTG, both of them forming part of the ACn content. Despite of the high amount of calcium silicates ( $C_3S$  and  $C_2S$ ) in the system, the presence of portlandite (CH) was not detected, except at later ages as a product of  $\beta$ -form belite ( $\beta$ - $C_2S$ )

hydration. This absence was deemed due to the CH reaction with ye'elimite at early ages to produce ettringite, and at later ages favors the degradation of AFt into AFm phases. This last effect was reflected as a decrease of AFt and increase of AFm amount from 28 to 180 days. The influence of the w/c ratio in the crystalline mineralogy was only in the stratlingite/katoite ratio, where the increment of w/c ratio favored the precipitation of stratlingite instead of katoite. The compressive strength of BAY mortars was improved by decreasing the w/c ratio, as expected; but **the most important result** was that **BAY cement mortar presents better mechanical behavior than non-active BYF** (48.7(6) wt% of  $\beta$ -C<sub>2</sub>S, 28.1(1.0) wt% of C<sub>4</sub>A<sub>3</sub>S, 14.9(2) wt% of C<sub>4</sub>AF, 1.3(2) wt% of CT, 2.6(5) wt.% of  $\gamma$ -C<sub>2</sub>S and 4.4(2) wt.% of C<sub>2</sub>AS), showing higher compressive strengths from the first day of hydration., even when that BYF cement presents a higher amount of ye'elimite. Thus, that result was attributed to the jointly presence of ettringite and C-S-H (from the hydration of ye'elimite and alite, respectively).

The optimal amount of a polycarboxylate based superplasticizer (SP) was determined by rheological studies, showing a significant improvement in the workability (decrease of the viscosity). After the optimization, the best amount to be added to the samples was 0.5 wt% (referred to active solids). The effect of the superplasticizer on the hydration behavior was also studied by isothermal calorimetry and *in-situ* Mo-LXRPD. This study showed that the polycarboxylate affects the kinetic of mayenite (C<sub>12</sub>A<sub>7</sub>) hydration; therefore, it inhibited the competitive hydration reaction between ye'elimite and mayenite. From the calorimetric study, this effect was observed as a decrease in the intensity of the main hydration peak, which is associated with precipitation of AFt and/or other aluminum hydrated phases, yielding to a reduction of 28% of the total heat released from BAY cement pastes after 2 days.

The use of fly ash in pastes and mortars did not show enough direct evidences of pozzolanic effect (reaction between fly ash and Ca<sup>2+</sup> and OH<sup>-</sup> free ions present in the pore solution). Nevertheless, it was found that the increment of FA (from 0 to

30 wt%) had two main effects on the hydrated phase assemblage of BAY: i) inhibited the belite hydration; therefore, ii) favored the AFt stability. From calorimetric studies the acceleration of the main peak, compared to the main signal of unblended BAY cement, was observed. This effect gives information concerning the FA capacity of creating nucleation centers for hydrated phases; this behavior is commonly known as "early filler effect". The increase of FA partial replacement also increased the mechanical development of BAY during the hydration time. This was attributed to the filler effect at early (nucleation centers) and later ages (pore space filler); but could too be justified as an indirect pozzolanic reaction, despite of the  $C_2S$  inhibition.

With the aim of understanding the influence and behavior of jointly hydration of alite and ye'elimite, a deeper study by *in-situ* SRXPD and isothermal calorimetry was carried out. The mixtures of pure alite and pure ye'elimite (orthorhombic and pseudocubic) systems with two alite/ye'elimite ratios (1.37 and 2.74) of both ye'elimite polymorphs were studied. Those samples were hydrated at water-to-solid ratios of 0.59 and 1.19 for alite/ye'elimite ratio of 2.74; and w/s ratios of 0.66 and 1.32 for alite/ye'elimite ratio of 1.37. Those w/s ratios correspond to 110% and 220% of stoichiometric water amount (i.e. the stoichiometric amount of water to full reaction of ye'elimite and alite), respectively. The results showed that alite hydration was highly affected by the hydration kinetic of ye'elimite, where due to the lower hydration kinetic of pseudocubic ye'elimite, alite started to react after one day. However, alite in presence of orthorhombic ye'elimite, began to react much faster, just after 10 hours of hydration. The main hydration products obtained from these hydrations were ettringite, monosulfoaluminate, stratlingite and C-S-H. Again, in these systems portlandite was not detected. After 7 days, the systems with pseudocubic ye'elimite and alite presented less hydration degree than in those systems with orthorhombic ye'elimite. This last behavior favors the stability and amount of AFt on the system. When the water-to-solid (w/c) ratio in the alite/ye'elimite ratio of 1.37 mixtures was increased, the kinetics of hydration of ye'elimite was hastened at half of their hydration time, favoring the rapid precipitation of ettringite (and monosulfoaluminate in systems with

orthorhombic ye'elimite). Likewise, independently of the alite/ye'elimite ratio, the increase of w/s ratio favored the hydration degree of alite and the respective formation of C-S-H and stratlingite.

It is important to emphasize that katoite did not precipitate in pure alite-ye'elimite systems, which is a relevant phase obtained in the hydration of BAY cement (even with the addition of fly ash). Its properties and influence on the mechanical development of BAY-cement are unknown. Consequently, these results give essential information about its formation mechanism in the studied BAY-cement system; it can be associated with the hydration of belite in an Al-rich environment and the joint hydration of ferrite and alite.

Finally, the “commercial binder” B83 (83 wt% of belite clinker supplied by Buzzi Unicem – Italy; plus 17 and 7 wt% of calcium sulfoaluminate clinker supplied by Belith S.P.R.L – Belgium and anhydrite, respectively) prepared with similar anhydrous mineralogy than BAY synthesized cement (alite/ye'elimite ratio 1.3) was studied with a w/c ratio of 0.4. These studies show that the main hydration products of B83 were ettringite, stratlingite, katoite, monosulfoaluminate and amorphous aluminum hydroxide, without precipitation of portlandite; i.e. the same mineralogy obtained from BAY cement hydration. Particularly, this “commercial binder” presented a hydration degree of alite of 77.5% at 180 days, while belite reached a hydration degree of 55%. This low hydration degree from calcium silicates favored the ettringite stability without any evidence of AFm formation. Additionally, the formation of stratlingite and katoite was favored in this Al-rich environment. However, that behavior was totally opposed for BAY cement hydration mechanism, where due to fast hydration of alite and late hydration of belite, the ettringite amount decreased showing an increase of AFm-type phases (monosulfoaluminate, hemicarbonate, stratlingite).

Moreover, the compressive strength of “commercial binder” B83 showed better values than BAY-cement mortars (without any fly ash addition) from the first hydration day. This mechanical development was related with the low porosity of

the paste of the cementitious mortars matrix, as well as the hydrated phases assemblage in it (i.e. ettringite stability and high amount, and elevated content of stratlingite).



UNIVERSIDAD  
DE MÁLAGA



## Resumen

El concreto está considerado como uno de los productos más fabricados debido a que es el componente primordial en el sector de la construcción. Donde la industria del cemento, elemento principal del concreto, es uno de los mayores contribuyentes de la emisión de los gases de efecto invernadero, generando cerca de una tonelada de dióxido de carbono (0.97 t) por tonelada de cemento portland ordinario (OPC, por sus siglas en inglés) fabricado. Haciéndolo, por lo tanto, responsable de hasta un 10% del total de CO<sub>2</sub> generado por el hombre, justo detrás de la industria energética. Teniendo en cuenta que para el 2050, respecto al año 1990, el desarrollo de la económica global podría causar un incremento cinco veces mayor sobre la producción del cemento mundial, se alcanzarían los 5 billones de toneladas de cemento producidas alrededor del mundo. Por lo tanto, se espera que las emisiones relacionadas con el cemento se vean incrementadas en un 260% en ese periodo (1990 – 2050), aún a pesar de las significativas mejoras en la eficiencia de producción que actualmente presenta este gremio. Por otro lado, la mitigación del cambio climático está volcada en la búsqueda de la reducción de los gases de efecto invernadero en general, y a la reducción del dióxido de carbono (CO<sub>2</sub>), en particular. Como consecuencia, el reto a afrontar por parte de la industria del cemento, está direccionado en la transformación del método actual de producción en un modelo de negocio sostenible, a la vez que se reducen sus emisiones.

Debido a este aspecto ambiental, la industria de cemento se encuentra bajo un creciente escrutinio, donde es necesario reducir la energía usada en el proceso

productivo del cemento portland, la cual está, a su vez, directamente asociada con las emisiones de dióxido de carbono. De igual manera, el cemento portland no es considerado el aglutinante ideal para todo tipo de aplicaciones, debido a que presenta problemas de durabilidad en ambientes particularmente agresivos. Por esta razón, actualmente hay un creciente interés en el desarrollo, caracterización e implementación de materiales alternativos al cemento portland que presenten comportamiento mecánico similar a un OPC.

El clínker OPC está compuesto principalmente por 4 fases cristalinas: ~65% en peso de alita ( $\text{Ca}_3\text{SiO}_5$ ;  $3\text{CaO} \cdot \text{SiO}_2$ ;  $\text{C}_3\text{S}$ ); ~ 15%p de belita ( $\text{Ca}_2\text{SiO}_4$ ;  $2\text{CaO} \cdot \text{SiO}_2$ ;  $\text{C}_2\text{S}$ ); ~ 15%p de ferrita ( $\text{Ca}_4\text{Al}_2\text{Fe}_2\text{O}_{10}$ ;  $4\text{CaO} \cdot \text{Al}_2\text{O}_3 \cdot \text{Fe}_2\text{O}_3$ ;  $\text{C}_4\text{AF}$ ) y ~5 %p de aluminato tricálcico o celita ( $\text{Ca}_3\text{Al}_2\text{O}_6$ ;  $3\text{CaO} \cdot \text{Al}_2\text{O}_3$ ;  $\text{C}_3\text{A}$ ). Su fase principal (la alita) es altamente demandante de calcita, generando por lo tanto, grandes cantidades de  $\text{CO}_2$  provenientes del proceso de descarbonatación de la misma, la cual es fuente principal de óxido de calcio, liberando, así, 0.58 t  $\text{CO}_2$  por cada tonelada de alita. Además, también está el hecho de que la temperatura de formación de la alita se encuentra cerca de  $1450^\circ\text{C}$ , requiriendo, en consecuencia, combustibles con alto poder calorífico. Una vez se obtiene el clínker, el cemento OPC es producido generalmente a partir de la conjunta molienda del mismo con un regulador de fraguado, donde el yeso es el mineral que principalmente se usa.

El mecanismo de hidratación de un cemento OPC consiste básicamente en dos tipos de reacciones que suceden simultáneamente. Estas reacciones, son la que se dan lugar a partir del silicato y el aluminato de calcio de manera independiente. Por una parte, la reacción del silicato de calcio consiste en la disolución de la alita en agua, seguida de la precipitación de silicato de calcio hidratado (C-S-H) en forma de gel o nanocristalina, y del hidróxido de calcio cristalino conocido como portlandita (CH). Por otra parte, la reacción del aluminato de calcio consiste en la hidratación del  $\text{C}_3\text{A}$  en presencia de una fuente de sulfato de calcio (usualmente yeso o hemihidrato de calcio), la cual

produce etringita (AFt;  $C_6As_3H_{32}$ ). Estas fases hidratadas (C-S-H y AFt) son las responsables del desarrollo de propiedades mecánicas con el tiempo, y el incremento de estas propiedades tras 28 días de hidratación, es debido a la lenta hidratación de la belita, cuya cinética es más lenta, y a su vez, también produce C-S-H y portlandita.

Por lo tanto, la obtención de un “eco-cemento alternativo” puede ser una opción frente al problema medioambiental del OPC. Este término de “eco-cemento alternativo” hace referencia a un material mineral fabricado por el ser humano, que cuando es molido en un polvo fino, reacciona con el agua o el  $CO_2$  lo suficientemente rápido, para producir una masa endurecida la cual pueda ser utilizada como aglutinante en un concreto o mortero. Este es el caso de los cementos ricos en ye'elemita y los cementos ricos en belita.

Los cementos ricos en ye'elemita ( $Ca_4Al_6SO_{16}$ ;  $3CaO.3Al_2O_3.CaSO_4$ ;  $C_4A_3S$ ), se conocen como cementos de sulfoaluminato de calcio (CSA por sus siglas en inglés) desde el año 1963, cuando Alexander Klein lo patentó como un cemento expansivo, con el objetivo de reducir el fenómeno de la retracción del OPC. El cemento CSA clásico, cuya fase principal es la ye'elemita (entre 40 – 70% en peso), se produce y utiliza en China desde los años 70 bajo el nombre de “Cemento de Tercera Generación”. Estos cementos son considerados ambientalmente eco-amigables por diversas razones, entre los que incluyen: i) el bajo requerimiento de caliza para alcanzar la composición mineralógica deseada (principalmente belita y ye'elemita) y ii) la baja temperatura de clinkerización, la cual se encuentra comprendida entre 1200 – 1300 °C (lo que representa ~200 °C menos que un cemento OPC). Las propiedades y aplicaciones de este tipo de material están fuertemente ligadas con diversos factores, tales como: i) la composición química y mineralógica del clíinker (principalmente asociada a la presencia de fases minoritarias como CA,  $CA_2$ ,  $C_{12}A_7$ ,  $C_4AF$ , CT, o  $C_2AS$ ); ii) la cantidad y tipo de fuente de sulfato de calcio utilizado; iii) la relación agua/cemento utilizada (w/c por sus siglas en inglés); o iv) la mezcla con otros aglutinantes, tales como los materiales cementantes suplementarios (SCMs por

sus siglas en inglés) o el mismo OPC. Las propiedades de este cemento CSA, pueden resumirse en que presentan un rápido fraguado, alta resistencia a la compresión a edades tempranas, buena durabilidad, capacidades autonivelantes y/o de compensación de la retracción. Sin embargo, debido a los grandes niveles de óxido de aluminio en estos cementos CSA (entre un 30 – 40%p), y al altísimo costo de la bauxita (fuente principal de aluminio a nivel mundial) necesaria como materia prima, estos cementos aun no son competitivos desde el punto de vista económico.

No obstante, recientes estudios y desarrollos han estado enfocados en los cementos belítico-ye'elemítico-ferrítico (BYF), cuya fase principal es la belita seguida de la ye'elemita (en términos de porcentaje en peso). Estos cementos BYF contienen hasta un 17% menos aluminio que los CSA, usándose en su reemplazo más cantidad de una fuente de hierro, lo cual permite la presencia de grandes cantidades de  $C_4AF$  en ellos. Estos cementos BYF usualmente contienen entre 40 – 50 %p de  $\beta$ - $C_2S$  y 20 – 30 %p de  $C_4A_3S$ . Su temperatura de clinkerización es similar a la de un CSA típico, estando cerca de los 1250 - 1300 °C (~200 °C menos que la temperatura de clinkerización del OPC). El mayor problema que presentan estos cementos ricos en belita es la diferencia que existe entre la extremadamente rápida reacción de la ye'elemita (durante las primeras 24 horas de hidratación), y la lenta reacción de la belita (en su forma beta), la cual se da a lugar después de los 28 días de hidratación. En un intento para solventar este problema, un sinfín de ideas han sido desarrolladas y parcialmente implementadas en los últimos años.

Una posible solución para solventar este problema es la activación de los clínkeres BYF a través de la estabilización de los polimorfos de alta temperatura de la belita, tales como  $\alpha$ - $C_2S$  y  $\alpha'$ - $C_2S$ . Esta activación puede realizarse utilizando la adición de elementos minoritarios como dopantes de estas fases a bajas temperaturas. Entre los tipos de dopantes más empleados para estabilizar estos dos polimorfos se encuentran el  $B_2O_3$ ,  $Na_2O$  o  $P_2O_5$ . Técnicamente, este

concepto del uso de dopantes ha sido implementado y patentado recientemente por la compañía cementera Lafarge, a través de un mega proyecto a escala industrial denominado AETHER™. Por lo tanto, actualmente, los cementos activados BYF son considerados como una de las alternativas más prometedoras del cemento OPC. Esto es apoyado por sus beneficios ambientales (menores emisiones de CO<sub>2</sub>), y el interés industrial, al poderse fabricar con la misma tecnología que un OPC. Sin embargo, es necesario evaluar el verdadero costo/beneficio antes que pueda ser implementado alrededor del mundo, debido a que sus materias primas son mucho más costosas que las que se usan en un cemento portland, y conocer sus prestaciones a medio y largo plazo.

Una alternativa diferente de activación de los cementos BYF, serían los cementos belíticos-ye'elemíticos-ternesíticos (BYT), donde la ternesita (Ca<sub>5</sub>Si<sub>2</sub>SO<sub>12</sub>; 4CaO.2SiO<sub>2</sub>.CaSO<sub>4</sub>; C<sub>5</sub>S<sub>2</sub>S) es una de las fases principales, junto con la belita y la ye'elemita. La ternesita (también conocida como sulfoespurrita) ha sido considerada por un tiempo como inactiva hidráulicamente hablando. Sin embargo, estudios recientes han mostrado que en presencia de fases ricas en aluminio (como el C<sub>4</sub>A<sub>3</sub>S, C<sub>12</sub>A<sub>7</sub>, CA, and CA<sub>2</sub>), la ternesita es altamente reactiva y capaz de formar C-S-H y etringita, las cuales son las principales fases hidratadas responsables de las propiedades mecánicas en los cementos OPC y CSA, respectivamente. Sin embargo, se hace estrictamente necesario desarrollar mayores investigaciones en el tema, donde se pueda evaluar su desempeño a largo plazo, es decir la evolución de su resistencia, su estabilidad dimensional y durabilidad.

Otra alternativa diferente de activación de los cementos BYF, es la obtención de conjunta de la alita y la ye'elemita. A estos cementos se les conoce como **belítico-alítico-ye'elemítico (BAY)** donde, dependiendo de su composición, su producción puede generar hasta un 18% menos CO<sub>2</sub> que un cemento OPC. La alita, fase principal del OPC, al hidratarse, otorga elevadas resistencias mecánicas a edades tempranas. Teniendo en cuenta lo anterior y lo que se

conoce del sulfoaluminato de calcio, la hidratación conjunta de la alita y la ye'elemite podrían favorecer, durante las primeras edades de hidratación, el desarrollo de altas resistencias a la compresión; mientras que la hidratación de la belita contribuiría con la resistencia pasados los 28 días de hidratación. Sin embargo, la producción de un cemento BAY representa un reto importante, debido a la diferencia que hay entre las temperaturas de formación y descomposición de estas dos fases (alita y ye'elemite, respectivamente). La formación de la alita requiere al menos  $\sim 1350$  °C; mientras que la ye'elemite comienza su descomposición por debajo de esa temperatura.

Recientes investigaciones enfocadas en la obtención de sistemas donde existan conjuntamente la alita y la ye'elemite, se han centrado en conseguir cementos alífticos-ye'elemíticos (conocidos como ACSA por sus siglas en inglés), donde la fase principal es alita (30 – 50 %p), seguida de belita (30 – 40 %p) y ye'elemite (5 – 20 %p). En estas investigaciones, la temperatura de formación de la alita se ha reducido a un rango entre 1250 - 1300 °C a través del uso de mineralizadores; entre ellos el más utilizado es el fluoruro de calcio (fluorita), junto de óxido de cobre, óxido de magnesio, óxido de titanio u óxido de zinc; o también ha sido logrado, a través de la estabilización de la ye'elemite con la adición de bario o estroncio, lo cual evita la descomposición a altas temperaturas de ésta. A pesar de los buenos resultados obtenidos en la mineralogía de los cementos ACSA, **a la fecha no se han encontrado evidencias, artículos o reportes de científicos enfocados en la síntesis de los cementos tipo BAY**, donde el contenido de alita pueda mitigar el gap que existe entre la reacción de la ye'elemite y  $\beta$ -belita. Por esta razón, se requiere una investigación profunda sobre su posible síntesis, el estudio de su verdadera mineralogía, su mecanismo de hidratación y el desarrollo de sus propiedades, todo esto comparándolo con un cemento BYF no activado.

De acuerdo con lo anterior, esta tesis doctoral se ha enfocado en el diseño, síntesis y caracterización de un cemento BAY, con y sin adición de cenizas

volantes (como material suplementario cementicio); así como también, un estudio profundo sobre el mecanismo de la hidratación conjunta de la alita y la ye'elemita. Además, a manera de comparación, se preparó una mezcla con dos clínkeres comerciales, un belítico y un sulfoaluminato de calcio; con los cuales se logró obtener un material con una mineralogía similar al BAY sintetizado en la primera etapa de la tesis.

Uno de los objetivos principales de esta Tesis, fue obtener un clínker BAY con el mayor contenido de alita y ye'elemita a partir del uso de materias primas naturales, tales como el caolín, la caliza, el yeso y arena rica en sílice. Este estudio fue llevado a cabo a dos escalas diferentes: i) la primera, a pequeña escala, denominada escala laboratorio, donde se sintetizaron ~7 g de clínker con diferentes composiciones de las fases objetivo, haciendo uso de 0.9 %p de fluorita ( $\text{CaF}_2$ ) como mineralizador. El proceso de clinkerización consistió en un calentamiento a 900 °C durante 30 min, utilizando una rampa de 5 °C/min; seguido de un nuevo calentamiento hasta los 1300 °C por 15 min, usando la misma rampa de subida. Una vez pasado el tiempo de residencia a la máxima temperatura (1300 °C/15 min), el clínker fue rápidamente enfriado usando convección forzada con aire. Este estudio mostró que la formulación de las materias primas jugó un papel importante en la mineralogía del clínker obtenido, donde con una formulación rica en óxido de hierro ( $\text{Fe}_2\text{O}_3$ ), la formación de la ye'elemita ( $\text{C}_4\text{A}_3\text{S}$ ) se vio significativamente afectada, favoreciendo así su descomposición en mayenita ( $\text{C}_{12}\text{A}_7$ ). Además, al disminuir el contenido de óxido de hierro e incrementar el contenido de  $\text{SO}_3$  (adicionando yeso) en la materia prima, se aumentó el contenido conjunto de la alita y la ye'elemita. Finalmente, se logró obtener un clínker compuesto por 16.0 %p de alita y 12.1 %p de ye'elemita, como máxima cantidad de ambos simultáneamente. Esto representa una relación alita/ye'elemita de ~1.3 en el clínker. Junto a estas dos fases, también se estaban presentes 60.3 %p de  $\text{C}_2\text{S}$ , 2.3 %p de  $\text{C}_{12}\text{A}_7$ , 7.0 %p de  $\text{C}_4\text{AF}$  y 2.3 %p de  $\text{C}_3\text{A}$ .

La segunda parte fue realizada a mediana escala, donde se prepararon 2 kg de clínker (denominado clínker “escalado”). Para llevar a cabo esto, las condiciones de síntesis y la formulación de materia prima (dosificación) fueron optimizadas. Los mejores resultados se alcanzaron cuando se utilizó un exceso de yeso (hasta conseguir un contenido total de  $\text{SO}_3$  de 4.3% en término de óxidos), y se calentó este nuevo crudo a 1300 °C durante 15 min. La caracterización del clínker BAY escalado, llevada a cabo por LXRPD y SEM-EDS, mostró que la composición final obtenida fue de 60.9(2) %p de  $\text{C}_2\text{S}$ , 6.9(2) %p de  $\text{C}_4\text{AF}$ , 0.6(1) %p de  $\text{Cs}$ , 10.4(1) %p de  $\text{C}_4\text{A}_3\text{S}$ , 13.5(2) %p de  $\text{C}_3\text{S}$ , 5.1(1) %p de  $\text{C}_{12}\text{A}_7$  y 2.6(1) %p de Fluorellestadita ( $\text{C}_7\text{S}_3\text{S}_3\text{F}$ ;  $6\text{CaO} \cdot 3\text{SiO}_2 \cdot 3\text{CaSO}_4 \cdot \text{CaF}_2$ ;  $\text{Ca}_{10}(\text{SiO}_4)_3(\text{SO}_4)_3\text{F}_2$ ). Donde nuevamente, se adquirió una relación alita/ye'elemite de ~1.3. La caracterización morfológica del clínker BAY escalado realizada por SEM-EDS, mostró que el tamaño promedio de partícula de la ye'elemite (el cual tiene una forma rómbica), la alita (la cual tiene una forma prismática) y la belita (cuya forma es esférica o redondeada) estuvo cercano a las 5  $\mu\text{m}$ . Finalmente, este clínker escalado se mezcló con 12 %p de anhidrita, lo cual corresponde a la cantidad estequiométrica necesaria para obtener etringita a partir del contenido de ye'elemite y aluminato de calcio (mayenita) presente en el clínker.

Es importante resaltar que el análisis de fases en el clínker BAY y sus productos de hidratación es una parte esencial de esta Tesis. La difracción de rayos-X (XRPD por sus siglas en inglés) combinada con la metodología Rietveld permitió cuantificar directamente el contenido cristalino de las fases presentes en la muestra. Esta técnica fue ampliamente usada para comprender la mineralogía de las muestras anhidras, y los mecanismos de hidratación tanto en el cemento BAY como en el sistema de alita-ye'elemite (mezcla de fases puras) estudiado. Por lo tanto, esto permitió correlacionar la mineralogía obtenida con el desarrollo de las propiedades mecánicas (resistencia a la compresión) de los correspondientes morteros.



El uso de RQPA (por sus siglas en inglés de Análisis Cuantitativo de Fases por Rietveld) usado para caracterizar clínkeres, cementos anhidros y pastas hidratadas no es una metodología fácil de aplicar debido a la cantidad apreciable de fases amorfas y/o de baja cristalinidad (ACn por sus siglas en inglés). El material amorfo, el cual es determinado indirectamente a partir de los datos de RQPA, está constituido por todas las fases amorfas, pero también está asociado a los problemas en el ajuste de las fases cristalinas analizadas (debido a su propio desorden interno) y a cualquier fase cristalina no incluida en el archivo de control de Rietveld. Como consecuencia, la cuantificación de las fases ACn es un punto de gran importancia para comprender los mecanismos de hidratación, en especial cuando los productos de hidratación pueden ser parte de ella, como es el caso del gel C-S-H, por ejemplo.

El estudio de la hidratación fue realizado usando LXRPD usando la metodología de estándar interno para determinar el ensamblaje de fases completo, incluyendo el contenido de ACn. Este método fue aplicado en las muestras hidratadas después de haber sido detenido su proceso de hidratación; en consecuencia, esto permitió obtener el contenido de ACn sin la presencia de agua no ligada. El agua libre (FW por sus siglas en inglés) fue determinado por la comparación de la pérdida de masa hasta los 600 °C, obtenido en las medidas de TG-DTG de las muestras hidratadas paradas y el agua total adicionada.

Otro objetivo importante comprendido en esta tesis, fue comprender el efecto de la relación agua/cemento usada, el contenido de superplastificante y la adición de ceniza volantes (FA) como SCMs en los mecanismos de hidratación de las pastas y en la resistencia a la compresión de los morteros del cemento BAY.

En un primer paso, se estudió el efecto de la relación w/c sobre la mineralogía cristalina del cemento BAY. En todos los casos, las fases hidratadas obtenidas, independientemente de la relación w/c usada, fueron la etringita (AFt), fases tipo AFm (las cuales contemplan al monosulfoaluminato y la stratlingita) y la katoita; y en una menor cantidad se identificó a través de TG-DTG, C-S-H e hidróxido de aluminio amorfo, los cuales forman parte del material ACn. En este sistema, a

pesar de tener un alto contenido de silicatos de calcio ( $C_3S$  y  $C_2S$ ), no se detectó portlandita (CH) por ninguna técnica, excepto a edades superiores a 28 días, donde procedía de la hidratación de la forma beta de la belita ( $\beta$ - $C_2S$ ). Su ausencia es asociada a que la portlandita reacciona con la ye'elemite a edades tempranas favoreciendo la producción de etringita, y a edades tardías, favorece la degradación de la etringita en monosulfoaluminato u otras fases tipo AFm. Este último efecto se vio reflejado en las pastas estudiadas, como una disminución en la cantidad de etringita y el subsecuente incremento de la cantidad de monosulfoaluminato, cuando se compara los resultados entre los 28 y 180 días de hidratación. El principal efecto de la relación w/c, sobre la mineralogía fue el aumento de la relación stratlingita/kaotita, al aumentar la relación w/c; el incremento de la relación w/c favoreció la precipitación de stratlingita en vez de la precipitación de katoita. El efecto observado de la relación w/c sobre la resistencia a la compresión, fue que al disminuir la relación w/c, la resistencia a la compresión incrementa, como era de esperarse.

El resultado más importante encontrado sobre el comportamiento de BAY, fue que **los morteros fabricados con el cemento BAY presentaron mejores resistencia a la compresión que los morteros de cemento BYF no activados** (cuya composición mineralógica era 48.7(6) %p de  $\beta$ - $C_2S$ , 28.1(1.0) %p de  $C_4A_3S$ , 14.9(2) %p de  $C_4AF$ , 1.3(2) %p de CT, 2.6(5) %p de  $\gamma$ - $C_2S$  y 4.4(2) %p de  $C_2AS$ ); desde el primer día de hidratación. Como el cemento BYF presentaba mayor cantidad de ye'elemite en su sistema, la mayor resistencia del BAY se atribuye a la coexistencia de la etringita y el gel C-S-H que provienen de la hidratación de la ye'elemite y la alita, respectivamente.

La cantidad óptima del superplastificante (SP) basado en policarboxilato, fue determinada a partir estudios reológicos, los cuales mostraron una significativa mejora en la homogeneidad y trabajabilidad (decrecimiento en la viscosidad) de las pastas preparadas. Después de la optimización, la mejor cantidad hallada para adicionar en las muestras fue de 0.5 %p de materia activa del aditivo

respecto al contenido en sólidos. Su efecto sobre el mecanismo de hidratación fue investigado a través del estudio *in-situ* en LXRPD con radiación Molibdeno y por medio de medidas calorimétricas. Estos resultados mostraron que el policarboxilato afecta la cinética de hidratación de la mayenita, lo cual inhibe la reacción simultánea y competitiva entre la ye'elemita y la mayenita. Del estudio calorimétrico, este efecto se vio reflejado como un decrecimiento en la intensidad del pico principal de hidratación, el cual se asocia con la precipitación del AFt y/u otras fases de aluminio hidratadas, presentando una reducción del 28% del calor total liberado a los 2 días de hidratación de la pasta de cemento BAY.

El uso de las cenizas volantes en las pastas y morteros no mostraron evidencias directas de efecto puzolánico (reacción entre la ceniza volante y los iones libres de  $\text{Ca}^{2+}$  y  $\text{OH}^-$  presente en la solución de poros). Sin embargo, se observó que la adición de FA (de 0 a un 30 %p), tuvo dos efectos principales en el ensamblaje de fases del cemento BAY: i) inhibió la hidratación de la belita; y por lo tanto, ii) favoreció la estabilidad del AFt. Del estudio calorimétrico, se observó una aceleración en el pico de hidratación principal, cuando se comparó con la señal observada en el cemento BAY sin mezclar con FA. Este efecto arrojó información relativa a la capacidad del FA en presentar puntos de nucleación para la formación de las fases hidratadas; a este comportamiento se le conoce comúnmente como "efecto filler temprano". Asimismo, al incrementarse el contenido de FA, se observó un aumento en las resistencias mecánicas. Este comportamiento de los morteros fue atribuido a un efecto filler temprano (puntos de nucleación), así como al relleno de poros por el aumento en contenido en sólidos; pero además podría ser justificado por un efecto de reacción puzolánica indirecta desconocida, la cual se dio lugar aún en el caso que la hidratación de la belita se vio inhibida.

Con el objetivo de comprender la verdadera influencia y comportamiento de la hidratación conjunta de la alita y la ye'elemita, se llevó a cabo un estudio más profundo a través de la hidratación *in-situ* por SXRPD y calorimetría isotérmica de un conjunto de muestras que contenían ambas fases (mezcla de fases

puras). Para hacer esto, se prepararon cuatro mezclas de alita con ye'elemite (tanto el polimorfo ortorrómbico como el pseudocúbico), con relaciones de alita/ye'elemite de 1.37 y 2.74. Estas muestras se hidrataron a relaciones de agua/sólido (w/s por sus siglas en inglés) de 0.59 y 1.19 para la relación de alita/ye'elemite de 2.74; y con relaciones de w/s de 0.66 y 1.32 para la relación de alita/ye'elemite de 1.37. Esas relaciones w/s corresponden al 110 y 220% de la cantidad de agua estequiométrica necesaria para su completa hidratación (es decir, la cantidad total de agua estequiométrica para dar lugar a la reacción de la ye'elemite y la alita), respectivamente, según la relación alita/ye'elemite usada. Los resultados mostraron que la hidratación de la alita está altamente afectada por la cinética de la hidratación de la ye'elemite, donde debido a la lenta hidratación de la ye'elemite pseudocúbica, la alita empezó a reaccionar/hidratarse después de un día. Sin embargo, la alita que estaba mezclada con la ye'elemite ortorrómbica, inició su reacción mucho más pronto, justo después de las 10 horas de hidratación. Los principales productos de hidratación obtenidos de estos sistemas fueron la etringita, monosulfoaluminado, stratlingita y C-S-H. Nuevamente, en este tipo de sistemas no se observó/presentó formación de portlandita. Después de 7 días de hidratación, los sistemas con alita y ye'elemite pseudocúbica presentaron menores grados de hidratación que los sistemas que conjuntamente estaba la alita con la ye'elemite ortorrómbica. Este comportamiento favoreció la estabilidad (y cantidad) de Aft en el sistema. Al aumentar la relación w/s en la mezcla con relación de alita/ye'elemite de 1.37, la cinética de hidratación de la ye'elemite se aceleró de tal forma, que acortó el tiempo de hidratación a la mitad, favoreciendo por lo tanto la rápida precipitación de la etringita (y de monosulfoaluminato en el caso de los sistemas con ye'elemite ortorrómbica). Asimismo, independientemente de la relación alita/ye'elemite, el incremento de la relación w/s, favoreció el grado de hidratación de la alita y la respectiva formación del C-S-H y la stratlingita.

Es importante resaltar que la katoita no se detectó/precipitó en los sistemas con fases puras de alita-ye'elemite, lo cual da indicios de su mecanismo de

formación/precipitación en el sistema BAY, donde se observó la presencia de katoita, incluso cuando se le adicionó ceniza volante. El efecto que presenta la katoita sobre el desarrollo de las propiedades mecánicas en el cemento BAY, aun es desconocido. Sin embargo, estos resultados obtenidos en las mezclas de fases puras, al igual que en las pastas de BAY, otorgan una información relevante sobre su mecanismo de formación, al asociarse con la hidratación de la belita en un ambiente rico en Al, al igual que de la hidratación conjunta de la alita y la ferrita.

Finalmente, se preparó una “mezcla de cemento comercial”, B83, cuya formulación consistía en un 83 %p de un clínker belítico suministrado por Buzzi Unicem con un 17 %p de clínker de sulfoaluminato de calcio suministrado por Belith, donde se adicionó 7 %p de anhidrita. Este cemento fue preparado de tal forma que su composición mineralógica fuese similar a la mineralogía del cemento BAY sintetizado (relación alita/ye'elemita de 1.3), el cual también fue estudiado con una relación w/c de 0.4. Este estudio mostró que los productos de hidratación principales fueron la etringita, la stratlingita, la katoita el monosulfoaluminato e hidróxido de aluminio amorfo; nuevamente sin la precipitación de portlandita (es decir, la misma mineralogía obtenida en la hidratación del cemento BAY). Particularmente, este “cemento comercial” B83 presentó un grado de hidratación de la alita de 77.5% a los 180 días, mientras que la belita alcanzó un grado de hidratación del 55%. Este bajo grado de hidratación de los silicatos de calcio favoreció en este sistema la estabilidad de la etringita, sin ninguna evidencia de la respectiva formación de AFm. Además, la formación de stratlingita y katoita se vio favorecida en este sistema rico en aluminio. Sin embargo, tal comportamiento fue totalmente opuesto al observado en el cemento BAY, donde debido a la rápida hidratación de la alita (la cual se consumió totalmente en los primeros 7 días de curado) y la tardía hidratación de la belita (a partir de los 28 días de curado, alcanzó un grado de hidratación del ~60% a los 180 días), la cantidad de la etringita se vio disminuida presentando un incremento en el contenido de las fases tipo AFm (monosulfoaluminato, hemicarbonato y stratlingita).

La resistencia a la compresión del “cemento comercial” B83 presentó, desde el primer día de hidratación, valores mayores que los correspondientes morteros de cemento BAY (sin la adición de cenizas volantes). Este desarrollo mecánico está relacionado con la baja porosidad de la pasta en la matriz cementicia del mortero, así como al ensamblaje de fases hidratadas dentro del mismo, es decir, la estabilidad y gran cantidad de etringita, y a un elevado contenido de stratlingita en el sistema.

# Introduction

## Background

Portland cement concrete, the most widely used manufactured material in the world, is made primarily from water, aggregates (rocks and sand), and Ordinary Portland cement (OPC). Since the first Portland cement was produced in 1843 by William Aspdin [1] there has been a continuous process of evolution in cement process technology and cement itself. However, since some years ago there has been also a significant increase in the research and development of new cementitious binders. The main impulse for this development is because the cement industry is one of the major contributors for greenhouse gases (GHG) emission [2,3]. In practice, the only greenhouse gas of concern here is  $\text{CO}_2$ , because the other greenhouse gases ( $\text{NO}_x$ ,  $\text{SO}_x$ , CO and particle material) are emitted in small amounts by the cement industry.

A typical Portland cement contains approximately: 50-70 wt% tricalcium silicate (alite;  $\text{C}_3\text{S}$ ), 15-30 wt% dicalcium silicate (belite;  $\text{C}_2\text{S}$ ), 5-10 wt% tricalcium aluminate (celite;  $\text{C}_3\text{A}$ ), 5-15 wt% calcium aluminoferrite (ferrite;  $\text{C}_4\text{AF}$ ), and up to 5 wt% gypsum ( $\text{CsH}_2$ ). Several other minor phases, such as alkaline sulfates, magnesium oxide (periclase; M) and/or calcium oxide (free lime;  $\text{C}_f$ ) are present only in small amounts or may be absent entirely [1,4,5]. Alite reacts with water rapidly and contributes to the early-age mechanical properties in Portland cement. The hydration reaction of belite is slower, so it contributes to the long-term mechanical properties development.  $\text{C}_3\text{S}$  and  $\text{C}_2\text{S}$  (~80 wt% of Portland cement), and their hydration forms calcium silicate hydrate (C-S-H) plus CH.

These C-S-H are the primarily responsible for the properties development in Portland cement, e.g. setting and compressive strength. Calcium silicate hydrate is usually referred as C-S-H because its composition is variable depending on the formation conditions. Gypsum is added to Portland cement clinker to regulate the hydration reactions of  $C_3A$  and  $C_4AF$ . The hydration reactions of  $C_3A$  and  $C_4AF$  with  $CsH_2$  form ettringite (AFt;  $C_6As_3H_{32}$ ), which contributes with mechanical properties at the early-ages [1,4,5].

Portland cement clinker is produced from high temperature heating (usually about 1400 - 1500 °C) of grinded natural raw materials such as limestone and clay, and then it is ground with gypsum to obtain cement [1,4]. OPC production typically emits about  $\sim 0.97$  t of  $CO_2$ /t of clinker [6,7]. This emission comes from two main sources: i) raw meal-derived  $CO_2$  is released from the calcination of limestone in the kiln (about 60 % of the total direct  $CO_2$  emissions); and ii) fuel-derived  $CO_2$  is released from combustion of the fuels used to heat the kiln (about 40 % of the total direct  $CO_2$  emissions) [3,6]. Thus, it is responsible for  $\sim 5$ –10% of the total man-made  $CO_2$  emissions [3,7,8]. In 2016, the worldwide Portland cement production reached 4200 Mt, meaning a grew up over of 82 % respect of 2005 production. Due to the global demand for concrete and future grow of the population, cement production for the future will be expected to reach up to 4.4 billion tons in 2050 (i.e. to increase 2.5 times between 2005 and 2050) [9–11]. As a consequence of this, the  $CO_2$  emissions will increase considerably.

## Alternatives to reduce $CO_2$ emission

Nowadays, the most effective way to reduce  $CO_2$  emissions from OPC manufacture is reducing the clinker factor, blending it with Supplementary Cementitious Materials (SCMs). These SCMs include natural rocks and minerals and industrial by-products, such as ground granulated blast furnace slag, fly ash, silica fume, calcined clays and limestone [12–14]. The main drawback of the use of SCMs in a high percentage, looking a mayor reduction of  $CO_2$ , is the low early compressive strength. Additionally, the durability of blended concretes is affected



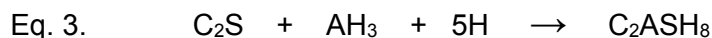
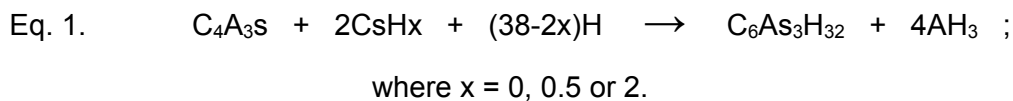
by SCMs. Thus, optimization of SCM characteristics can only partly improve these issues.

Facing with the need to reduce CO<sub>2</sub> emissions, the Portland cement industry and scientific community implicated in it, have been also considering the development of “alternative low-carbon binders” not based on Portland clinkers (and their corresponding new standards) [3,8,15–17]. The term “alternative low-carbon cement binder” is used to refer a man-made mineral material that, when ground to a fine powder, is capable of reacting rapidly enough with water and/or CO<sub>2</sub> in such a way, to produce a hardened mass which can be used as the binder in a concrete or mortar [3,12,16]. Belite-rich cements and ye’elimite-rich cements are within these alternatives [18,19,28–30,20–27].

Since alite is the most abundant phase in Portland cement, it requires high lime contents and high formation temperature [1,4]. The substitution of the main phase by belite in the cement, maintaining the same mineralogy (i.e. C<sub>2</sub>S-C<sub>3</sub>S-C<sub>3</sub>A-C<sub>4</sub>AF in the system) result in up to 12% reduction of CO<sub>2</sub> due to the lower limestone requirement and less fuel required for both limestone decarbonation and formation of C<sub>3</sub>S. They are commonly known as high belite cements (HBC) [16,18,20,22–24,30]. The clinkering temperature for HBC is usually close to 1350 °C, which is about 100 °C lower than the average for OPC, which lead to somewhat lower kiln heat consumption, so on less use of fuel. Physically, they preserve satisfying long-term properties due to the lower alkalinity of the pastes. However, substituting the main phase, C<sub>3</sub>S, by C<sub>2</sub>S compromises the early-age property development due to the slow reactivity of this phase. In addition, the consumption of electricity during the grinding process is higher due to its little porosity. This renders the HBC unusable in nearly any field of practice.

Ye’elimite (C<sub>4</sub>A<sub>3</sub>S)-rich cements, also known as calcium sulfoaluminate (CSA) cements, surged as another alternative to OPC. This was developed by the China Building Materials Academy in the 1970s, with the intention of manufacturing self-stressed concrete pipes to capitalize on the expansive properties of this material [31,32]. These cements were produced by adding

gypsum to CSA clinkers, which are mainly composed with around 40 - 70 wt% of ye'elimite [26,28,33–36], which has the lowest calcium oxide content than any cement phase (i.e. ~50, 44, 41, and 20% less unit mass of CaO than C<sub>3</sub>S, C<sub>2</sub>S, C<sub>3</sub>A and C<sub>4</sub>AF, respectively [3]), thus reducing the limestone requirement for obtaining it. In addition, CSA clinkers contain belite, ferrite and other minor components as secondary phases. These minor phases can be anhydrite or free lime, calcium aluminates (such as CA and/or C<sub>12</sub>A<sub>7</sub>), perovskite (CT) and/or gehlenite (C<sub>2</sub>AS) [28,37,38]. The latter two phases can be regarded as non-hydraulic. C<sub>3</sub>A is not usually present in CSA cements. In addition, the CSA clinkers present high porosity that permits the use of less energy to be grinded [32,39]. Nowadays, they are interground with different levels of calcium sulfate source (such as gypsum, hemihydrates and anhydrite) in order to obtain different properties depending on the amount and kind of calcium sulfate used. Within these properties are rapid-hardening, high-early strength, expansive, self-levelling or self-stressing [34,40–42]. These properties are mainly due to the rapid formation of ettringite from the reaction of ye'elimite with calcium sulfate source (Eq. 1), and variable quantities of amorphous gel phases (such as aluminum hydroxide and/or C-S-H). Another hydrated phases that can be present and influence on the CSA properties are monosulfoaluminate and stratlingite from the hydration of C<sub>4</sub>A<sub>3</sub>S (Eq. 2) and the hydration of C<sub>2</sub>S with AH<sub>3</sub> (Eq. 3), respectively.



The temperature needed to produce sulfoaluminate cements ranges from 1200 to 1300 °C, which is ~200 °C lower than that for Portland cement clinkers.

Limestone, bauxite and gypsum are the main raw materials involved in the manufacture. Depending on the composition, CSA cements emit about 25 to 35% less CO<sub>2</sub> during their manufacturing compared to OPC. Nevertheless, unlike Portland cement, CSA cements do not have a defined phase composition range; it is generally referred to cements that have the same basic components of C<sub>4</sub>A<sub>3</sub>S and C<sub>2</sub>S, but the composition and amount of the minor phases vary significantly. Furthermore, production of such cements requires bauxite as a principal raw material, and this makes them relatively expensive compared to Portland cements [8,15,16]. That restricts them to niche applications.

In an attempt to overcome the disadvantages present in HBC and CSA cements, but keeping the advantage of the low-CO<sub>2</sub> emissions, recent studies, mainly in Europe, have been focused on systems with intermediate compositions [2,16,21,39,43,44]. Therefore, recently an alternative range of compositions that contain less ye'elimite and higher belite contents has been developed, and represents a better compromise in terms of cost and CO<sub>2</sub> emissions. Current researches are focused on so-called belite – ye'elimite – ferrite (BYF) cements, where belite is the main phase and not ye'elimite [16,28,45–48]. They can be considered as intermediate cements between OPC and CSA cements, with the absence of alite. Due to the lower calcite demanding of their formulations, i.e. 20–30% less limestone than OPC, less carbon dioxide emissions are produced from decarbonation in the kilns. Additionally, the clinkering temperature of BYF, typically near to 1250 – 1350 °C, is lower than that for OPC, 1400 – 1450 °C. Thus, BYF clinkers are also easier to grind than OPC with the consequent energy saving and indirect emission depletion. Consequently, the manufacturing of BYF releases ~20% less CO<sub>2</sub> than OPC [2,12,16,28,49]. Taking into account all these advantages, different compositions found in the ternary system C<sub>4</sub>A<sub>3</sub>S-C<sub>2</sub>S-others phases are now contemplated by different patents, as it is listed in Figure Int.1 [50]

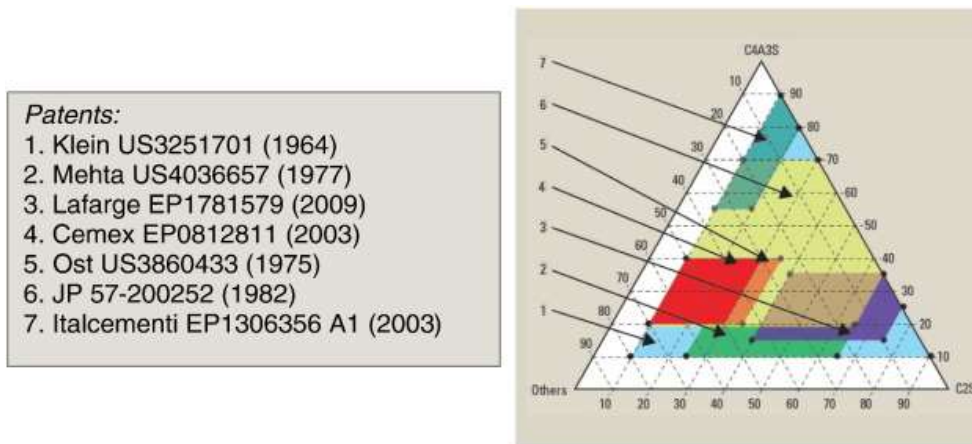


**Figure Int.1.** Patents in the system  $C_4A_3S$ - $C_2S$ -others. Taken from [50], Copyright (2015) with permission from Elsevier (Annex III).

However, the main problem of the belite-rich cements is the gap in reactivity between the extremely fast-reacting ye'elimite and the slow-reacting belite. This gap is reflected in the low mechanical strengths developed at intermediate hydration ages (from 1 to 28 days). To solve this problem, several ideas have been developed and partially implemented in the recent years, as it will be described below.

## Ways to overcome the disadvantages of BYF

A possible solution to increase the reactivity during hydration consists on the stabilization of high temperature-more reactive polymorphs of belite, such as  $\alpha$ - $C_2S$  and  $\alpha'$ - $C_2S$  forms. It is known that belite presents five crystalline polymorphs ( $\beta$ ,  $\alpha$ ,  $\alpha'_L$ ,  $\alpha'_H$  and  $\gamma$ ) [1,4]. Recent researchs have found two other belite polymorphs. These two forms of belite, known as XRD-amorphous- $C_2S$  and  $x$ - $C_2S$ , are considered higher reacted than alite [50,51]. However, it is necessary a deeper investigation about their obtaining and stabilization into cements. The  $\beta$ -form is present in OPC, HBC, CSA and non-active BYF clinkers. Despite of being unstable at low temperatures, high temperature modifications can be stabilized by rapid cooling, appropriate particle size and the incorporation of foreign ions. It

has been demonstrated that Ba is beneficial for the  $\alpha$  stabilization; Mg, P, K, B, Sr and S, promote the formation of  $\alpha'$ -C<sub>2</sub>S forms and increase its hydraulic properties, where specifically P and Sr favors  $\alpha'_H$  and  $\alpha'_L$  respectively. Whereas the  $\beta$ -polymorph can be stabilized by a broad range of elements, such as B, Na, K, Ba, Mn, Cr, Al, S or their combinations [23,52–55]. For this reason, there is an increasing interest on the role of dopants in the stabilization of belite polymorphs and their hydration behavior [25,36,48,56,57]; taking especial importance for stabilization purposes the use of B<sub>2</sub>O<sub>5</sub>, Na<sub>2</sub>O and P<sub>2</sub>O<sub>5</sub> [21,44,48,49,52,56–60]. In addition, belite-activated BYF cements can gain strength at similar rates as OPC over a wide range of temperatures, and give acceptable durability in many standard tests due to their low alkalinity, as shown in the report of EU's "Aether" Life+ project (see Figure Int.2) [16,38,61,62]. Technically, this cement concept was implemented as part of a large-scale experiment in which 5500 tons of active BYF (AETHER™) with the composition of 55, 25 and 15 wt% of  $\alpha'_H$ -C<sub>2</sub>S, C<sub>4</sub>A<sub>3</sub>S and C<sub>4</sub>AF, respectively, were prepared [61,62]. However, the cost of raw materials is greater than that for OPC, although according to Gartner [2,12,16] this may not be an economic factor once the projected CO<sub>2</sub> emissions costs (taxes) have been factored in. The development and testing of active BYF cements will show promise and could in time lead to the establishment of new codes and standards [38].

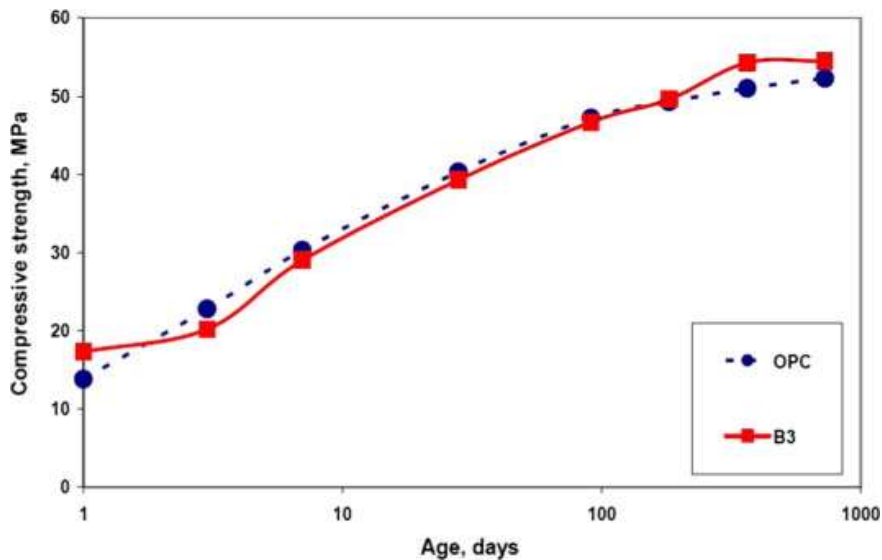


**Figure Int.2.** Compressive strength of BYF compared to OPC at  $w/c = 0.55$ ,  $300 \text{ kg/m}^3$  for pilot batch of BYF (B3) compared to OPC (CEM1 42.5) at  $20 \text{ }^\circ\text{C}$ . Taken from [38]. Copyright (2012) with permission from Elsevier (Annex III).

A different alternative is the so-called belite-ye'elimite-(ferrite)-ternesite (BY(F)T) cement, in which besides belite and ye'elimite, the ternesite ( $\text{C}_5\text{S}_2\text{S}$ ) is a main phase [63,64]. Although ternesite (also known as sulfospurrite or calcium sulfosilicate) has traditionally been regarded as non-hydraulically active phase [1,4,28,65]. Previous research on systems containing  $\text{CaO}$ ,  $\text{SiO}_2$ ,  $\text{Al}_2\text{O}_3$  and  $\text{CaSO}_4$  indicated that at  $\sim 1200 \text{ }^\circ\text{C}$ , ternesite was formed as an intermediate phase instead of belite and anhydrite, in addition to ye'elimite. The results showed that at  $1150 - 1250 \text{ }^\circ\text{C}$ , belite reacted with anhydrite to form ternesite, which decomposed to the above two components at temperatures higher than  $1250 \text{ }^\circ\text{C}$  [64,66]. Recent studies have shown that it is activated in presence of amorphous  $\text{AH}_3$ . It hydrates yielding ettringite and C-S-H, the main hydration products in CSA and OPC cements respectively, and the phases to which they owe their mechanical properties (i.e. compressive strength and durability). Stratlingite may also form with or instead of C-S-H [63,66,67]. Even, according to the literature, sulfospurrite is a reactive phase as part of BYF systems and it is more reactive than belite [63,64]. Bullerjahn *et al* [63] proposed a two-stage

method for ternesite formation in BYF systems, in which clinker is synthesized at 1250 °C/1h and then cooled within the furnace to 1100 °C (during 30 min), and finally clinkered at 1100 °C/1h followed by rapid cooling in air. Hanein *et al.* [68], proposed a single-stage process at temperatures over 1200 °C, on the partial pressure of SO<sub>2</sub> and O<sub>2</sub>. Thus, the system BYF-ternesite is able to close the gap between the reactivity of ye'elimite and belite. However, further work on the long-term performance of BY(F)T cements should be performed, such as that related to strength development, dimensional stability and durability, and the effects of variability of the calcium sulfate source.

Another way to close the gap between the reactivity of ye'elimite and belite is the introduction of alite in the BYF system. The production of such cements is, however, associated with significant challenges since there are inherent difficulties with the incompatibility of the formation/decomposition temperatures of alite and ye'elimite respectively. Alite formation is favored by the presence of melted phases (without any additive) at a temperature of, at least, 1350 °C [1,4,69], while ye'elimite decomposition/dissolution takes place above 1350 °C and it is enhanced by melting phases [58,70,71]. Fortunately, recent research focused on obtaining alite – calcium sulfoaluminate cements (known as ACSA), with C<sub>3</sub>S (30 – 50 wt%) as the main phase, followed by C<sub>2</sub>S (30 – 40 wt%) and C<sub>4</sub>A<sub>3</sub>S (5 – 20 wt%) phases [72,73,82–87,74–81]. There are two approaches to obtain both coexisting phases : i) the addition of a small amount of fluorite (and/or CuO [87], MgO [76,77], TiO<sub>2</sub> [81], ZnO [75]) to the raw mixture to promote the coexistence of both phases at temperature ranging 1230 and 1300 °C [72,73,88–91]. The rate of alite formation at lower temperatures is increased by lowering its free energy relative to belite [88–92]; ii) the addition of BaO or SrO to the raw material transforms ye'elimite into barium (or strontium) calcium sulfoaluminate and promotes the coexistence of alite and ye'elimite at temperatures between 1350 and 1380 °C [5,89,93,94]. Despite of those results, **there only are few works where belite-alite-ye'elimite-(ferrite) - BAY(F) clinker was synthesized** [75,79,86]. Thus, further investigation on their synthesis, clinker mineralogy, hydration mechanism and mechanical properties is needed.

The effect of the different mineralizers on the clinkering, hydration mechanism and mechanical properties of  $C_3S$ - $C_4A_3S$  based (ACSA cement) system will be explained below.

## ***Synthesis of alite-ye'elimite systems***

Extensive research on the formation and coexistence of alite and ye'elimite phases with doping minor elements has been carried out, which could reduce both the viscosity and the formation temperature of the liquid phase, promoting the formation of  $C_3S$ . Odler *et al* [95,96] investigated the  $SO_3$ -rich Portland clinkers containing simultaneously alite and ye'elimite, burning (at  $\sim 1250 - 1300$  °C during 30 min) a pertinent mixture of chemical reagents (i.e.  $CaCO_3$ ,  $SiO_2$ -quartz,  $Al_2O_3$ ,  $Fe_2O_3$ , and  $CaSO_4$ , that contained no more than 0.1 wt% of foreign ions) with 0.5 wt% of  $CaF_2$ . Portland clinkers with an exceptionally good grindability, due to their high porosity, could be obtained. Liu *et al* [76,77] produced the clinker at temperatures between 1250 °C and 1300 °C by adding 0.25 wt% of  $CaF_2$  and different amounts of MgO as mineralizers to natural raw materials (limestone, clay, gypsum and fly ash). They concluded that the addition of MgO at about 2–5 wt% can improved the burnability of raw meal, promoting the absorption of free lime and the formation of  $C_3S$  and  $C_4A_3S$ . Ma *et al* [87] reported that the coexistence of  $C_4A_3S$  and  $C_3S$  could be achieved in the clinker, using limestone, gypsum, clay and fly-ash, as a raw meal, by adding  $CaF_2$ , and up to 1 wt% of CuO at 1300 °C. Liu *et al* [81] showed that a smaller amount of  $TiO_2$  (up to 1 wt%) and 0.25 wt%  $CaF_2$ , could improve the burnability of the raw mixture (chemical reagents and natural raw materials), accelerating the absorption of free lime, and promoting the formation of more minerals of  $C_3S$  and  $C_4A_3S$ , at 1300 °C for 30 min. Perez-Bravo *et al* [75] studied the effect of the addition of zinc oxide and calcium fluoride on the formation of  $C_3S$  and  $C_4A_3S$  in ACSA materials; finding that 1300 °C/15 min was a suitable clinkering temperature, and the optimum amount to be added of ZnO and  $CaF_2$  were of 1.0 wt% of each one.



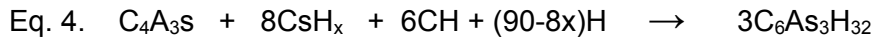
Recently, a new strategy to produce cements with alite and ye'elimite has been published by Ma *et al* [85], which consists on a two-step clinkering cycle, one to form alite at 1450 °C in a sulfate-rich raw meal, and a second one to recrystallise ye'elimite at 1250 °C. Moreover, in current studies, the addition of only 1 wt% of CaF<sub>2</sub> as mineralizer was the main way to achieve the coexistence of ye'elimite and alite in the production of ACSA clinker at 1300 °C [72,73,79]. There is not doubt about the contribution of calcium fluoride to the formation of C<sub>3</sub>S at lower temperatures instead of formation of C<sub>2</sub>S [88–92]. Another way newly found to favor the formation and coexistence of alite and ye'elimite was by the co-synthesis of 20 wt% of ferrite (C<sub>4</sub>AF) at 1350 °C for 60 min, maintaining the molar proportion between Fe<sub>2</sub>O<sub>3</sub> and Al<sub>2</sub>O<sub>3</sub> in 1/3 [86].

### ***Hydration of alite-ye'elimite systems***

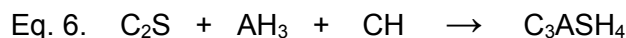
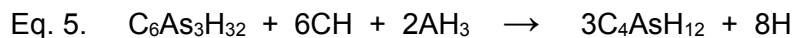
Former studies have mainly focused on ACSA clinker production and physical properties, but only a few studies have reported detailed hydration data, such as calcium–silicate–hydrates (C–S–H) and AFt composition. Li *et al* [97] showed that the main hydration products from an alite–ye'elimite cement synthesized by the two-stage firing process [85] with 67.0 and 4.8 wt% of alite and ye'elimite respectively, were ettringite, portlandite and C-S-H. The AFt formed in presence of portlandite is expansive, and the presence of CH accelerated the hydration of C<sub>4</sub>A<sub>3</sub>S to form it. Additionally, Duvallet *et al* [79] presented the hydration of three different ACSA cements with an intermediate composition of 27.2 wt% C<sub>3</sub>S, 25.4 wt % C<sub>2</sub>S, 17.9 wt% C<sub>4</sub>A<sub>3</sub>S and 23.4 wt% C<sub>4</sub>AF with 15.0 wt% CsH<sub>2</sub>; alite and ye'elimite were totally consumed after 28 curing days, while ferrite persisted through 6 months. Respect to crystalline hydration product development, ettringite was the only phase formed after 5 hours of hydration. Then, portlandite was formed at 24 h, followed by monosulfoaluminate and hemicarbonate at 7 hydration days. These two latter phases came from the conversion of ettringite to monosulfoaluminate at later ages. Some samples also showed katoite (silicious hydrogarnet; C<sub>3</sub>ASH<sub>4</sub>) as a hydrated product after 28 days of hydration. Hu *et al* [74] presented that the hydrated crystalline phases of ACSA cement with 57.2

and 1.1 wt% of alite and ye'elimite, respectively, were AFt at 12 h, CH at 5 h and AFm at 3 d. Over time, ettringite phase peaks increased in these samples (at 3, 5, 12 h and 1 d). After 1 day, the ettringite was degraded to form AFm phases (monosulfoaluminate), becoming larger at 28 days. Finally, Chitvoranund *et al* [72] reported the hydration mechanism of a ACSA cement, that contain around 50 and 10 wt% of alite and ye'elimite, respectively. During the first hours, mainly reacts the alite, while ye'elimite starts to dissolve after 2 days; giving as main hydration products calcium–silicate–hydrates (C–S–H), ettringite, monosulfoaluminate and portlandite.

Summarizing, during the first hydration hours, ettringite is the main crystalline hydration product together with amorphous aluminum hydroxide (no detected by LXRPD) [98,99]. Ettringite is formed in these systems from the dissolution of  $C_4A_3S$  and  $C_sH_x$  ( $x = 0, 0.5$  or  $2$ ) (see Eq. 1). Once the sulfate source is depleted and there is enough water available, monosulfoaluminate (AFm) is formed (see Eq. 2) [42,100,101]. In addition, ye'elimite and calcium sulfate in presences of portlandite (CH) enhances the formation of AFt (Eq. 4) [102–104].



Furthermore, and independently of the kinetic of the reaction,  $C_3S$  produces amorphous C-S-H gel and portlandite (CH). This portlandite, at later age, favors the demotion of AFt into AFm phases (Eq. 5) [102,103,105]. Furthermore, at later ages, katoite formation could come from  $C_2S/C_3S$  in presences of amorphous  $AH_3$  and/or CH (Eq. 6 and Eq. 7) [106–109].





## ***Properties of alite-ye'elimite systems***

Strength, hardening properties (stability in dimensions), and durability are required as the ultimate performance for cement-based materials and concrete. However, whether these are realized or not depends on the rheological properties of the fresh materials [110]. Rheology is the science that studies the flow and deformation of the matter under the influence of a mechanical force. This technique is wide used on fresh cement to know its workability/flowability [110–115]. The workability/flowability can be improvement by the use of additives (such as plastisizers or superplastisizers) to obtain more homogeneous mixtures and hence, improved mechanical properties [26,114,116,117]. However, there are not any reports about the fresh behavior of ACSA systems.

As mentioned in the section above, there are several studies where the effect of mineralizers and/or mineralogy on the mechanical strength was analyzed. Liu *et al* [76] presented that the content of MgO in the clinker, in a range from 2.0 to 5.0 wt%, improved the strengths development of the cement, reaching up to ~74.1, ~89.3 and ~119.3 MPa at 3, 7 and 28 d, respectively; and the final setting time is shortened. If the MgO content reaches about 8.0 wt%, the strength of the cement decreases to 106.3 MPa at 28 d and the setting time is extended. Liu *et al* [81] reported that a proper amount of TiO<sub>2</sub> can increase the strength of cement, especially for clinkers with higher amounts of C<sub>3</sub>S (~56 wt%), to which 1.0 wt% TiO<sub>2</sub> can increase the strength of cements at different hydration ages prominently (i.e. ~80, ~100 and ~125 MPa at 3, 7 and 28 d respectively). When the amount of TiO<sub>2</sub> is over 1.0 wt% the setting time of cement would be obviously delayed up to final setting time of ~185 min. Li *et al* [97] reported that the alite-ye'elimite cement clinker synthesized by reformation (refers to the clinker annealed at 1250 °C for 1 h to form ye'elimite from C<sub>3</sub>A and Cs reaction) with 67.0 and 4.8 wt% of C<sub>3</sub>S and C<sub>4</sub>A<sub>3</sub>s respectively, yielded values of 30.0, 42.3 and 55.8 MPa at 1, 3

and 28 days, respectively. The early strength of the cement at 1 and 3 days was 48.5% and 27.4% higher, respectively, than PII 52.5 Portland Chinese cement (under the Chinese standard). Hu *et al* [74] showed that the mechanical behavior of alite-belite-ye'elimite cement with 57.2, 25.0 and 1.1 wt% of  $C_3S$ ,  $C_2S$  and  $C_4A_3S$  respectively; was higher than that of OPC at 1 and 3 days, but lower at 28 days. The early compressive strengths were increased by approximately 27% and 17%, respectively. Finally, Chitvoranund *et al* [72] presented a ACSA cement mortar (that contained around 50 and 10 wt% of alite and ye'elimite respectively), that gained strength rapidly through 7 curing days and continued to gain strength at a slower rate through 28 days. Likewise, from 1 to 7 d, the compressive strength of the corresponding ACSA mortars increased by three times (i.e. 10.1, 30.8 and 35.2 MPa at 1, 7 and 28 d respectively).

Despite these results, these ACSA cements present more  $CO_2$  emission than BYF cements, due to it has high content of  $C_3S$  (main phase) and few content of  $C_4A_3S$ , needing more amounts of limestone to be synthesized.

## Overview of the thesis

The main aim of this work consists on obtaining a cementitious system that presents lower carbon dioxide emissions, good mechanical performance and optimal durability. This PhD thesis presents the preparation and hydration of an active BYF cement with the maximum content of alite and ye'elimite, hereinafter known as belite-alite-ye'elimite cement (BAY). The corresponding mortars showed high early compression strength values due to the coexistence of alite and ye'elimite. Moreover, the addition of fly ash (FA), as possible SCMs, was evaluated; it will also contribute to the  $CO_2$  footprint reduction of this eco-cement, generating economic savings due to the reuse of industrial by-product and less clinker requirements. Additionally, to understand the hydration mechanisms of alite with ye'elimite, a study of a mixture of pure alite and pure ye'elimite was carried out. Finally, for the sake of comparison, a blended material from

commercial belite cement and calcium sulfoaluminate cement, called hereafter "commercial binder" B83, was prepared and evaluated, which has similar mineralogical composition to BAY cement manufactured.

This thesis includes 8 chapters, including this introduction. Chapter 1 describes the materials and methodology followed to carried out this investigation. Chapter 2 presents the synthesis of BAY clinkers from natural raw materials, in a small (~ 7 g) and medium (~ 2 kg) scales. Chapter 3 presents the hydration: water-to-cement ratio effects on the hydrated phase mineralogy, hydration mechanism, rheological behavior and mechanical development. Chapter 4 shows a deeper study on the hydration of mixtures of pure alite and pure ye'elite to understand the hydration mechanism in BAY cement. Chapter 5 reports the effects of fly ash addition on BAY cement hydration, rheological behavior and mechanical properties. Chapter 6 presents the results of hydration and mechanical properties of "commercial binder" B83. Finally, Chapter 7 provides the conclusions and future recommendations from this research.



UNIVERSIDAD  
DE MÁLAGA

## Objetives

The main aim of this PhD thesis was to understand the hydration mechanism and mechanical behavior of Belite-Alite-Ye'elimate systems to be correlated with BAY cements and compared with non-active BYF. The specific objectives of this study are described below:

- ✓ To optimize the synthesis of BAY clinkers at laboratory level, and to dosage the raw materials to achieve high jointly contents of  $C_3S$  and  $C_4A_3S$  through the use of  $CaF_2$  as mineralizer.
- ✓ To optimize the scaling process (temperature and residence time) to obtain ~2 kg of that clinker.
- ✓ To understand the effect of water/cement ratio (w/c), superplasticizer content and addition of class F - fly ash, on the rheological behavior and hydration mechanism of pastes and compressive strength of mortars.
- ✓ To synthesize and characterize pure phases related to BAY: alite and ye'elimate to study the jointly hydration mechanism of these phases with anhydrite and different water/cement ratios.
- ✓ To study the behavior of a mixture of a commercial belite clinker with calcium sulfoaluminate clinker, named hereafter as "commercial binder" clinker, whose mineralogical composition by the mixture is similar to the BAY clinker obtained in the scaling process.



UNIVERSIDAD  
DE MÁLAGA



# 1. Materials and Methods

In this study three types of cementitious materials were used: i) BAY clinker/cement/pastes/mortars (without and with fly ash), ii) mixture of pure phases (alite, ye'elimite and anhydrite), and iii) a commercial belite clinker mixed with calcium sulfoaluminate clinker, named as “commercial binder” B83.

The description of the synthesis (including raw materials, reagents and procedure) of BAY clinkers, and pure phases (pseudocubic and orthorhombic ye'elimite, and alite), including the preparation of the corresponding mixture is shown below. In addition, information about both commercial belite and calcium sulfoaluminate clinkers used for the preparation of the “commercial binder” study is also given below. Finally, the methodology used to characterize anhydrous and hydrated samples is also detailed.

## 1.1. Materials

### 1.1.1. Belite-Alite-Ye'elimite (BAY) clinkers and cements

The different BAY clinkers prepared at the first stage, likewise the scaled-up BAY clinker, were prepared from the combination of white kaolin (NC-35 *Caolines Vimianzo - Spain*), mineral limestone, sand, iron oxide corrector and gypsum (all from *Financiera y Minera cement factory - Spain*). The oxide composition, from XRF, of all these raw materials is shown in Table 1.1. Calcium fluoride reagent-grade (>99%, Sigma-Aldrich) was added to each raw material mixture as mineralizer, as reported in [118].

**Table 1.1.** Elemental composition of raw materials determined by XRF (in oxide wt%)

Raw material	Limestone	Sand	Kaolin	Iron Source	Gypsum	Anhydrite	Class F Fly Ash <sup>+</sup>
Oxide							
CaO	54.0	3.1	-	0.3	33.4	40.1	4.5
Al <sub>2</sub> O <sub>3</sub>	0.2	1.8	35.2	0.8	1.2	-	26.4
SO <sub>3</sub>	-	-	-	3.3	34.6	56.1	
Fe <sub>2</sub> O <sub>3</sub>	0.1	2.4	1.1	74.8	0.9	0.1	7.4
SiO <sub>2</sub>	0.8	85.0	47.5	3.3	4.8	1.0	52.7
K <sub>2</sub> O	-	0.5	1.9	-	2.2	-	3.6
Na <sub>2</sub> O	-	-	0.1	-	0.1	0.4	
MgO	0.5	1.9	0.2	-	1.5	0.5	1.9
P <sub>2</sub> O <sub>5</sub>	-	-	-	-	0.1	-	0.3
Lol*	44.4	5.2	13.8	17.6	23.6	1.3	1.6

Lol\*: Loss of Ignition at 1050 °C. \*Data from literature [119]

The BAY cement was made by adding 12 wt% of anhydrite, as calcium sulfate resource (its stoichiometric amount of calcium sulfate respect to ye'elimite and calcium aluminate contents) to fulfill reaction of ettringite formation. Anhydrite (Cs) was previously prepared by heating at 700 °C for 60 min (heating rate of 10 °C/min) a commercial micronized gypsum (CsH<sub>2</sub>) from *BELITH S.P.R.L. (Belgium)*, with the aim to obtain a calcium sulfate source with a slow dissolution. For the fly ash (FA) study, the BAY cement was blended with 15 and 30 wt% of class F fly ash (provided by power station *Lada – Spain*). Its chemical composition is also shown in Table 1.1. All these samples were labeled as FA#BAY, where # represents the weight percent of FA referred to the total solid content.

### 1.1.2. Alite-Ye'elimite-Anhydrite mixture

Four alite-ye'elimite-anhydrite (C<sub>3</sub>S/C<sub>4</sub>A<sub>3</sub>S/Cs) mixtures were prepared. Two samples were mixed with orthorhombic ye'elimite and the other two samples were mixed with pseudocubic ye'elimite. The phase mixture ratios of

$C_3S/C_4A_3S/Cs$  were 48.6/35.5/15.9 and 65.4/23.9/10.7, where alite/ye'elimite ratios were 1.37 and 2.74, respectively. These samples were labeled as  $n137$  and  $n274$ , where “ $n$ ” represents polymorph of ye'elimite used (“ $o$ ” orthorhombic and “ $c$ ” pseudocubic). Ye'elimite polymorphs (orthorhombic and pseudocubic) were synthesized following Cuesta *et al* procedure [120,121] using  $CaCO_3$  (99.95%, Alfa Aesar),  $Al_2O_3$  (99.997%, Alfa Aesar), and  $CaSO_4 \cdot 2H_2O$  (98%, Sigma-Aldrich) reagent-grade. In addition, to stabilize the pseudocubic ye'elimite polymorph,  $Fe_2O_3$  (99.945%, Alfa Aesar),  $SiO_2$  (99.5%, Alfa Aesar) and  $Na_2CO_3$  (99.999%, Sigma-Aldrich) reagent-grade were also used. Monoclinic III alite was supplied by *Sarl Mineral Research Processing (France)*. Anhydrite used was the same prepared from micronized gypsum previously mentioned. The values of  $D_{v50}$ , described below, in the *Particle Size Distribution Section*, of pseudocubic ye'elimite, orthorhombic ye'elimite, anhydrite and monoclinic alite were 5.9, 9.0, 8.9 and 13.8  $\mu m$ , respectively. The  $D_{v90}$  values (defined below, in the *Particle Size Distribution Section*) were 21.3, 28.7, 26.9 and 35.8  $\mu m$ , respectively, for the pseudocubic ye'elimite, orthorhombic ye'elimite, anhydrite and monoclinic alite, see Figure 4.14 in *Pure phases hydration study Section*.

### 1.1.3. “Commercial binder”, B83

A “commercial binder” named as B83 was made mixing 78 wt% of a belite clinker supplied by Buzzi Unicement (Italy) with 16 wt% of calcium sulfoaluminate clinker – CSA (from BELITH S.P.R.L. - Belgium) and 6 wt% of anhydrite used before. The aim was to compare with the mineralogical and mechanical behavior of BAY cement (also labeled as FA0BAY). The “commercial binder” B83 was blended in a micro-Deval machine (A0655, Proeti S.A., Spain) at 100 rpm with 5 steel balls of 30 mm to improve the powder homogeneity. The average particle size of B83,  $d_{v50}$ , was  $\sim 20 \mu m$ . Table 1.2 shows chemical and mineralogical composition of both commercial clinkers.

**Table 1.2.** Chemical and mineralogical composition for the two clinkers (belite and CSA) determinate by XRF and Rietveld quantitative phase analysis (RQPA) quantification respectively.

<i>FRX</i> <b>Oxide,</b> <b>wt%</b>	<b>CSA</b> <b>clinker*</b>	<b>Belite</b> <b>clinker</b>	<i>RQPA,</i> <b>wt%</b>	<b>CSA</b> <b>clinker</b>	<b>Belite</b> <b>clinker</b>
CaO	42.0	59.6	$\beta\text{C}_2\text{S}$	18.7(2)	50.5(3)
SiO <sub>2</sub>	8.2	22.9	$\alpha\text{C}_2\text{S}$	4.3(1)	-
Al <sub>2</sub> O <sub>3</sub>	33.8	5.2	$\text{oC}_4\text{A}_3\text{S}$	60.8(3)	-
Fe <sub>2</sub> O <sub>3</sub>	2.4	2.1	CT	3.7(1)	-
SO <sub>3</sub>	8.8	5.4	M	0.9(1)	2.3(1)
K <sub>2</sub> O	0.2	1.1	C <sub>3</sub> S	-	15.0(2)
Na <sub>2</sub> O	<0.1	0.3	C <sub>4</sub> AF	-	7.5(2)
MgO	2.7	2.9	CsH <sub>0.5</sub>	-	0.6(1)
P <sub>2</sub> O <sub>5</sub>	0.1	-	C <sub>3</sub> A	-	0.9(1)
TiO <sub>2</sub>	1.5	-	CH	-	0.2(1)
SrO	0.1	-	ACn	11.6(1)	21.8(1)
ZrO <sub>2</sub>	0.1	-	R <sub>wp</sub>	8.19	7.68
F	-	0.1			

\* Data from literature [119]

#### 1.1.4. Polycarboxylate-based material as superplasticizer (SP)

A commercial polycarboxylate-based superplasticizer (SP), Floadis 1623 (supplied by Adex Polymer S.L., Madrid, Spain), with a 25 wt% of active matter, was used to improve the homogeneity and workability of pastes and mortars (FA#BAY and B83). The amount of SP in every system was optimized through the rheological behavior of the corresponding pastes.

## 1.2. Samples preparation

### 1.2.1. Clinker preparation

For the preparation of clinkers at “small” scale, all raw materials mixed with fluorite were homogenized in an agate mortar throughout 30 min. Then, the mixtures were dye-pressed (~3 g and 20 mm of diameter). Three pellets (~9 g) were placed into Pt/Rh crucibles of 50 ml of volume and heated in a bottom loading furnace HOB 33-3/16 (Hobersal, Spain) at 900 °C at a heating rate of 5 °C/min and held at that temperature for 30 min. Next, the temperature was raised at the same rate to the final temperature (1300°C) and held for 15 min. Finally, the clinkers were quenched to room temperature (RT) using forced air convection, ground and sieved through a 75 µm mesh.

For the preparation of the scaled-up clinker (“medium” scale), the raw meal was pre-homogenized for 90 min in a micro-Deval machine (A0655, Proeti S.A., Spain) at 100 rpm with steel balls (9 balls of 30 mm, 10 balls of 18 mm and 20 of balls of 10 mm). The mixture was dye-pressed (pellets of ~30 g and 55 mm of diameter), and the clinkering conditions were optimized. Three pellets (~90 g) were heated at 1280 or 1300 °C (at same heating rate used before for “small” scale) and held for 15 min or 30 min. All samples were quenched to RT using forced air convection. Once the clinkering conditions were optimized, seven pellets (~30 g and 55 mm of diameter each one) were placed into a large Pt/Rh crucible of 325 ml of volume, and heated at 1300 °C for 15 min. This process was repeated ten times to obtain a total of ~2 kg of clinker. The pellets of clinker were ground using a vibration disc mill until a size of  $d_{v50}$  close to 10 µm was achieved.

### 1.2.2. Paste preparation

The hydration of the pastes was deeply studied. All samples were mixed using distilled water. BAY cement (also known as FA0BAY cement) pastes were prepared at w/c ratios of 0.4 and 0.5. FA15BAY and FA30BAY cements were

mixed at a w/c ratio of 0.4. FA0BAY and FA30BAY pastes were also prepared at a w/c ratio of 0.57 (which corresponds a water-to-binder ratio of 0.4 in FA30BAY), and characterized only at selected ages.

All these pastes were prepared by mechanical stirring at 800 rpm in a plastic beaker following EN196-3 time procedure, and introduced into a hermetically closed polytetrafluoroethylene (PTFE) cylinder mold during 24 hours at 20 °C [40]. After that time, they were demolded and stored within water at 20 °C until the age of study. Then, the samples were characterized after 1, 7, 28, 90 and 180 days of hydration.

In addition, samples *n137* were mixed at a water/solid ratio of 0.66 and 1.32, and *n274* were prepared at a water/solid ratio of 0.59 and 1.19. The w/s ratio of 0.66 and 0.59 correspond to the stoichiometric amount of water with 10% of excess for *n137* and *n274* respectively, according to Eq. 1 (*Introduction section*). The w/s value of 1.32 and 1.19 are the double of the previous values to study the effect of large water excess on hydration mechanisms. These pastes were prepared by hand stirring using a spatula in a plastic beaker following EN196-3 time procedure. The used curing mold depended on the X-ray diffraction technique followed. For the *in-situ* synchrotron X-ray powder diffraction (SXRPD) study, all anhydrous mixtures were mixed with 20 wt% SiO<sub>2</sub> (99.5%, Alfa Aesar) as an internal standard [122]. The corresponding pastes were loaded into glass capillaries of 0.7 mm of diameter with a syringe. The capillaries were sealed with grease. For the *ex-situ* laboratory X-ray powder diffraction (LXRPD) study, *n137* pastes at a w/s ratio of 1.32 were poured and kept into hermetically closed PTFE cylinder molds [40] for 1 day. Then they were demolded and stored at 20 °C within distilled water until 7 days of hydration.

Finally, B83 pastes were prepared at a w/c ratio of 0.4. The same preparation methodology than FA#BAY samples was followed.

### 1.2.3. Stopping hydration of pastes

The pastes, at the selected curing ages, were crushed in an agate mortar prior to stopping hydration. The stopping hydration method consists on a solvent exchange in a Whatman system (70 mm diameter Whatman filter with a pore size of 2.5  $\mu\text{m}$  and a Teflon support) using first acetone (in samples of FA#BAY and B83 cement) or isopropanol (in *n*137 samples) twice and finally diethyl ether once. The stopped powder samples were stored in a plastic eppendorf tube inside of a closed desiccator (without vacuum application) with silica gel to avoid further hydration and/or carbonation [56,119]. FA#BAY and B83 cement pastes were stopped at 1, 7, 28, 90, and 180 hydration days. The *n*137 samples were stopped at 7 hydration days and were compared with *in-situ* SXRPD study.

### 1.2.4. Mortar preparation

FA#BAY and B83 cement mortars were prepared according to EN196-1 standard procedure, at a cement/sand ratio of 1/3 and w/c ratio of 0.40, with the optimum amount of superplasticizer (previously optimized through rheological studies). CEN EN196-1 standard sand was used. Cubes ( $3 \times 3 \times 3 \text{ cm}^3$ ) were cast and cured at  $20 \pm 1 \text{ }^\circ\text{C}$  and 99% relative humidity (RH) for 24 h; then the cubes were demolded and submerged in a water bath at  $20 \pm 1 \text{ }^\circ\text{C}$  until testing (compressive strength) at the same curing age than pastes were stopped and characterized (1, 7, 28, 90, and 180 days).

## 1.3. Analytical Methods

### 1.3.1. Laboratory X-ray Powder Diffraction (LXRPD)

Laboratory X-ray powder diffraction (LXRPD) measurements were carried out on both anhydrous and stopped-hydration samples. Powder patterns for anhydrous clinkers were collected using monochromatic  $\text{CuK}\alpha_1$  radiation ( $\lambda = 1.5406 \text{ \AA}$ ) on

an X'Pert Pro MPD (PANalytical B.V., Netherlands) diffractometer with X'Celerator detector. Data were acquired with an angular scan of 5-70° (2 $\theta$ ), with step size of 0.016° and step time of 300 s yielding a 160 min pattern. The samples were rotated during data collection at 16 rpm in order to enhance particle statistics.

Powder patterns for the anhydrous cements and stopped pastes were also recorded on a D8 ADVANCE (Bruker AXS, Germany) diffractometer, using monochromatic MoK $\alpha_1$  radiation ( $\lambda = 0.7093 \text{ \AA}$ ) with LYNXEYE XE 500  $\mu\text{m}$  linear dispersive energy detector, optimized for high-energy radiation, with the maximum opening angle. This diffractometer works on transmission geometry and samples are placed between kapton foils and are rotated at 10 rpm during data collection. Data were collected from 3° to 27° (2 $\theta$ ). To determine the amorphous and crystalline non-quantified (ACn) [122] content, an internal standard approach was employed [122,123]. As internal standard, Quartz (99.56%, ABCR GmbH & Co. KG) was added to the samples to a total content of ~20 wt%. The mixtures (sample-standard) were homogenized for 15 min in an agate mortar.

In addition, an *in-situ* LXRPD study of FA0BAY with/without addition of superplasticizer was performed to understand its effect on early hydration. To do so, LXRPD were collected on the same D8 ADVANCE diffractometer by using an Anton Paar MHC-trans chamber. Data were collected at 25°C and relative humidity (RH) value of 95%. X-ray diffraction patterns were collected every 15 min. All patterns were measured between 2° and 27° (2 $\theta$ ) with a step size of 0.017° and counting time of 0.5 s per step (total time per pattern 10 minutes).

### 1.3.2. Synchrotron X-ray Powder Diffraction (SXRPD)

An *in-situ* study of the hydration of the mixture of pure phases, alite-ye'elimite-anhydrite, was carried out by SXRPD. All patterns have been collected in the



Materials Science and Powder Diffraction station (MSPD - BL04) located at ALBA, the Spanish Synchrotron Radiation Facility (Barcelona, Spain). Patterns were collected in Debye-Scherrer (transmission) mode [124] with a wavelength of 0.61878(3) Å. The diffractometer is equipped with a MYTHEN detector system especially suited for time-resolved experiments and extremely good signal-to-noise ratio experiments. The glass capillaries of 0.7 mm of diameter were rotated at 20 rpm during data collection to improve diffracting particle statistics. The overall data acquisition time was 6 min per pattern. Several patterns at different hydration times were collected for every sample over the angular range from 2 to 40° (2 $\theta$ ). SXRPD patterns were normalized taking into account the loss of X-ray beam flux with time due to the electron beam current decline in the storage ring. Normalized SXRPD patterns were analyzed by using the Rietveld methodology in order to obtain RQPA. Internal standard methodology has been also used with SXRPD data using 20 wt% SiO<sub>2</sub> (99.5%, Alfa Aesar).

### 1.3.3. Rietveld methodology and ACn quantification

Once a good powder diffraction pattern was collected from LXRPD or SXRPD, all the cementitious phases were identified using the X'Pert High Score Plus program from PANalytical with reference structures from PDF database and Inorganic Crystal Structure Database (ICSD). Then, the patterns were analyzed by direct Rietveld method using GSAS software package [125] by using a pseudo-Voigt peak shape function [126] with the asymmetry correction included [127] to obtain RQPA. The refined overall parameters were: phase scale factors, background coefficients, unit cell parameters, zero-shift error, peak shape parameters (including anisotropic broadening correction when appropriated) and preferred orientation coefficient, if needed (March–Dollase ellipsoidal preferred orientation correction algorithm [128]).

The Amorphous and Crystalline non-quantified content present in the samples prepared with the internal standard was calculated comparing the weight value

of the standard,  $W_{st}$ , with the obtained value from RQPA,  $R_{st}$ , to obtain a quantification of amorphous phases [122].

### **1.3.4. Scanning electron microscopy (SEM) and Field emission scanning electron microscopy (FE-SEM)**

A fracture cross-section of a selected clinker pellet (scaled-up BAY\_4) was performed in a Jeol JSM-6490LV (Japan) scanning electron microscope using secondary electrons at 20 kV, to study the morphology of the phases. Prior to SEM observation, the sample was gold coated (by sputtering during 10 min until obtain 30 nm of thickness) to improve the conductivity of the sample and observation.

Moreover, a field emission scanning electron microscope (FE-SEM) (Helios Nanolab 650 dual beam from FEI) was used to study the phase distribution of polished scaled-up BAY\_4 clinker. Backscattering electron (BSE) images were acquired at 15 kV with a retractable CBS backscatter detector (annular solid-state device) that inserts and rests directly underneath the final lens of the system. EDS (energy dispersive X-ray spectroscopy) analysis was acquired using a X-Max 50 mm<sup>2</sup> detector from Oxford Instruments with AZtec software (v.1.0).

### **1.3.5. Specific surface measurement**

A Blaine specific surface is an estimation of the surface area per unit mass of a powder, expressed in cm<sup>2</sup>/g. The Blaine surface area is determined indirectly by measuring the time of a known volume of air passing through a pellet of powder with an effective pressure. The Blaine surface area of all anhydrous powder samples were measured following ASTM C 204-05 procedure.

Furthermore, the specific surface area of anhydrous samples was carried out by BET (Brunauer-Emmett-Teller) methodology. These measurements were performed in an automatic MICROMERITICS ASAP 2020 (Micromeritics

Instrument Corp, GA, USA). Isotherms at low partial pressures of the inert gas ( $N_2$ , at room temperature) were used to determine specific surface areas. The total surface area of the powders was calculated using the Langmuir theory and the BET generalization. The BET method gives results two to three times higher than the air permeability values (Blaine method) because it includes internal surfaces present in microcracks or in pores open at only one end.

### 1.3.6. Particle size distribution (PSD)

The particle size distribution of powder anhydrous samples was measured by laser diffraction in isopropanol suspension using a Malvern MasterSizer S (UK) instrument. The powders were previously dispersed in isopropanol in test tubes using an ultrasonic bath. The suspension is irradiated by a laser beam that diffracts on the particles and the diffracted beam is recorded by a detector. From the measurement, information such as  $D_{v50}$  (maximum particle diameter below which 50% of the sample volume exists - also known as the median particle size by volume), and  $D_{v90}$  (maximum particle diameter below which 90% of the sample volume exists) can be obtained.

### 1.3.7. Isothermal calorimetry

An eight channel TAM Air Isothermal conduction calorimetry (TA Instruments, USA) was used to study the heat evolution from hydration reactions at 25 °C for 72 hours. An admix automatic device was used to mix 2 g of anhydrous samples and the corresponding amount of water inside the calorimeter for 2 minutes, with the aim to avoid any data loss at the beginning of the reaction. In the reference vessel, the same sample measured (2 g) was used, due to it has similar heat capacity. The reference vessel is used to reduce the signal-to-noise ratio and to correct both measurement and temperature gadget. Each channel is independent from the other channels and was calibrated for 24 hours before any experiments were made.

### 1.3.8. Thermogravimetric analysis (TG)

Thermogravimetry and differential thermogravimetry (TG-DTG) analyses were carried out in a SDT-Q600 analyzer from TA Instruments (New Castle, DE) under dry air atmosphere (flow rate of 100 ml/min), over the temperature range 20-1000 °C with a heating rate of 10 °C/min. Open platinum crucibles were used and the sample weight was approximately 40 mg. TG-DTG studies were performed on powder from the stopped-hydration pastes to examine the thermal decomposition of hydrated phases up to 600 °C, to quantify phases, including the free water content. Data were processed using TA Instruments Universal Analysis 2000.

### 1.3.9. Rheological measurements

Rheological measurements of the cement pastes were carried out to optimize the superplasticizer content. A viscometer (Model VT550, Thermo Haake, Karlsruhe, Germany) with a serrated coaxial cylinder sensor, SV2P, provided with a solvent trap to reduce evaporation was used. Flow curves were obtained with controlled rate (CR) measurements using a two-stage measuring program. First, the shear rate was increased with ramp times of 6 s from 0 to 100 s<sup>-1</sup>, for a total of 11 ramps. Second, the shear rate was decreased from 100 to 0 s<sup>-1</sup> following the same ramp times. Before starting the rheological measurement, the pastes were pre-sheared for 30 s at 100 s<sup>-1</sup>.

### 1.3.10. Mercury intrusion porosimetry - MIP

MIP was carried out to characterize the connected pore network and the size of the pore entries on FA#BAY and B83 paste samples at 180 curing days, for the sake of comparison. The cylindrical pieces (15 mm length and 10 mm diameter) of around 2 g mass were first immersed in isopropanol for 72 h, and then dried at 40 °C until their weight was stable. The surface of this cylinder was removed prior to the analysis. Micromeritics AutoPore IV 9500 porosimeter (Micromeritics

Instrument Corporation, Norcross- GA, US) was used, which is capable of measuring porosity in the range from 1 mm down to 2 nm. The pressure applied by the intrusion porosimetry ranged from 0 to 300 MPa. A constant contact angle  $\theta$  of  $130^\circ$  was assumed for data evaluation.

### 1.3.11. Solid-state nuclear magnetic resonance (NMR)

Solid state magic angle spinning nuclear magnetic resonance was performed on stopped-hydration pastes to characterize the local atomic structure of  $^{29}\text{Si}$  and  $^{27}\text{Al}$  nuclei.  $^{27}\text{Al}$  and  $^{29}\text{Si}$  MAS-NMR spectra were recorded on a Bruker AVIII HD 600 NMR spectrometer (Bruker AXS, Germany) with magnetic field 14.1 T, operating at 156.4 MHz with a 2.5 mm triple-resonance DVT probe using zirconia rotors at 20 and 15 kHz spinning rates (respectively for  $^{27}\text{Al}$  and  $^{29}\text{Si}$ ).

$^{27}\text{Al}$  MAS-NMR experiment was performed with (Hpdcc) and without (One pulse)  $^1\text{H}$  decoupling by applying a single pulse ( $p/12$ ), an excitation pulse of 1  $\mu\text{s}$ , 5.0 s relaxation delay and 200 scans. The chemical shift was referenced to an external solutions of 1 M of  $\text{Al}(\text{NO}_3)_3$ .

$^{29}\text{Si}$  MAS-NMR experiments were performed with  $^1\text{H}$  decoupling (cw sequence) by applying a single pulse ( $p/2$ ), an excitation pulse of 5  $\mu\text{s}$ , 30 s relaxation delay and 10800 scans. The chemical shift was referenced to an external solution of tetramethylsilane (TMS).

### 1.3.12. Compressive strengths

The compressive strength of all mortars ( $3 \times 3 \times 3 \text{ cm}^3$  cubes) was measured following the EN 196-1 protocol in a Model Autotest 200/10 W (Ibertest, Spain) press. The compressive strength values were calculated by dividing the total maximum load indicated by the testing machine (KN) by the specimen area ( $900 \text{ mm}^2$ ). The final results were obtained as an average of three compressions

values. The testing curing ages were 1, 7, 28, 90, and 180 days, which correspond to the same studied curing times of pastes. The strength results were compared between them and with non-active BYF published elsewhere [48].

## 2. Clinkering and scaled-up of BAY

In this chapter, belite-alite-ye'elimite (BAY) clinkers were synthesized from natural materials, as described in the *Materials and Methods Section*. The primary goal was to synthesize BAY clinker with maximal jointly content of alite and ye'elimite. The procedures developed for “small” and “medium” scales are explained. The term “small” scale refers up to 10 g of final clinker and the term “medium” scale or scaled-up refers up to around 2 kg of final clinker. The phase content of all resulting clinkers was analyzed and quantified using laboratory X-ray diffraction combined with the Rietveld methodology. The scaled-up clinker (“medium scale”) was analyzed by SEM methodology combined with EDS analysis to know both the morphology and phase distribution. Finally, cements were prepared with the scaled-up clinker by adding anhydrite to control hydration reactions. Part of this work has been published in *Clinkering and hydration of Belite-Alite-Ye'elimite cement* [118] (see Annex I).

### 2.1. BAY clinkering optimization

#### 2.1.1. Dosage optimization

Four BAY clinker attempts were carried out at “small scale” to find the correct dosage of raw materials to obtain the maximal jointly content of alite and ye'elimite, as reported in paper # 1 [118] (Annex I). The four BAY clinkers, as described in the *Materials and Methods section*, were prepared by mixing natural raw materials with 0.75 wt% of calcium fluoride [75–78,85], which corresponds to 0.9 wt%  $\text{CaF}_2$  when only the amount of oxides (after carbonation) is considering.

Table 2.3 reports the expected phase composition of the four clinkers, named as BAY\_# referred to the attempt number, the elemental oxide composition of each mixture and the amount of the raw materials used in their preparation.

**Table 2.3.** Targeted mineralogical phase assemblage (in wt%) of BAY clinkers, nominal elemental composition of raw mixtures (expressed as oxides) excluding H<sub>2</sub>O and CO<sub>2</sub> and raw materials dosages (wt%). Taken from [118]. Copyright (2017) with permission from Elsevier (Annex III).

	BAY_1	BAY_2	BAY_3	BAY_4
Targeted composition (wt%)				
C <sub>2</sub> S	55	55	50	45
C <sub>4</sub> A <sub>3</sub> S	15	20	15	18
C <sub>3</sub> S	15	20	25	30
C <sub>4</sub> AF	15	5	5	5
Cs	---	---	5	2
Elemental composition of raw material (wt%)				
CaO	58.1	59.1	59.7	60.0
Al <sub>2</sub> O <sub>3</sub>	10.8	11.2	8.8	10.2
SO <sub>3</sub>	2.1	2.6	4.9	3.5
Fe <sub>2</sub> O <sub>3</sub>	5.5	2.4	2.4	2.4
SiO <sub>2</sub>	22.6	23.9	23.4	23.0
CaF <sub>2</sub>	0.9	0.9	0.9	0.9
Raw material (wt%)				
White limestone	67.1	67.3	65.7	67.3
Sand	5.6	6.2	8.3	6.5
Gypsum	3.6	4.8	9.0	6.4
Iron source	4.2	1.4	1.4	1.4
White kaolin	18.9	19.7	15.1	17.8
Fluorite (mineralizer)	0.6	0.6	0.6	0.6



Figure 2.3 shows LXRPD patterns of all BAY clinkers attempts, “small scale”, and Table 2.4 shows their mineralogical composition determined by Rietveld method, normalized to 100 wt% of crystalline phases.

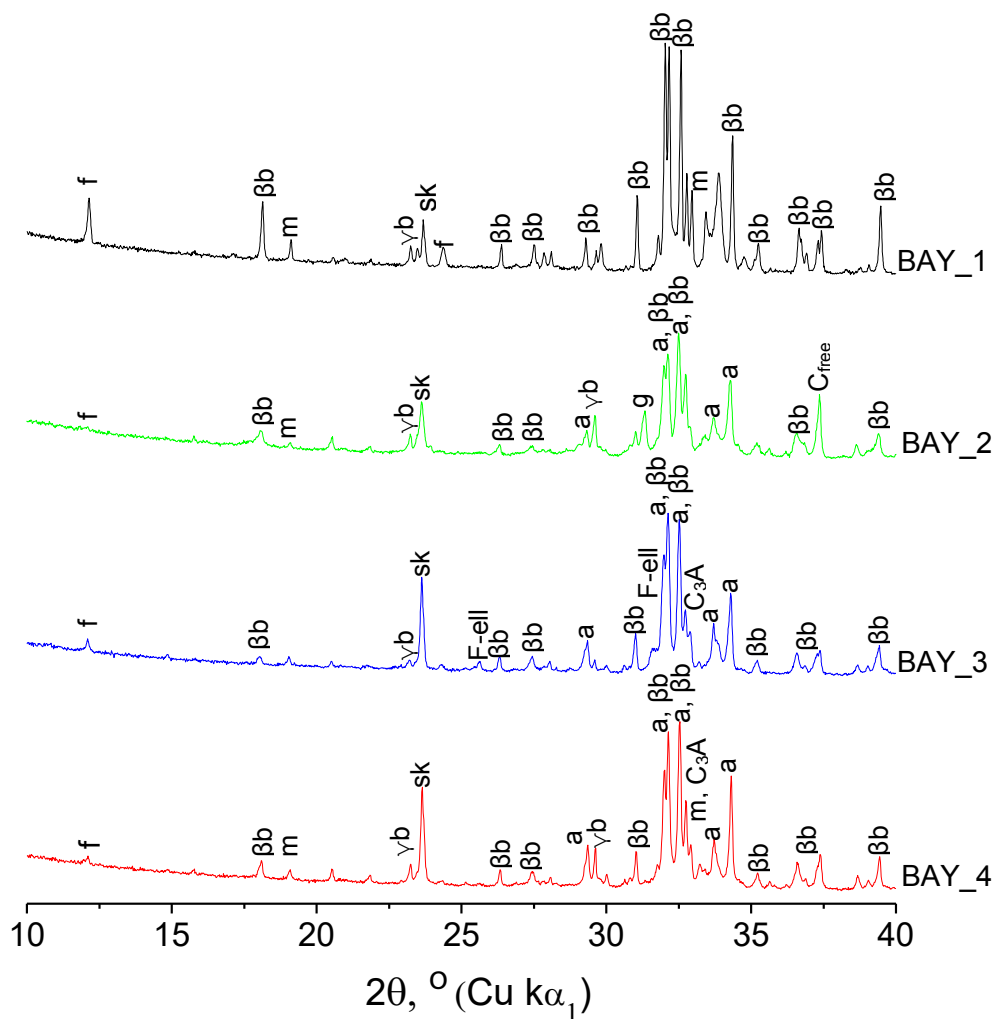


**Figure 2.3.** LXRPD patterns for BAY clinkers with monochromatic  $\text{CuK}\alpha_1$  ( $\lambda=1.5406\text{\AA}$ ). sk ( $\text{C}_4\text{A}_3\text{S}$ ), f ( $\text{C}_4\text{AF}$ ),  $\beta\text{b}$  ( $\text{bC}_2\text{S}$ ),  $\gamma\text{b}$  ( $\text{gC}_2\text{S}$ ), m ( $\text{C}_{12}\text{A}_7$ ), a ( $\text{C}_3\text{S}$ ), F-ell (Fluorellestadite), g ( $\text{C}_2\text{AS}$ ),  $\text{C}_{\text{free}}$  (Free lime),  $\text{C}_3\text{A}$ . Modified from [118]. Copyright (2017) with permission from Elsevier (Annex III).

**Table 2.4.** Direct RQPA (wt%) for BAY clinkers (taken from [118]). Copyright (2017) with permission from Elsevier (Annex III).

Phase	BAY_1	BAY_2	BAY_3	BAY_4
$\beta$ -C <sub>2</sub> S	65.0(1)	44.9(3)	59.9(2)	51.8(2)
$\gamma$ -C <sub>2</sub> S	2.7(1)	12.2(2)	2.9(2)	8.5(2)
C <sub>4</sub> AF	22.0(2)	8.2(2)	7.6(1)	7.0(1)
Cs	-	-	0.5(2)	-
o-C <sub>4</sub> A <sub>3</sub> S	3.5(1)	1.9(1)	9.7(2)	9.1(4)
c-C <sub>4</sub> A <sub>3</sub> S	-	7.9(1)	0.6(2)	3.0(4)
C <sub>3</sub> S	-	13.0(3)	13.1(2)	16.0(2)
C <sub>12</sub> A <sub>7</sub>	6.6(1)	2.1(8)	-	2.3(1)
Fluorellestadite	-	-	5.0(3)	-
C <sub>3</sub> A	-	-	0.8(1)	2.3(1)
C <sub>2</sub> AS	-	7.0(3)	-	-
Free lime	-	2.7(1)	-	-
R <sub>wp</sub>	4.33	6.37	5.89	5.40

In the first attempt, in BAY\_1, there was no evidence of alite; only a high amount of belite ( $\beta$ -C<sub>2</sub>S and  $\gamma$ -C<sub>2</sub>S polymorphs) and ferrite, 67.7 and 22.0 wt% respectively, with a minimal quantity of pseudocubic ye'elimite and mayenite (3.5 and 6.6 wt% respectively), as can be seen in Table 2.4 and Figure 2.3. The high amount of iron oxide in this dosage affected the formation of alite despite the amount of fluorite and calcium sulfate added. In addition, the iron oxide content favored the decomposition of ye'elimite into mayenite [70]. It is known that a Al<sub>2</sub>O<sub>3</sub>/Fe<sub>2</sub>O<sub>3</sub> ratio between 1.5 and 2.5 in OPC systems helps the formation of liquid which favors the ion diffusivity [4,129]. In this specific case, due to high amount of Fe<sub>2</sub>O<sub>3</sub> in the system favors the quantity of liquid phase and its viscosity promote the decomposition of C<sub>4</sub>A<sub>3</sub>S into C<sub>12</sub>A<sub>7</sub>; and the sulfate in liquid phase generated by C<sub>4</sub>A<sub>3</sub>S decomposition inhibits the reaction of CaO with belite, consequently suppressing the C<sub>3</sub>S formation [79,86,130,131].

In the second attempt, BAY\_2, it was decided to change the targeted amount of the phases. The desired content of C<sub>4</sub>AF was reduced to 5 wt%, both alite and

ye'elimite contents were tried to rise up to 20 wt%, and the amount of belite was fixed in 55 wt%. After the clinkering process, a significant amount of both polymorphs of belite, jointly with alite and ye'elimite polymorphs (57.1, 13.0 and 9.8 wt% respectively) were present, which are the main phases of BAY systems [72,74,75,77,79,85,93,118]. In addition, ferrite, mayenite, gehlenite and free lime were also detected. BAY\_2 was also ruled out due to the presence of free lime, because it is a revealing indicator that the clinkering process was not finished at 1300 °C. Furthermore, there was a non-negligible existence of gehlenite, which is considered an inert intermediate phase in ye'elimite-based systems [37,132]. Alike, there was 12.2 wt% of  $\gamma$ -C<sub>2</sub>S of total amount of belite in this clinker, and it is known that this phase is hydraulically inactive [133].

In the third attempt (BAY\_3 targeted composition shown in Table 2.3), the objective was to increase the amount of C<sub>3</sub>S and C<sub>4</sub>A<sub>3</sub>S present in the clinker, respect to BAY\_1. BAY\_3 clinker contained belite (gamma and beta polymorphs), alite, ye'elimite (pseudocubic and orthorhombic polymorphs), ferrite, anhydrite, C<sub>3</sub>A and fluorellestadite (62.8, 13.1, 10.3, 7.6, 0.5, 0.8 and 5.0 wt%, respectively). In this case, the increases of alite and ye'elimite were not significant, and there also was fluorellestadite (F-ellestadite). That phase comes from reaction between CaF<sub>2</sub>, C<sub>2</sub>S and Cs [91,134], which is a non-hydraulic intermediate phase and is stable up to 1240 °C, where it began to decompose into C<sub>2</sub>S and a liquid phase [132,135]. Despite the presence of this inert phase, it was possible to jointly obtain C<sub>3</sub>S, C<sub>4</sub>A<sub>3</sub>S and C<sub>2</sub>S in a considerable good quantity.

Finally, in the fourth attempt, BAY\_4, the targeted of alite and ye'elimite were increase again, obtaining 16.0 and 12.1 wt%, respectively, without anhydrite and fluorellestadite in it. Additionally, it presented aluminum phases (C<sub>12</sub>A<sub>7</sub> and C<sub>3</sub>A specifically) which are highly hydraulic ones [4,5].

According to this, it is good to remark that the maximum alite/ye'elimite mass ratio achieved was 1.3, both in BAY\_3 and BAY\_4, for this reason they were the most promising candidates to be scaled-up. Although in all clinkers the phase

assemblage was quite different to their targeted phase composition, it can be seen that three of them include high percentages of both alite and ye'elimite jointly with belite. BAY\_3 and 4 attempts were used for further optimization and characterization.

## 2.1.2. Mineralizer optimization

Three assays were carried out to study the mineralizer (fluorite –  $\text{CaF}_2$ ) effect on the synthesis and phase assemblage of the BAY\_3 dosage. The objective was to increase the quantity of  $\text{C}_3\text{S}$  and  $\text{C}_4\text{A}_3\text{S}$ , and decrease/eliminate the formation of F-ellestadite. Table 2.5 shows the raw materials dosages and elemental oxides composition for the three attempts realized with BAY\_3. The clinkering was carried out also at “small scale” as detailed in the *Materials and Methods Section*. Hereafter BAY\_3 clinkers will be named as BAY3\_x, where x stands for the amount of calcium fluoride in wt% (x= 0.6, 0.9 and 1.2).

**Table 2.5.** Raw materials dosages (wt%) and nominal elemental composition of raw mixtures (expressed as oxides) for BAY\_3 attempts.

	BAY3_0.6F	BAY3_0.9F*	BAY3_1.2F
Raw material (wt%)			
White limestone	65.8	65.7	65.5
Sand	8.3	8.3	8.3
Gypsum	9.0	9.0	9.0
Iron source	1.4	1.4	1.4
White kaolin	15.1	15.1	15.0
Fluorite (mineralizer)	0.4	0.6	0.8
Elemental composition of raw material (wt%)			
CaO	59.8	59.7	59.5
$\text{Al}_2\text{O}_3$	8.8	8.7	8.7
$\text{SO}_3$	4.9	4.9	4.9
$\text{Fe}_2\text{O}_3$	2.4	2.4	2.4
$\text{SiO}_2$	23.5	23.4	23.3
$\text{CaF}_2$	0.6	0.9	1.2

\*Corresponds to BAY\_3 attempt explicated in section 2.1.1.

Table 2.6 gives the Rietveld quantitative phase analysis, normalized to 100 wt% of crystalline phases, for all samples, where the targeted phase assembly was not achieved independently of the amount of fluorite added. The mineralogical results show that the increasing of  $\text{CaF}_2$  favors the decomposition of  $\text{C}_4\text{A}_3\text{S}$  into  $\text{C}_3\text{A}$  [5,70], from 10.6 to 8.4 wt% with the addition of 0.6 to 1.2 wt%, respectively, since fluorite helps the formation of liquid/molten in the clinker [88–90]. However,  $\text{C}_3\text{S}$  contents were lower than expected. When 0.6 wt% of  $\text{CaF}_2$  was added, only 6.9 wt% of alite was quantified. However, when 1.2 wt% of  $\text{CaF}_2$  was added, 8.5 wt% of alite was formed, but also F-ellestadite was present, meaning that the calcium fluoride addition was too high. According to these results it was not possible to obtain a higher quantity of alite and ye'elimite together without a significant content of F-ellestadite. As a conclusion of these results, calcium fluoride has to be added in 0.9 wt% to promote the optimum  $\text{C}_3\text{S}$  formation and to avoid  $\text{C}_4\text{A}_3\text{S}$  decomposition.

**Table 2.6.** Direct RQPA (wt%) for BAY\_3 clinkers synthesized with different amounts of  $\text{CaF}_2$ .

Phase	BAY3_0.6F	BAY3_0.9F*	BAY3_1.2F
$\beta\text{-C}_2\text{S}$	71.9(1)	59.9(2)	59.2(2)
$\gamma\text{-C}_2\text{S}$	3.6(1)	2.9(2)	2.0(1)
$\text{C}_4\text{AF}$	5.4(2)	7.6(1)	10.8(3)
Cs	0.5(1)	0.5(2)	0.5(1)
o- $\text{C}_4\text{A}_3\text{S}$	10.2(1)	9.7(2)	8.1(2)
c- $\text{C}_4\text{A}_3\text{S}$	0.4(1)	0.6(2)	0.3(1)
$\text{C}_3\text{S}$	6.9(3)	13.1(2)	8.5(1)
Fluorellestadite	0.4(1)	5.0(3)	7.5(1)
$\text{C}_3\text{A}$	0.6(1)	0.8(1)	3.2(1)
$R_{\text{wp}}$	5.74	5.89	5.32

\*Corresponds to BAY\_3 attempt explicated in section 2.1.1.

## 2.2. BAY clinker scaled-up

According to the results obtained in Sections 2.1.1 y 2.1.2, the BAY\_4 attempt was finally chosen due to the absence of fluorellestedite and the highest

percentages of alite and ye'elimite (16.0 and 12.1 wt%, respectively). The clinkering conditions had to be optimized for the scaled-up samples: temperature and dwelling time at that temperature. The scaled-up material obtained in this step was named as scBAY\_4. Table 2.7 reports the normalized crystalline composition of scBAY\_4 assays under different clinkering conditions. In all cases, the quantity of ye'elimite was reduced to the half and the amount of mayenite was doubled; It means that the solid reaction at this scale (~90 g of sample) favors the ye'elimite decomposition into mayenite [70] and a loss of sulfur as SO<sub>2</sub>. In addition, in the sample clinkered at 1280°C for 15 min only ~11 wt% of alite was obtained; when the sample was heated at 1300°C for 30 min a decrease of the alite amount to almost to the half was quantified, while the sample clinkered at 1300°C for 15 min (same condition used in small scale) presented 16.2 wt% of alite. For these reasons, 1280°C/15 min and 1300°C/30 min thermal processes were discarded.

**Table 2.7.** Mineralogical composition (RQPA in wt%) for scBAY\_4 clinker with 0.9 wt% CaF<sub>2</sub> at different thermal treatments. Taken from [118]. Copyright (2017) with permission from Elsevier (Annex III).

Phase	1280 °C 15 min	1300 °C 15 min	1300 °C 30 min	1300 °C 15min with excess of sulfur*
β-C <sub>2</sub> S	60.0(2)	56.3(2)	62.2(1)	59.4(2)
γ-C <sub>2</sub> S	3.2(1)	4.1(1)	3.6(1)	1.5(1)
C <sub>4</sub> AF	6.0(3)	6.4(2)	6.0(2)	6.9(2)
Cs	1.3(2)	0.9(2)	1.1(2)	0.6(1)
oC <sub>4</sub> A <sub>3</sub> S	5.0(1)	5.2(2)	5.6(1)	10.4(1)
C <sub>3</sub> S	11.7(2)	16.2(1)	8.9(1)	13.5(2)
C <sub>12</sub> A <sub>7</sub>	11.3(1)	9.5(1)	10.4(1)	5.1(1)
C <sub>3</sub> A	0.1(1)	1.2(1)	1.3(1)	---
Free lime	1.4(1)	0.9(3)	0.6(1)	---

\* Also contains 2.6(1) wt% of F-ellestadite

The next step followed was to modify the amount of  $\text{SO}_3$  in the dosage, by adding an excess of sulfur (up to a total amount of 4.3 wt% of  $\text{SO}_3$ , supplied as gypsum) to the raw materials to favor the ye'elimite formation/stabilization and compensate the loss of sulfur as  $\text{SO}_2$ . Table 2.7 and Figure 2.4 show the final mineral crystalline composition of the clinker (2 kg) obtained, where the amount of ye'elimite increased up to 10.4 wt% and the amount of alite was 13.5 wt%. It must be noted that this clinker shows an alite/ye'elimite ratio of 1.3 (similar to that for small pellets selected from Table 2.4).

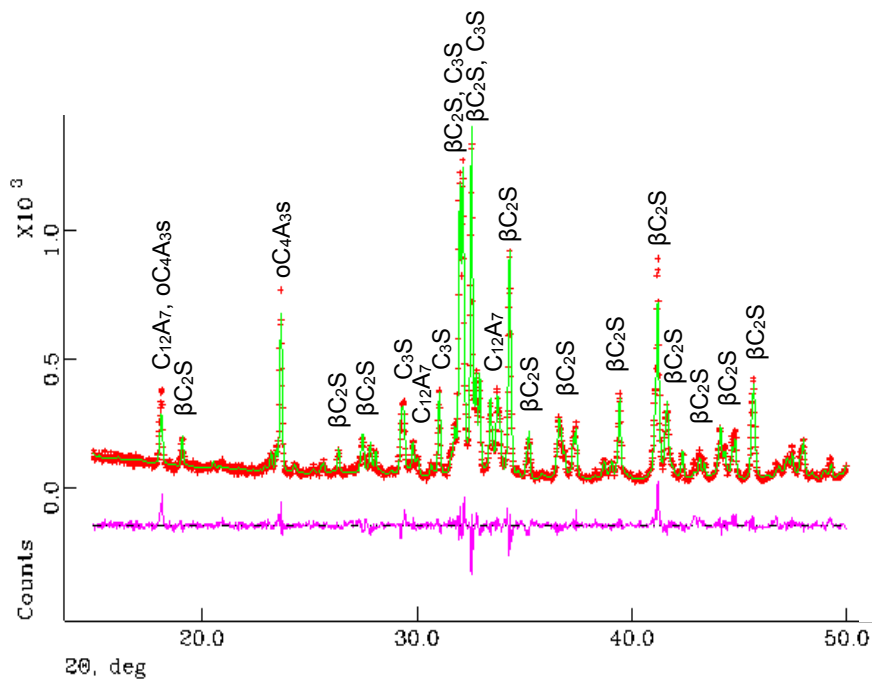
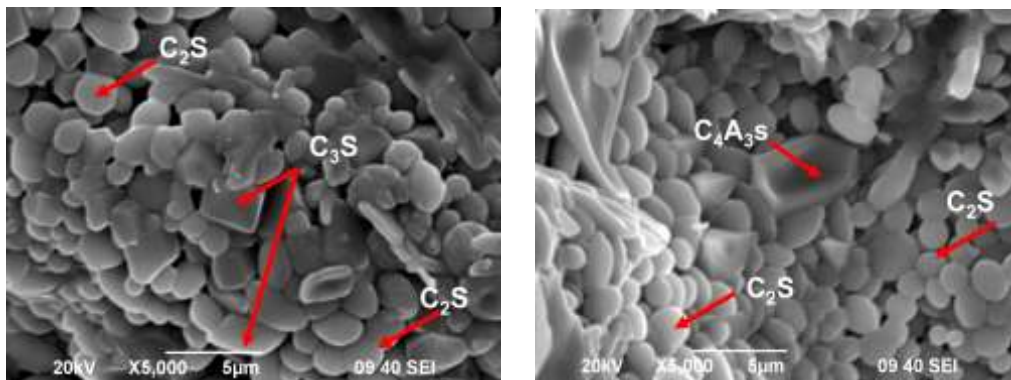


**Figure 2.4.** Rietveld plot of scBAY\_4 (~90 g of sample) at 1300 °C for 15 min and excess of sulfate, measured by XRPD with monochromatic  $\text{CuK}\alpha_1$  ( $\lambda=1.5406\text{\AA}$ ) radiation

Finally, these clinkering conditions (1300°C/15 min and excess of sulfur) were selected to prepare a total of 2 kg of scBAY\_4 clinker, in batches of ~210 g of sample. Every batch showed the same mineralogical composition than that prepared in batch of ~90 g (scBAY\_4 with excess of  $\text{SO}_3$  at 1300 °C for 15 min, Table 2.7). It is worth to highlighting that the synthesis of the scaled-up clinker,

releases 13.4% less  $\text{CO}_2$  than OPC (7.2% is related to the decarbonation of the raw materials, and the remaining is due to the reduction of fuel and milling electricity).

Figure 2.5 shows the SEM micrographs of the fresh fracture surface of the scaled-up clinker, where the morphology and distribution of phases can be observed. In the clinker, spherical particles ( $< 5 \mu\text{m}$ ) of belite, prismatic particles of alite (Figure 2.5 left side) and rhombic particles ( $\sim 4 \mu\text{m}$ ) of ye'elimite (Figure 2.5 right side) can be observed. As reported by Perez-Bravo *et al* [75] and Lu *et al* [78,93], ye'elimite has a rhombic decahedron shape.



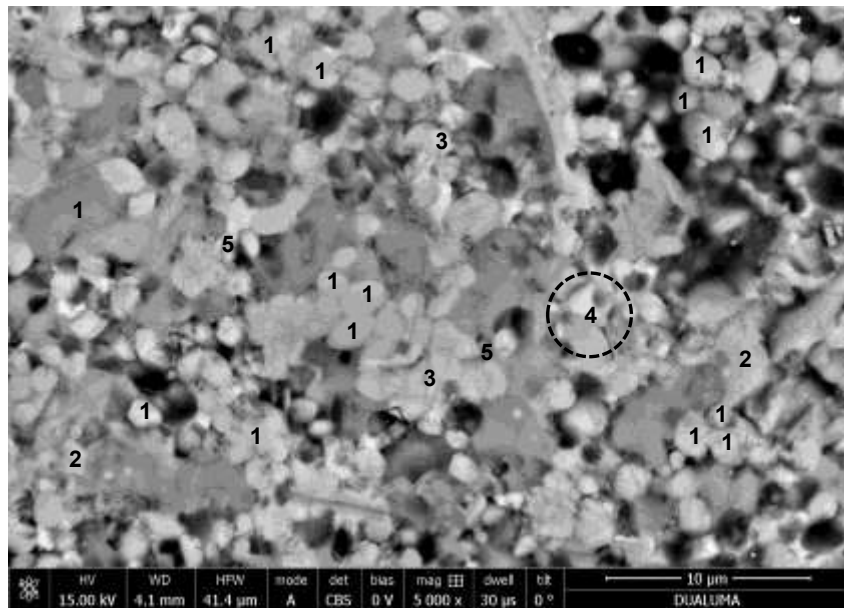
**Figure 2.5.** SEM micrographs of fresh fracture surface of scBAY\_4 clinker (taken from [118]). Copyright (2017) with permission from Elsevier (Annex III).

Figure 2.6 shows a FE-SEM micrograph of the polished scaled-up clinker where the EDS analysis was performed. It can be observed rounded particles of  $\text{C}_2\text{S}$  (labeled as 1), which composition was confirmed by EDS analysis. Table 2.8 represents the atomic ratio analysis results compared with stoichiometric atomic ratios of the phases.

Prismatic particles of alite were not so clearly observed in Figure 2.6, but EDS analysis confirms that particles labeled as 2, clearly matches with alite. EDS



analysis was also helpful to identify  $C_4A_3S$  (labeled as 3), where rhombic shape particles were not evidently found. Isolated points of other phases were also detected, which corresponds to F-ellestadite (labeled as 5) and subcooled phases (labeled as 4). Due to the small particle size (i.e. less than  $1\ \mu\text{m}$ ) of  $C_{12}A_7$  and  $C_4AF$ , it was not possible to differentiate them in subcooled phase. Black holes were observed in Figure 2.6, which correspond to porosity that favors the grinding of the material.



**Figure 2.6.** Backscatter electron (BSE) image of scBAY4 clinker (FE-SEM), where 1 ( $\beta C_2S$ ), 2 ( $C_3S$ ), 3 ( $C_4A_3S$ ), 4 (subcooled phase) and 5 (Fluorellestadite). Modified micrograph from [118]. Copyright (2017) with permission from Elsevier (Annex III).

**Table 2.8.** Average atomic ratio obtained by EDS in sc-BAY4 clinker, where “n” stands the number of measurements (points) analyzed. Theoretical atomic ratios of clinker phases are also included. Taken from [118]. Copyright (2017) with permission from Elsevier (Annex III).

Atomic ratio	n	Si/Ca	Al/Ca	S/Ca	Fe/Ca	F/Ca
Experimental EDS ratios						
C <sub>2</sub> S	12	0.47(2)	0.07(5)	0.03(3)	0.01(5)	--
C <sub>3</sub> S	4	0.31(7)	0.05(2)	0.08(4)	0.02(3)	--
C <sub>4</sub> A <sub>3</sub> S	5	0.05(1)	1.31(6)	0.25(2)	--	--
Subcooled phase*	5	0.06(4)	1.07(11)	0.07(8)	0.40(3)	--
Fluorellestadite	3	0.31(5)	0.31(13)	0.25(2)	--	0.26(10)
Theoretical stoichiometric ratios						
C <sub>2</sub> S		0.50	--	--	--	--
C <sub>3</sub> S		0.33	--	--	--	--
C <sub>4</sub> A <sub>3</sub> S		--	1.50	0.25	--	--
C <sub>4</sub> AF		--	0.50	--	0.50	--
C <sub>12</sub> A <sub>7</sub>		--	1.17	--	--	--
Fluorellestadite		0.30	--	0.30	--	0.20

\*Mainly consists on C<sub>4</sub>AF and C<sub>12</sub>A<sub>7</sub>

### 2.3. BAY cement preparation

Once the scBAY\_4 was completely obtained, BAY cement was prepared by mixing it with 12 wt% of anhydrite (as sulfate source), which corresponds to the stoichiometric amount that reacts completely with all calcium aluminates present in scBAY\_4 (ye'elimite and mayenite) to form ettringite. The cement showed a Blaine surface area of ~5200 (±24) cm<sup>2</sup>/g and d<sub>v,50</sub> of around 4 μm (see Figure 2.7).

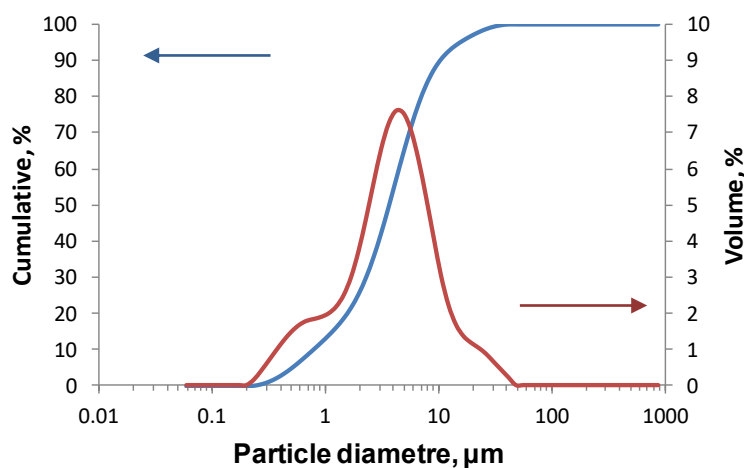


Figure 2.7. Particle size distribution of BAY cement.

## 2.4. Summary

Belite-alite-ye'elinite clinkers were successfully synthesized by combining natural raw materials, where the dosage has presented an important influence on the mineralogical composition. High amounts of  $\text{Fe}_2\text{O}_3$  significantly affected the formation of the ye'elinite and favored its decomposition into mayenite (i.e. BAY\_1). The quantity of  $\text{C}_3\text{S}$  and  $\text{C}_4\text{A}_3\text{S}$  increased by decreasing the amount of iron oxide and by increasing the amount of  $\text{SO}_3$  in the range of study (added as gypsum). The maximum percentages of alite and ye'elinite (16.0 and 12.1 wt% respectively) were obtained in BAY\_4 clinker, with a alite/ye'elinite ratio of 1.3. In addition, the mineralizer ( $\text{CaF}_2$ ) effect on the mineralogical composition was also studied, where the optimal quantity to be added in this system was 0.9 wt% (taking into account the amount of oxides).

In a second step, using the BAY\_4 clinker formulation, the scaled-up was carried out. The thermal conditions (clinkering temperature and dwelling time) had to be fine-tuned up for the preparation of 2 kg of scBAY\_4 clinker; the best results were obtained heating the sample at 1300 °C for 15 min, and adding an excess amount of  $\text{SO}_3$  up to a total amount of 4.3 wt%. The final scBAY\_4 clinker

showed a  $C_3S/C_4A_3S$  ratio of 1.3, same to that obtained in a previous step. That clinker was constituted by a high proportion of rounded particles of  $C_2S$ , individual points of prismatic particles of  $C_3S$  and rhombic shape particles of  $C_4A_3S$ . The clinker scBAY\_4 was quite porous, which favored the grinding.

Finally, the scBAY\_4 clinker was mixed with its stoichiometric amount of anhydrite (12 wt%) to completely react with calcium aluminates to form ettringite.

All these results have allowed to fulfill the specific objectives of synthesis and scaling-up optimization.

## 3. BAY cement hydration and mechanical behavior

This chapter studies the hydration of both BAY cements and mortars at water/cement ratios of 0.4 and 0.5 through the combination of independent techniques. They were characterized at 1, 7, and 28 days of hydration. The main goal was to unravel the hydration mechanism of this cement, the effect of water-to-cement ratio and the corresponding mechanical properties. The behavior of the cement pastes at very early-age was investigated by rheology. Quantitative X-ray powder diffraction with Rietveld analysis were the main techniques used to investigate the content of crystalline and ACn phases in pastes. Thermogravimetric analysis (TG-DTG) was employed to confirm the mineralogy of the pastes and to determine the chemically bounded water. Finally, the mechanical behavior of the mortars, as compressive strengths, was analyzed. Part of this work has been published in *Clinkering and hydration of Belite-Alite-Ye'elimite cement* [118] and in *Influence of Fly Ash blender on hydration and physical behavior of Belite-Alite-Ye'elimite cement* [136] (see Annex I).

### 3.1. Early-age behavior of fresh pastes

The reduction of the w/c from 0.5 to 0.4 caused a dramatic loss of workability in pastes and mortars. To overcome that drawback and assure the preparation of homogeneous pastes and mortars at a low w/c ratio, it is essential the addition of the right amount (and type) of additive, viz. a superplasticizer (SP). It will improve the homogeneity of the cementitious systems due to the better dispersion of the

particles and, consequently will reduce their viscosity; consequently, pastes and mortars will develop higher performances.

Figure 3.8 shows the flow curves of BAY pastes prepared at w/c ratios of 0.4 and 0.5. The former contains a small amount of superplasticizer, 0.1 wt%, since it was too viscous to be prepared without it. This fact confirms the needing of the addition and optimization of the right amount of superplasticizer, mainly when the water is reduced. Both pastes of Figure 3.8 show a shear thinning behavior, where the paste with the lowest water content shows the highest viscosity values (i.e. 3.9 and 1.8 Pa·s for w/c 0.4 and 0.5, respectively, at 100 s<sup>-1</sup>, from the up-curve), as expected.

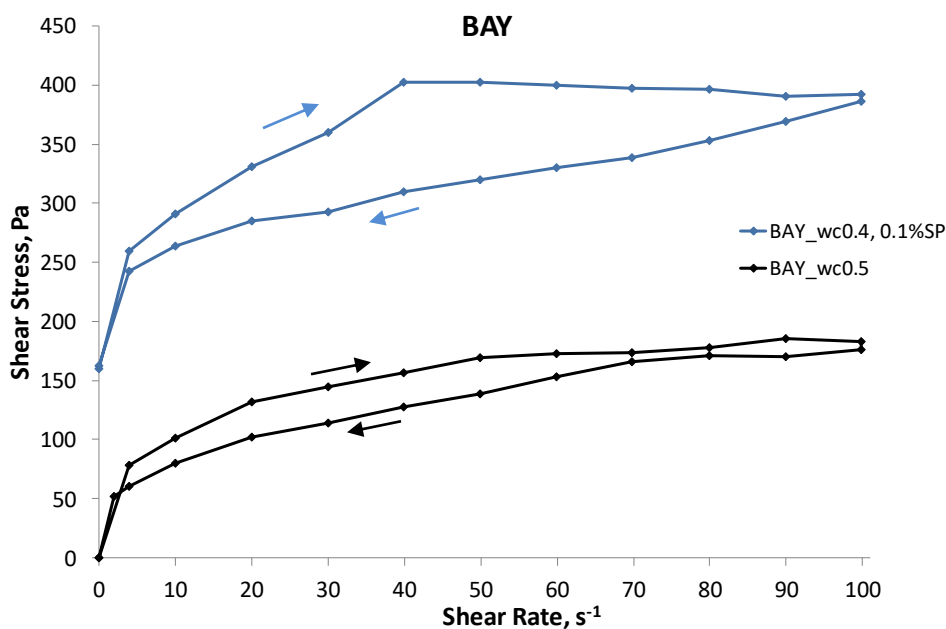


**Figure 3.8.** Flow curves of BAY pastes prepared at water/cement ratios of 0.4 (with 0.1wt% superplasticizer) and 0.5 (without superplasticizer).

Figure 3.9 shows the flow curves of BAY pastes prepared at a w/c of 0.4 and different SP contents. The down-curves of all those pastes of Figure 3.9 were adjusted to the Bingham model, Eq. 8, from 100 to 10 s<sup>-1</sup> where  $\tau$  is the shear stress,  $\tau_0$  is the yield stress,  $\mu$  is the plastic viscosity, and  $\dot{\gamma}$  corresponds to the shear rate.

Eq. 8

$$\tau = \tau_0 + \mu \cdot \dot{\gamma}$$

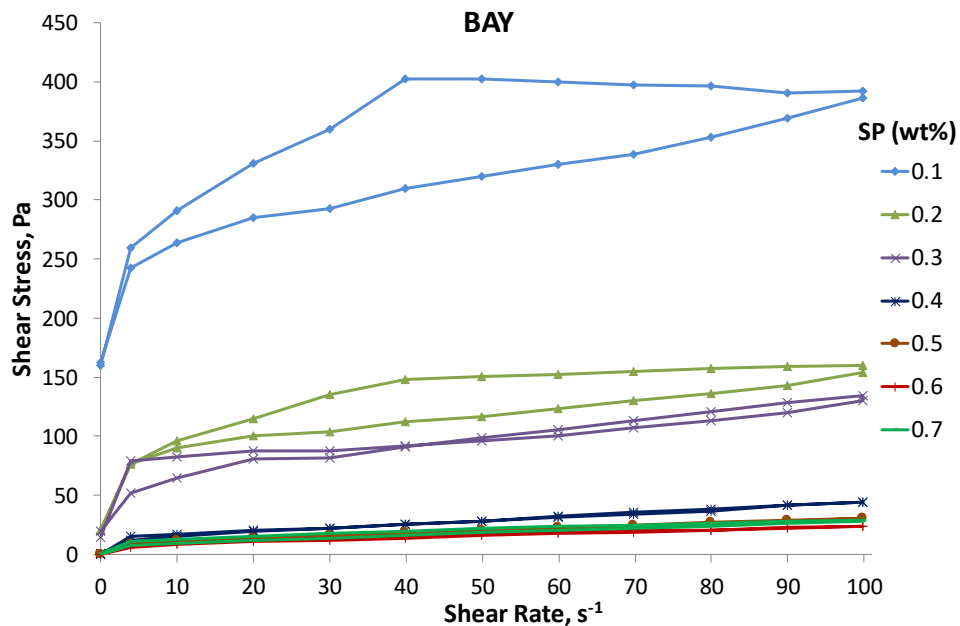


**Figure 3.9.** Flow curves of BAY pastes at  $w/c = 0.4$  and different superplasticizer contents. Modified from [136].

Table 3.9 depicts the thixotropy values and both plastic viscosity and apparent yield stress values obtained from the Bingham fitting for the BAY pastes prepared at  $w/c=0.4$  and different SP contents. In general, the yield stress is a consequence of the interparticle forces, so these links are often broken irreversibly by shear [137,138]. Here, the apparent yield stress values, obtained by extrapolation using the Bingham model [139], are only shown for the sake of comparison.

**Table 3.9.** Rheological properties of the fresh BYA paste prepared at w/c=0.4 and different SP contents.

SP (wt%)	Apparent Yield Stress (Pa)	$\eta_{\text{plastic}}$ (Pa·s)	Thixotropy (Pa/s)
0.1	255.2	1.27	5324.0
0.2	84.6	0.66	2205.0
0.3	74.0	0.51	749.5
0.4	10.4	0.26	53.0
0.5	9.0	0.22	58.3
0.6	7.7	0.20	157.0
0.7	7.9	0.20	269.9

Figure 3.10 shows the deflocculation curve of the pastes shown in Figure 3.9. The values were taken from the up-curves at the shear rate of  $100 \text{ s}^{-1}$ . Here, up-curves have been selected to compare up-curves and down-curves (through plastic viscosity). The inset corresponds to the same values but at different scale. In all cases (Figures 3.9, 3.10 and Table 3.9), by adding SP, the viscosity (apparent, shown in Figures 3.9 and 3.10, and plastic, shown in Table 3.9) of all pastes decreases to a minimum value, which corresponds to the optimum amount. From there, the viscosity of all pastes was kept constant or even increased. On the one hand, minimum values of viscosity were achieved when 0.5 and 0.6 wt% of SP were added (Figure 3.10 and Table 3.9), being slightly lower for 0.6 wt% in both cases. However, the small difference in viscosity does not justify the extra-addition of additive; in addition, the paste with 0.5 wt% SP shows a lower thixotropic cycle (Table 3.9). Furthermore, the amount of 0.4 wt% SP was discarded since the viscosity of that paste is higher than the selected one (with 0.5 wt% SP), and a small variation in the addition of the additive would increase considerably the viscosity. On the other hand, the apparent yield point values decrease by increasing the SP content in the range of study.



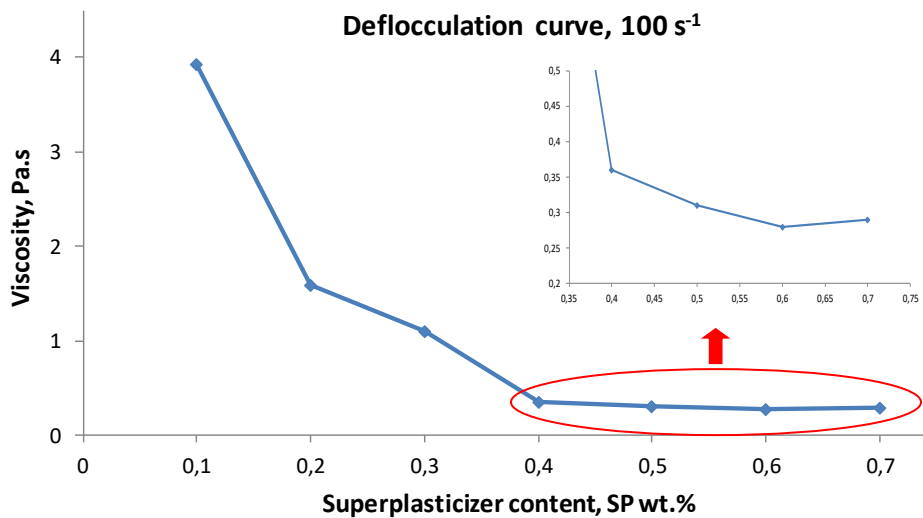


**Figure 3.10.** Deflocculation curve of BAY pastes with w/c ratio of 0.4 and different SP content at the shear rate of  $100 \text{ s}^{-1}$ . The inset corresponds to the same figure but at different scale.

The hydration of the paste (and the properties of the corresponding mortar) prepared at a w/c 0.5 was firstly studied; since the viscosity of that paste was good enough to work with it, the effect of SP was not studied. However, as explained before, the paste prepared at a w/c of 0.4 needed SP to be prepared; because of that, both mineralogical and mechanical comparative studies of this paste/mortar was performed on with 0.5 wt% SP (and w/c=0.4).

## 3.2. Mineralogical behavior of BAY pastes

The RQPA results of BAY cement pastes with time (water-to-cement ratio of 0.4 and 0.5, the former with SP) including both ACn (amorphous and crystalline non-quantified) and free water (FW) contents, are shown in Table 3.10 ACn contents were derived as detailed in *Materials and Methods Section*. FW was calculated taking into account the added water and the combined water determined by TG-DTG, according to Eq. 9. shows the mineralogical evolution vs time of BAY at a w/c of 0.4, as a representative example.

$$\text{Eq. 9} \quad FW = \%Water_{added} - \frac{BW_{ATD} * \%Cement}{100 - BW_{ATD}}$$

where  $BW_{ATD}$  : stands for the mass loss up to 600 °C from TG curves.

**Table 3.10.** RQPA (wt%) for BAY pastes at w/c 0.4 (with SP) and w/c 0.5. Taken from [118]. Copyright (2017) with permission from Elsevier (Annex III).

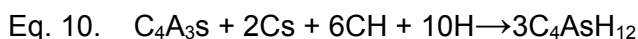
Phases	w/c=0.4				w/c=0.5			
	t <sub>0</sub>	1d	7d	28d	t <sub>0</sub>	1d	7d	28d
$\beta$ -C <sub>2</sub> S	29.5(3)	32.1(1)	33.1(2)	28.9(2)	27.6(3)	30.6(1)	29.0(2)	24.0(2)
$\gamma$ -C <sub>2</sub> S	0.8(1)	1.0(1)	1.3(1)	2.2(1)	0.8(1)	1.5(1)	1.5(1)	1.3(1)
C <sub>4</sub> AF	2.6(1)	2.3(1)	-	-	2.4(1)	0.8(1)	-	-
Cs	6.6(1)	-	-	-	6.2(1)	-	-	-
C <sub>4</sub> A <sub>3</sub> S	5.0(1)	1.4(1)	-	-	4.7(1)	1.2(1)	-	-
C <sub>3</sub> S	6.8(2)	2.6(1)	0.9(1)	-	6.4(2)	2.1(1)	0.9(1)	-
C <sub>12</sub> A <sub>7</sub>	3.8(1)	2.0(1)	-	-	3.6(1)	1.1(1)	-	-
F-ellestadite	2.2(2)	2.7(1)	2.6(1)	2.6(1)	2.1(2)	3.5(1)	2.6(1)	2.4(1)
partially C-S-H <sup>a</sup>	-	-	0.8(2)	1.1(2)	-	0.4(2)	1.2(2)	1.6(2)
AFm <sup>b</sup>	-	0.4(1)	2.4(1)	3.0(1)	-	0.9(1)	2.2(1)	3.0(1)
AFt	-	20.8(2)	16.0(2)	16.6(2)	-	15.1(2)	10.2(2)	12.7(2)
Katoite	-	-	2.4(2)	3.7(2)	-	1.1(1)	1.8(1)	2.5(1)
C <sub>2</sub> ASH <sub>8</sub>	-	1.2(1)	4.7(2)	5.0(2)	-	-	5.2(2)	5.3(2)
ACn	14.0(2)	20.9(2)	26.1(2)	28.6(2)	13.1(2)	24.7(2)	29.4(2)	34.8(2)
FW	28.6(-)	12.6(-)	9.7(-)	8.3(-)	33.3(-)	17.1(-)	16.0(-)	12.5(-)

a. As clinotobermorite

b. As monosulfoaluminate



cements should be composed also for C-S-H gel. However, crystalline CH was not detected by LXRPD or TGA-DTG in these systems. Therefore, it is speculated that the portlandite has reacted to form AFt, AFm (monosulfoaluminate) and katoite, following Eq. 4., Eq. 10 and Eq. 6 respectively.



Stratlingite ( $C_2ASH_8$ ) and katoite ( $C_3ASH_4$  or siliceous hydrogarnet) were other hydration products detected by LXRPD (Figure 3.11) Stratlingite is an AFm-type phase and comes from the hydration of silicates ( $C_2S$  and/or  $C_3S$ ) in presence of  $AH_3$  [106,142]. In this specific case,  $C_2ASH_8$  is obtained from the reaction of  $C_3S$  with  $AH_3$ . Katoite is a hydration product that can be formed by different reactions, shown in Eq. 6, Eq. 7 and Eq. 11. The results presented here suggest that part of katoite is produced from Eq. 11 by the reaction of alite with ferrite. Then, when ferrite is completely reacted, more katoite is formed from CH (Eq. 7).



The katoite formed from Eq. 11 can present a significant amount of aluminum substituted by iron, as reported Alvarez-Pinazo *et al* [56]. The A/F ratio was estimated in katoite with general formula  $C_3A_{1-x}F_xSH_4$ , using the equation  $a=0.16x+12.29$  [56]. being  $a$  the unit cell parameter. In these systems,  $x$  is  $\sim 0.7$  and  $\sim 0.5$  for w/c ratios of 0.4 and 0.5, respectively. Taking into account these values of  $x$ , it can be said that  $\sim 80$  wt% of the hydrated ferrite crystallized as katoite, in both systems. And, it speculates that the remaining 20 wt% of the ferrite has yielded amorphous/highly distorted AFm.

Analyzing Table 3.10, it can be observed that only  $\sim 50$  wt% of the dissolved silicates phases ( $C_3S$  and  $C_2S$ ) have crystallized as C-S-H (quantified as clinotobermorite), stratlingite and katoite; and  $\sim 60$  wt% of the dissolved aluminate-bearing phases ( $C_4A_3S$ ,  $C_{12}A_7$  and  $C_4AF$ ) have crystallized as AFt and monosulfoaluminate. As a result,  $\sim 50$  wt% and 40 wt% of the silicate and

aluminate content, respectively should be as ACn phase(s). Its composition may be mainly C-S-H gel and aluminum hydroxide gel, as were detected by TG-DTG, Figure 3.12.

Figure 3.12 shows TG-DTG plots of the evolution of BAY pastes with  $w/c=0.4$  (with SP) (Figure 3.12a) and  $w/c=0.5$  (Figure 3.12b) ratios at all the studied ages. The presumed composition of the amorphous hydrated phases was checked through thermogravimetric technique. In all samples, three mass loss signals were observed. The first one, near to  $\sim 110$  °C, it is due to the overlapped processes among the dehydration of C-S-H and the loss of 32 water molecules from ettringite [105,143,144]. The second group of signals was found between 120 and 220 °C, and it is associated to the dehydration of AFm-type phases. It is known that AFm-phases can be monosulfate, stratlingite and/or  $C_4AH_x$  (hydroxy-AFm phase with  $x = 12$  to 19 depending on relative humidity). According to Matschei *et al.*[109], AFm-type phases generally can form solid solutions, with a maximum of  $\sim 50$  mol%  $OH^-$  incorporated into the sulfate-AFm and  $\sim 3$  mol% of  $SO_4^{2-}$  incorporated into  $C_4AH_x$ . As can be seen in Figure 3.11, the AFm-type phases identified in these systems were monosulfate phase and stratlingite. As it has been mentioned, crystalline portlandite was not detected by TG-DTG (absence of a signal at  $\sim 450$  °C). This is in agreement with Winnefeld & Barlag [102], Trauchessec *et al.* [145] and Hargis *et al.* [103]. At early hydration hours, the formation of AFt it is favored [105,109] following Eq. 4. After calcium sulfate and ye'elimite reacted completely (24 h), portlandite (from the hydration of  $C_3S$ ), started to react with  $AH_3$  and AFt to produce AFm-type phases [72,103,145]. Monosulfoaluminate formed above 7 days should come from Eq. 5. The third signal located at  $\sim 270$  °C was associated to the dehydroxylation of amorphous aluminum hydroxide, in concordance to the absence of crystalline gibbsite in LXRPD patterns.

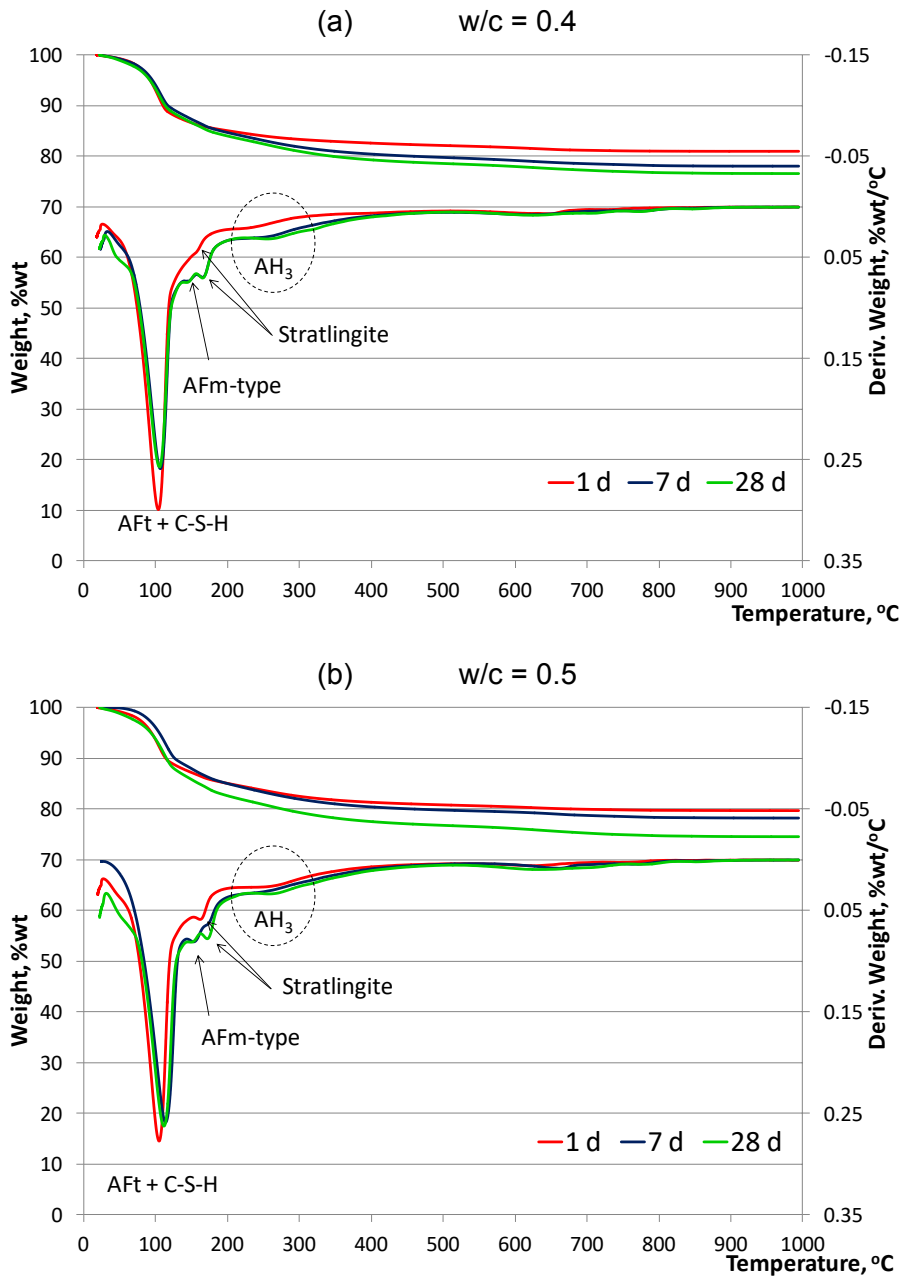


**Figure 3.12.** Thermogravimetric plots of BAY cement pastes after 1, 7 and 28 days of hydration. (a)  $w/c=0.4$  and (b)  $w/c=0.5$ . Taken from [118]. Copyright (2017) with permission from Elsevier (Annex III).

### 3.3. Compressive strength development of BAY mortars

The compressive strength of BAY mortars at different curing ages is shown in Figure 3.13. The results of a non-active belite sulfoaluminate (BYF) mortar (prepared with anhydrite, as calcium sulfate source) [48] is also shown for the sake of comparison. The most important result is that all mortars prepared with the BAY cement developed higher compressive strengths than non-active BYF-mortars [48], independently of the amount of w/c used. As expected, the compressive values in BAY-mortars increase by decreasing the water content and by increasing the curing time. BAY-mortar at a w/c of 0.4 at 1 day of hydration showed a higher compressive strength value than the same mortar prepared with w/c ratio of 0.5 after 3 days of hydration (~25.5 and ~21 MPa, respectively). After 28 curing days, BAY mortars reached a compressive strength of ~34.5 and ~26 MPa, at w/c of 0.4 and 0.5, respectively. All of this can be explicated for the good particles dispersion and low porosity reached with less water-to-cement ratio and use of optimal superplasticizer.

The higher compressive strength values from BAY-mortars than BYF-mortars is correlated to the presence of alite, in spite of BAY cements has lower amount of ye'elemite (~10 wt%) in contrasts of BYF cements (~30 wt%). This is likely due to the higher AFt contents (resulting from  $C_4A_3S$  and  $C_{12}A_7$  hydration) present at any age, combined with the higher density related to the lower water content and presence of C-S-H gel phase.

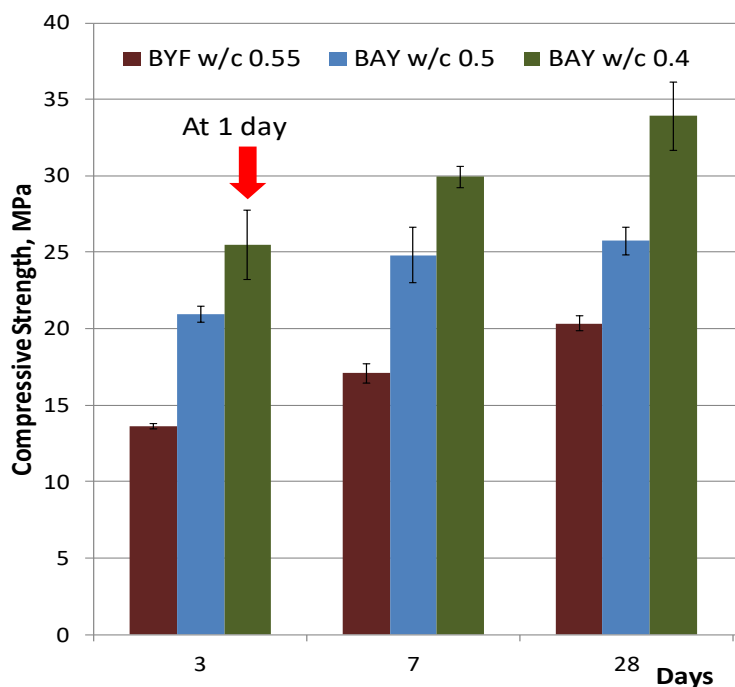


**Figure 3.13.** Compressive strengths of BAY cements as a function of w/c ratio and time. Non-active BYF is presented for comparison [48]. Taken from [118].

Copyright (2017) with permission from Elsevier (Annex III)

### 3.4. Summary

BAY with water-to-cement ratio of 0.5 showed a low viscosity, implying a fine workability and dispersion of the particles. When the w/c ratio was reduced to 0.4, the viscosity significantly increased, avoiding the preparation of homogeneous pastes (Figure 3.8). To overcome this drawback, a rheological study of the effect of the addition of polycarboxylate-based superplasticizer was performed with the conclusion that the optimum amount of the additive for pastes prepared at w/c ratio of 0.4 was 0.5 wt% SP.

In a second step, the mineralogical evolution of BAY pastes was analyzed by LXRPD and TG-DTG. Independently of the water-to-cement ratio used, the main hydration phases obtained were AFt, AFm-type phases (as monosulfoaluminate



and stratlingite) and katoite (as siliceous hydrogarnet). Ill-crystalline C-S-H gel was also detected in minor quantities. Amorphous aluminum hydroxide was quantified by the internal standard methodology, combining LXRPD and TG-DTG. Crystalline portlandite was not detected in the pastes likely due to the early formation of AFt, katoite, stratlingite and late monosulfoaluminate.

Finally, the mechanical strengths development was studied through a compressive test. BAY mortars ( $w/c=0.5$ ) developed higher compressive strengths than non-active BYF mortars ( $w/c=0.55$ ), at any hydration time (i.e. 24.8 and 17.1 MPa respectively, at 7 days). These values have been improved (up to 29.9 MPa at 7 days) by decreasing the water content ( $w/c$  ratio of 0.4) and the addition of superplasticizer. Later, after 28 days of curing, BAY mortars reached ~34.5 and ~26 MPa for samples prepared at the  $w/c$  ratio of 0.4 and 0.5, respectively.

All these results have allowed to fulfill part the specific objective of understanding of effect of  $w/c$  ratio on the hydration mechanism and compressive strength of BAY.



UNIVERSIDAD  
DE MÁLAGA

## 4. Pure phase hydration study

In this chapter, a study on different mixtures of pure phases (alite, ye'elinite and anhydrite) is presented to firstly unravel their hydration kinetics, and secondly, to be compared with the BAY cement behavior. Eight mixtures of pure phases (*Materials and Methods Section*) with different alite/ye'elinite and water-to-solid ratios were prepared, and the details are given in Table 4.11. The w/s ratio of 0.66 and 0.59 correspond to the stoichiometric amount of water with 10 wt% of excess for *n137* and *n274* respectively, according to Eq. 1 (*Introduction section*). The w/s values of 1.32 and 1.19 are the double of the previous values to study the effect of large water excess on hydration mechanisms. The pastes were studied through both *in-situ* and *ex-situ* X-Ray Powder Diffraction (XRPD). The *in-situ* hydration study was carried out by Synchrotron XRPD (SXRPD) and isothermal calorimetry during the first 48 hours. Moreover, a SXRPD pattern at 7 days of hydration was also collected. The ACn contents were determined by internal standard methodology [122]. The *ex-situ* study was carried out by Laboratory XRPD (LXRPD) to calculate the full mineralogical composition by Rietveld refinements and ACn contents by the internal standard method [122,146]. TG-DTG was used to calculate the free water content (see Chapter *BAY cement hydration and mechanical behavior* section 3.2), and *o137\_132* and *c137\_132* samples were also studied through Nuclear Magnetic Resonance (NMR) at 7 days of hydration. These results will be submitted for publication soon [147].



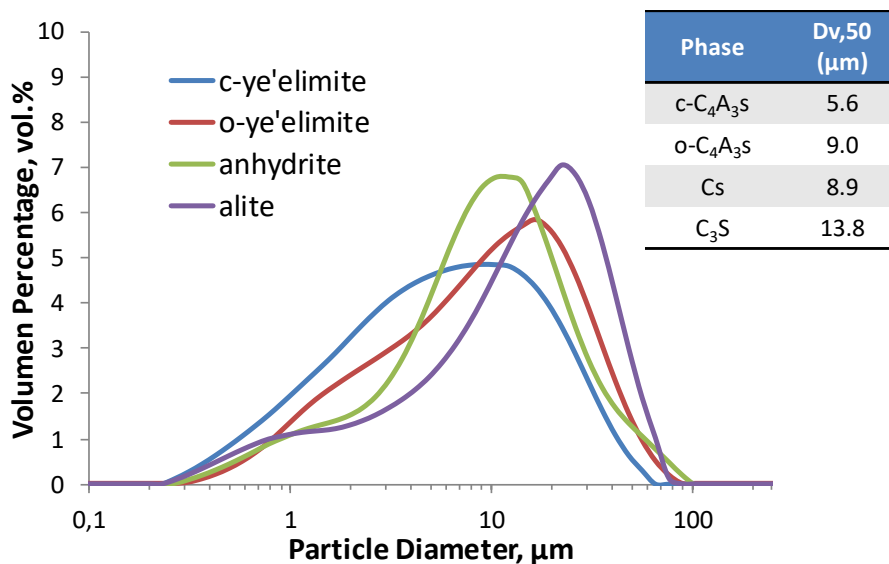
**Table 4.11.** Pure phase mixture compositions, in weight percentages (wt%).

Mixture nomenclature	o-C <sub>4</sub> A <sub>3</sub> S	c-C <sub>4</sub> A <sub>3</sub> S	Cs	C <sub>3</sub> S	C <sub>3</sub> S/C <sub>4</sub> A <sub>3</sub> S	w/s
o137_0.66	35.5	-	15.9	48.6	1.37	0.66
o137_1.32	35.5	-	15.9	48.6	1.37	1.32
o274_0.59	23.9	-	10.7	65.4	2.74	0.59
o274_1.19	23.9	-	10.7	65.4	2.74	1.19
c137_0.66	-	35.5	15.9	48.6	1.37	0.66
c137_1.32	-	35.5	15.9	48.6	1.37	1.32
c274_0.59	-	23.9	10.7	65.4	2.74	0.59
c274_1.19	-	23.9	10.7	65.4	2.74	1.19

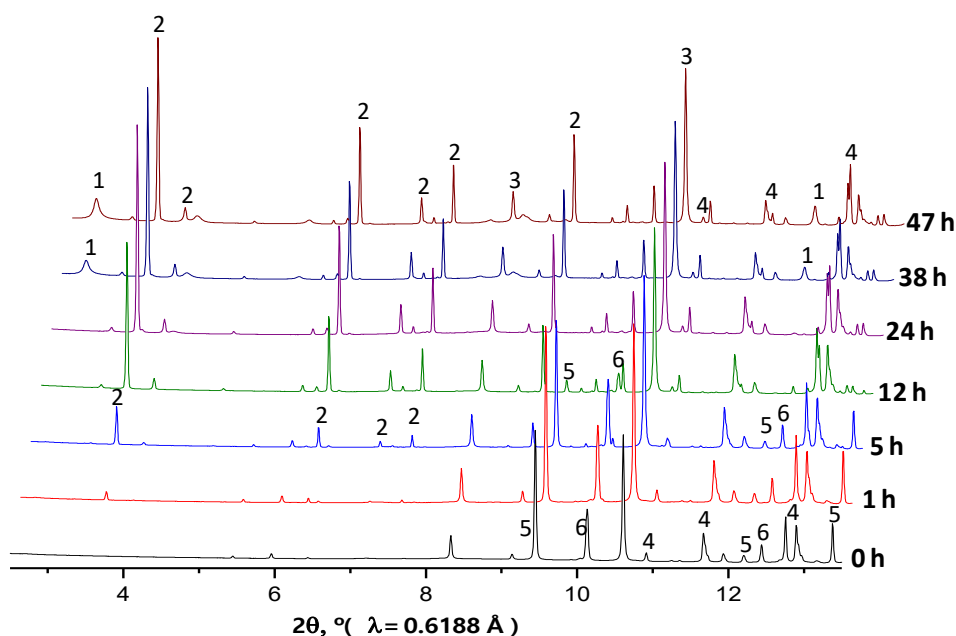
#### 4.1. *In-Situ* SXRPD hydration study

Figure 4.14 shows the particle size distribution (PSD) of the pure phases used in this study. Most of them show a bimodal behavior, with peaks centered at 1-2  $\mu\text{m}$  and 10-30  $\mu\text{m}$ . The values of  $D_{v,50}$  are also presented in the Figure 4.14. Particle size distribution of C<sub>4</sub>A<sub>3</sub>S (pseudocubic and orthorhombic), Cs and C<sub>3</sub>S powders., where all of them are between 5.6 and 14  $\mu\text{m}$ ; the smallest value corresponds to c-C<sub>4</sub>A<sub>3</sub>S (with a polydisperse behavior), and the largest one to C<sub>3</sub>S.

The effect of w/s ratio, ye'elimite polymorphism and the amount of alite jointly with anhydrite were studied during the hydration. Figure 4.15 depicts the raw SXRPD patterns at different times of hydration of c137\_132 mixtures. Figure 4.16 shows Rietveld plots of c137\_132 and o137\_132 mixtures after 24 hours of hydration, as representative examples.

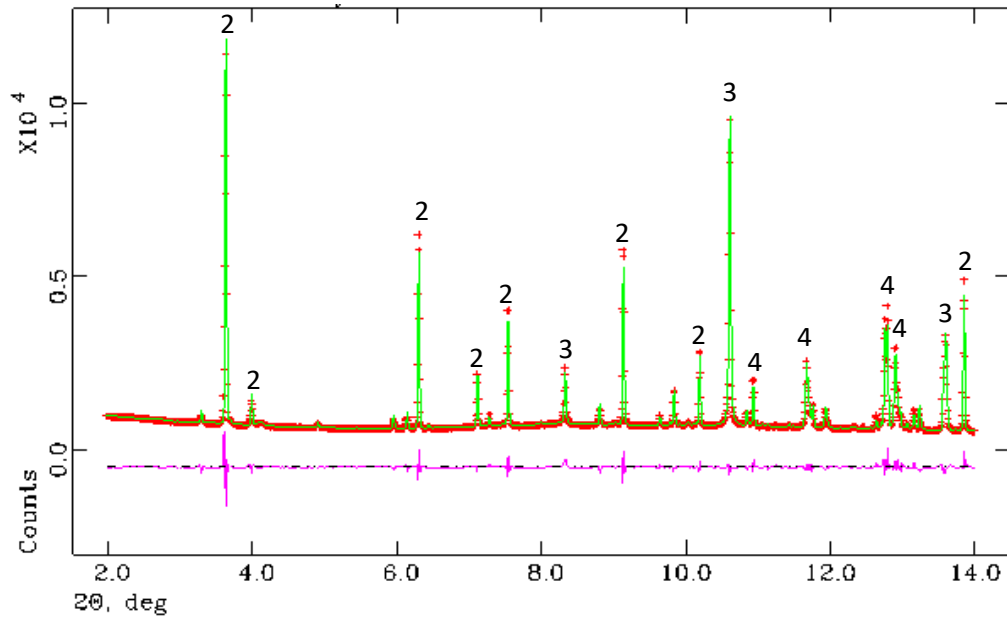


**Figure 4.14.** Particle size distribution of C<sub>4</sub>A<sub>3</sub>S (pseudocubic and orthorhombic), Cs and C<sub>3</sub>S powders.



**Figure 4.15.** *In-situ* SXRPD hydration evolution of c137\_132. 1 (stratlingite), 2 (ettringite), 3 (Quartz as internal standard), 4 (alite), 5 (pseudocubic ye'elimite) and 6 (anhydrite).

(a)



(b)

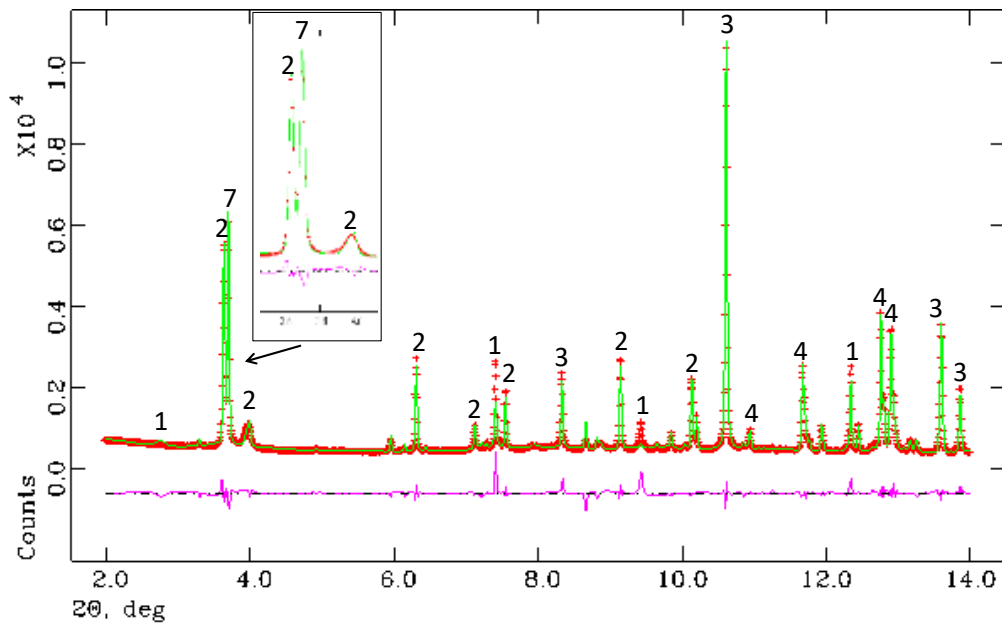


**Figure 4.16.** Rietveld plots of (a) c137\_132 and (b) o137\_132 at 24 hours of hydration. 1 (stratlingite), 2 (ettringite), 3 (Quartz as internal standard), 4 (alite) and 7 (monosulfoaluminate).

Tables A1 to A8 (see *Annex II*) give RQPA including the ACn and free water (FW) contents determined by internal standard methodology. Figure 4.17 shows full phase content evolution of c137 and o137 at different w/s ratios, where heat flow curves are also included. Figure 4.18 provides the full phase content evolution and heat flow curves of c274 and o274 at different w/s ratios. From all these Figures, two phenomena can be clearly described. Firstly, the reaction kinetics of polymorphs of ye'elimite were totally different in presence of anhydrite (as a calcium sulfate source) and alite. Orthorhombic ye'elimite, independently of w/s and alite/ye'elimite ratios, reacted faster than pseudocubic ye'elimite, even when it shows a bigger average particle size; i.e. it completely reacts at ~10 hours while pseudocubic ye'elimite needs ~20 hours in all the compositions. This is in agreement with Cuesta *et al* [101] and Jansen *et al* [148]. Secondly, alite did not start to react until ye'elimite was completely consumed, independently of the polymorphism. The main crystalline hydration products of these systems were AFt, monosulfoaluminate and stratlingite. Moreover, the phase assemblage was not strongly affected by water-to-solid ratio or polymorphism of ye'elimite.

The calorimetric curves, Figure 4.17 and Figure 4.18 (black line), present a strong peak within the first 25 minutes (0.4 hours) since mixing, known as the induction period. This peak is clearly associated with the dissolution (heat of wetting of the cement), and hydration of ye'elimite to form ettringite (purple asterisk) [101,148]. The hydration of orthorhombic and pseudocubic ye'elimite was published elsewhere [101] and the total heat evolved after 7 days was ~570 and ~550 J/g, respectively. The higher amount of heat released by the samples with the orthorhombic polymorph at 25 minutes corroborates the quicker reactivity of that phase when compared with the samples pseudocubic polymorph in spite of the amount of water and the amount of alite. Table 4.12 gives the degree of reaction of ye'elimite calculated from the calorimetric data, considering that it has reacted with water at 25 minutes.

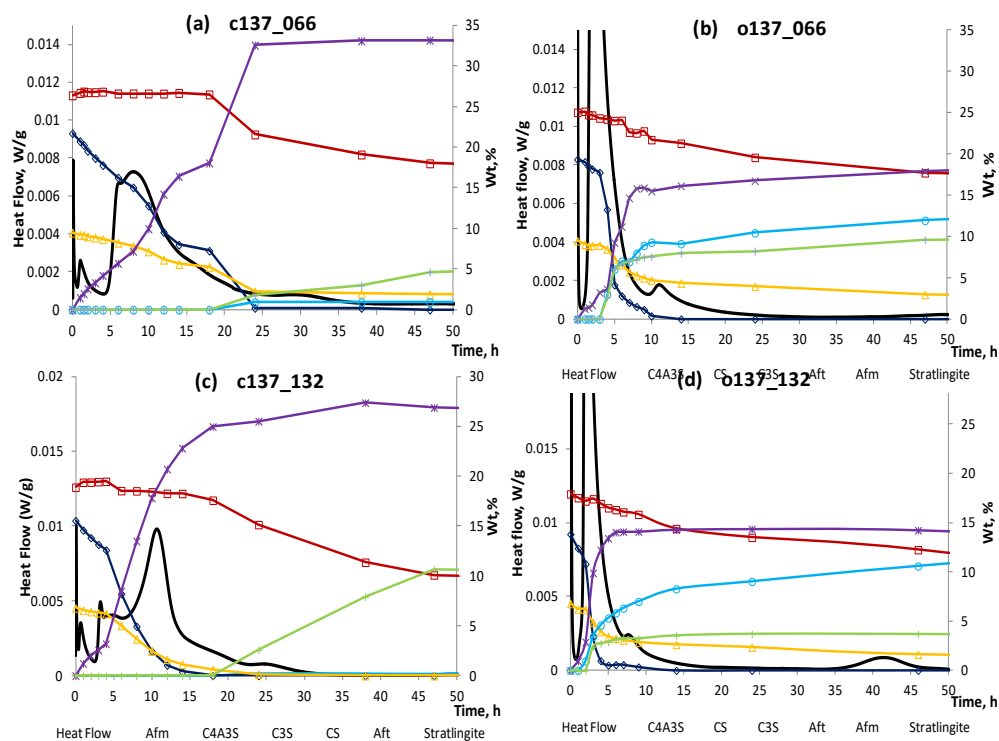


**Figure 4.17.** Heat flow and mineralogical in-situ hydration evolution of (a and c) c137 and (b and d) o137. In each plot, the left-hand vertical axis shows the rate of heat release, and the right-hand vertical axis shows the weight percent amount of the phases. Black line: Heat flow, blue diamond:  $C_4A_3S$ , yellow triangle: Cs, red square:  $C_3S$ , purple asterisk: Aft, light blue circle: AFm and green cruise:  $C_2ASH_8$ .

**Table 4.12.** Degree of reaction of ye'elimite in all the samples calculated from calorimetric data at 25 minutes (0.4 hours).

Samples	w/s ratio	Degree of reaction
		$\alpha_{0.4h}, \%$
c137	0.66	0.8
	1.32	1.0
o137	0.66	1.4
	1.32	1.8
c274	0.59	0.8
	1.19	0.9
o274	0.59	1.3
	1.19	1.5



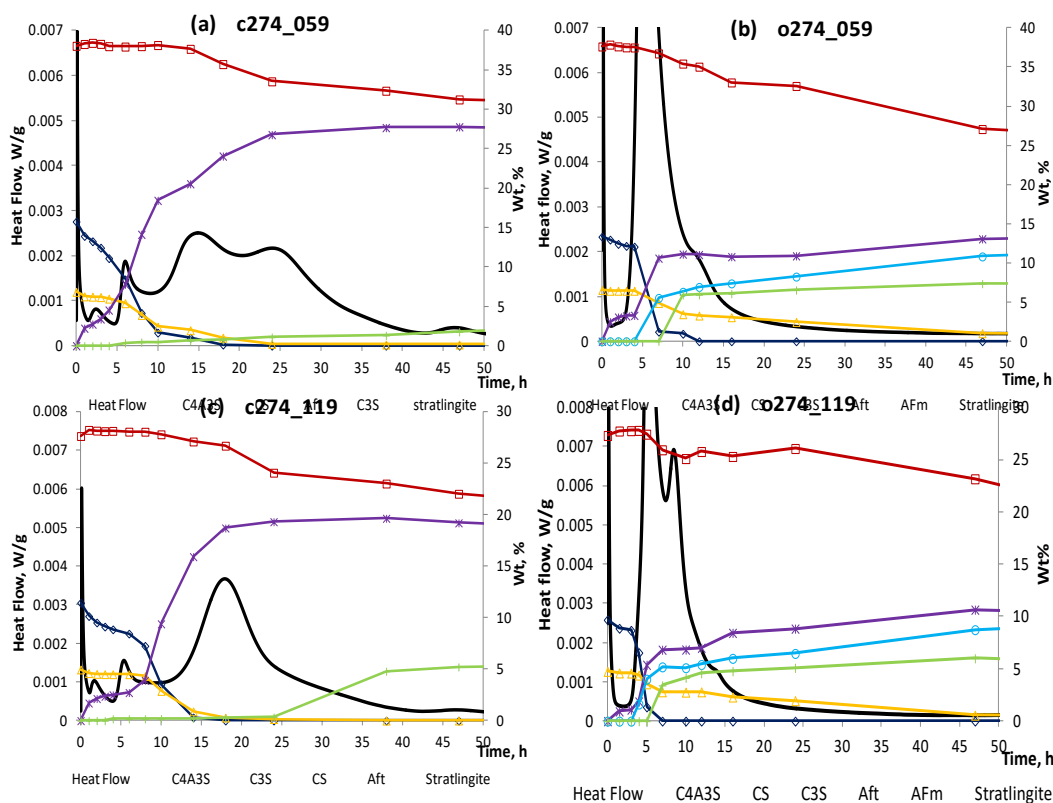


**Figure 4.18.** Heat flow and mineralogical in-situ hydration evolution of (a and c) c274 and (b and d) o274. In each plot, the left-hand vertical axis shows the rate of heat release, and the right-hand vertical axis shows the weight percent amount of the phases. Black line: Heat flow, blue diamond:  $C_4A_3S$ , yellow triangle: Cs, red square:  $C_3S$ , purple asterisk: AFt, light blue circle: AFm and green cruise:  $C_2ASH_8$ .

The degree of reaction of ye'elimitite determined by RQPA is given in Table 4.13. It is worth to highlight that the degree of reaction of ye'elimitite at 25 minutes is much prone to errors due to the low variation in percentages. Consequently, it has not been calculated. The degree of reaction of orthorhombic ye'elimitite in all the mixtures is higher than that of pseudocubic after 5 hours of hydration, confirming the slower pace of hydration of the latter. It is important to highlight that during the induction period, small amounts of ettringite were precipitated

without the dissolution of anhydrite, as previously published [101,148,149]. After that period at around 1.5 and 5 h for o137 and c137, respectively, a fast formation of ettringite jointly with dissolution of ye'elimite and anhydrite was detected.

**Table 4.13.** Degree of reaction (%) of ye'elimite in each mixture at selected times calculated from RQPA.

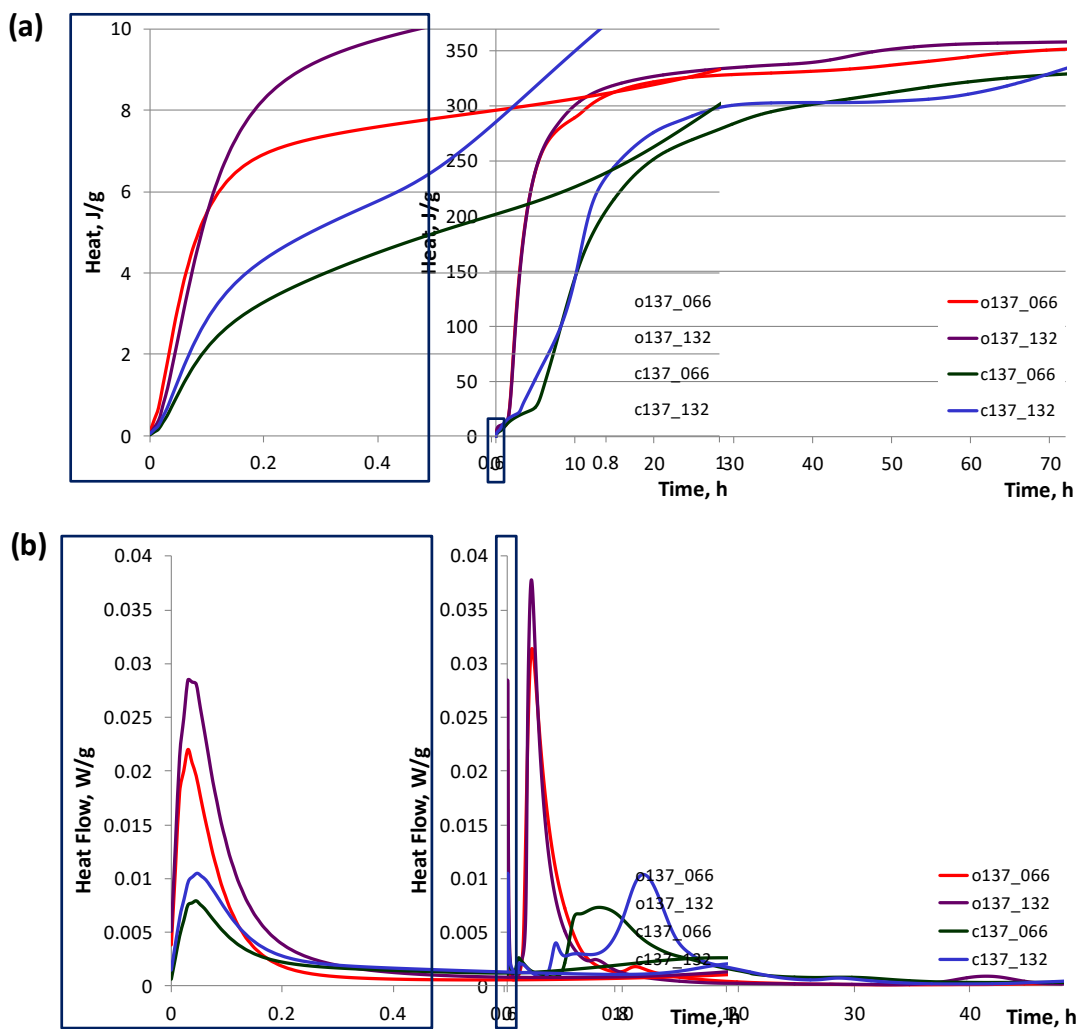
Samples	w/s ratio	$\alpha_{1.5h}$	$\alpha_{5h}$	$\alpha_{10h}$	$\alpha_{18h}$	$\alpha_{48h}$
c137	0.66	6.7	21.4	41.1	66.6	100
	1.32	8.3	32.9	84.2	100	100
o137	0.66	4.3	78.6	98.1	100	100
	1.32	15.9	95.8	100	100	100
c274	0.59	6.9	24.6	69.1	99.1	100
	1.19	8.4	38.3	89.5	100	100
o274	0.59	11.6	47.4	93.2	100	100
	1.19	16.8	86	100	100	100

Figure 4.19 show (a) the cumulative heat and (b) the heat flow for o137 and c137 mixtures. A broad signal of heat flow between 5 to 25 hours (Figure 4.17a and Figure 4.17c) and a sharp peak between 0.5 and 10 hours (Figure 4.17b and Figure 4.17d) were detected from hydration of c137 and o137, respectively. The total heat at 10 h of hydration was ~150 J/g and ~300 J/g, for pseudocubic and orthorhombic bearing mixtures, respectively, showing again the slower hydration kinetic of mixtures with pseudocubic ye'elimite.

In addition, the calculated total heat from RQPA was estimated by considering the total heat flow evolved for pure phases. Orthorhombic- $C_4A_3S$  and pseudocubic- $C_4A_3S$ , according to Eq. 1 (*Introduction Section*), would release ~575 and ~550 J/g [101], respectively. Moreover, alite releases 517 J/g [4], according to Eq. 12. Figure 4.20 shows both the experimental (calorimetry) and calculated (XRPD) total heat (cumulative), where the similarity is reasonably satisfactory.



where both  $x$  and  $y$  may vary over a wide range.



**Figure 4.19.** a) Total heat (cumulative) and b) heat flow curves of c137 and o137.

The insets of the Figures (left side) correspond to the first minutes of hydration

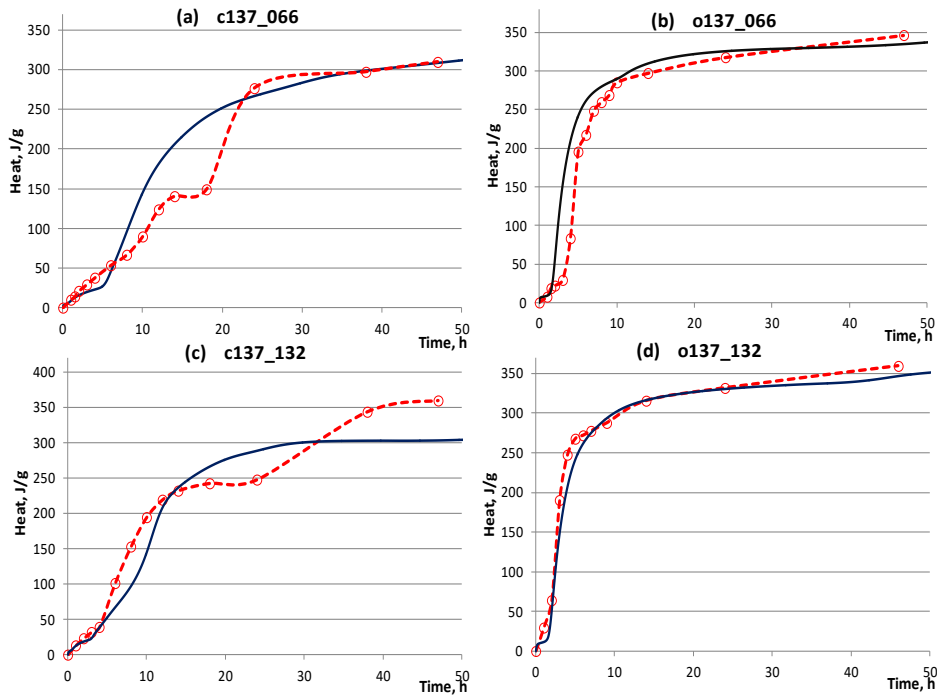
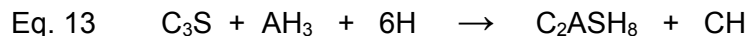


**Figure 4.20.** Comparison between measured (blue solid line) and calculated with RQPA results (red dash line) of heat for c137 and o137 mixtures at different water/solid ratios.

In o137 mixtures, some amounts of AFm-type phases (as monosulfoaluminate and stratlingite) also crystallized at early age (4 and 2 hours of hydration for w/s of 0.66 and 1.32, respectively), Figure 4.17. As reported by Winnefeld & Barlag [144] and Cuesta *et al* [101], the slow dissolution of anhydrite releases very little sulfate ions to the pore solution (unsaturated pore solution), favoring the formation of monosulfoaluminate, instead of ettringite. The amount of AFt in c137 mixtures was higher than in o137 samples at any time due to the formation of monosulfoaluminate in the latter mixtures.

The stratlingite comes from the amorphous aluminum hydroxide and partial dissolution of alite (Eq. 13), starting its precipitation close to 4 h in o137 mixtures. Furthermore, in c137 mixtures, the stratlingite formation started at 18 h when the mayor dissolution of alite occurs. Monosulfoaluminate was not observed at any

time as a consequence of the slow dissolution pace of both pseudocubic ye'elimite and anhydrite.



In general, the formation of stratlingite was observed in heat flow curves as a hump at ~8 and ~18 hours of hydration, for o137 and c137, respectively (Figure 4.17). The formation of stratlingite was enhanced by the rapid dissolution of orthorhombic ye'elimite, releasing amorphous aluminum hydroxide that moves the equilibrium to the right in Eq. 13. In both systems (c137 and o137), the increase of w/s ratio favored the dissolution and reactivity of C<sub>3</sub>S and C<sub>4</sub>A<sub>3</sub>S, Table 4.13. When w/s ratio raised from 0.66 to 1.32, the degree of reaction of C<sub>4</sub>A<sub>3</sub>S increased significantly, allowing the C<sub>3</sub>S to start reacting. However, the total heat after 48 hours of hydration of these samples, independently of the w/s used, was ~300 J/g and ~350 J/g, for c137 and o137, respectively, Figure 4.19a.

Figure A1 and Figure A2 (see Annex II) show the RQPA (in-situ SXRPD) of mixtures with 1.37 and 2.74 alite/ye'elimite ratios, respectively, where ACn and free water contents are included, as well as the RQPA at 7 days (from the in-situ SXRPD study). The main hydrated phases from C<sub>3</sub>S were stratlingite and C-S-H gel. The latter was quantified as part of ACn.

Samples c274 and o274 showed the same mineralogical phase assemblage and same tendency exhibited by the previous detailed samples, where orthorhombic ye'elimite reacts much faster than pseudocubic form, Figure 4.18. Figure 4.21 shows total heat and heat flow curves for c274 and o274 at different w/s ratios. At 15 h, when both ye'elimites have completely reacted, Table 4.12 and Table 4.13, and the total heat released for c274 and o274 were ~70 and ~200 J/g, respectively.

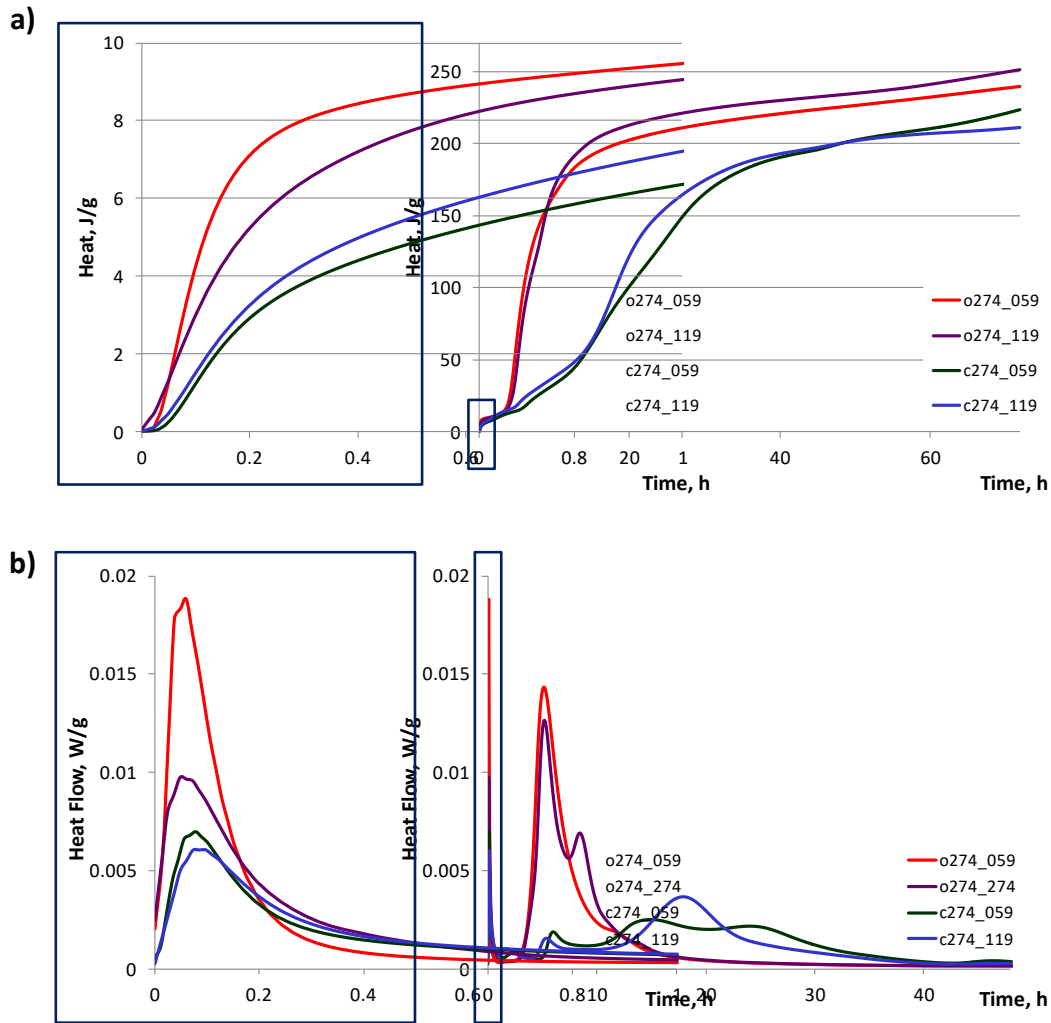


**Figure 4.21.** a) Total heat (cumulative) and b) heat flow curves of c274 and o274.

The insets of the figures (left side) correspond to the first minutes of hydration

The cumulative heat displayed after 48 h by c274 and o274, independently of the w/s used, were about ~200 and ~230 J/g respectively. Similar as in the previous mixtures, during the induction peak a small amount of AFt crystallized without the dissolution of Cs. Monosulfoaluminate was not detected in the pseudocubic ye'elimite mixtures. However, in o274 mixtures, the precipitation of AFt increased considerably jointly with monosulfoaluminate co-precipitation, after the induction

peak around at 4 h, Figure 4.18 and Figure A2 (Annex II) The raise of water/solid ratio from 0.59 to 1.19 did not affected the mixtures with orthorhombic ye'elinite. However, in the mixture with the pseudocubic form, both alite dissolution and precipitation of stratlingite are enhanced, were larger amounts of stratlingite were precipitated. This may be justify by the availability of water.

The mineralogical composition of all samples at 7 hydration days (168 hours) is given in Table 4.14. Analyzing Table 4.14, Tables A1-A8 (Annex II) and Figures A1-A2 (Annex II), it can be observed that the amount of AFt slightly decreases and monosulfoaluminate was formed (Eq. 5) due to the rich siliceous environment caused by the dissolution of C<sub>3</sub>S and formation of C-S-H, as reported by Trauchessec *et al* [145] and Chitvoranund *et al* [72]. A similar effect was observed in samples of BAY cements [74,118], where a high amount of C<sub>3</sub>S and C<sub>2</sub>S were reacting.

**Table 4.14.** Mineralogical composition in weight (wt%) at 7 days (168 hours) of *in-situ* SXRPD hydration study.

Sample w/s ratio	c137		o137		c274		o274	
	0.66	1.32	0.66	1.32*	0.59	1.19	0.59	1.19
<b>Phases</b>								
AFt	32.7(1)	24.4(1)	21.5(1)	11.0(3)	25.6(2)	15.1(1)	15.3(2)	9.2(3)
AFm	0.7(2)	0.5(1)	15.7(2)	18.3(2)	-	5.4(2)	14.7(3)	9.7(4)
Stratlingite	8.2(3)	9.8(2)	9.9(4)	3.2(5)	6.2(6)	6.7(3)	7.1(5)	5.3(5)
C <sub>3</sub> S	14.3(4)	7.9(3)	15.4(3)	1.2(2)	27.7(4)	14.0(5)	20.2(4)	1.2(3)
Hemicarbonate	0.1(1)	1.3(1)	-	1.9(2)	0.7(1)	1.4(1)	-	2.0(1)
Cs	1.4(1)	-	1.3(1)	-	0.2(2)	-	0.3(1)	-
CH	-	-	-	-	-	0.6(1)	-	3.6(1)
ACn + FW	42.6(1)	56.0(1)	36.2(1)	62.9(1)	39.7(1)	56.7(1)	42.4(1)	68.9(1)

\*Also 1.3(1) of C-S-H as clinotobermorite.

It is noticeable that crystalline portlandite and gibbsite were not detected in the first 48 h of hydration in any system (c137, o137, c274 and o274). The lack of precipitation of CH was expected and it is associated to the enhanced hydration of C<sub>4</sub>A<sub>3</sub>S that favors the early-AFt formation [102,103,150]. Moreover, the lack of

crystalline  $AH_3$  is associated with the formation of stratlingite (Eq. 13) [105,151]. A small amount of crystalline portlandite was detected, only after 7 days of hydration in the in-situ study, in the samples c274 and o274 prepared at a w/s ratio of 1.19, see Table 4.14. This is correlated with the higher amounts of  $C_3S$  and water that favors the formation of C-S-H (as a gel) and CH. As previously discussed, pseudocubic ye'elimite mixtures produced higher amounts of ettringite than orthorhombic ye'elimite samples, under similar hydrating conditions. This is due to orthorhombic ye'elimite presents a higher kinetic of hydration than pseudocubic ye'elimite, consequently when orthorhombic ye'elimite reacts with the anhydrite slow dissolved, favors the jointly formation of Aft and monosulfoaluminate

Table 4.15 shows the degree of hydration of alite in all samples; as mentioned before, by increasing the water-to-solid ratio to double (from 0.66 and 0.59 to 1.32 and 1.19, respectively), the hydration of alite was favored, achieving up to 95% of hydration degree and an increment on the ACn content, see Table 4.14, Tables A1-A8 (Annex II) and Figures A1-A2 (Annex II).

**Table 4.15.** Hydration degree of alite at 24, 48 hours, and 7 days from RPQA

Samples	w/s ratio	$\alpha_{24h}, \%$	$\alpha_{48h}, \%$	$\alpha_{7d}, \%$
c137	0.66	20	29	39
	1.32	20	32	58
o137	0.66	22	32	46
	1.32	25	47	92
c274	0.59	12	18	27
	1.19	11	20	49
o274	0.59	11	25	46
	1.19	13	28	95

These results indicate that alite reactivity is clearly influenced by the kinetics of reaction of ye'elimite. Stratlingite formation only occurred during the first 48 h, later it was not seen significant precipitation increase, see Tables A1 to A8 in the



Annex II. The change of  $C_3S/C_4A_3S$  ratio from 1.37 to 2.74 favors the AFt degradation to monosulfoaluminate, at 7 days. These systems of samples showed a high competition between the hydration of ye'elimite, anhydrite and alite. Due to slower hydration of pseudocubic ye'elimite and anhydrite, the alite hydration is retarded and permitted the stabilization and high precipitation of AFt. While the high hydration kinetic of orthorhombic ye'elimite with the slow dissolution of anhydrite, promoted the monosulfoaluminate formation (due to the lack of sulfate in the environment), likewise dissolution of alite at early age giving stratlingite and amorphous C-S-H. Owing the increment of  $C_3S/C_4A_3S$  ratio from 1.37 to 2.74, the cumulative heat flows decreased in  $\sim 120$  and  $\sim 100$  J/g for the samples with orthorhombic and pseudocubic ye'elimite respectively.

## 4.2. *Ex-Situ* hydration study

For the sake of comparison, two selected samples were hydrated during 7 days by *ex-situ* technique (LXRPD) as detailed in the Chapter 1 *Materials and Methods*. The selected samples were c137\_132 and o137\_132. These samples (after stopping the hydration) were characterized by LXRPD, TG-DTG and  $^{29}\text{Al}$  and  $^{27}\text{Si}$  NMR. Table 4.16 shows the comparative of mineralogical content of those samples at 7 days by *in-situ* and *ex-situ* hydration methodologies. Comparing the results, it is clear that the same products of hydration were formed, but the methodology of preparation affected their percentage [142]. Furthermore, it has to be highlighted that not only the hydration methodology affects; the use of quartz as internal standard (added to anhydrous samples) enhanced the reactivity of all phases in the in-situ hydration study, giving higher amorphous contents and AFm in the case of o137\_132. For example, 19.5(4) wt% of Aft were detected in o137\_132 by *ex-situ* method, and by *in-situ* method 11.0(3) and 18.3(2) wt% of AFt and AFm were quantified, respectively. Stratlingite precipitation was improved when *ex-situ* hydration was used, given 20.5(7) and 12.5(8) wt% in o137\_132 and c137\_132 respectively.

**Table 4.16.** Comparative mineralogical composition of c137\_132 and o137\_132 at 0 and 7 days

Phases	o137_132		
	<i>t = 0h</i>	<i>in-situ</i>	<i>ex-situ</i>
C <sub>4</sub> A <sub>3</sub> S	13.8 (1)	-	-
Cs	6.8 (1)	-	-
C <sub>3</sub> S	17.9 (4)	1.2(2)	4.0(3)
AFt	-	11.0(3)	19.5(4)
AFm	-	18.3(2)	1.4(1)
C <sub>2</sub> ASH <sub>8</sub>	-	3.2(5)	20.5(7)
HemiCO <sub>3</sub> *	-	1.9(2)	2.2(2)
C-S-H**	-	1.3(1)	2.2(2)
ACn+FW	4.6(1)+56.9 <sup>a</sup> =61.5	62.9(2)	21.8(2)+28.5 <sup>b</sup> =50.3
c137_132			
	<i>t = 0h</i>	<i>in-situ</i>	<i>ex-situ</i>
C <sub>4</sub> A <sub>3</sub> S	15.5 (1)	-	-
Cs	6.8 (1)	-	-
C <sub>3</sub> S	18.9 (3)	7.9(3)	11.0(3)
AFt	-	24.4(1)	23.7(4)
AFm	-	0.5(1)	0.9(1)
C <sub>2</sub> ASH <sub>8</sub>	-	9.8(2)	12.5(8)
HemiCO <sub>3</sub> *	-	1.3(1)	1.2(1)
ACn+FW	1.9(1)+56.9 <sup>a</sup> =58.8	56.0(1)	17.1(2)+33.5 <sup>b</sup> =50.7

\*HemiCO<sub>3</sub> as hemicarbonat (AFm)

\*\* C-S-H as clinotobermorite

a. Theoretical free water content

b. Free water calculated from TG-DTG analysis

Figure 4.22 shows the thermogravimetric curves of c137\_132 and o137\_132 at 7 days after *ex-situ* hydration and stopping procedure. The first mass loss observed between 50 and 130 °C is assigned to dehydration of ettringite and C-S-H [105,118,143,144]. Its individual identification and quantification for a comparative analysis with RQPA results was not possible due to their overlapping. A second mass loss region between 130 and 220 °C is assigned to dehydration of AFm-type phases [48,118,144]. AFm-type phases in these samples, according with the results of LXRPD (Table 4.14), were considered as

monosulfoaluminate and stratlingite. Being the mass loss signal centered on  $\sim 180$  °C corresponds to the dehydration of stratlingite (marked as an asterisk in Figure 4.22) [56,118,152,153]. The mass loss from between 230 and 320 °C is related to the dehydroxilation of aluminum hydroxide [118,144,154]. This aluminum hydroxide obviously is amorphous since it was not detected in LXRPD (see Table 4.14). Nevertheless, portlandite was not identified by TG-DTG, as expected, which presents a typical dehydroxilation loss around 450 °C [153,155,156]. This confirms that CH favors the early formation of AFt (Eq. 4) [105,109,150] and later reacts with  $AH_3$  and AFt to produce AFm-type phases (Eq. 5) [72,103,145]. The total mass loss associated with bonded water (from room temperature up to 600 °C) for c137\_132 and o137\_132 were  $\sim 35.1$  and  $\sim 39.7$  wt% respectively, while the mass loss associated with decarbonation process were  $\sim 0.9$  and  $\sim 1.3$  wt%, respectively. These values are in agreement with the results from LXRPD (Table 4.14).

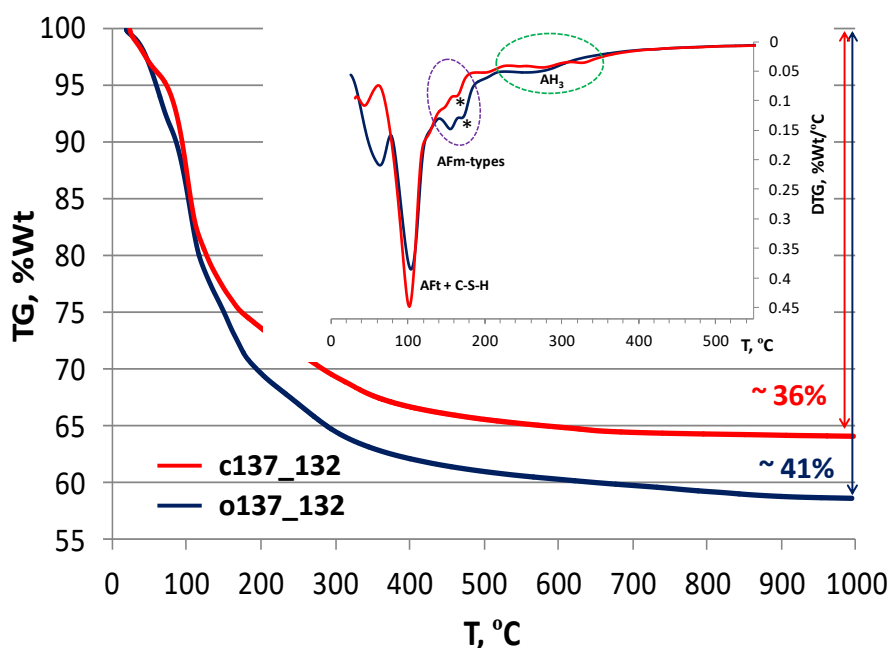


**Figure 4.22.** TG-DTG of c137\_132 and o137\_132 at 7 curing days.

\* Stratlingite as AFm-type phase

Figure 4.23 and Figure 4.24 gives  $^{27}\text{Al}$  and  $^{29}\text{Si}$  MAS-NMR spectra and the deconvolution signals of c137\_132 and o137\_132 at 7 days of hydration, respectively. Table 4.17 presents a summary of the mineralogical content detected by NMR spectra and their related composition. In a general view,  $^{27}\text{Si}$  NMR spectrum (left side of Figure 4.23) presents two wide regions: one between -67 to -76 ppm related to  $\text{Q}^0$  (isolated  $\text{SiO}_4$  tetrahedron) of anhydrous alite [157–159], and another one between -77 to -90 ppm associated with  $\text{Q}^n$  ( $n = 1, 2$  or  $3$ , refers to the number of tetrahedrons linked by oxygen bonds to the previous tetrahedron [159]) of C-S-H and  $\text{Q}^2$  of stratlingite [157–162].  $^{29}\text{Al}$  NMR spectrum (right side of Figure 4.23) shows a small peak at 61.4 ppm (mark as asterisk in Figure 4.23) attributed to tetrahedrally ( $\text{Al}^{\text{IV}}$ ) coordinated aluminum of stratlingite [142,161]; two intense signals around 13 ppm are related to AFt and between 11.8 to 8 ppm are associated with  $\text{Al}^{\text{VI}}$  in AFm-type phases and amorphous  $\text{AH}_3$  [98,148,161,163–168].

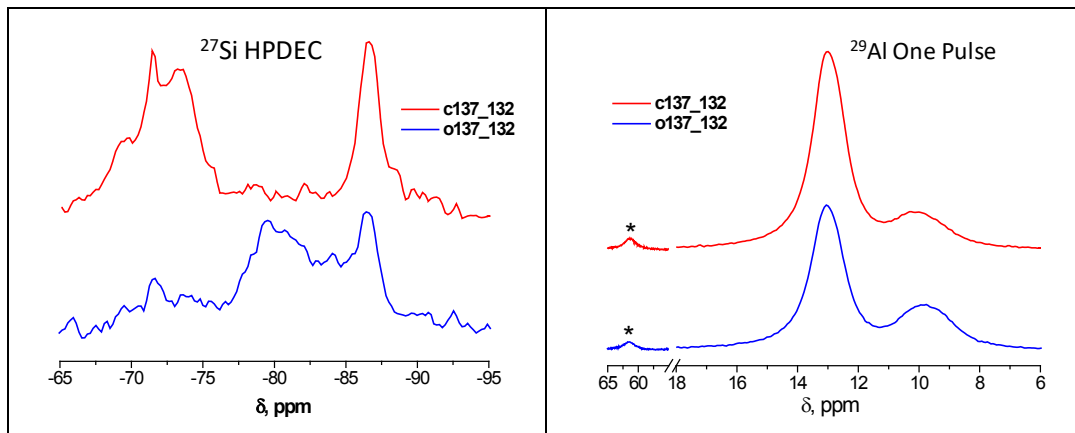


**Figure 4.23.**  $^{27}\text{Si}$  HPDEC (left) and  $^{29}\text{Al}$  One pulse (right) MAS-NMR spectra of stopped-pastes of c137\_132 (blue) and o137\_132 (red) at 7 curing days.  
\*Stratlingite signal ( $\text{Al}^{\text{IV}}$ ).

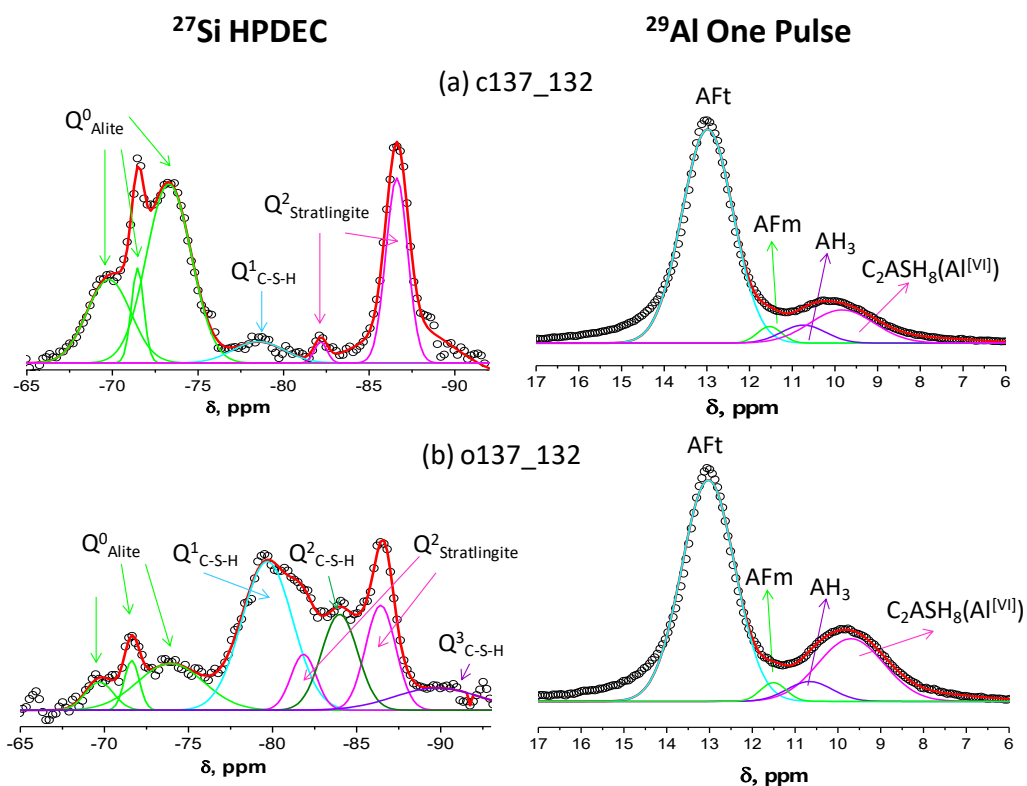


**Figure 4.24.** Deconvolution of  $^{27}\text{Si}$  (left) and  $^{29}\text{Al}$  (right) MAS-NMR spectra of (a) c137\_132 and (b) o137\_132 at 7 days of hydration. Each spectrum includes experimental (dots) and its deconvoluted spectrum (red line) with individual contribution from each sites.

**Table 4.17.** Relative area percentages (%) from deconvolution of  $^{29}\text{Si}$  and  $^{27}\text{Al}$  MAS-NMR spectra of c137\_132 and o137\_132 pastes

Samples	$^{29}\text{Si}$ MAS-NMR			$^{27}\text{Al}$ MAS-NMR			
	$\text{C}_3\text{S}$	$\text{C}_2\text{ASH}_8$	C-S-H	AFt	AFm	$\text{AH}_3$	$\text{C}_2\text{ASH}_8$
c137_132	70.6	23.4	6.0	70.9	2.6	5.1	21.4
o137_132	23.3	11.5	52.1	64.0	2.6	4.9	28.6

For c137\_132, six chemical shifts were observed by  $^{27}\text{Si}$  HPDEC-MAS-NMR and their related positions are presented in the left side of Figure 4.24a. Peaks at around -70.0, -71.5, -73.5 ppm were related to  $\text{Q}^0$  of alite [157–159]. Peaks

detected at around -79.0, -82.2 and -86.6 were correlated to  $Q^1$  of C-S-H [157–159,162,169], and  $Q^{2(2Al)}$  and  $Q^2$  of stratlingite [161,163,165], respectively. Eight chemical shifts were observed for o137\_132 by the same technical characterization ( $^{27}Si$  HPDEC-NMR). Their related positions are deconvoluted in the left side of Figure 4.24b.  $Q^0$  species of alite were also found at -70.0, -71.5, -73.5 ppm.  $Q^1$ ,  $Q^2$  and  $Q^3$  species of C-S-H were found at -79.0, -84.0 and -89.8 ppm, respectively [157–159].  $Q^3$  indicates a more densely cross-linked silicate network in C-S-H with lower Ca/Si ratios [157,169]. In addition,  $Q^{2(2Al)}$  and  $Q^2$  species of stratlingite were detected at around -82.2 and -86.6 ppm respectively. From Table 4.17 it can be observed that c137\_132 and o137\_132 samples presented a non-hydrated alite relative content of 71 and 23% (relative area percentage), respectively. These values are in agreement with the results of LXRPD (Table 4.16), where non-hydrated alite represents a 58.2 and 22.3 % of total  $C_3S$  in the samples c137\_132 and o137\_132, respectively. Moreover, the amount of amorphous C-S-H gel determined by MAS-NMR study is ~6 and 52% (relative area percentage), Table 4.17, for c137\_132 and o137\_132, respectively. From this last result, the peak centered on ~110 °C in TG-DTG (Figure 4.22) is mainly to the decomposition of AFt in c137\_132, while in o137\_132 may be due to the latter but also to the decomposition of amorphous C-S-H gel. The MAS-NMR study has unraveled that, for the same w/c ratio, the reaction of alite is strongly influenced by the chemical environment. In the orthorhombic ye'elimite sample, the formation of jointly AFm with AFt reduces the amount of amorphous  $AH_3$ . This fact has a strong effect in the hydration products from alite being amorphous C-S-H gel formation clearly favored, instead of stratlingite, Table 4.17. In terms of mechanical strengths, this mixture should develop higher mechanical strengths.

Four chemical shifts were identified in  $^{29}Al$  One pulse MAS-NMR spectra (right side of Figure 4.24), in both samples. Their relative position and contributions are presented in Figure 4.24 and Table 4.17 respectively. A narrow signal at 13.0 ppm was assigned to ettringite [98,164–166] and broader signals at 11.5, 10.7

and 9.7 ppm correspond to AFm,  $AH_3$  and octahedrally coordinated aluminum ( $Al^{VI}$ ) of stratlingite, respectively [98,142,161,164,167]. From Table 4.17, Aft presented the main differences of areas between c137\_132 and o137\_132. In c137\_132 corresponds to 71%, while in o137\_132 corresponds to 64% (relative area percentage). These results are in agreement with LXRPD results, where c137\_132 produces more ettringite than o137\_132, Table 4.16. Additionally, the relative content of stratlingite was 21 and 29% for c137\_132 and o137\_132, respectively, in agreement with LXRPD and TG-DTG results.

### 4.3. Summary

On the basis of the study performed in this chapter the following conclusions can be drawn:

1)  $C_3S$  hydration was influenced by the kinetic of ye'elimite dissolution and reaction, and it began to react after ye'elimite reacted completely. In mixtures with orthorhombic and pseudocubic ye'elimite, alite depletion started after 10 and 20 hours respectively, since orthorhombic ye'elimite reacts faster than the pseudocubic polymorph. The main products from alite reaction were stratlingite and amorphous C-S-H gel. The formation of calcium hydroxide (as portlandite or amorphous) was not detected, as expected. The w/s ratio also affected the kinetic of hydration of alite. The mixtures with orthorhombic ye'elimite and higher w/s ratio presented, after 7 days, a higher hydration degree. Consequently, higher amounts of C-S-H and stratlingite were obtained. The mixtures with pseudocubic ye'elimite, even after 7 days of hydration, presented high amounts of non-reacted  $C_3S$ . Moreover, the main hydration product from the reaction of alite is stratlingite, while in the orthorhombic ye'elimite sample, the main phase is amorphous C-S-H gel.

2) By calorimetry, the hydration of both system is characterized by an initial period and induction period, followed by a maxima signals associated with the main hydration. In mixtures with pseudocubic ye'elimite the maxima signal was

displayed as a wide maxima signal, due to the retarded hydration of this ye'elimite. However, this effect favors the stability and amount of ettringite. The maxima signal in mixtures with orthorhombic ye'elimite was exhibited as a narrow peak associated with the quick precipitation of AFt, favoring the jointly formation of AFm (as monosulfoaluminate).

The results obtained in this chapter can be compared with those of BAY-cement pastes (Chapter 3 *BAY cement hydration and mechanical behavior*), and here, many hypotheses have been clarified. The dependence of  $C_3S$  hydration on the kinetic of hydration of ye'elimite justifies the presence of alite in BAY-pastes systems after 7 days of hydration. In those systems, the main hydration product of alite reactivity is stratlingite followed by C-S-H gel. Calcium hydroxide is not precipitated from  $C_3S$ , due to the formation of AFt at early ages and AFm-type phases at later ages. Katoite phase was not detected in the mixtures studied in this chapter. Consequently, in the BAY-pastes katoite should come from the hydration of  $C_2S$  and the joint reaction between  $C_3S$  and  $C_4AF$ .

All these results have allowed to fulfill the specific objective of understanding of effect of w/c ratio and alite/ye'elimite ratio on the hydration mechanism on alite-ye'elimite systems and permitted correlate these results with the hydration behavior of BAY.



## 5. Influence of Fly Ash addition on BAY cement hydration and properties

This chapter presents a study of the effect of class F - fly ash (FA) on the mineralogical and mechanical behavior of the laboratory prepared BAY cement. This study was carried out on pastes and mortars of FA#BAY samples (where # corresponds to 0, 15 and 30 wt% of FA referred to the total solid content) at the constant water-to-cement ratio of 0.4. FA#BAY mixtures presented a trimodal particle size distribution, where their  $D_{v50}$  and  $D_{v90}$  increased with the presence of FA. That is due to the larger size of fly ash compared with BAY-cement (Figure 5.25). The blended FA#BAY pastes and mortars were studied up to 180 days of hydration. Moreover, FA0BAY and FA30BAY cements were selected to be also hydrated at a w/c of 0.57, with the aim of understanding the w/c effect (the latter corresponds a w/s of 0.40). The potential pozzolanic effect was analyzed by RQPA, isothermal calorimetry, thermogravimetric analysis, mercury intrusion porosimetry (MIP) and MAS-NMR spectroscopy in FA#BAY pastes and compressive strength measurements in FA#BAY mortars. The effect of the FA on the fresh pastes and the optimization of the superplasticizer content was studied through rheological measurements. Part of this work has been published in *Influence of Fly Ash blending on hydration and physical behavior of Belite-Alite-Ye'elimate cement* [136].



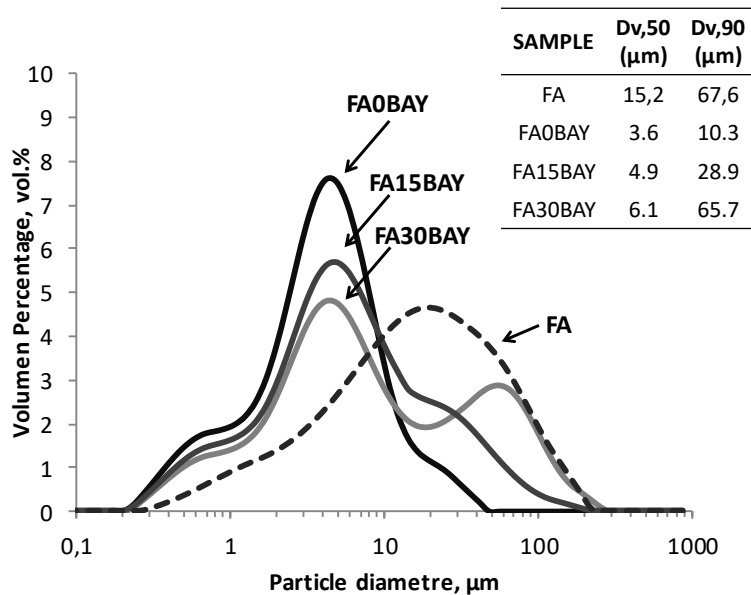


Figure 5.25. Particle size distribution of FA#BAY powders. Modified from [136].

## 5.1. Rheological behavior

As described in Chapter 3 *BAY cement hydration and mechanical behavior*, BAY paste (hereafter FA0BAY) prepared at w/c ratio of 0.4 needed the addition of superplasticizer, and the optimum amount of the studied polycarboxylate-based superplasticizer was 0.5 wt% referred to the solid (cement) content.

In this chapter, BAY pastes were prepared with different amounts of FA. Table 5.18 gives the amount of cement, FA and water used in the preparation of the three studied pastes. FA#BAY pastes were prepared at a constant w/c ratio of 0.4, giving a water-to-solid (w/s) ratio of 0.40, 0.34 and 0.28 for FA0BAY, FA15BAY and FA30BAY, respectively, they also needed the addition of SP. Thus, the percentage of SP was also optimized in FA15BAY and FA30BAY pastes through rheological studies.

**Table 5.18.** Proportion of cement, fly ash and water used in pastes.

<b>SAMPLE</b>	<b>w/c ratio</b>	<b>w/s ratio</b>	<b>Cement, wt%</b>	<b>FA, wt%</b>	<b>Water, wt%</b>
<b>FA0BAY</b>	0.40	0.40	71.4	0	28.6
	0.57	0.57	63.7	0	36.3
<b>FA15BAY</b>	0.40	0.34	63.4	11.2	25.4
<b>FA30BAY</b>	0.40	0.28	54.7	23.4	21.9
	0.57	0.40	50.0	21.4	28.6

Figure 5.26a and Figure 5.26b show the flow curves of FA15BAY and FA30BAY pastes, respectively, with different superplasticizer contents. Pastes without SP were not measured due to the heterogeneity of the samples and high viscosity, as it happened for FA0BAY.

In all pastes, the viscosity decreased by increasing the addition of SP down to a minimum value; after that, the viscosity was kept constant or even slightly increased. Moreover, when a low SP content, 0.2 wt%, was added, both pastes showed a wide thixotropic cycle (3290 and 4500 Pa/s for FA15BAY and FA30BAY pastes, respectively) and high viscosity; however, the thixotropic cycle is almost negligible when the SP content was close to the optimum one.

The evolution of the viscosity with the SP content can be observed on detail in Figure 5.27, where the deflocculation curves of both pastes, taken from the up-curves at the shear rate of  $100 \text{ s}^{-1}$ , are shown. From this figure, it can be observed how the viscosity of the pastes increased by increasing the FA content since the solid loading also increased. In FA15BAY-family, similar to FA0BAY-family (see Figure 3.10), samples with 0.4, 0.5 and 0.6 wt% SP show the lowest viscosity values (480, 420 and 430 mPa.s at  $100 \text{ s}^{-1}$ , respectively) and similar rheological behaviors, where the paste with 0.5 wt% SP also shows the smallest thixotropic cycle (217, 138 and 165 Pa/s for pastes with 0.4, 0.5 and 0.6 wt%, respectively), Figure 5.26.

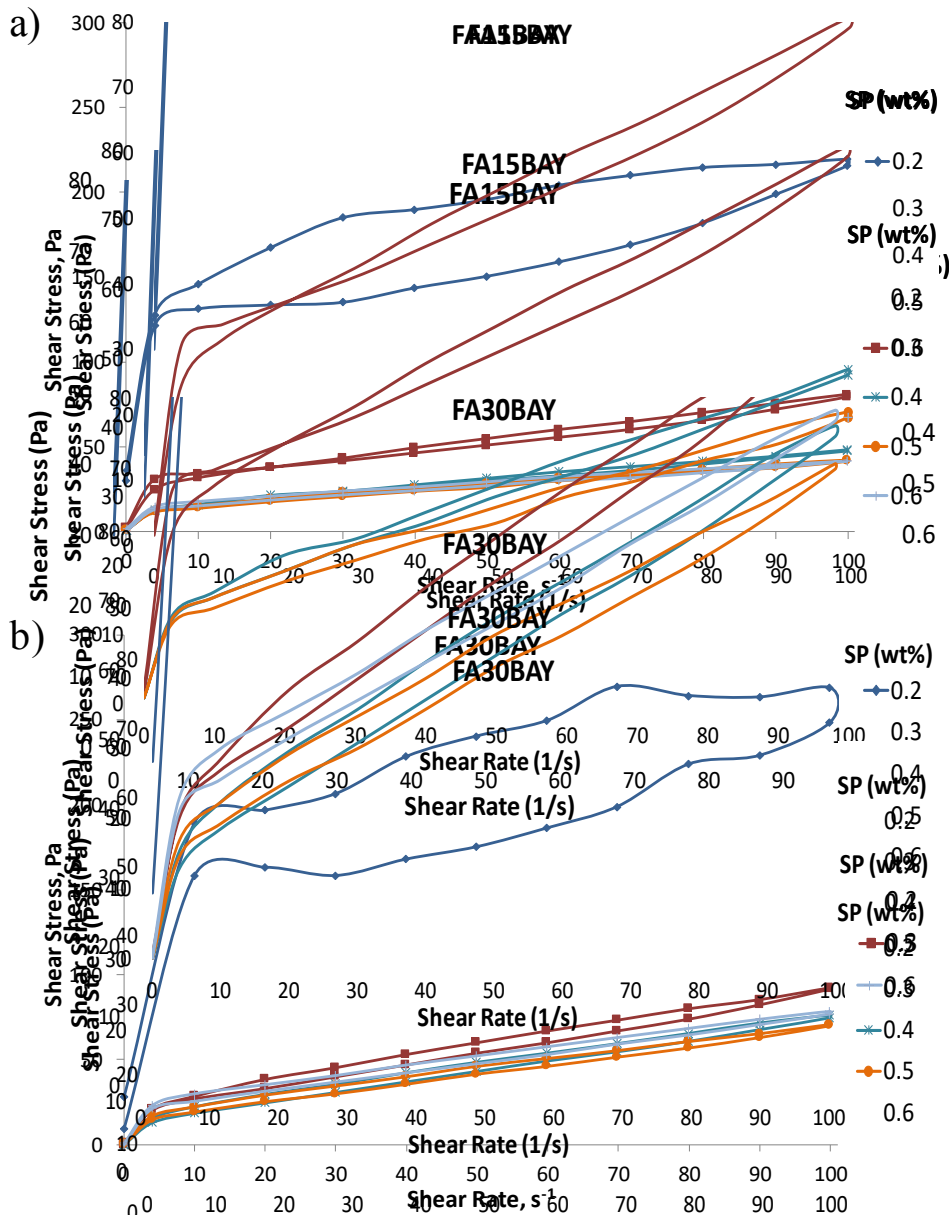


**Figure 5.26.** Flow curves of (a) FA0BAY, (b) FA15BAY and (c) FA30BAY pastes at  $w/c = 0.4$  and different superplasticizer contents. Taken from [136].

The same behavior is observed in FA30BAY-family, where the paste with 0.5 wt% SP shows the lowest viscosity and thixotropic cycle values. The viscosity in FA30BAY slightly increased when the SP content was raised up to 0.6 wt% (780 mPa.s). All these results made us to conclude that there is a range of SP content that will assure good dispersion of particles (from 0.4 to 0.6 wt%), where 0.5 wt% of polycarboxylate-based SP was the optimal amount for all FA#BAY pastes. It is worth to highlight that the particle size of the FA is higher than that of the cement, and consequently powder mixtures with higher FA contents will have higher particle sizes according to Figure 5.25. However, the optimized amount of SP in the three pastes is the same (or similar) between them, since it is related not only with the size of the particles, but also with their nature.

Pastes and mortars were prepared with the optimized amount of SP, 0.5 wt%, for further hydration and mechanical properties studies.

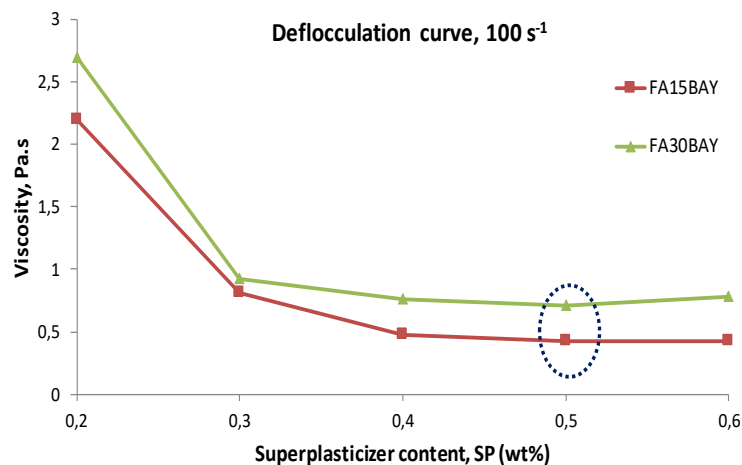


**Figure 5.27.** Deflocculation curves of FA15BAY (red) and FA30BAY (green) pastes at the shear rate of  $100 \text{ s}^{-1}$ . Modified from [136].

## 5.2. Isothermal calorimetric studies

### 5.2.1. Effect of superplasticizer on FA0BAY early-age hydration

The effect of the superplasticizer on the hydration of the BAY-cement pastes was studied. This study was carried out through isothermal calorimetric analysis and *in-situ* Mo-LXRPD (described in *Materials and Methods* section 1.3.1). The phase assemblage within the first hours of hydration obtained by *in-situ* RPQA-LXRPD and their heat flow are shown in Figure 5.28.

The heat displayed during the first 12 minutes, known as initial period, was associated with the partial dissolution of Cs,  $C_{12}A_7$ ,  $C_3S$  and  $C_4A_3S$ , and the quick early-precipitation of ettringite [144,149,170]. After 5 minutes of hydration, the sample without SP reaches a maximum heat flow of  $0.052 \pm 0.008$  W/g, while the sample with SP reaches about half of it ( $\sim 0.024 \pm 0.001$  W/g). That difference in the released heat is assigned to the effect of the SP on the aluminum-based phase rate dissolution and its corresponding hydrates precipitation. Previous works have reported that polycarboxylate-based superplasticizers have a retarder effect on the hydration of Al-rich phases in cement pastes [26,116,117]. Once the initial period finished, an induction period was not clear in these systems, giving directly a broad signal in the sample without SP (Figure 5.28a) and a hump in the sample with 0.5 w% SP (Figure 5.28b) centered at around 8 h in both samples. In both systems, the hydration of alite was slower than ye'elimite and mayenite, as expected when alite is in presence of aluminates phases [105,118,145,162].

This is in agreement with the results reported in the previous chapter (*Pure phase hydration study*). From this study, it can be highlighted that superplasticizer has had a retarder hydration effect on Cs and mayenite, while ye'elimite shows the same dissolution behavior in both systems. Thus, this type of SP seems to affect

the hydration of Al-bearing phases but not the hydration of ye'elite in this system.

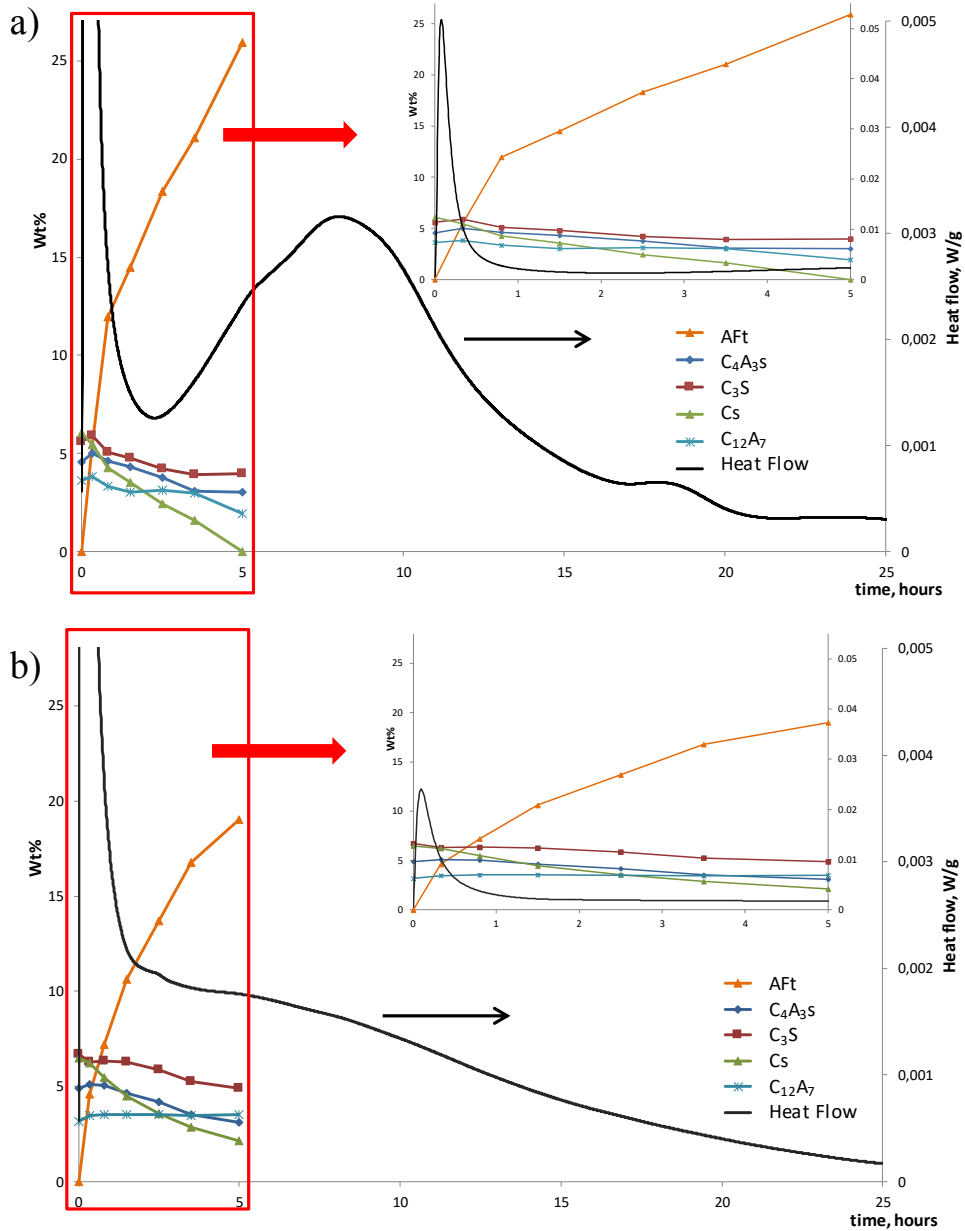


**Figure 5.28.** Phase evolution of FA0BAY paste prepared (w/c=0.40) (a) without superplasticizer and (b) with 0.5 wt% of superplasticizer. Isothermal calorimetric heat flow curves are shown as black lines. Taken from [136].

The total heat released by FA0BAY without and with SP is shown in Figure 5.29. It is clear that the addition of 0.5 wt% superplasticizer (referred to solid content) favors the slow down on the dissolution of  $C_{12}A_7$  and Cs and consequently, the released heat flow is lower. After 48 hours of hydration, a total heat of 130 J/g and ~180 J/g evolved by FA0BAY with and without SP, respectively, represents a ~28% of less heat.

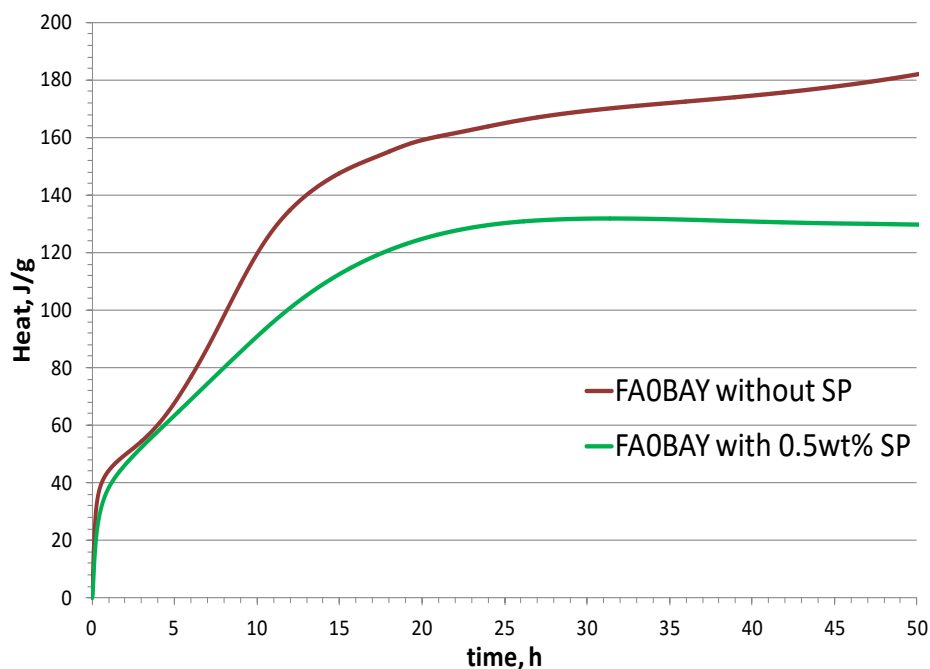


**Figure 5.29.** Cumulative heat released by FA0BAY prepared without (red line) and with (green line) superplasticizer.

### 5.2.2. Effect of FA substitution on heat released

The influence of the FA replacement on the heat released by BAY cement pastes was studied using isothermal calorimetry. The addition of FA changes both the rate of heat evolution and the total amount of heat evolved. Figure 5.30a and Figure 5.30b show the heat evolution and cumulative heat, respectively, of the three FA#BAY pastes prepared at a w/c constant ratio of 0.4 and 0.5 wt% of SP (referred to the total solid content). Calorimetry heat flows of the samples (Figure



5.30a) show two significant signals, the dissolution peak and a shoulder once the initial period finished. These data clearly show the effect of the addition of fly ash.

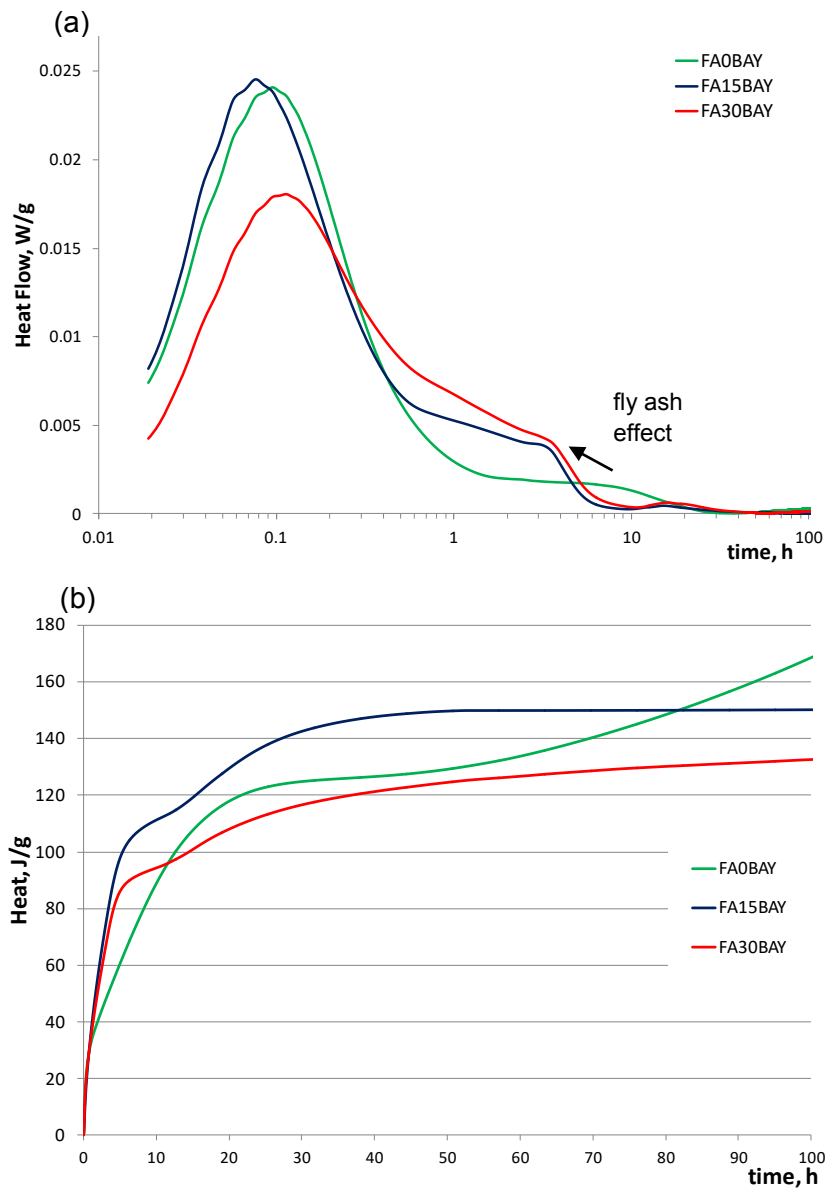


**Figure 5.30.** Normalized heat flow (a) and cumulative heat (b) per gram of solid for FA#BAY pastes prepared at a constant w/c of 0.4 and 0.5 wt% SP.

The first peak, Figure 5.30a, is associated with the partial dissolution of  $C_3S$ ,  $C_{12}A_7$ , Cs and  $C_4A_3S$ , and reached maximum values of  $\sim 24$ , 25 and 18 mW/(g of solid for FA#BAY), at 6, 5, and 6 minutes of hydration, for FA0BAY, FA15BAY and FA30BAY, respectively. It indicates that the released heat due to the dissolution of those phases was slightly favored when 15 wt% of FA was added, but it was lower when 30 wt% of FA was present. The second signal (shoulder), displayed in the calorimetric curves, was centered at 8 h for FA0BAY, and released  $\sim 0.002$  W/g; with the addition of FA, it was increased to  $\sim 0.005$  W/g and accelerated up to 3-4 h, indicating an increase on the early reactivity. Taking into account that FA does not react at early ages, the observed effect should be related to the nucleation effect of FA that favors the formation of hydrates, also known as filler effect [13,119,152,171,172]. Figure 5.30b shows the cumulative heat being higher at the first 10 h in FA15BAY and FA30BAY than FA0BAY (i.e. 111, 95 and 90 J/g, respectively). Moreover, after 36 hydration hours, the maximum cumulative heats of pastes with FA reached asymptote values of 145 and 120 J/g for FA15BAY and FA30BAY respectively, while FA0BAY continues growing up. Finally, at 72 h, the cumulative heat of FA#BAY were 170, 150 and 130 J/g for 0, 15 and 30 wt% of FA, respectively. These results could be explicated as follows: i) during the first 10 hours, the filler-nucleation effect of FA favors the precipitation of ettringite from aluminate-rich phases, ii) between 10 to 36 hours, there is an oversaturation of nucleation points, despite of the high availability of particles, acting hereafter as a phase content diluter and iii) from 36 h to 3 days,  $C_3S$  begins to react increasing the heat flow in FA0BAY, while in FA15BAY and FA30BAY,  $C_3S$  has reacted more quickly (through the first 24 hours of hydration).

### 5.3. Hydration studies of FA#BAY binders

The effects of the addition of fly ash on the hydration behavior of the pastes were studied up to 180 curing days. The results of RQPA and TG-DTG of pastes

hydrated at 1, 3, 7, 28, 90 and 180 curing days are shown in Table 5.19 and Figure 5.31 respectively. All pastes were prepared at a w/c ratio of 0.4 and with 0.5 wt% SP, as optimized before.

$C_4A_3S$  and  $C_3S$  totally disappeared after 1 and 7 days of hydration, respectively. Table 5.19, in all cement pastes. The hydration of ye'elimite with anhydrite forms ettringite (or monosulfoaluminate) and aluminum hydroxide (amorphous or crystalline gibbsite); while the hydration  $C_3S$  produces amorphous C-S-H gel and portlandite. However, crystalline aluminum hydroxide (called gibbsite) or crystalline portlandite were not detected by LXRPD. These data are in agreement with the results found in the pure phases mixtures studied before (see chapter 4 *Pure phase hydration study*). Moreover, crystalline CH was not detected by TG-DTG, except after 28 hydration days in FA0BAY, where a small endothermic signal around 450 °C was detected (Figure 5.31a). These results are in agreement with Winnefeld *et al* reports [102,151] where portlandite was not detected in systems associated with jointly content of ye'elimite, silicates and anhydrite. As mentioned before, portlandite favors the formation of AFm-type phases, i.e. monosulfoaluminate, stratlingite [102,103,105,118,142] and katoite [4] at later ages. In addition, the formation of AFm-type phases increase while AFt contents decrease from 28 to 180 days of hydration in FA0BAY, Table 5.19. The hydration of the silicon-bearing phases (alite and belite) has yielded a Si-rich environment where AFt is unstable [72,149]. Furthermore, in this system rich in silicon-bearing phases and aluminum hydroxide, the stratlingite crystallization was favored [4,106,142]. Moreover, the presence of stratlingite was detected even at 1 day in FA0BAY paste, and at 7 days in FA15BAY and FA30BAY pastes. This is in agreement with the TG-DTG results, Figure 5.31. In all cases, two typical decomposition groups of signals were found: i) the first one, between 50 to 120°C, assigned to the overlapped dehydration of C-S-H and AFt [102,105,118,143]; due to the overlapping of these signals is not possible to compare these results with those obtained by LXRPD. ii) The second group of signal corresponds to the dehydration of AFm-types phases, where the

dehydration of monosulfoaluminate happens between 120 and 180 °C [102,118,144], while the dehydration of stratlingite is located at 180 and 220 °C [48,106,118,152,173]. Although crystalline CH should be formed from the hydration of C<sub>3</sub>S, the formation of ettringite at first hydration hours could be favored from the Ca<sup>2+</sup> and OH<sup>-</sup> rich environment [102,105,109]. Later, when the calcium sulfate and ye'elimite have been reacted completely (after 24 h), portlandite reacts with aluminum hydroxide and AFt forming AFm-type phases [103,145]. For this reason, portlandite was not detected by TG-DTG, where its characteristic mass loss is centered on 450 °C [102,103,145].

Belite showed its typical hydration behavior, where only after 28 days, this phase started to react with water. But, in FA15BAY and FA30BAY this reaction was even lower than in FA0BAY (as an example, β-C<sub>2</sub>S reacts ~41, 25 and 8% from 28d to 90d, for pastes with 0, 15 and 30 wt% FA, respectively). The lower reactivity of belite with the increasing amount of FA may be attributed to the low amount of water used, i.e. w/c=0.4, which means w/s of 0.40, 0.34 and 0.28, for 0, 15 and 30 wt% of FA, respectively. Consequently, a question was open at this stage: Is the lower reactivity of belite due to the lower amount of water?. In order to answer this question, FA0BAY and FA30BAY pastes were also prepared at a w/c ratio of 0.57 (the latter has a w/s ratio of 0.4). Table 5.20 shows RQPA results of both pastes at 28 and 90 days. Belite showed the same pace of hydration in both samples, i.e. the hydration degree of belite in FA0BAY was more or less constant independently of the w/c ratio. In addition, the belite hydration was inhibited in FA30BAY at any w/c ratio. As a consequence, the hydration behavior of belite was not influenced by the w/c ratio under these experimental conditions, but it seems to be influenced by the addition of FA. Besides that, the w/c ratio affected the phase assemblage, concretely, the katoite/stratlingite ratio, where pastes prepared at w/c=0.4 presented both phases, while samples with w/c of 0.57 only contained stratlingite, shown in Table 5.21.

**Table 5.19.** RQPA results (wt%) on cement pastes, as a function of hydration time obtained from LXRPD for FA#BAY pastes (w/c=0.4 and 0.5 wt% SP), including ACn and free water (FW) contents. Taken from [136]

Phases	FA0BAY <sup>a</sup>						FA15BAY						FA30BAY					
	t <sub>0</sub>	1d	7d	28d	90d	180d	t <sub>0</sub>	1d	7d	28d	90d	180d	t <sub>0</sub>	1d	7d	28d	90d	180d
<b>C<sub>4</sub>A<sub>3</sub>S</b>	5.1(1)	1.3(1)	-	-	-	-	5.3(1)	2.4(1)	-	-	-	-	4.3(1)	1.0(1)	-	-	-	-
<b>γ-C<sub>2</sub>S</b>	1.2(1)	1.3(1)	1.3(1)	1.3(1)	1.1(1)	1.0(1)	1.5(2)	1.4(1)	1.3(1)	1.4(1)	0.8(1)	0.8(1)	1.4(1)	1.1(1)	1.2(1)	1.3(1)	0.8(1)	1.1(1)
<b>β-C<sub>2</sub>S</b>	32.3(1)	32.9(1)	32.4(1)	27.9(1)	16.5(2)	14.4(3)	25.0(2)	28.6(2)	28.1(2)	27.2(2)	20.3(2)	18.6(2)	19.8(2)	23.2(2)	23.2(2)	21.5(2)	19.8(2)	19.8(2)
<b>C<sub>3</sub>S</b>	7.9(2)	3.0(2)	1.0(1)	-	-	-	7.4(3)	2.4(2)	-	-	-	-	6.0(2)	1.5(1)	-	-	-	-
<b>C<sub>12</sub>A<sub>7</sub></b>	4.3(1)	2.0(1)	-	-	-	-	3.6(1)	1.9(1)	-	-	-	-	2.7(1)	1.6(1)	-	-	-	-
<b>F-ellestadite</b>	2.2(1)	3.0(2)	2.7(1)	2.3(1)	3.2(3)	3.0(3)	3.4(3)	3.4(2)	2.3(2)	2.5(1)	2.6(1)	2.1(1)	3.1(3)	2.3(1)	2.0(1)	2.1(1)	2.3(2)	2.2(2)
<b>C<sub>4</sub>AF</b>	3.3(1)	2.6(1)	-	-	-	-	2.6(1)	2.7(1)	0.2(1)	-	-	-	2.1(1)	1.6(1)	-	-	-	-
<b>Cs</b>	7.1(1)	-	-	-	-	-	5.6(1)	-	-	-	-	-	4.7(2)	-	-	-	-	-
<b>Mullite</b>	-	-	-	-	-	-	0.5(1)	0.5(1)	1.0(1)	1.0(1)	2.1(1)	2.1(1)	1.9(2)	2.1(2)	2.4(2)	2.1(1)	2.3(1)	1.6(1)
<b>Quartz</b>	-	-	-	-	-	-	0.4(1)	0.4(1)	0.4(1)	0.4(1)	0.4(1)	0.4(1)	0.6(1)	0.7(1)	0.7(1)	0.7(1)	0.7(1)	0.7(1)
<b>C-S-H<sup>b</sup></b>	-	-	1.0(1)	1.0(1)	1.4(1)	1.1(1)	-	-	0.4(1)	1.4(1)	7.0(3)	6.7(3)	-	-	-	1.0(1)	2.1(1)	3.4(1)
<b>AFm</b>	-	-	2.4(1)	3.0(1)	5.0(1)	5.3(1)	-	-	1.2(1)	1.2(1)	1.6(1)	0.6(1)	-	-	1.8(1)	1.3(1)	0.9(1)	0.3(1)
<b>AFt</b>	-	19.5(1)	16.4(1)	16.6(1)	12.5(2)	12.7(3)	-	17.5(1)	15.3(1)	15.0(1)	15.4(2)	15.2(2)	-	14.9(2)	13.9(1)	13.4(1)	13.3(2)	13.4(2)
<b>Katoite</b>	-	-	4.0(2)	7.1(2)	4.1(2)	3.2(2)	-	-	2.8(2)	4.0(2)	4.8(2)	5.5(2)	-	-	2.6(2)	2.2(3)	3.1(3)	2.7(2)
<b>Stratlingite</b>	-	2.1(2)	5.4(3)	6.3(3)	6.4(3)	9.2(7)	-	-	4.8(4)	6.5(4)	6.6(4)	7.3(2)	-	-	1.7(1)	1.9(2)	2.8(2)	2.8(2)
<b>ACn</b>	8.1	19.7	23.6	26.2	45.4	48.2	19.3	27.5	33.8	32.4	32.5	38.8	31.3	40.9	43.9	47.0	47.7	49.4
<b>FW</b>	28.6	12.6	9.7	8.3	5.9	2.9	25.4	11.3	8.5	7.0	5.2	2.2	21.9	9.1	6.7	5.4	4.3	2.7

a. Also contains 0.1 and 0.3 wt% of CH at 90 and 180 days respectively.

b. C-S-H as clinotobermorite.

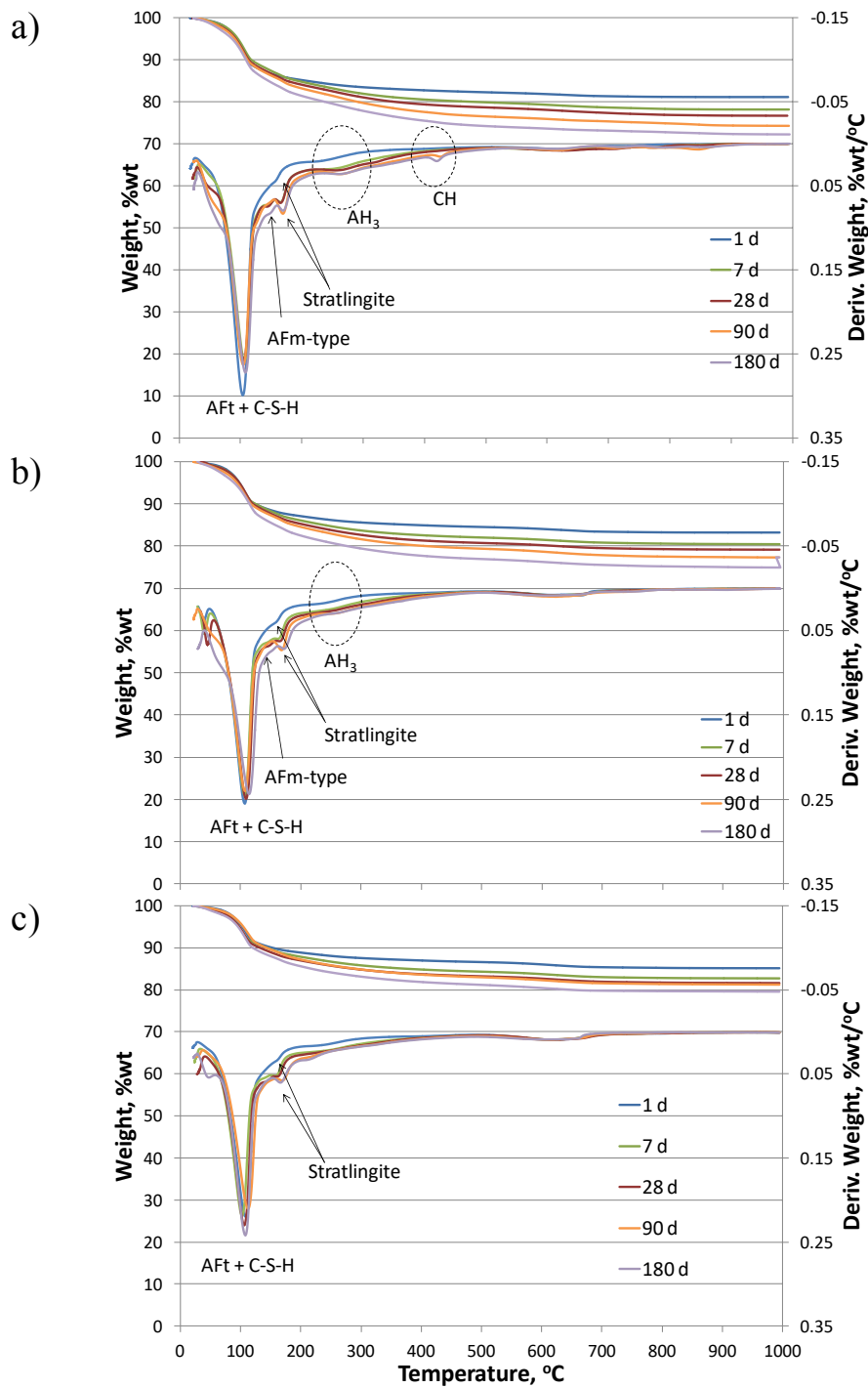


**Figure 5.31.** Thermogravimetric and differential thermogravimetric analyses (TG-DTG) of (a) FA0BAY, (b) FA15BAY and (c) FA30BAY pastes, with  $w/c=0.4$  prepared with 0.5 wt% of superplasticizer. Taken from [136]

**Table 5.20.** RQPA comparative results (wt%) on cement pastes of FA0BAY and FA30BAY prepared at w/c of 0.57, as a function of hydration time obtained from LXRPD. Taken from [136].

Phases	FA0BAY			FA30BAY		
	w/c 0.57			w/c 0.57		
	t <sub>0</sub>	28d	90d	t <sub>0</sub>	28d	90d
<b>C<sub>4</sub>A<sub>3</sub>S</b>	4.5(1)	-	-	4.0(1)	-	-
<b>γ-C<sub>2</sub>S</b>	1.1(1)	1.9(2)	1.4(2)	1.2(1)	1.1(1)	1.1(1)
<b>β-C<sub>2</sub>S</b>	28.8(1)	28.4(2)	16.5(2)	18.1(2)	18.3(2)	18.1(2)
<b>C<sub>3</sub>S</b>	7.1(2)	-	-	5.5(2)	-	-
<b>C<sub>12</sub>A<sub>7</sub></b>	3.8(1)	-	-	2.5(1)	-	-
<b>F-ellestadite</b>	2.0(1)	2.5(2)	2.4(2)	2.9(1)	1.4(2)	1.5(2)
<b>C<sub>4</sub>AF</b>	2.9(1)	-	-	2.0(1)	-	-
<b>Cs</b>	6.3(1)	-	-	4.3(2)	-	-
<b>Mullite</b>	-	-	-	1.8(1)	2.5(1)	2.2(1)
<b>Quartz</b>	-	-	-	0.6(1)	0.7(1)	0.7(1)
<b>C-S-H<sup>b</sup></b>	-	1.4(1)	3.6(1)	-	5.1(1)	3.0(1)
<b>AFm</b>	-	5.7(1)	5.6(1)	-	3.4(1)	4.6(1)
<b>AFt</b>	-	24.0(2)	12.7(3)	-	15.4(2)	15.0(2)
<b>Katoite</b>	-	-	-	-	-	-
<b>Stratlingite</b>	-	7.5(3)	9.5(4)	-	2.2(2)	2.0(2)
<b>ACn</b>	7.2	12.0	22.4	28.7	36.5	40.6
<b>FW</b>	36.3	16.6	15.1	28.5	13.6	11.2

a. Also contains 0.1 and 0.3 wt% of CH at 90 and 180 days respectively.

b.C-S-H as clinotobermorite.

**Table 5.21.** Comparative content (wt%) of katoite and stratlingite on FA0BAY at 28 days, as a function of w/c ratio used.

Phases	w/c ratio		
	0.4	0.5	0.57
C <sub>3</sub> ASH <sub>4</sub>	3.7(2)	2.5(1)	-
C <sub>2</sub> ASH <sub>8</sub>	5.0(2)	5.3(2)	7.5(3)

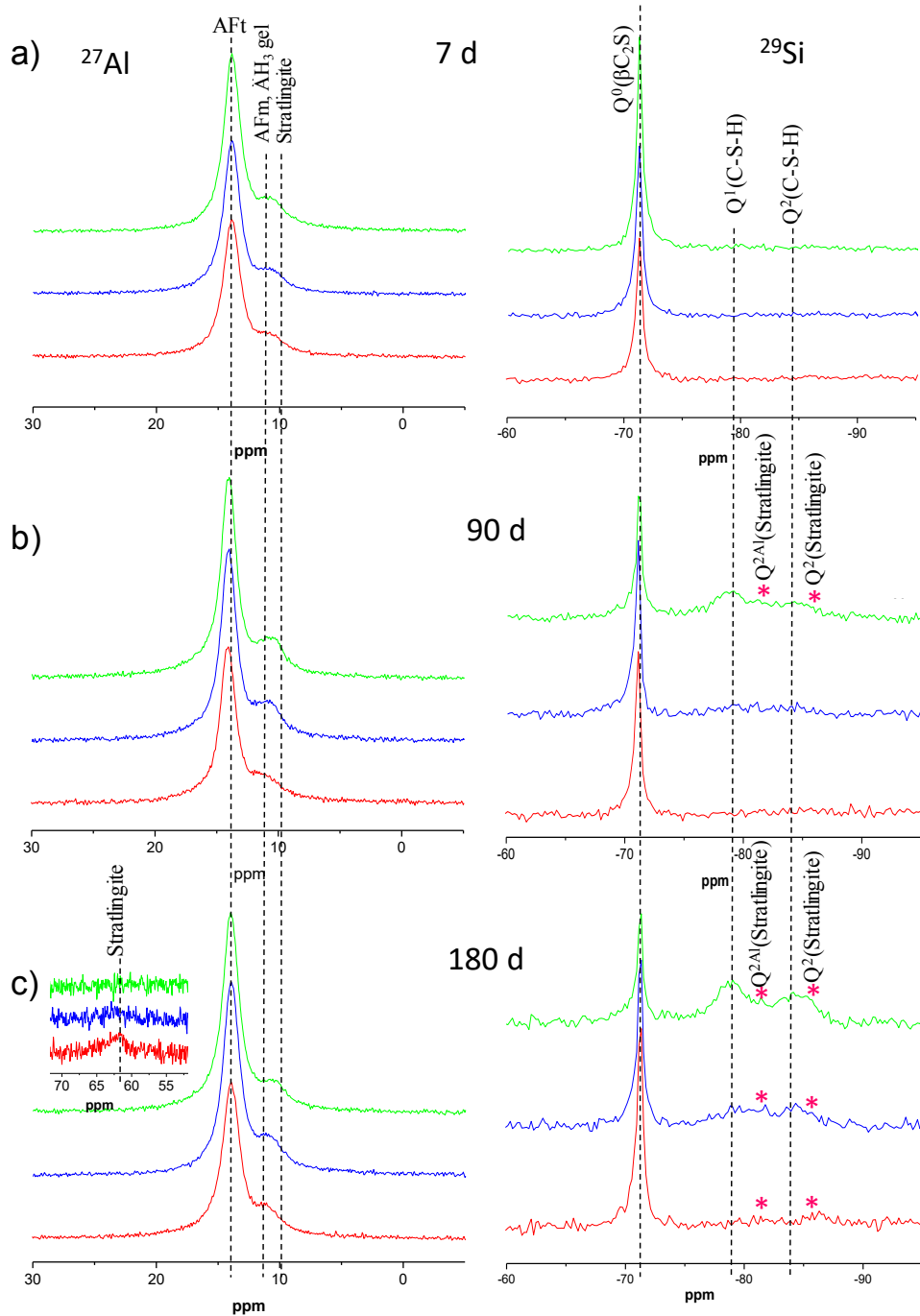


**Figure 5.32.**  $^{27}\text{Al}$  (left) and  $^{29}\text{Si}$  (right) MAS-NMR of FA#BAY pastes at a) 7 days, b) 90 days and c) 180 days. FA0BAY in green line, FA15BAY in blue line and FA30BAY in red line. Inset at 180 days are the signal of  $\text{Al}^{\text{IV}}$  of stratingite multiplied x10 for a sake of better representation. Modified from [136]



Figure 5.32 shows  $^{27}\text{Al}$  and  $^{29}\text{Si}$  MAS-NMR spectra of FA#BAY pastes at 7, 90 and 180 hydration days.  $^{27}\text{Al}$  MAS-NMR spectra (Figure 5.32, left site) shows  $\text{Al}^{\text{VI}}$  octahedrally-coordinated zone, where AFt is located at  $\sim 13.8$  ppm [161,164,174]. The wide signal located at about 9-11 ppm can be assigned to the overlapping contribution of AFm-type phases (stratlingite and monosulfoaluminate) and aluminium hydroxide [36,98,161,174]. The inset at 180 curing days corresponds to  $\text{Al}^{\text{IV}}$  tetrahedrally-coordinated zone. The signal observed at  $\sim 62$  ppm is assigned to  $\text{Al}^{\text{IV}}$  of stratlingite [142,161]. The signals of AFm-type phases and aluminium hydroxide are present in all the pastes at any time. For a better understanding, the deconvolution of  $^{29}\text{Al}$  MAS-NMR of FA0BAY at 180 days, shown in Figure 5.33 was performed, as an example. Here, the wide signal associated with AFm-type phases and amorphous aluminum hydroxide was composed by 45% of stratlingite, 35% of amorphous-AH<sub>3</sub> and 20% of monosulfoaluminate, centered at  $\sim 10.1$ ,  $\sim 11.2$  and  $\sim 12.1$  ppm respectively [36,98,161,174]. This is in agreement with TG-DTG results for this paste.

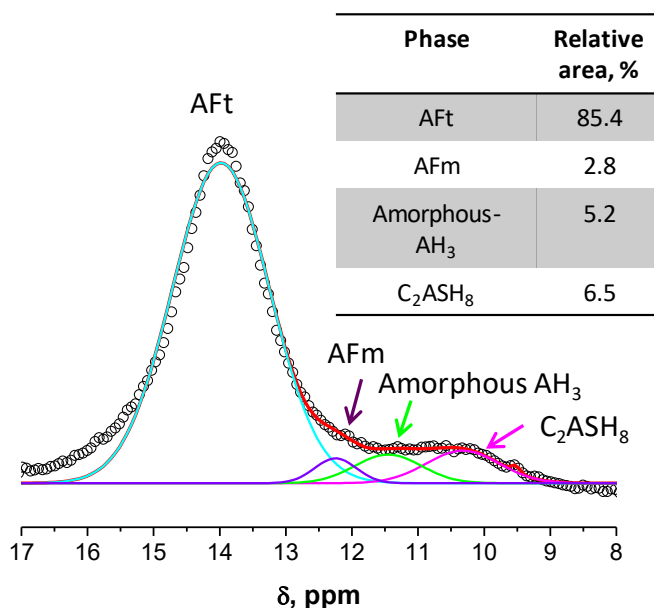


**Figure 5.33.** Deconvolution of  $^{29}\text{Al}$  MAS-NMR spectra of FA0BAY at 180 days. Each spectrum includes experimental (dots) and its deconvoluted spectrum (red line) with individual contribution of AFt (blue line), amorphous-AH<sub>3</sub> (green line), AFm (purple line) and stratlingite (pink line).

$^{29}\text{Si}$  MAS-NMR spectra of all samples (Figure 5.32, right side) showed near at -72 ppm a signal corresponding to isolated  $\text{SiO}_4$  tetrahedra ( $\text{Q}^0$  sites) of non-hydrated belite [159,164,169]. After 90 days of hydration, FA0BAY paste showed two small peaks at around -79 and -84 ppm, which may be assigned to  $\text{Q}^1$  and  $\text{Q}^2$  species of C-S-H gel, respectively.  $\text{Q}^1$  and  $\text{Q}^2$  represent the end chain and middle chain of  $\text{SiO}_4$  tetrahedron, respectively [157–159]. Later, at 180 days, those two peaks also appeared with shoulders centered at -82 and -86 ppm, corresponding to  $\text{Q}^{2(2\text{Al})}$  and  $\text{Q}^2$  of stratlingite [161,174]. Figure 5.32c shows wide peaks between -75 to -88 ppm in 180 days in FA15BAY paste  $^{29}\text{Si}$  MAS-NMR spectra, associated with  $\text{Q}^1$  and  $\text{Q}^2$  of C-S-H and  $\text{Q}^2$  of stratlingite. In FA30BAY paste those characteristics peaks were not clearly observed. To obtain deeper information from these data, the deconvolution of FA#BAY at 180 days spectra, shown in Figure 5.34, was carried out. Here, FA0BAY and FA15BAY at 180 days showed the characteristic  $\text{Q}^1$  and  $\text{Q}^2$  signals of C-S-H, although they are slightly weaker in FA15BAY. The presence of C-S-H at later ages in these samples proves its origin from the belite hydration. On the other hand, these signals were not detected in FA30BAY sample, confirming that the belite hydration was inhibited (see Figure 5.34c). In all cements the characteristic  $\text{Q}^2$  and  $\text{Q}^{2(2\text{Al})}$  signals of stratlingite were detected, corroborating the results obtained by LXRPD and TG-DTG (Table 5.19 and Figure 5.31).

The fact that the stratlingite peak at 62 ppm ( $^{27}\text{Al}$  MAS-NMR at 180 days) was more pronounced than the peaks observed by  $^{29}\text{Si}$  MAS NMR in FA30BAY, suggests that the tetrahedral layer in this phase presents higher amount of  $\text{Al}^{\text{IV}}$  than  $\text{Si}^{\text{IV}}$ . [106,142]

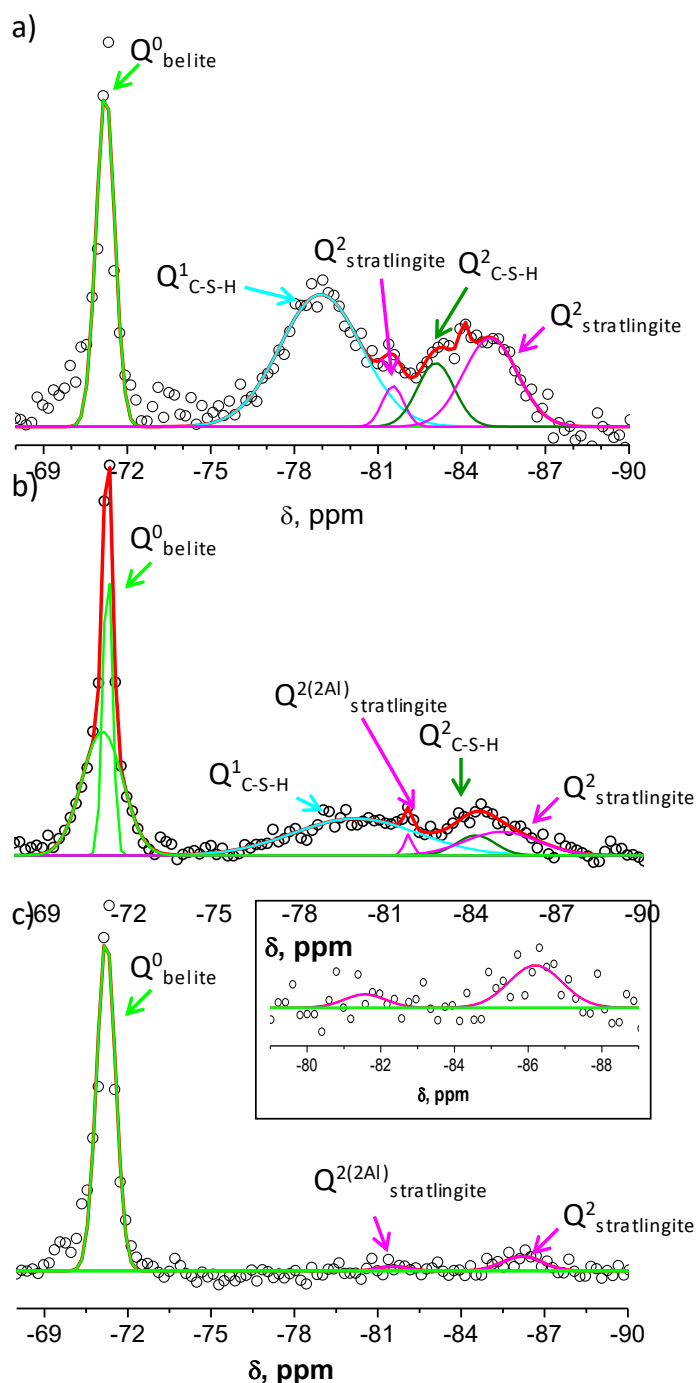


**Figure 5.34.** Deconvolution of  $^{27}\text{Si}$  MAS-NMR spectra of (a) FA0BAY, (b) FA15BAY and (c) FA30BAY at 180 days. Each spectrum includes experimental (dots) and its deconvoluted spectrum (red line) with individual contribution of C<sub>2</sub>S (light green line), C-S-H gel (blue and dark green line) and stratlingite (pink line).

## 5.4. Mechanical behavior of FA#BAY binders

The compressive strengths of FA#BAY mortars are shown in Figure 5.35. Here, it can be seen that the increment of FA content favored the increasing compressive strength at any age. The percentages (increase) the measured strength values of those mortars referred to FA0BAY, at the same ages, are shown in Table 5.22. These values indicate that the increase is important at early ages (1 and 7 days). This increase in mechanical strengths at early ages may be due to the filler effect and to the consequent reduction of porosity and pore size. However, the increases after 28 days, despites of inhibition of belite hydration, might be considered as an indirect experimental result of pozzolanic reaction, although at a small degree. However, the significant changes in phase assemblages with time and amount of FA are not enough to justify the raise in compressive strengths. Consequently, the porosity and pore size distribution of the pastes was studied at 180 hydration days, Figure 5.36, where the pore size diameter decreases by increasing the FA content. Moreover, the open porosity of pastes also decreases with the FA content (16, 13 and 9 vol% for FA0BAY, FA15BAY and FA30BAY respectively). Therefore, the increasing compressive strength can be justified by a decreasing in porosity with increasing FA content, mainly due to a filler effect, as reported by Winnefeld *et al* [152] and Garcia-Mate *et al* [119].

**Table 5.22.** Increase of the strength (in percentage) referred to FA0BAY-mortar at the same ages.

Mortar		Curing age, days				
		1	7	28	90	180
FA15BAY	percentage (%)	15	21	5	19	6
FA30BAY	percentage (%)	43	42	24	24	19

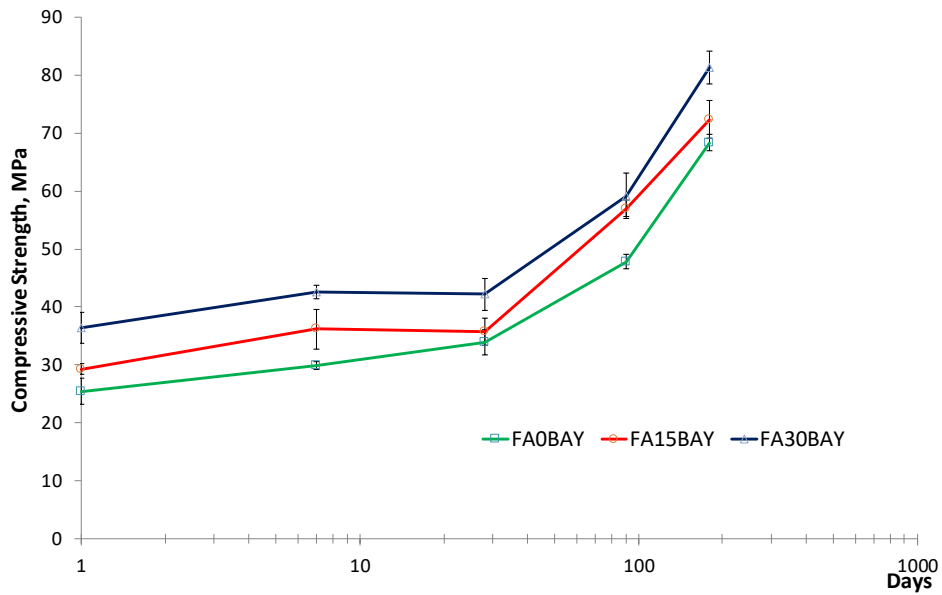


Figure 5.35. Compressive strength of FA#BAY.

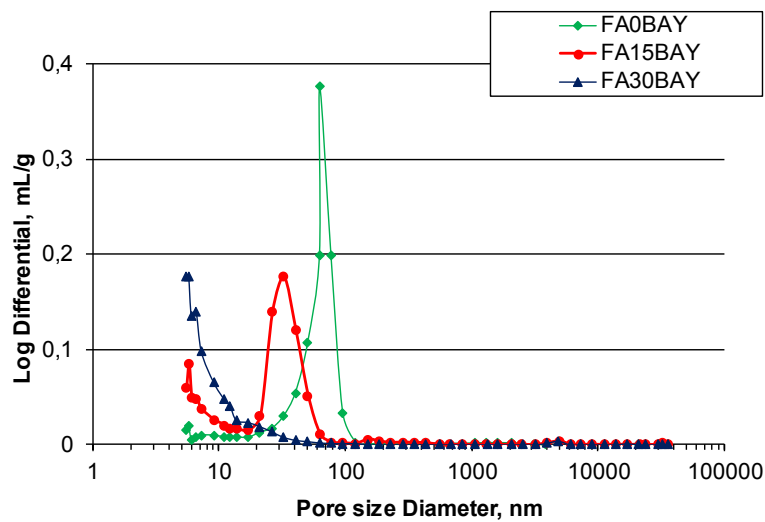


Figure 5.36. Pore size distribution of FA#BAY pastes at 180 hydration days. Taken from [136].



## 5.5. Summary

The role of FA replacement on the hydration mechanism of BAY cement was studied, as a possible SCMs. Firstly, the amount of a polycarboxylate-based SP was optimized (0.5 wt% of the active matter referred to solids) to assure the homogeneity of the pastes, and the effect on the pastes hydration was also studied.

The calorimetric studies reveals that, the use of polycarboxylate-based superplasticizer, in this BAY cement (FA0BAY), mainly affected the rate of hydration of  $C_{12}A_7$ , inhibiting the competitive reaction between  $C_{12}A_7$  and  $C_4A_3S$ .

Secondly, the effect of FA addition was investigated through calorimetric studies, and the results showed that fly ash prompts the second exothermic peak to appear before and shorten induction period. This peak is attributed to the aluminate-phases consumption and the corresponding production of AFt. However, detailed analysis did not provide any evidence that there was any reaction of the FA itself at early hours of hydration. Thus, these results reveal that FA initially works as a filler, giving nucleation points for the formation of hydrated phases.

Moreover, the presence of fly ash had a small impact on the hydration mechanism or kinetics of BAY cement pastes. FA0BAY showed slightly different chemical hydration behavior than FA15BAY and FA30BAY. In all systems, the main hydration products were AFt, AFm-phases (monosulfoaluminate and stratlingite) and katoite. The increase of FA had a significant impact on the hydration of belite and hence on the C-S-H formation. Both of which were lower than in the paste without fly ash (FA0BAY). This impact favors the AFt stability, which suffers a considerable decrease after 28 hydration days in FA0BAY. The compressive strength was increased with the fly ash amount replacement and time evolution. On the one hand, the early age mechanical strength increase is thought to be related to the filler effect which decreases the porosity on the

pastes. On the other hand, the compressive strength enhanced after 28 days without significant belite depletion (FA15BAY and FA30BAY), with a reduction on total porosity and open pore size diameter, and higher total heat of hydration after the same ages, might be considered as an indirect evidence of some degree of pozzolanic reaction.

It is important to foreground that the increase of water content on BAY cement systems (from w/c of 0.40 to 0.57) affected the  $C_3ASH_4/C_2ASH_8$  ratio, i.e. higher w/c contents favor the higher contents of stratlingite and lower contents of katoite (see Table 5.21). These different mineralogical phase assemblages may have an impact on the mechanical strengths; however, this needs more research.

All these results have allowed to fulfill the specific objective of understanding of effect of w/c ratio, use of polycarboxylate as superplasticizer and percentage of addition of FA on the rheological behavior, heat flow, hydration mechanism and compressive strength of BAY.



UNIVERSIDAD  
DE MÁLAGA



## 6. “Commercial binder” study associated with BAY cement

This chapter describes the hydration mechanism and mechanical behavior of a mixture of a commercial belite Portland cement with a commercial calcium sulfoaluminate cement, as described in Chapter *Materials and Methods section 1.1.3*. The mixture will be named hereafter as B83. For the sake of comparison, this cement was formulated with a similar mineralogy than FA0BAY, where  $C_3S/C_4A_3S$  ratio was near to 1.37.

Cement pastes and mortars were prepared at a water/cement ratio of 0.4 and were studied at 1, 7, 28, 90 and 180 days of hydration. At early-age, the rheological behavior of the cement pastes was investigated. Moreover, the heat released by this cement was also analyzed. LXRPD with Rietveld analysis was the main technique used to investigate the content of crystalline and ACn phases in pastes. Thermogravimetric analysis (TG-DTG) was employed to confirm the mineralogy of the pastes and to calculate the ACn content. Finally, the mechanical behavior, as compressive strength, of these mortars was measured and correlated with the composition.

### 6.1. Optimization of the superplasticizer content

The amount of the polycarboxylate based-superplasticizer was optimized for this paste through rheological studies. Figure 6.37 shows the flow curves of the B83 paste prepared with different SP contents. In general, the viscosity of these

pastes is lower than the corresponding FA0BAY pastes, even without SP. This may well be related with the larger particle size of B83 cement powder (19.9 and 180  $\mu\text{m}$  for  $D_{v50}$  and  $D_{v90}$ , respectively) than the laboratory-prepared FA0BAY cement powder (3.6 and 10.3  $\mu\text{m}$  for  $D_{v50}$  and  $D_{v90}$ , respectively). It corresponds to a lower surface area (1.2 and 1.4  $\text{m}^2/\text{g}$  for B83 and FA0BAY, respectively), and thus lower particle interactions.

As it happened before, a small addition of SP, e.g. 0.1 wt%, decreased drastically the viscosity of B83 pastes (from 870 to 260  $\text{mPa}\cdot\text{s}$  at  $100 \text{ s}^{-1}$  for pastes with 0 and 0.1 wt% SP respectively). By adding SP, the viscosity decreases until a minimum value, associated with the optimum amount of SP. From there, the viscosity of was kept constant. Figure 6.37 shows the deflocculation curve using the values from the up-curves at the shear rate of  $100 \text{ s}^{-1}$ , where the optimum value was achieved when 0.4 wt% SP was added (126  $\text{mPa}\cdot\text{s}$  at  $100 \text{ s}^{-1}$ ).

To deeply study the effect of the SP on the mechanical strength of the mortars, and check the effect of slightly diminishing the amount of SP, they were prepared with 0.3 and 0.4 wt%. Pastes were prepared with 0.35 wt% of SP as a mean value between 0.3 and 0.4 wt%, because the slightly decrease in SP amount does not affect drastically the hydrated phase assemblage.

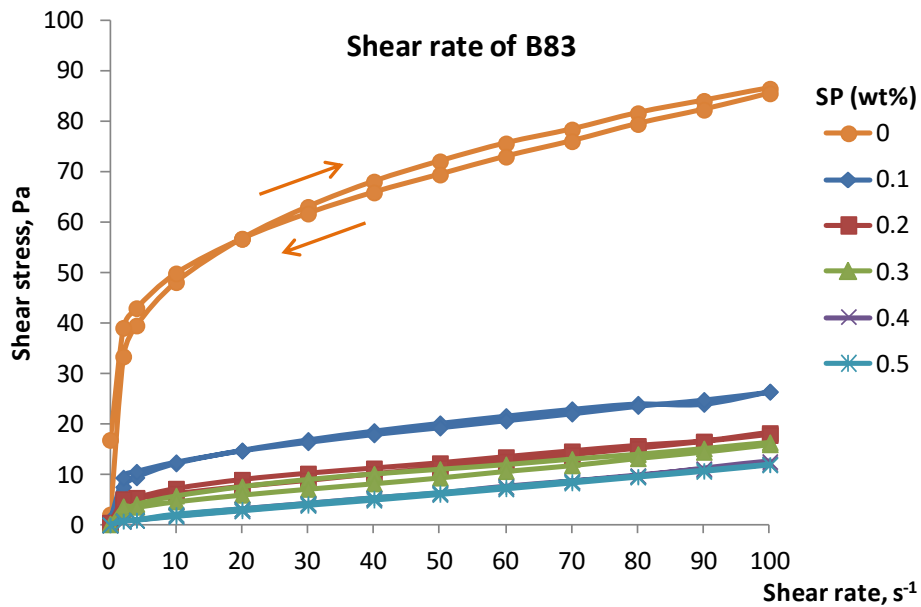


Figure 6.37. Flow curves of B83 pastes with different superplasticizer contents (water/cement ratio of 0.4).

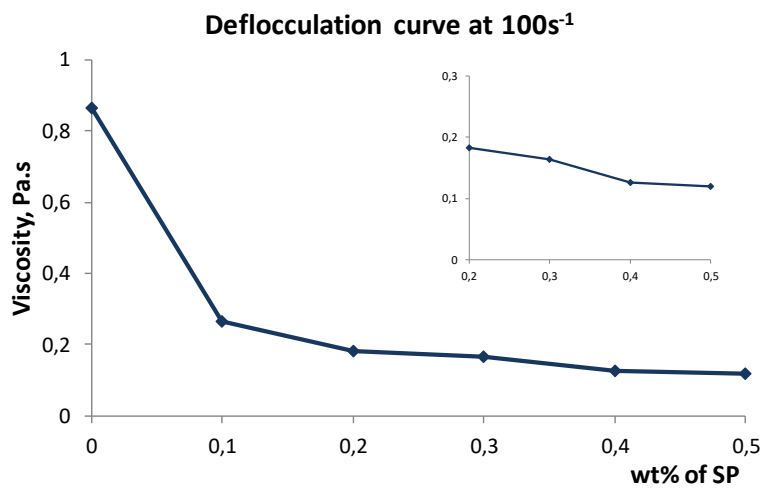


Figure 6.38. Deflocculation curve of B83 pastes prepared at a w/c ratio of 0.4 and different SP contents at the shear rate of 100 s<sup>-1</sup> (values taken from the up-curves). Inset shows an amplified zone between 0.2 and 0.5 wt% of SP



## 6.2. Isothermal calorimetric behavior

As detailed in previously chapters, the heat produced by the pastes is a good indication of their early-age hydration behavior. For this reason, Figure 6.39a and Figure 6.39b show the heat flow curves and cumulative heat, respectively, released by B83. The curves of FA0BAY pastes are also shown for the sake of comparison. Both pastes show an intense signal during the initial period and a hump immediately after the initial period depletion [72,79,105,136].

In the case of B83, the released heat during the initial period (from 0 to 0.3 h, Figure 6.39a) is assigned to the partial dissolution of anhydrite and ye'elimite and the initial precipitation of ettringite [144,149,170], is assigned to the partial dissolution of anhydrite and ye'elimite and the initial precipitation of ettringite, as detailed in previous chapters (Chapter 4 *Pure phase hydration study* and Chapter 5 *Influence of Fly Ash addition on BAY cement hydration and properties*). The heat released during this initial period was slightly higher in B83 than FA0BAY (20 and 18 J/g respectively) despite its larger particle size; this may be due to the different amounts of  $C_4A_3S$ , being 7.1 and 5.1 wt% for B83 and FA0BAY, respectively.

Similar to FA0BAY, B83 does not present a clear induction period, directly showing a hump centered at around 2.5 hydration hours. This hump can be considered as the main hydration/precipitation signal. B83 shows an higher and more accelerated signal, 108 J/g at 3.5 hours, than FA0BAY (78 J/g located at ~8h, Figure 6.39b), indicating that the former reacts faster. Considering the similar mineralogy of both cement powders, and the experience acquired from the pure-phases mixture studies, the main peak may well be associated with the precipitation of AFt and AFm-type phases (monosulfoaluminate and/or stratlingite) [72,136]

B83 paste shows a cumulative heat release different than FA0BAY, Figure 6.39b, which reflects the previous observations of their heat flow. During the first 5

hours, B83 released twice the total heat of FA0BAY (~120 and ~60 J/g respectively). And after 72 h, B83 and FA0BAY reached cumulative heats of 185 and 142 J/g respectively.

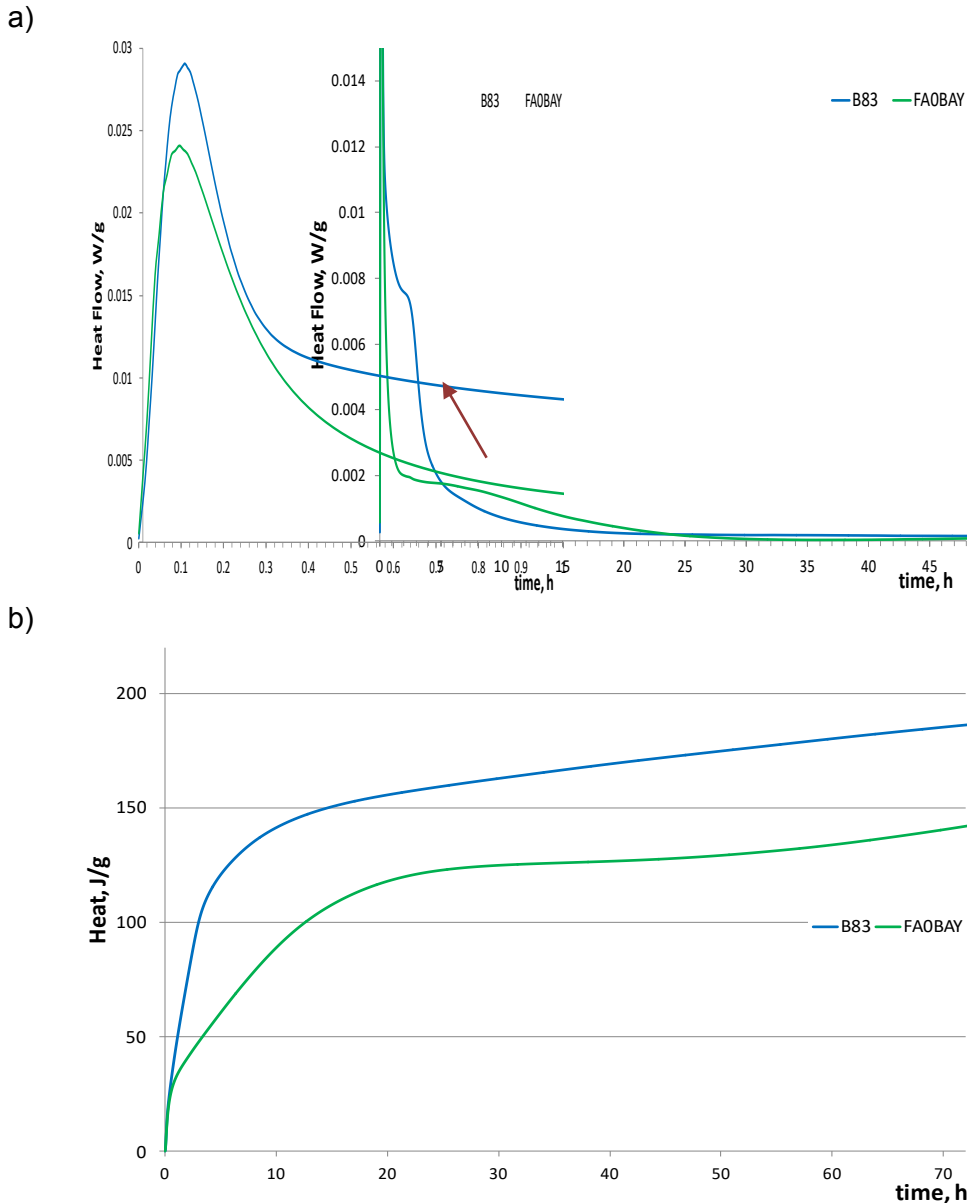


**Figure 6.39.** Heat flow (a) and total heat (b) of B83 (blue line) and FA0BAY (green line).



### 6.3. Hydration mechanism in B83

The RQPA for the hydration of B83 pastes (water-to-cement ratio of 0.4 and 0.35 wt% SP) including both ACn and FW contents, is shown in Table 6.23, and Mo LXRPD patterns are showing in Figure 6.40. The results show that the main hydration products obtained were AFt, stratlingite and katoite. After 1 day,  $C_4A_3S$  and Cs reacted quickly and contributed to the formation of crystalline AFt and amorphous aluminum hydroxide; same that happened in FA0BAY cement hydration. The amorphous content formed from these cement at early ages should be composed mainly for amorphous- $AH_3$ . Despite of fast reaction of ye'elimite, the hydration of alite in B83 was a little bit slower, only 74% of degree of reaction compared to FA0BAY, where after 7 days had reacted 100% (Chapter 3 *BAY cement hydration and mechanical behavior*). In B83, even after 180 days, there was anhydrous alite remaining in the system, representing a remnant of 22% of the initial content. This fact may be due to a passivation of the system, i.e. remaining alite is covered by hydrated products and free water is not reaching it.

In addition,  $\beta$ -belite showed a typical slow reactivity that, after 28 days of hydration, presented an important depletion, reaching at 180 days a hydration degree of 55%. It is known that alite and belite reacts with water to produce C-S-H gel and crystalline portlandite. However, the precipitation of CH was not detected by LXRPD in B83, as expected from the previous studies. Additionally, CH was not detected by TG-DTG, except after 180 hydration days where a small peak around 450 °C was detected (see Figure 6.41). These results are in agreement with several studies, where crystalline portlandite was not detected in systems containing jointly ye'elimite and alite [102,105,118,136,151] because CH favors reaction of ye'elimite with calcium sulfate source to produce early ettringite [102,105,118,136] and the formation of late AFm-type phases (as monosulfoaluminate and stratlingite) [102,103,105,118,142]. In this amorphous aluminum hydroxide rich system, the formation of stratlingite from silicates

phases ( $C_2S$  and  $C_3S$ ) is favored from the first day [4,106,142], reaching a maximum content of 13.8 wt% at 180 d.

Katoite was detected at 90 hydration days, where ferrite, alite and belite had reached a reaction degree of ~ 69, 78 and 12%, respectively. This result confirms the hypothesis suggested: for belite-alite-ye’elimitite systems, where katoite mainly comes from hydration of  $C_2S$ , CH and  $AH_3$  (Eq. 6), and from  $C_3S$  with  $C_4AF$  (Eq. 11). Furthermore, due to the lower hydration degree of alite, after 180 days AFt did not present a significant decrease, just reaching a degradation of ~9% respect to AFt content at 1 hydration day. Contrary to FA0BAY, where the degradation degree of AFt was ~ 35%.

**Table 6.23.** RQPA (wt%) for B83 pastes.

Phases	Curing age, days					
	$t_0=0$	1	7	28	90	180*
$C_3S$	8.9(5)	4.8(3)	2.3(3)	2.5(4)	2.0(3)	2.0(3)
$C_2S$	29.0(5)	32.9(3)	34.0(3)	34.5(3)	25.5(5)	13.1(6)
$C_3A$	0.7(1)	0.7(1)	-	-	-	-
$C_4AF$	5.4(2)	3.5(2)	3.6(2)	2.9(2)	1.7(2)	1.1(2)
$C_4A_3S$	7.1(2)	1.4(8)	-	-	-	-
MgO	1.6(1)	1.5(8)	1.5(7)	1.4(1)	1.2(1)	1.3(1)
Cs	4.9(1)	-	-	-	-	-
AFt	-	20.4(3)	20.3(3)	20.3(3)	18.5(4)	18.6(4)
Stratlingite	-	4.3(3)	9.7(6)	3.7(4)	6.0(5)	13.8(1)
Katoite	-	-	-	-	1.0(3)	1.1(3)
AFm	-	-	-	-	0.8(3)	0.8(2)
Can	13.8(2)	19.1(1)	20.2(1)	25.7(2)	37.6(2)	47.7(2)
FW	28.6	11.5	8.3	9.0	5.6	0.1

\*Also 0.5(1) wt% of CH.







All these results are in agreement with TG-DTG, where the same zones detected in FA0BAY were observed. A first peak centered at around  $\sim 110$  °C, was attributed to overlapped dehydration signals of AFt and C-S-H [102,105,118,136,143], and did not allow the correlation with LXRPD results. A second series of peaks located between 120 and 220 °C were assigned to the dehydration of AFm-type phases, where stratlingite displays its characteristic mass loss peak close to 180 °C [48,106,118,136,152,173]. This last peak was increasing during the hydration time, confirming the results obtained by LXRPD. Finally, around 230 to 300 °C, a kind of broad peak associated was detected and associated with amorphous  $AH_3$  [98,118].

#### 6.4. Compressive strength of B83 mortars

Compressive strength tests were performed on B83 mortars with 0.3 and 0.4 wt% of SP, prepared at a constant w/c ratio of 0.4. These data were compared to FA0BAY mortars. The compressive strength values measured up to 180 days for B83 and FA0BAY are shown in Figure 6.42. Here, it can be seen that at 1 day, FA0BAY and B83 presented similar compressive strength values ( $\sim 26$ ,  $\sim 26$  and  $\sim 27$  MPa for FA0BAY and B83 with 0.3 and 0.4 wt% SP respectively). This can be explain by inspecting Table 5.19 and Table 6.23. In both systems, B83 and FA0BAY, the phase assemblage after one day is more or less the same,  $\sim 20$  wt% of AFt,  $\sim 20$  wt% of ACn and  $\sim 12$  wt% of free water. Nevertheless after 1 day, B83 mortars always showed higher compressive strengths than FA0BAY mortars, reaching values at 180 curing days of  $\sim 79$  and  $\sim 81$  MPa for B83 with 0.3 and 0.4 wt% SP, respectively; while FA0BAY reached a compressive strength of  $\sim 68$  MPa. In order to understand this behavior, Table 5.19 and Table 6.23, were analyzed in detail. Main differences between both systems are: i) AFt did not present a high degradation grade in B83, consequently after 180d,  $\sim 19$  wt% of AFt was present while FA0BAY contains  $\sim 13$  wt%; ii) the amount of stratlingite was higher in B83 than in FA0BAY,  $\sim 13$  and  $\sim 9$  wt%, respectively and the amount of katoite was smaller; finally, iii) the amount of free water is also slightly different,

being almost zero in B83. Therefore, we can speculate that the increasing compressive strengths in this system depends on the higher amounts of AFt and stratlingite, and the lower amount of katoite and free water.

As expected, the compressive values in B83 increase by increasing the curing time and the amount of superplasticizer. This can be explained for the better homogeneity of the cementitious matrix (particles dispersion), the lower viscosity, and lower porosity reached in B83 with the use of optimal superplasticizer.

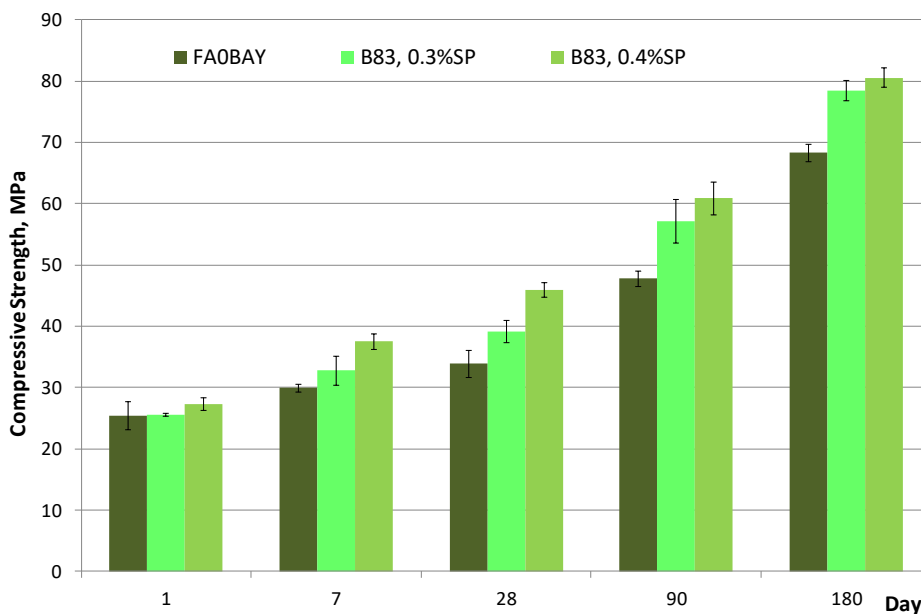


**Figure 6.42.** Compressive strength of FA0BAY ( $w/c=0.4$  and  $0.5$  wt% SP) and B83 ( $w/c=0.4$ ) with  $0.3$  and  $0.4$  wt% of SP

## 6.5. Summary

In this chapter, the study of the hydration behavior and mechanical properties of B83 cement (a mixture of belite clinker with calcium sulfoaluminate clinker) was carried out, and compared with the FA0BAY system. Firstly, the amount of superplasticizer was optimized ( $0.4$  wt% SP) through rheological measurements.

In a second step, the calorimetry behavior of B83 and FA0BAY was compared. During the initial period (around first 15 min of hydration), they presented same heat release reaching similar values to 26 mW/g (representing a total heat of about 20 J/g). This peak was associated with partial dissolution of  $C_4A_3S$  and Cs and initial precipitation of AFt. After that, the heat flow of B83 showed an acceleration and increasing hump at ~2.5 h (in relation to FA0BAY main peak showing also a hump at ~8 h), associated with precipitation of hydration products. In addition, the cumulative heat of B83 showed a different trend than FA0BAY; during the first 5 hours of hydration reached twice the heat of FA0BAY (~120 and ~60 J/g, respectively), due to the acceleration and increased of the main peak. Finally, they reached a constant heat of ~185 and ~140 J/g, respectively.

In a third step, the mineralogical evolution was analyzed, where the main hydration products were ettringite, AFm-type phases (stratlingite and monosulfoaluminate), katoite and amorphous  $AH_3$ . Surprisingly, B83 showed a different chemical hydration behavior than FA0BAY, with a lower hydration degree of alite, and a typical hydration behavior of belite after 28 days. This silicate behavior favored the AFt stability, which did not present a considerable decrease after 28 days. In addition, the rich aluminum hydroxide in this system favored the precipitation of stratlingite after 1 day, and a small amount of katoite after 90 hydration days.

Finally, the compressive strength of B83 mortars was evaluated and compared with FA0BAY. B83-mortars, during the studied curing time, always showed higher values of compressive strength than FA0BAY mortars; although at 1 day they exhibited the same compressive strength (around ~26 MPa). This mechanical behavior was assigned to higher amounts of AFt and stratlingite and lower amount of free water which may yield to a high density in the pastes due to less porosity than FA0BAY.

All these results have allowed to fulfill the specific objective of understand and compare the hydration and compressive strength of BAY and a blended binder.



UNIVERSIDAD  
DE MÁLAGA

# Conclusions and Perspectives

## Conclusions

This PhD thesis can be gathered in four parts correlated between them. In a first part the synthesis process (at laboratory scale) of Belite-Alite-Ye'elimite (BAY) cement was studied and optimized. In a second part, the effects of water-to-cement (w/c) ratio, superplasticizer and class F fly ash (FA) addition on the hydration mechanism and mechanical behavior of BAY cement were investigated. In the third part, the effects of the polymorphism of ye'elimite, water-to-solid (w/s) ratio and alite/ye'elimite ratio on the jointly hydration mechanism of ye'elimite, anhydrite and alite were evaluated. And last but not least, the fourth part, is focused on the hydration behavior and mechanical development of a "commercial binder", named B83, formulated with similar mineralogy of the synthesized BAY cement, but mixing belite clinker with calcium sulfoaluminate clinker.

All those study have allowed to fulfill the main objective of understand the hydration mechanism and mechanical behavior of belite-alite-ye'elimite systems.

In the first part, BAY clinkers were successfully synthesized by combining natural raw materials, where the oxide dosage and the addition of a mineralizer ( $\text{CaF}_2$ ) presented an important influence on the mineralogical composition. The quantities of alite ( $\text{C}_3\text{S}$ ) and ye'elimite ( $\text{C}_4\text{A}_3\text{S}$ ) increased with the addition of  $\text{SO}_3$  (as gypsum) and decreased by adding  $\text{Fe}_2\text{O}_3$ . On the one hand, the iron oxide favors the decomposition of ye'elimite into mayenite, on the other hand the

decomposition of  $C_4A_3S$  inhibits the reaction of CaO with  $C_2S$ , consequently suppressing the alite formation. According to these, the maximum percentages of alite and ye'elimite quantified in BAY clinkers were 16.0 and 12.1 wt%, respectively, representing an alite/ye'elimite ratio of 1.3. The optimum clinkering conditions to prepare 2 kg of BAY was 1300 °C for 15 min, and the optimum dosage had 0.9 wt% of fluorite and an excess of gypsum up to total amount of 4.3 wt% of  $SO_3$  (referred to the oxides).

Form the second part, BAY hydration, the following conclusions can be drawn:

- The increase of the water-to-cement ratio does not affect the hydration product assemblage of the system, that mainly contained ettringite (AFt) and AFm-type phases (as monosulfoaluminate and stratlingite) and katoite. Moreover, the ACn phase was indirectly quantified, and its composition should be mainly C-S-H and amorphous aluminum hydroxide ( $AH_3$ ). The presence of crystalline calcium hydroxide, as portlandite (CH), only was present until later ages when belite ( $\beta$ - $C_2S$ ) began to react. This absence is adjudged to: i) CH at early-ages stimulate the reaction of ye'elimite with anhydrite to produce AFt; and ii) CH at later ages favors the demotion of AFt into AFm-type. This last effect was observed in all BAY samples, where AFm-type phases content increased while AFt content decreased from 28 to 180 hydration days, independently of w/c ratio used. The main effects of w/c ratio on the mineralogical behavior observed were: i) the kinetics of reaction of ye'elimite, alite and belite were improved when w/c ratio increases, as expected. And ii) the katoite/stratlingite ratio decreased when w/c ratio increased.

The effect of w/c ratio on mechanical properties was as expected: the reduction of w/c favors the compressive strength of BAY. However, the decrease of water content in lab-synthesized BAY cement required the use

of superplasticizer to improve the workability and the homogeneity of the cementitious matrix; for this reason, its effect will be explained below.

- The use of the optimal amount of superplasticizer, 0.5 wt%, determined through rheological studies, the better homogeneity related to the particle repulsion favored the workability of the cement pastes, even when FA was added, with the direct effect on the viscosity reduction. The samples with and without the addition of SP did not show significant mineralogical changes at ages longer than 24 h. However, in the first 24 hours, it was detected through isothermal calorimetry and in-situ Mo-LXRPD, that the SP influences on the kinetics of hydration of mayenite ( $C_{12}A_7$ ), which yields ye'elimite to react first. This effect was reflected in the heat flow as a decrease of the main peak intensity, associated with precipitation of hydrated products, giving a reduction of the total heat of about ~ 28% after 2 days.
- The addition of FA as supplementary cementitious material (SCMs) in BAY, showed a vaguely impact on hydration products, where their main hydrated phases were AFt, monosulfoaluminate, stratlingite and  $AH_3$ , the same as in unblended cement. But the increase of FA amount impacted considerably on the kinetic reaction of belite (by inhibiting it), hence favored the AFt stability due to absences of Si-rich environment (C-S-H gel) and portlandite. From the calorimetric studies, as expected, the early-age FA addition effect was associated with a filler behavior, giving nucleation points to form hydrated phases.

The compressive strength values during the 180 hydration days increased with the increasing FA addition on BAY cement. During the first 28 days, this can be attributed to the filler effect (nucleation points and pores space filler); but after that, despite of the insignificant belite depletion, it might be considered as an indirect evidence of a kind of pozzolanic reaction.

It is important to highlight that all samples of the studied BAY (with and without fly ash) presented, from the first hydration day, higher compressive strengths than non-active belite-ye'elimite-ferrite (BYF) cement [48], reaching after 28 days higher compressive strengths than non-active BYF at 120 days (~ 34.5 and ~32.2 MPa respectively).

In the section about the hydration of the mixture of pure phases, the following conclusions can be remarked:

- The kinetic of hydration of alite was highly affected by the polymorphism of ye'elimite, where it began to react after the complete hydration of ye'elimite. Since the orthorhombic ye'elimite reacted faster than pseudocubic ye'elimite, the initial depletion of  $C_3S$  was carried out after 10 and 20 hydration hours, respectively. The main crystalline products obtained from this jointly reaction were AFt, monosulfoaluminate and stratlingite. Again, the absent of crystalline CH is a fact. When alite jointly reacts with orthorhombic ye'elimite, higher amounts of C-S-H (as ACn content) were detected from higher hydration degree of  $C_3S$ . The reactivity of alite in presence of pseudocubic ye'elimite was delayed, due to the slower kinetic of pseudocubic than orthorhombic ye'elimite; Thus anhydrous alite was presented even after 7 days of hydration, which favors the stability and quantity of AFt.
- The water-to-solid ratio mainly affected the kinetic hydration of the jointly alite, ye'elimite and anhydrite, where the increase of w/s showed an acceleration of ye'elimite hydration reducing its hydration time to the half, hence favored the quick precipitation of ettringite (and monosulfoaluminate in orthorhombic ye'elimite). But, independently on alite/ye'elimite ratio, the hydration degree of alite and its respective stratlingite and C-S-H formation are always favored by increasing w/s ratio.



- The hydration of alite/ye'elimite mixtures show initial period, induction period followed by a maxima signals during the main hydration. The maxima signal in mixtures with pseudocubic ye'elimite were displayed as a wide signal, corresponding to the retarded hydration of this ye'elimite. And the maxima signal in mixtures with orthorhombic ye'elimite was exhibited as a narrow peak associated with the AFt precipitation. The alite/ye'elimite ratios mainly affected the evolved heat flow. When alite/ye'elimite ratio was 1.37, the main peak was located before 20 hours of hydration, and the maximum values of ~37 and ~10 mW/g for orthorhombic and pseudocubic ye'elimite respectively were reached, at ~ 2 and ~11 hours of hydration, respectively. When the alite/ye'elimite ratio was 2.74, the main peak was delayed, centered between 3 to 20 hours for orthorhombic ye'elimite, and 5 to 40 hours for pseudocubic ye'elimite; maximum values of ~14 and ~3 mW/g were reached at around ~5 and ~18 hydration hours, respectively. These results are because the hydration enthalpy of ye'elimite is higher than that for alite (~ 560 [101,148] and ~ 515 J/g [4]), and from their independent kinetics of hydration.

Comparing these results with the BAY hydration mineralogy, it can be underlined that, in this jointly alite-ye'elimite-anhydrite system, katoite was not detect. This result yields an important information relative to katoite formation: it seems that its formation needs not only alite to react in an aluminate rich environment but also needs the reactivity of ferrite.

Finally, in the "commercial binder" (B83) part, the following conclusions were obtained:

- The heat flow showed by B83 was slightly different to that for BAY cement, where the main peak was accelerated and increased from the quick precipitation of AFt and stratlingite in the system; reaching, therefore, the double of total heat during the first 5 hours of hydration compared to BAY (~120 J/g and ~60 J/g for B83 and BAY, respectively).

- The main hydration products of B83 were AFt, AFm-type phases (stratlingite and monosulfoaluminate), katoite and amorphous aluminum hydroxide. In this system, alite did not react completely reaching a maximum hydration degree of 77.5% at 180 days, while belite reacted normally after 28 hydration days, reaching at 180 days, a hydration degree of ~ 55%. Thus, this slower alite hydration favored the AFt stability without a considerable AFm formation (demotion degree of AFt at 180 days was only ~ 8.8%). This behavior is contrary of that of BAY cement, where due to the total hydration of alite and partial hydration of belite, after 28 hydration days, ettringite showed a significant demotion with a corresponding increase of AFm-type phases. In addition, the stratlingite and katoite precipitation were favored in both rich aluminum hydroxide environments.
- The compressive strength values obtained from B83 mortars, after 1 days of hydration showed higher values than BAY-cement (without fly ash addition). This mechanical behavior was associated with the higher amount of AFt (higher stability), higher amount of stratlingite and lower free water, that cause lower porosity of the cementitious matrix.

## Perspectives

During this work, the study of an unexplored field has been started: the activation of belite cement with the jointly rich content of alite and ye'elimite, its hydration mechanism and mechanical properties (understanding as compressive strength). Although a good basis has been laid with the current work, there are still several points that should be assessed in the future.

- The synthesis of BAY clinker was possible by the use of 0.9 and 4.3 wt% of fluorite and  $\text{SO}_3$ , respectively. But it is known that MgO and CuO (up to 1.5 and 2.0 wt%, respectively) favor the coexistence of alite and ye'elimite. The use of one of them, may increase  $\text{C}_3\text{S}$  and  $\text{C}_4\text{A}_3\text{S}$  amounts, keeping the

alite/ye'elinite ratio near to 1. All of this is something that should be considered in futures works.

- Lab-synthesized BAY clinker contains  $\beta$ -form of belite, which presents a slow kinetic of hydration; the activation of belite with boron may be considered, with the aim of obtaining a highly reactive belite, without a decrease of the amount and ratio of alite and ye'elinite. It is important to highlight that in the hydration of this system the stability of AFt could be comprised, but this has to be studied.
- In this thesis, anhydrite was used as calcium sulfate source, thus, further research may be performed to determine the influence of type and amount of calcium sulfate source (i.e. gypsum, hemihydrate or anhydrite) in BAY hydration mechanism and performances
- In this research, polycarboxylate-based superplasticizer was used to improve the homogeneity of BAY pastes (blended and unblended) when the w/c was reduced to 0.4. Its direct influence on the setting time and the effect of other kinds of superplasticizers and/or retarders could be studied.
- In the hydrated phase assemblage of BAY, portlandite was not detected owing to its consumption to form late AFm-type phases, mainly from AFt. The use of calcined clay or nano-SiO<sub>2</sub> particles could be considered, as a supplementary cementitious materials, with the aim of favoring the early formation of C-S-H and possibly inhibition on the demotion of ettringite.
- Before BAY cements could be used, it is needed to establish their long-term durability. The understanding of how the AFt degradation and the presence of AFm-type phases and/or katoite can affect on the later properties such as shrinkage/expansion, chemical resistance, freeze-thaw, carbonation, heavy metals encapsulation, and so on.



UNIVERSIDAD  
DE MÁLAGA

## **Annex I:**

# **Papers published or submitted**



Paper # 1. *Clinkering and hydration of Belite-Alite-Ye'elimite cement* [118]

## Clinkering and hydration of belite-alite-ye'elimite cement

D. Londono-Zuluaga <sup>a,b</sup>, J.I. Tobón <sup>b</sup>, M.A.G. Aranda <sup>a,c</sup>, I. Santacruz <sup>a</sup>, A.G. De la Torre <sup>a,\*</sup><sup>a</sup> Departamento de Química Inorgánica, Cristalografía y Mineralogía, Universidad de Málaga, 29071 Málaga, Spain<sup>b</sup> Grupo del Cemento y Materiales de Construcción, CEMATEC, Universidad Nacional de Colombia, Facultad de Minas, Medellín, Colombia<sup>c</sup> IMAA Synchrotron, Campus de la Udm 2-26, E-08290, Cerdanyola del Vallès, Barcelona, Spain

## ARTICLE INFO

## Article history:

Received 13 July 2016

Received in revised form

21 February 2017

Accepted 10 April 2017

Available online 12 April 2017

## Keywords:

Belite-alite-calcium sulfoaluminate cement

Clinkering

Hydration

Compressive strength

## ABSTRACT

Some belite-ye'elimite-ferrite (BYF) cements present low mechanical strengths mainly due to the slow reactivity of belite. A solution to this problem may be the activation of BYF clinkers by preparing them with a consistence of alite and ye'elimite, which are known as belite-alite-ye'elimite (BAY) cements.

The objective of this work was the preparation of BAY mortars that show higher mechanical strengths than BYF mortars. In order to attain this, the clinkering conditions to prepare BAY-clinker (2 kg) with the following mineralogical composition 60.6 (2) wt% of belite, 14.3 (2) wt% of alite and 10.4 (1) wt% of ye'elimite were optimized (900 °C/30 min–1300 °C/15 min). The hydration mechanism of cement pastes [with 12 wt% of anhydrite and water-to-cement ratios of 0.4 and 0.5] was studied through laboratory X-ray powder diffraction and thermo-analyses. Finally, BAY mortars with higher compressive strengths than BYF-mortars were obtained (viz. 24.8 and 17.1 MPa for BAY and BYF mortars at 7 days of hydration, respectively).

© 2017 Elsevier Ltd. All rights reserved.

## 1. Introduction

Ordinary Portland cement (OPC), which contains alite<sup>1</sup> (C<sub>2</sub>S) as the primary mineralogical phase, is used extensively all over the world. However, the production of OPC has the disadvantage of generating large amounts of carbon dioxide from limestone calcination, and requires a high synthesis temperature, between 1450 and 1500 °C [1]. Therefore, the production of OPC clinker counts for about 5% of the total anthropogenic CO<sub>2</sub>-emissions. An environmental strategy for reducing the negative effect of CO<sub>2</sub> footprint of the OPC industry consists on the development of eco-cements composed by less calcite demanding phases, such as belite (C<sub>2</sub>S) and ye'elimite (C<sub>4</sub>A<sub>3</sub>S<sub>3</sub>, also called Klein's compound) [2]. That is the case of clinkers based on calcium sulfoaluminate (CSA) which are more environmentally friendly than OPC [2,3], as their production releases up to 35% less CO<sub>2</sub> than the latter. Depending on the raw meal composition, CSA clinkers may contain more than 50 wt% of ye'elimite and other minor phases such as belite, ferrite (C<sub>2</sub>A<sub>2</sub>F), anhydrite (C<sub>2</sub>S<sub>2</sub>), gehlenite (C<sub>2</sub>AS), mayenite (C<sub>12</sub>A<sub>7</sub>) or C<sub>3</sub>A [4–9]. These materials are commonly used for niche applications: this is

partially due to their high cost related to the large alumina content needed for their fabrication.

Recently, belite-ye'elimite-ferrite (BYF) [2] (also known as belite-calcium sulfoaluminate (BCSA) or sulfobelite) cements have been studied as potential OPC substitutes [6,10–14]. The mineralogical composition of BYF includes belite and ye'elimite as main and secondary phases, respectively. However, it has been published [13] that a non-active BYF mortar with 33 wt% of β-belite and 19 wt% of orthorhombic-ye'elimite as main phases showed a technological problem associated to their low mechanical strengths achieved at early-medium hydration ages (viz. compressive strengths of ~8 MPa at 7 days of hydration) mainly due to the slow reactivity of belite [13]. A possible solution to this problem goes through the production of cements which jointly contain belite, alite and ye'elimite, which could be named as belite-alite-ye'elimite (BAY) cements [15–22], since alite is responsible for early mechanical strengths in OPC. Their manufacture may release 15% less CO<sub>2</sub> than OPC, depending on their composition. The reaction of alite and ye'elimite with water will develop cements with high mechanical strengths at early ages, while belite will contribute to strength developments at later ages. However, they are difficult to prepare due to the formation/decomposition temperature incompatibility between C<sub>2</sub>S and C<sub>4</sub>A<sub>3</sub>S<sub>3</sub>: alite begins to be formed at ~1300 °C [1], and ye'elimite starts its decomposition at 1300–1350 °C [23–25]. Fortunately, this can be overcome by the addition of minor

\* Corresponding author.

E-mail address: rgl@umma.es (A.G. De la Torre).

<sup>1</sup> Cement nomenclature will be used: C—CaO, S—SiO<sub>2</sub>, A—Al<sub>2</sub>O<sub>3</sub>, F—Fe<sub>2</sub>O<sub>3</sub>, S—SO<sub>3</sub>, and H—H<sub>2</sub>O.<http://dx.doi.org/10.1016/j.cemconcomp.2017.04.002>  
0958-9465/© 2017 Elsevier Ltd. All rights reserved.

quantities of fluorite [18,26] or oxides such those derived from Mg [21], Cu [19], Mn [17], Ti [16] or Zn [15], in the raw materials.

The main objective of the present work is to produce scaled-up belite-elite-yeelimite clinker (~2 kg) from common raw materials to produce mortars developing higher mechanical strengths than belite-yeelimite-ferrite mortars. All the parameters involved in the process (clinkering conditions, hydration mechanism of the cement pastes and water-to-cement ratio) and mechanical properties were studied.

## 2. Experimental

### 2.1. Materials

#### 2.1.1. Synthesis of clinkers

Four BAY clinkers were prepared by mixing natural limestone, sand, iron oxide (byproduct of the sulfuric acid industry) and gypsum (all of them from Financiera y Minera cement factory, Spain) with kaolin (ref. NC-35 from Caolinos Viminazo, Spain). The chemical composition of the raw materials was determined by X-ray fluorescence (XRF) and is given in Table 1. Table 2 reports the targeted composition of the four clinkers, named as BAY\_# referred to the essay number, the amount of each raw material used in their preparation, and the elemental composition (expressed as oxides) of each mixture. Fluorite (>99%, Sigma-Aldrich) was added to each raw material mixture as mineralizer (0.6 wt% in the raw material dosage). The amount of  $\text{CaF}_2$  in the raw materials was 0.9 wt% when only the amount of oxides (after carbonation) is taking into account. All these mixtures were homogenized in an agate mortar throughout 30 min. Then, the mixtures were dye-pressed (~3 g and 20 mm of diameter). The pellets were placed into Pt/Rh crucibles and heated at 900 °C at a heating rate of 5 °C/min and held at that temperature for 30 min. Next, the temperature was raised at the same rate to the final temperature (1300 °C) and held for 15 min. Finally, the clinkers were quenched to room temperature (RT) using forced air convection, ground and sieved through a 75  $\mu\text{m}$  mesh.

#### 2.1.2. Scale-up

BAY\_4 was scaled-up to 2 kg (called hereafter sc-BAY\_4). The raw meal, with the appropriate amounts of the starting materials (see Table 2), was pre-homogenized for 90 min in a micro-Deval machine (A0655, Proest S.A., Spain) at 100 rpm with steel balls (9 balls of 30 mm, 10 balls of 18 mm and 20 of balls of 10 mm). The mixture was dye-pressed (pellets of ~30 g and 55 mm of diameter), and the clinkering conditions were optimized. Three pellets (~90 g) were heated at 900 °C (heating rate of 5 °C/min) and held for 30 min, and then, they were further heated at 1260 or 1300 °C (at same heating rate) and held for 15 min or 30 min. All samples were quenched to RT using forced air convection. Once the clinkering

**Table 1**  
Elemental composition of raw materials determined by XRF (in oxide wt%).

Raw material	limestone	Sand	Kaolin	Iron Source	Gypsum
Oxide					
CaO	54.0	3.1	–	0.3	33.4
$\text{Al}_2\text{O}_3$	0.2	1.8	35.2	0.8	1.2
$\text{SiO}_2$	–	–	–	33.5	34.6
$\text{Fe}_2\text{O}_3$	0.1	2.4	1.3	74.8	0.9
$\text{SO}_3$	0.8	85.0	47.5	3.3	4.8
$\text{K}_2\text{O}$	–	0.5	1.9	–	2.2
$\text{Na}_2\text{O}$	–	–	0.1	–	0.1
MgO	0.5	1.9	0.2	–	1.5
$\text{P}_2\text{O}_5$	–	–	–	–	0.1
Loss*	44.4	5.2	13.8	17.6	23.6

Loss\*: loss of ignition at 1050 °C.

**Table 2**  
Targeted mineralogical phase assemblage (in wt%) of BAY clinkers, raw material dosages (wt%) and nominal elemental composition of raw mixtures (expressed as oxides) including  $\text{H}_2\text{O}$  and  $\text{CO}_2$ .

	BAY_1	BAY_2	BAY_3	BAY_4	sc-BAY_4
Targeted composition (wt%)					
$\text{C}_2\text{S}$	35	35	30	45	45
$\text{C}_3\text{A}$	15	20	15	18	18
$\text{C}_4\text{AF}$	15	20	25	30	30
$\text{C}_2\text{AF}$	15	3	3	3	5
$\text{C}_3\text{S}$	–	–	5	2	2
Raw material (wt%)					
limestone	67.1	67.3	65.7	67.3	66.3
sand	5.6	6.2	8.3	6.5	6.4
gypsum	3.6	4.8	9.0	6.4	7.7
iron source	4.2	1.4	1.4	1.4	1.4
kaolin	18.9	19.7	15.1	17.8	17.9
fluorite	0.6	0.6	0.6	0.6	0.6
Elemental composition of Raw material (wt%)					
CaO	58.1	59.1	59.7	60.0	59.5
$\text{Al}_2\text{O}_3$	10.8	11.2	8.8	10.2	10.1
$\text{SiO}_2$	2.1	2.6	4.9	3.5	4.3
$\text{Fe}_2\text{O}_3$	5.5	2.4	2.4	2.4	2.3
$\text{SO}_3$	22.6	23.9	23.4	23.0	22.8
$\text{CaF}_2$	0.9	0.9	0.9	0.9	0.9

conditions were optimized, seven pellets (~30 g and 55 mm of diameter) were placed into a large Pt/Rh crucible, and heated at 1300 °C for 15 min. This process was repeated ten times to obtain a total of ~2 kg of clinker. The clinkered pellets were ground using a vibration disc mill until an average particle size,  $d_{50}$ , close to 10  $\mu\text{m}$ .

#### 2.1.3. Cement preparation

Cements were prepared by mixing sc-BAY\_4 clinker with 12 wt% of anhydrite which corresponds to the stoichiometric content to complete the reactions with ye'elimite and other calcium aluminates to form ettringite. The resulting cement powder was homogenized for 30 min in a micro-Deval machine at 100 rpm without balls. Anhydrite ( $\text{C}_2\text{S}$ ) was previously prepared by heating commercial micronized gypsum ( $\text{C}_2\text{S} \cdot \text{H}_2\text{O}$ , marketed by BELJIN S.P.R.L. (Belgium), at 700 °C for 60 min (heating rate of 10 °C/min). The cement showed a Blaine surface area of ~5200 ( $\pm 24$ )  $\text{cm}^2/\text{g}$ .

#### 2.1.4. Cement paste preparation

All cement pastes were prepared with deionized water using two different water-to-cement (w/c) mass ratios, 0.4 and 0.5, in a stirrer according to UNE-EN 196–3. The paste with the lowest water content (w/c = 0.4) was prepared with 0.5 wt% (of active matter referred to the cement content) of a commercial polycarboxylate-based superplasticizer (Fisoads 1623, with 25 wt% of active matter) to improve the workability of the paste. Both pastes were poured into hermetically closed polytetrafluoroethylene (PTFE) cylinder shape molds (2.8  $\text{cm}^3$  of volume each) and rotated during the first 24 h, at 20  $\pm 1$  °C [27]. Then, samples were taken out and stored within deionized water at 20  $\pm 1$  °C. The cement pastes, at 1, 7 and 28 days of hydration, were ground into fine powder in an agate mortar, and the hydration was stopped as reported to Ref. [13].

## 2.2. Characterization

#### 2.2.1. Laboratory X-ray powder diffraction (LXRPD) data collection and analysis

LXRPD studies were performed on anhydrous materials and stopped hydration pastes. Powder patterns for anhydrous materials were recorded on an X'Pert MPD PRO diffractometer (PANalytical)

using monochromatic  $\text{CuK}\alpha_1$  radiation ( $\lambda = 1.54059 \text{ \AA}$ ) [Ge (111) primary monochromator] and X'Celerator detector. Data were collected from  $5^\circ$  to  $70^\circ$  ( $2\theta$ ), with stepsize of  $0.016^\circ$  and step time of 300 s yielding a 160 min pattern. The samples were rotated during data collection at 16 rpm in order to enhance particle statistics. Powder patterns for the stopped pastes were recorded on a D8 ADVANCE DaVinci (Bruker AXS, Germany) diffractometer (BRUKER) using monochromatic  $\text{MoK}\alpha_1$  radiation ( $\lambda = 0.7093 \text{ \AA}$ ) [Ge (111) primary monochromator] with LYNXEYE XE 500  $\mu\text{m}$  linear dispersive energy detector. Data were collected from  $3^\circ$  to  $35^\circ$  ( $2\theta$ ). To determine the amorphous and crystalline non-quantified (ACn) [28] content, an internal standard approach was employed [29,30]. As internal standard, quartz (99.56%, ABCR GmbH & Co. KG), was added to the samples to a total content of  $\sim 20 \text{ wt\%}$ . The mixtures (sample-standard) were homogenized for 20 min in an agate mortar.

All the patterns were analyzed by the Rietveld method using GSAS software package [31] by using a pseudo-Voigt peak shape function [32] with the asymmetry correction included [33] to obtain Rietveld Quantitative Phase Analysis (RQPA). The refined overall parameters were: phase scale factors, background coefficients, unit cell parameters, zero-shift error, peak shape parameters and preferred orientation coefficient, if needed [March–Dollase ellipsoidal preferred orientation correction algorithm [34]]. The crystal structure descriptions used for all phases were given in Refs. [28] and [35], and updated crystallographic descriptions were used for orthorhombic [36] and pseudo-cubic [37] ye'elimite.

#### 2.2.2. Scanning electron microscopy (SEM)

The fracture cross-section of a selected clinker pellet (sc-BAY\_4) was observed in a Jeol JSM-6490LV (Japan) scanning electron microscope using secondary electrons at 20 kV. Prior to SEM observation, the sample was gold sputtered.

The same clinker pellet was mounted in epoxy resin and was progressively diamond polished down to  $3 \mu\text{m}$ . A field emission scanning electron microscope (FE-SEM) (Helios Nanolab 650 dual beam from FEI) was used. BSE images were acquired at 15 kV with a retractable CBS backscatter detector (annular solid-state device) that inserts and rests directly underneath the final lens of the system. EDS analysis was performed with a X-Max 50  $\text{mm}^2$  detector from Oxford Instruments with AZtec software (v.1.0).

#### 2.2.3. Thermal analysis

Differential thermal (DTA) and thermogravimetric (TGA) analyses were performed in a SDT-Q600 analyzer from TA instruments (New Castle, DE) for a ground fraction ( $\sim 30 \times 10^{-3} \text{ g}$ ) of every paste after stopping hydration. The temperature was varied from room temperature to  $1000^\circ\text{C}$  at a heating rate of  $10^\circ\text{C}/\text{min}$ . Measurements were carried out in open platinum crucibles under air flow ( $100 \text{ mL}/\text{min}$ ). The weight loss from RT to  $600^\circ\text{C}$  was computed to be water (chemically bounded water) and that from  $600$  to  $1000^\circ\text{C}$  was considered as  $\text{CO}_2$ . Table 3 lists the corresponding data.

**Table 3**

Weight loss and loss on ignition (LOI) obtained from TGA measurements for all pastes.

w/c ratio	Paste age (days)	Weight loss RT-600 °C (%)	Weight loss 600-1000 °C (%)	LOI at 900 °C (%)
0.4	1	18.3	0.7	17.5
	7	20.8	1.2	19.3
	28	22.1	1.3	20.1
0.5	1	18.3	0.7	19.7
	7	20.6	0.8	24.4
	28	23.8	1.0	28.0

#### 2.2.4. Compressive strengths

Standard mortars were prepared at a cement/sand ratio of 1/3 and water/cement ratios of 0.4 and 0.5 according to UNE-EN196-1. CEN EN196-1 standard sand was used. The same superplasticizer used for cement pastes (0.5 wt% of active matter referred to cement content) was used to prepare the mortars with w/c ratio of 0.4, to improve the workability. Cubes ( $30 \times 30 \times 30 \text{ mm}^3$ ) were cast and cured at  $20 \pm 1^\circ\text{C}$  and 99% relative humidity (RH) for 24 h; then the cubes were demolded and cured within a water bath at  $20 \pm 1^\circ\text{C}$  until testing (3, 7 and 28 days for mortars prepared at w/c ratio of 0.5, and 1, 7 and 28 days for mortars prepared at w/c ratio of 0.4). The compressive strength of cubic mortars was measured in a Model Autotest 200/10 W (Ibertest, Spain) press.

### 3. Results and discussion

#### 3.1. Synthesis of clinkers and scale-up methodology

Fig. 1 shows LXRDP patterns of all BAY clinkers and Table 4 reports their mineralogical composition determined by Rietveld method, normalized to 100 wt% of crystalline phases. Numbers in brackets indicate the error from Rietveld method (not standard deviation). In general, free lime was not observed (except for BAY\_2 where  $\sim 2 \text{ wt\%}$  was quantified) revealing that the clinkering process was finished at  $1300^\circ\text{C}$ , which is  $150^\circ\text{C}$  lower than that commonly used for OPC clinkers. Although the phase assemblage of all clinkers was somewhat different to their targeted phase composition, three of them contain high percentages of both alite and ye'elimite,

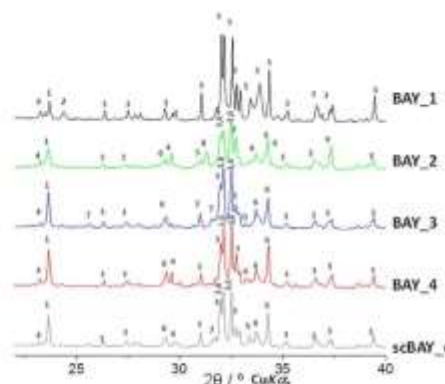


**Fig. 1.** LXRDP patterns for BAY clinkers with monochromatic  $\text{CuK}\alpha_1$  ( $\lambda = 1.5406 \text{ \AA}$ ). Where 1 ( $\text{C}_1\text{A}_1$ ), 2 ( $\text{C}_2\text{A}_1$ ), 3 ( $\beta\text{-C}_2\text{S}$ ), 4 ( $\gamma\text{-C}_2\text{S}$ ), 5 ( $\text{C}_3\text{A}$ ), 6 ( $\text{C}_4\text{A}$ ), 7 (F), 8 ( $\text{C}_3\text{A}$ ), 9 (Free lime), 0 ( $\text{C}_3\text{A}$ ).



336

D. Lendino-Jadaga et al. / *Cement and Concrete Composites* 80 (2017) 323–346

**Table 4**  
RQPA (wt%) for BAY clinkers (3 g pellets).

Phase	BAY_1	BAY_2	BAY_3	BAY_4
B-C <sub>2</sub> S	65.0 (1)	44.9 (3)	59.9 (2)	51.8 (2)
γ-C <sub>2</sub> S	2.7 (1)	12.2 (2)	2.9 (2)	8.3 (2)
C <sub>3</sub> Af	22.0 (2)	8.2 (2)	7.6 (1)	7.0 (1)
C <sub>3</sub> S	–	–	0.3 (2)	–
α-C <sub>4</sub> A <sub>3</sub> f	3.5 (1)	1.9 (1)	0.7 (2)	0.1 (4)
α-C <sub>4</sub> A <sub>3</sub> S	–	7.9 (1)	0.6 (2)	3.0 (4)
C <sub>2</sub> S	–	13.0 (3)	13.1 (2)	76.6 (2)
C <sub>12</sub> A <sub>7</sub>	6.6 (1)	2.1 (0)	–	2.9 (1)
Fluorellestite	–	–	3.0 (3)	–
C <sub>3</sub> A	–	–	0.8 (1)	2.3 (1)
C <sub>3</sub> AS	–	7.0 (3)	–	–
Free lime	–	2.7 (1)	–	–
R <sub>90</sub>	4.33	6.37	5.89	5.40

jointly with belite and ferrite. The maximum percentages of alite and ye'elimite were 36.0 (2) and 12.1 (4) wt%, respectively, for BAY\_4 (see Table 4). This yields an alite/ye'elimite mass ratio of 1.3. The low-temperature polymorph of dicalcium silicate, γ-C<sub>2</sub>S, was found in all the clinkers. This phase increases its unit cell volume about 12% when compared to β-form producing powdered clinkers and, in addition, it is hydraulically inactive; therefore its presence is undesirable in clinkers. It is formed on cooling by the polymorphic transformation, β-C<sub>2</sub>S → γ-C<sub>2</sub>S below 500 °C. The formation of γ-C<sub>2</sub>S is enhanced by i) prolonged holding times at high temperatures, ii) slow cooling rates, and iii) the absence of foreign ions that stabilize the β-form. The presence of γ-C<sub>2</sub>S phase in these laboratory clinkers is associated mainly with the latter factor. In addition, a more efficient quenching process could have reduced the presence of this component. Moreover, small amounts of mayenite (C<sub>12</sub>A<sub>7</sub>) and C<sub>3</sub>A were also found in the clinkers. Since these phases are hydraulically active, their presence in the clinkers has to be taken into consideration to prepare the corresponding cements. In addition, fluorellestite (F-ellestite) [38,39], which is an inert phase [40], is present in BAY\_3. From these results, BAY\_1 was ruled out due to the absence of alite and BAY\_2 presented both free lime and non-negligible percentages of gehlenite (C<sub>2</sub>AS), which has been described as an intermediate phase in the mechanism of formation of CSA clinkers which does not present hydraulic properties [8,41]. According to these results, BAY\_3 and BAY\_4 were the most promising candidates to be scaled-up, and BAY\_4 was finally chosen due to the absence of fluorellestite.

In a second step, a large amount of BAY\_4 was prepared, so the clinkering conditions had to be again fine-tuned, including both the

highest temperature and the dwelling time at that temperature, as described in the Experimental section. Table 5 gives the RQPA for sc-BAY\_4, using -90 g mixtures (3 pellets of -30 g each) each time, under three different thermal treatments (1300 °C/15 min, 1300 °C/30 min, and 1280 °C/15 min). In the three cases, the amount of ye'elimite was drastically reduced and mayenite was doubled since the solid diffusion favored the mayenite formation instead of ye'elimite, and there was a loss of sulfur as SO<sub>2</sub> as determined by XRF, Table 5. Samples clinkered at 1300 °C for 30 min show a reduction of the alite amount to half, and when samples were heated at 1280 °C for 15 min, only ~1 wt% of alite was obtained; then, both thermal processes were discarded. Pellets clinkered at 1300 °C for 15 min show the highest percentages of alite and ye'elimite in the range of the study, so these clinkering conditions were selected for further studies. In the following step, an excess of sulfur (to a total amount of 4.3 wt% of SO<sub>2</sub>, supplied as gypsum) was added to the raw materials to compensate the loss of sulfur as SO<sub>2</sub> and to favor ye'elimite formation/stabilization. This final elemental composition of sc-BAY\_4 raw material is also included in Table 2. These clinkering conditions were selected for further studies. Table 5 reports the final mineralogical composition of the as-obtained clinker (2 kg), where the amount of ye'elimite increased up to 10.4 (1) wt%. The elemental composition of this clinker determined by XRF is also included in Table 5, confirming a higher amount of retained sulfur, comparing Tables 2 and 5. It must be noted that this clinker shows an alite/ye'elimite ratio of 1.3 (similar to that for small pellets). A total of 2 kg, in batches of ~210 g, were obtained following these clinkering conditions, which show the same mineralogical composition than that prepared in batches of ~90 g with the same pellet size. Phase assemblage of individual batches was checked prior to be mixed showing a standard deviation of less than 2% in all the phases. Taking into account the final composition of the scaled-up clinker (and the used raw materials) and the clinkering temperature, a total reduction of 13.4% of CO<sub>2</sub> emission, compared to OPC, is expected, which comprises 7.2% due to the decarbonation of the raw materials, and the remaining is related to the reduction of fuel and electricity [3].

Fig. 2 shows SEM micrographs, at different magnifications, of the fracture surface of a clinkered sc-BAY\_4 pellet, where prismatic particles of C<sub>2</sub>S (Fig. 2b), rounded particles of C<sub>3</sub>S (<5 μm) (Fig. 2b and c) and rhombic particles (~4 μm) of ye'elimite (Fig. 2c) were identified; the shape of ye'elimite is known to be rhombic dodecahedron [15,42]. The sample is highly porous (Fig. 2a), which should favor the grinding of the material. Moreover, to have a deeper insight on the composition of clinker phases, EDS measurements of polished sections were also performed. Table 6 includes the atomic

**Table 5**  
RQPA (wt%) for sc-BAY\_4 clinker at different thermal cycles. Elemental composition of clinkers selected to be scaled-up determined by XRF.

Phase	1300 °C/15 min	1300 °C/30 min	1280 °C/15 min	1300 °C/15 min with excess of sulfur*
B-C <sub>2</sub> S	56.3 (2)	62.2 (1)	60.0 (2)	59.4 (2)
γ-C <sub>2</sub> S	4.1 (1)	3.6 (1)	3.2 (1)	1.5 (1)
C <sub>3</sub> Af	6.4 (2)	6.0 (2)	6.0 (3)	8.9 (2)
C <sub>3</sub> S	0.9 (2)	1.1 (2)	1.3 (2)	0.6 (3)
α-C <sub>4</sub> A <sub>3</sub> f	5.2 (2)	5.6 (1)	5.0 (1)	10.4 (1)
C <sub>2</sub> S	16.2 (1)	8.9 (1)	11.7 (2)	13.5 (2)
C <sub>12</sub> A <sub>7</sub>	0.5 (1)	10.4 (1)	11.3 (1)	5.1 (1)
C <sub>3</sub> A	1.2 (1)	1.3 (1)	0.1 (1)	–
C <sub>3</sub> AS	0.9 (3)	0.6 (1)	1.4 (1)	–
CaO	61.3	–	–	59.4
Al <sub>2</sub> O <sub>3</sub>	10.9	–	–	11.8
SO <sub>2</sub>	2.4	–	–	3.0
Fe <sub>2</sub> O <sub>3</sub>	2.2	–	–	2.3
SiO <sub>2</sub>	22.9	–	–	23.5

\* Also contains 2.6 (1) wt% of fluorellestite.

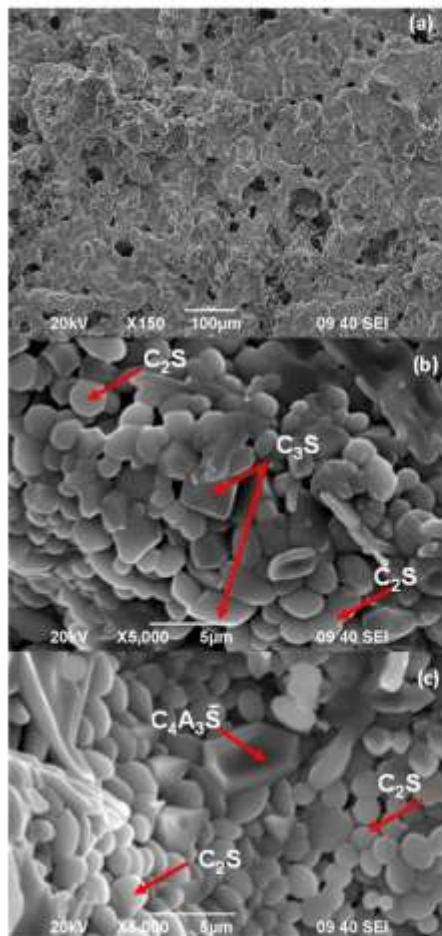


Fig. 2. SEM micrographs of sc-BAY\_4.

ratios obtained by EDS and the corresponding values of the stoichiometric phases for the sake of comparison. Fig. 3 shows a BSE image (FE-SEM) with the particles labeled according to atomic ratios obtained by EDS. Rounded particles presented an average composition close to belite as expected. The prismatic particles of alite are not so clearly observed in the polished section, but EDS analysis of particles labeled as 2 in Fig. 3 clearly matches with that of alite. The same can be argued for ye'elimite, labeled as 3 in Fig. 3. Due to small particle size, i.e. less than 1  $\mu\text{m}$ ,  $\text{C}_4\text{AF}$  and  $\text{C}_{12}\text{A}_7$  were not detected isolated.

Table 6

Average atomic ratios obtained by EDS in sc-BAY clinker;  $n$  stands for the number of measurements (points) analyzed. Theoretical atomic ratios of clinker phases in (curves) are also included.

Atomic ratio	$n$	Si/Ca	Al/Ca	S/Ca	Fe/Ca	F/Ca
Experimental EDS ratios						
$\text{C}_2\text{S}$	32	0.47 (2)	0.07 (3)	0.53 (3)	0.01 (5)	–
$\text{C}_3\text{S}$	4	0.31 (7)	0.05 (2)	0.68 (4)	0.02 (3)	–
$\text{C}_4\text{A}_3\text{S}$	5	0.05 (1)	1.31 (6)	0.25 (2)	–	–
Subcooled phase <sup>a</sup>	5	0.06 (4)	1.07 (13)	0.57 (8)	0.40 (3)	–
Fluorellesatite	3	0.31 (5)	0.31 (13)	0.25 (2)	–	0.26 (10)
Theoretical stoichiometric ratios						
$\text{C}_2\text{S}$	0.50	–	–	–	–	–
$\text{C}_3\text{S}$	0.33	–	–	–	–	–
$\text{C}_4\text{A}_3\text{S}$	–	1.50	0.25	–	–	–
$\text{C}_4\text{AF}$	–	–	–	0.50	–	–
$\text{C}_{12}\text{A}_7$	–	1.17	–	–	–	–
Fluorellesatite	0.30	–	0.30	–	–	0.20

<sup>a</sup> Mainly consists on  $\text{C}_4\text{AF}$  and  $\text{C}_{12}\text{A}_7$ .

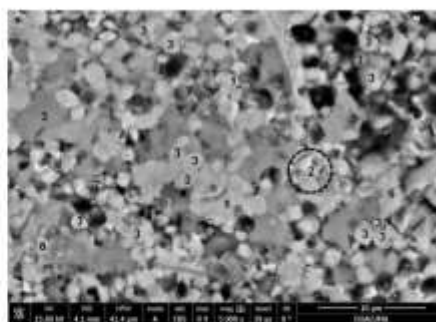


Fig. 3. Backscatter electron (BSE) micrograph (FE-SEM) of sc-BAY clinker. Where 1 ( $\text{C}_4\text{A}_3\text{S}$ ), 2 (subcooled phase), 3 ( $\text{C}_4\text{AF}$ ), 4 ( $\text{C}_3\text{S}$ ), 5 ( $\text{C}_2\text{S}$ ), and 7 (Fluorellesatite).

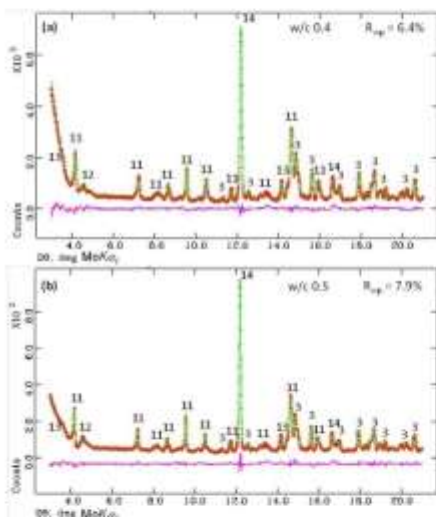
### 3.2. Hydration of BAY cement pastes

Table 7 shows the RQPA for the hydration of the sc-BAY\_4 cement (with 12 wt% of anhydrite) pastes; this table includes both ACN and free water (FW) contents. FW was estimated by the difference between the added water and the combined water determined by TGA. Table 3. As representative examples, Fig. 4 shows the Rietveld plots for sc-BAY\_4 hydrated at 28 days ( $w/c = 0.4$  and  $w/c = 0.5$  for Fig. 4a and b, respectively). From Table 7, it can be seen that both anhydrite and ye'elimite were consumed within the first day of hydration, independently of the water content. The main hydration products are ettringite (AFt), two AFm-type phases: monosulfaluminate ( $\text{C}_4\text{A}_3\text{S} \cdot \text{H}_{12}$ ) and stratlingite ( $\text{C}_2\text{S} \cdot \text{ASH}_3$ ), katoite ( $\text{C}_3\text{ASH}_4$ ), and C-S-H (partially quantified as clinotobermorite with the approximate chemical composition of  $\text{C}_6\text{S}_3\text{O}_{17}(\text{H}_2\text{O})_2$ ) [43]. Ye'elimite reacts with anhydrite to form ettringite (AFt) and amorphous hydrated aluminum hydroxide (i.e. crystalline gibbsite was not detected). Belite showed a typical hydration behavior, and only after 28 days, a small amount of this phase reacted with water. Alite was almost consumed at 7 days of hydration. In OPC, this phase reacts with water to form C-S-H (amorphous calcium silicate hydrate) and portlandite. However, in this hydrated aluminum hydroxide-rich system the following reaction may be carrying out to form stratlingite [1], reaction #1):

**Table 7**  
RQPA (wt%) for sc-BAY\_4 pastes.

Phases	w/c = 0.4				w/c = 0.5			
	<i>t</i> <sub>0</sub>	7d	28d	28d	<i>t</i> <sub>0</sub>	7d	28d	28d
β-C <sub>2</sub> S	29.5 (3)	32.1 (1)	33.1 (2)	28.9 (2)	27.6 (3)	30.6 (1)	29.0 (2)	24.0 (2)
γ-C <sub>2</sub> S	0.8 (1)	1.0 (1)	1.3 (1)	2.2 (1)	0.8 (1)	1.5 (1)	1.5 (1)	1.3 (1)
C <sub>3</sub> A	2.6 (1)	2.3 (1)	–	–	2.4 (1)	0.8 (1)	–	–
C <sub>3</sub> S	6.6 (1)	–	–	–	6.2 (1)	–	–	–
C <sub>4</sub> A <sub>3</sub> S <sub>3</sub>	5.0 (1)	1.4 (1)	–	–	4.7 (1)	1.2 (1)	–	–
C <sub>2</sub> S	0.8 (2)	2.6 (1)	0.0 (1)	–	6.4 (2)	2.1 (1)	0.0 (1)	–
C <sub>2</sub> A <sub>3</sub>	3.8 (1)	2.0 (1)	–	–	3.6 (1)	1.1 (1)	–	–
Ferrihydrite	2.2 (2)	2.7 (1)	2.6 (1)	2.6 (1)	2.1 (2)	3.5 (1)	2.6 (1)	2.4 (1)
Monosulfoaluminate	–	–	0.8 (2)	–	–	0.4 (2)	1.2 (2)	1.6 (2)
AFm	–	0.4 (1)	2.4 (1)	3.0 (1)	–	0.9 (1)	2.2 (1)	3.0 (1)
Katoite	–	29.8 (2)	16.0 (2)	16.6 (2)	–	15.1 (2)	10.2 (2)	12.7 (2)
Stratlingite	–	1.3 (1)	2.4 (2)	3.7 (2)	–	1.1 (1)	1.8 (1)	2.5 (1)
ACn	–	1.2 (1)	4.7 (2)	5.0 (2)	–	–	5.2 (2)	5.3 (2)
ACn	14.0 (2)	20.0 (2)	26.1 (2)	24.0 (2)	11.1 (2)	24.7 (2)	20.4 (2)	34.8 (2)
FW	28.6 (–)	12.6 (–)	8.7 (–)	8.3 (–)	33.3 (–)	17.1 (–)	16.0 (–)	12.5 (–)

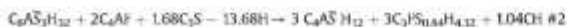
\* Monosulfoaluminate, with chemical formula [Ca<sub>2</sub>Al<sub>2</sub>(OH)<sub>6</sub>SO<sub>4</sub>·nH<sub>2</sub>O].



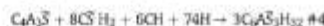
**Fig. 4.** Rietveld plot of sc-BAY\_4 pastes at 28 days of hydration with monochromatic MoK<sub>α</sub> (λ = 0.7093 Å) radiation. a) w/c = 0.4 and b) w/c = 0.5. Numbers stand for 11 (C<sub>2</sub>S), 12 (AFm), 13 (Stratlingite) and 14 (Quartz as internal standard).



After 7 days of hydration, ferrite has completely reacted. Recently, the reactivity of ferrite in the presence of silicates has been published [44], in which AFm is consumed to give mono-sulfoaluminate and katoite, reaction #2:



However, portlandite was not detected by LXRPD or DTA-TG in these systems. Consequently, we can speculate that calcium hydroxide is being consumed to form katoite [1] (reaction #3), AFm (reaction #4) or monosulfoaluminate (reaction #5) [45], as all these phases are detected by LXRPD.



Moreover, from Table 7, it can be observed that only ~60 wt% of the dissolved aluminate-bearing phases (C<sub>4</sub>A<sub>3</sub>S<sub>3</sub>, C<sub>12</sub>A<sub>7</sub> and C<sub>4</sub>A<sub>3</sub>) has crystallized as AFm and AFn. Consequently, ~40 wt% of the aluminate content may be as ACn phase(s), mainly as an aluminum hydroxide gel, as detected by DTG-TGA, Fig. 5. In addition, ~50 wt% of the dissolved silicates phases (C<sub>2</sub>S and C<sub>3</sub>S) has crystallized as C-S-H, stratlingite and katoite. As reported by Alvarez-Pinazo et al. [13], katoite may present a significant amount of aluminum substituted by iron. The Al<sup>3+</sup> ratio was estimated in katoite with general formula C<sub>3</sub>A<sub>1-x</sub>Fe<sub>x</sub>S<sub>4</sub>, using the equation  $\alpha = 0.31x - 22.29$  [13]. In these systems,  $x$  is ~0.7 and ~0.5 for w/c ratios of 0.4 and 0.5 respectively. With these results, it can be said that ~80 wt% of the hydrated ferrite crystallized as katoite.

It has to be highlighted that the amount of stratlingite was lower in these pastes at any time, when compared to the hydrating behavior of BYF reported elsewhere [13,46]. This may be due to the lower reactivity of helite in sc-BAY\_4 (~10% at 28 days) compared to that in a BYF cement paste (A10B6, paste prepared with 10 wt% of anhydrite at w/c 0.55) (~37% at 28 days of hydration) [46]. It must be noted that the pH values of the corresponding pastes are likely different which may play a role. In any case, more research is needed to fully clarify the hydration mechanisms.

The evolution of the amorphous phases with time was checked through thermal analyses. Fig. 5 shows DTG-TGA plots of all the studied pastes at w/c = 0.4 (Fig. 5a) and w/c = 0.5 (Fig. 5b). Three

- de Torre, I., León-Rozsa, M.A.G., Aranda, R., Rietveld quantitative phase analysis of Ye'elimite-containing cements, *Cem. Concr. Res.* 42 (2012) 960–971.
- [36] A. Cuervo, A.G. De la Torre, E.R. Leizaola, V.R. Pérez, P. Reynak, A. Aysela, C. Frutieria, M.A.G. Aranda, 3D structure, atomistic simulation, and phase transition of inachinometric ye'elimite, *Chem. Mater.* 23 (2011) 1580–1587.
- [37] A. Cuervo, A.G. De la Torre, E.R. Leizaola, I. Santacruz, M.A.G. Aranda, Pseudocubic crystal structure and phase transition in doped Ye'elimite, *Cryst. Growth Des.* 14 (2014) 5126–5163.
- [38] I. Pajares, A.G. De la Torre, S. Martínez-Ramírez, F. Puertas, M.T. Blanco-Varela, M.A.G. Aranda, Quantitative analysis of mineralogical white Portland clinker: the structure of Haasferritine, *Powder Diff.* 17 (4) (2002) 281–286.
- [39] S. Gieseler-Kulina, M.T. Blanco-Varela, Solid state phase relationship in the  $\text{CaO}-\text{SO}_3-\text{Al}_2\text{O}_3-\text{CaF}_2-\text{CaSO}_4$  system, *Cem. Concr. Res.* 23 (1993) 475–482.
- [40] F. Puertas, M.T. Blanco-Varela, A. Palomo, T. Vázquez, Behaviour of a new white cement fabricated with raw materials containing  $\text{CaF}_2$  and  $\text{CaSO}_4 \cdot 2\text{H}_2\text{O}$ , Part I: hydration process, *ZKG Int.* 50 (1997) 212–220.
- [41] G.S. Li, G. Walesta, L.M. Gartner, Montreal, Canada, in: Formation and Hydration of Low- $\text{CO}_2$  Cements Based on Belite, Calcium Sulfoaluminate and Calcium Aluminoferrite, Proceedings of the 12th ICCI, 2007, TH3–15.3.
- [42] L. Linghao, Ch Jun, Ch Xin, L. Jianing, Y. Runsheng, Study on a cementing system taking alite-calcium borate sulphoaluminate as main mineral, *J. Mater. Sci.* 40 (2005) 4035–4438.
- [43] S. Morino, E. Bonaccorsi, T. Arzufforzi, The real structure of clinobermudite and tribromite 9A: OD character, polytypes, and structural relationships, *Eur. J. Mineral.* 12 (2000) 411–428.
- [44] N. Chittaramand, F. Winnefeld, C.W. Hängl, S. Santhopraj, B. Lothenbach, Synthesis and hydration of alite-calcium sulfoaluminate cement, *Adv. Con. Res.* 29 (2017) 101–111.
- [45] C.W. Hängl, A.P. Kirchheim, F.J.M. Monteiro, L.M. Gartner, Early age hydration of calcium sulfoaluminate (synthetic ye'elimite,  $\text{C}_3\text{A}_3\text{S}$ ) in the presence of gypsum and varying amounts of calcium hydroxide, *Cem. Concr. Res.* 48 (2013) 105–115.
- [46] G. Alvarez-Finazo, I. Santacruz, M.A.G. Aranda, A.G. De la Torre, Hydration of belite-ye'elimite-ferite cements with different calcium sulfate sources, *Adv. Con. Res.* 28 (2016) 529–543.
- [47] J.I. Tobón, J. Piya, M.V. Borrachero, L. Sottano, G.J. Rintropo, Determination of the optimum parameters in the high resolution thermogravimetric analysis (HR-TGA) for cementitious materials, *J. Therm. Anal. Calorim.* 107 (2012) 231–238.
- [48] F. Winnefeld, S. Barlag, Calorimetric and thermogravimetric study on the influence of calcium sulfate on the hydration of ye'elimite, *J. Therm. Anal. Calorim.* 101 (2010) 949–957.
- [49] K. Traucheneck, J.M. Meehling, A. Leornie, A. Roux, B. Le Rolland, Hydration of ordinary Portland cement and calcium sulfoaluminate cement blends, *Cem. Concr. Compos.* 58 (2015) 106–114.
- [50] T. Matschei, B. Lothenbach, F.P. Glasser, Thermodynamic properties of Portland cement hydrates in the system  $\text{CaO}-\text{Al}_2\text{O}_3-\text{SO}_3-\text{CaSO}_4-\text{CaCO}_3-\text{H}_2\text{O}$ , *Cem. Concr. Res.* 37 (10) (2007) 1339–1400.
- [51] I. Santacruz, A.G. De la Torre, G. Alvarez-Finazo, et al., Structure of shuftegitte and effect of hydration methodology on microstructure, *Adv. Con. Res.* 28 (1) (2016) 11–22.
- [52] F. Winnefeld, S. Barlag, Influence of calcium sulfate and calcium hydroxide on the hydration of calcium sulfoaluminate clinker, *ZKG Int.* 12 (2009) 42–53.
- [53] K. Traucheneck, J.M. Meehling, A. Leornie, A. Roux, B. Le Rolland, Impact of anhydrite proportions in a calcium sulfoaluminate cement and Portland cement blend, *Adv. Con. Res.* 28 (5) (2014) 325–333.

**Paper # 2. Influence of Fly Ash blender on hydration and physical behavior of Belite-Alite-Ye'elimite cement [136]**

Cover Letter

Dr. Ángeles G. De la Torre  
Departamento de Química Inorgánica  
Facultad de Ciencias  
Universidad de Málaga  
29071 - MÁLAGA, Spain  
Int- 34-952131877, Fax: Int- 34-  
952131870  
<http://webpersonal.uma.es/~mgd/>  
[mgd@uma.es](mailto:mgd@uma.es)

Málaga, 13<sup>th</sup> October, 2017

Dear Prof. Michael C. Forde,

Construction and Building Materials Editor-in-Chief

I have the pleasure to submit on-line for publication in *Construction and Building Materials* as a research article the work entitled "*Influence of Fly Ash blending on hydration and physical behavior of Belite-Alite-Ye'elimite cement*" authors: Diana Londono-Zuluaga, Jorge Iván Tobón, Miguel A. G. Aranda, Isabel Santacruz, Angeles G. De la Torre.

This paper deals with the characterization of three eco-cements, containing belite, alite and ye'elimite (BAY), with the addition of fly ash (0, 15 and 30 wt%). The main aim of this work has been the understanding of the effect of addition of fly ash on BAY cement hydration mechanisms and its impact on mechanical strengths.

The key findings of this work are:

- (1) The amount of a polycarboxylate based superplasticizer has been optimized for the blended BAY cement with fly ash in order to prepare homogeneous pastes with low viscosity values.
- (2) The isothermal calorimetric study reveals that the superplasticizer affects the hydration behaviour of calcium aluminate phases in BAY.
- (3) The presence of fly ash has inhibited the AF<sub>n</sub> decomposition, since this phase was unstable in the cement without fly ash after 28 days, while it was not decomposed in the cement with 30 wt% of fly ash.
- (4) High additions of fly ash inhibited the reactivity of belite.
- (5) We only have found indirect evidence of pozzolanic chemical reaction, since the compressive strengths of mortars increased with the fly ash addition, mainly due to decrease in the porosity (and pore size) of the corresponding mortars.
- (6) The increase of water content of these types of systems (w/c of 0.40 to 0.57) has affected the katoite/stratlingite ratio, i.e. higher w/c contents yielded to higher contents of stratlingite and lower ones of katoite.

I look forward to hearing from you.

Yours Sincerely,

Ángeles. G. De la Torre

\*Manuscript

[Click here to view linked References](#)

*Manuscript to be submitted to construction and building materials*

**Influence of Fly Ash blending on hydration and physical behavior of Belite-Alite-  
Ye'elimite cement**

Londono-Zuluaga, D.<sup>1,2</sup>, Tobón, J.L.<sup>2</sup>, Aranda, M.A.G.<sup>1,3</sup>, Santacruz, I.<sup>1</sup>, De la Torre, A.G.<sup>\*1</sup>

1. Departamento de Química Inorgánica, Cristalografía y Mineralogía, Universidad de Málaga, 29071 Málaga, Spain

2. Grupo del Cemento y Materiales de Construcción, CEMATCO, Universidad Nacional de Colombia, Facultad de Minas, Medellín, Colombia

3. ALBA Synchrotron, Carrer de la Llum 2-26, E-08290 Cerdanyola del Vallès, Barcelona, Spain

\*Corresponding author. Tel.: +34952131877; fax: +34952131870. E-mail: [mgd@uma.es](mailto:mgd@uma.es)

Cement nomenclature: C=CaO, S=SiO<sub>2</sub>, A=Al<sub>2</sub>O<sub>3</sub>, F=Fe<sub>2</sub>O<sub>3</sub>,  $\bar{S}$ =SO<sub>3</sub> and H=H<sub>2</sub>O



## 1 Abstract

2 Three cement containing belite-alite-ye'elimite cement blended with 0, 15 and 30 wt% of fly ash have been  
3 characterized. The contribution of fly ash to the hydration reactions resulted in both the partial inhibition of  
4 Aft degradation and belite reactivity, even after 180 days. The compressive strength was enhanced with the  
5 increase of fly ash addition (68, 73 and 82 MPa for 0, 15 and 30 wt% of fly ash, respectively at 180d),  
6 mainly due to a decrease of the porosity and pore size. Pozzolanic reaction has not been proved directly but  
7 there are indirect evidences.

8 **Keywords**— Belite-alite-ye'elimite cement; Fly ash; Hydration; Rietveld method; Phase evolution; NMR;  
9 Compressive strength.

10

## 11 1. Introduction

12 An environmental strategy for reducing the negative effect of CO<sub>2</sub> footprint of the Portland Cement (PC)  
13 industry, consists on its partial substitution by reactive industrial by-products, such as fly ash [1,2]. Fly ash  
14 (FA) is the major solid waste generated from coal-firing power stations. From power station perspective,  
15 they are looking for ways to exploit fly ash disposal in an economically advantageous way. However, from  
16 the building industry perspective, FA is looked upon as a supplementary cementitious material (SCM)  
17 which is used in mass, conventional and high performance concrete as a cement replacement material [3].  
18 Furthermore, the addition of FA to cement can modify its properties, such as reduced hydration heat and  
19 thermal cracking in concrete at early ages, improved workability of fresh mortar/concrete mix, improved  
20 durability and ultimate strength increase [3,4]. Despite the benefits offered by OPC cement/concrete  
21 blended with FA, high amount of fly ash utilization is still not achieved due to various limitations, such as  
22 variability in its mineralogy and chemical compositions [5].

23 Another alternative to reduce CO<sub>2</sub> emission consists on the development of eco-cements composed by less  
24 calcite demanding phases, such as belite and ye'elimite. That is the case of calcium sulfoaluminate (CSA)



UNIVERSIDAD  
DE MÁLAGA



## **Annex II:**

# ***In-situ* hydration evolution of pure phase mixtures.**

The tables and figures given in this annex show the RQPA results including ACn and free water (FW) determined by internal standard methodology of the XRD in-situ study of mixtures of pure phases.

**Table A1.** RQPA results (wt%) of the *in-situ* hydration study of c137\_066.

Phases Age (h)	C <sub>4</sub> A <sub>3</sub> S	Cs	AFt	AFm	C <sub>2</sub> ASH <sub>8</sub>	Hemi- CO <sub>3</sub> <sup>a</sup>	C <sub>3</sub> S	ACn+FW
0	21.7	9.5	-	-	-	-	26.4	42.4
1	20.7	9.2	1.5	-	-	-	26.4	42.2
1.5	20.3	9.2	2.0	-	-	-	26.4	42.2
2	19.5	9.0	2.6	-	-	-	26.4	42.5
3	18.7	8.9	3.3	-	-	-	26.4	42.7
4	17.8	8.7	4.2	-	-	-	26.4	42.7
6	16.3	8.2	5.7	-	-	-	26.4	43.3
8	15.0	7.8	7.2	-	-	-	26.4	43.5
10	12.8	7.2	10.0	-	-	-	26.4	43.6
12	9.6	6.2	14.2	-	-	-	26.4	43.6
14	8.0	5.6	16.4	-	-	-	26.4	43.5
18	7.3	5.3	18.1	-	-	-	26.4	43.0
24	0.2	2.0	32.0	0.9	1.7	-	21.2	41.9
38	-	2.0	33.1	0.9	3.0	-	19.1	41.6
47	-	1.9	33.2	0.9	4.6	-	18.0	41.3
168*	-	1.4	32.7	0.7	8.2	0.1	14.3	42.6

a.Hemi-CO<sub>3</sub> : Hemicarbonate

\*168 h = 7 days of hydration

**Table A2.** RQPA results (wt%) of the *in-situ* hydration study of c137\_132.

Phases Age (h)	C <sub>4</sub> A <sub>3</sub> S	Cs	AFt	AFm	C <sub>2</sub> ASH <sub>8</sub>	Hemi- CO <sub>3</sub> <sup>a</sup>	C <sub>3</sub> S	ACn+FW
0	15.5	6.8	-	-	-	-	18.9	58.8
1	14.6	6.6	1.2	-	-	-	18.9	58.7
2	13.8	6.4	2.0	-	-	-	18.9	58.8
3	13.2	6.3	2.6	-	-	-	18.9	59.1
4	12.6	6.2	3.2	-	-	-	18.9	59.1
6	8.2	5.0	8.5	-	-	-	18.6	59.7
8	4.9	3.7	13.5	-	-	-	18.5	59.3
10	2.5	2.5	17.8	-	-	-	18.4	58.8
12	1.1	1.6	20.7	-	-	-	18.3	58.3
14	0.4	1.1	22.8	-	-	-	18.3	57.4
18	-	0.6	25.0	-	-	-	17.6	56.8
24	-	0.1	25.5	0.2	2.6	0.4	15.1	56.0
38	-	-	27.4	0.2	7.9	0.7	11.4	52.4
47	-	-	26.9	0.2	10.7	1.1	10.1	51.0
168*	-	-	24.5	0.2	9.8	1.3	7.9	56.0

a. Hemi-CO<sub>3</sub> : Hemicarbonat

\*168 h = 7 days of hydration

**Table A3.** RQPA results (wt%) of the *in-situ* hydration study of o137\_066.

Phases	C <sub>4</sub> A <sub>3</sub> S	Cs	AFt	AFm	C <sub>2</sub> ASH <sub>8</sub>	C <sub>3</sub> S	ACn+FW
Age (h)							
0	19.3	9.5	-	-	-	25.0	46.1
1	19.1	9.1	1.3	-	-	25.0	45.7
1.5	18.5	8.9	1.4	-	-	24.7	46.5
2	18.2	8.9	1.7	-	-	24.7	46.5
3	17.8	8.9	3.2	-	-	24.4	45.7
4	13.3	8.5	3.6	3.0	2.7	24.2	44.7
5	4.1	7.3	9.3	6.0	6.1	24.0	43.1
6	2.8	6.6	11.2	7.0	6.7	24.0	41.8
7	2.0	5.7	14.7	6.9	7.0	22.6	41.0
8	1.5	5.3	15.8	7.9	7.2	22.5	39.7
9	1.1	4.9	15.8	8.6	7.4	22.4	40.1
10	0.4	4.7	15.8	9.0	7.6	21.7	40.8
14	-	4.4	16.1	9.1	8.0	21.3	41.2
24	-	4.0	16.8	10.4	8.2	19.6	41.0
47	-	3.0	17.9	12.0	9.6	17.7	39.9
168*	-	1.3	21.5	15.7	9.9	15.4	36.2

\*168 h = 7 days of hydration

**Table A4.** RQPA results (wt%) of the *in-situ* hydration study of o137\_132.

Phases Age (h)	C <sub>4</sub> A <sub>3</sub> S	Cs	AFt	AFm	C <sub>2</sub> ASH <sub>8</sub>	C <sub>3</sub> S	ACn+FW
0	13.8	6.8	-	-	-	17.9	61.5
1	12.4	6.2	0.9	-	-	17.5	62.9
2	10.8	6.2	2.9	1.0	-	17.2	62.0
3	3.4	4.9	9.9	3.5	2.4	17.2	58.7
4	1.0	3.9	12.2	4.6	2.7	16.9	58.6
5	0.5	3.4	13.4	5.3	2.9	16.5	57.9
6	0.5	3.2	14.1	5.8	3.1	16.3	56.8
7	0.5	3.1	14.2	6.3	3.3	16.1	56.6
9	0.3	2.9	14.2	6.9	3.3	15.7	56.6
14	-	2.6	14.3	8.3	3.5	14.4	56.9
24	-	2.4	14.4	9.0	3.7	13.5	57.0
47	-	1.6	14.4	10.4	3.7	12.3	57.6
168 <sup>a*</sup>	-	-	11.0	18.3	3.2	1.4	62.9

a. Also 1.9 wt% of C-S-H (as clinotobermorite) and 1.3 wt% of hemicarbonate.

\*168 h = 7 days of hydration

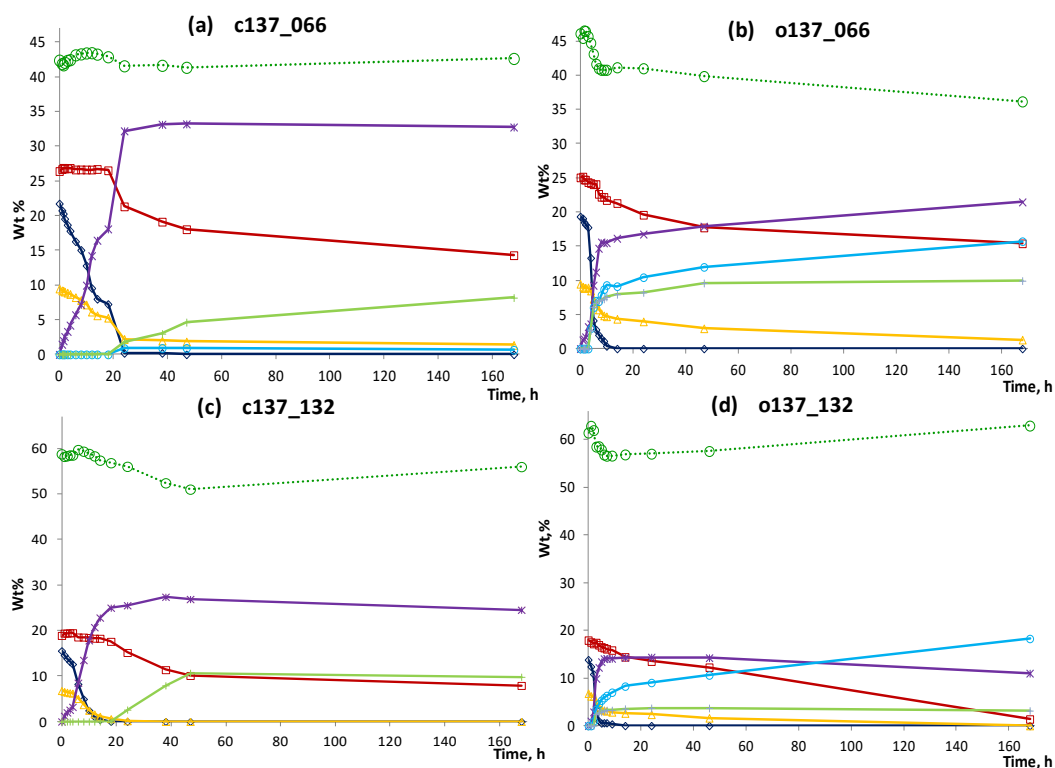


**Figure A1.** Phase assemblage during 168 hours (7 days) of hydration of (a and c) c137 and (b and d) o137. Dark green circle: ACn+FW, blue diamond: C<sub>4</sub>A<sub>3</sub>S, yellow triangle: Cs, red square: C<sub>3</sub>S, purple asterisk: AFt, light blue circle: AFm and green cross: C<sub>2</sub>ASH<sub>8</sub>.

**Table A5.** RQPA results (wt%) of the *in-situ* hydration study of c274\_059.

Phases Age (h)	C <sub>4</sub> A <sub>3</sub> S	Cs	Aft	C <sub>2</sub> ASH <sub>8</sub>	Hemi- CO <sub>3</sub> <sup>a</sup>	C <sub>3</sub> S	ACn+FW
0	15.8	6.8	-	-	-	38.1	39.3
1	13.9	6.3	2.2	-	-	38.1	39.5
2	13.3	6.2	2.7	-	-	38.1	39.6
3	12.4	6.2	3.4	-	-	38.1	39.9
4	11.1	6.0	4.5	-	-	38.0	40.3
6	8.4	5.4	7.8	0.4	-	38.0	40.1
8	4.2	3.9	14.1	0.4	-	38.0	39.3
10	1.7	2.4	18.4	0.5	-	38.0	39.1
14	1.0	2.0	20.6	0.6	-	37.7	38.1
18	0.1	1.0	24.1	0.7	-	35.8	38.3
24	-	0.2	26.8	1.1	-	33.6	38.3
38	-	0.2	27.7	1.3	0.3	32.4	38.2
47	-	-	27.8	1.8	0.3	31.3	38.9
168*	-	-	25.6	6.2	0.7	27.7	39.9

\*168 h = 7 days of hydration

**Table A6.** RQPA results (wt%) of the *in-situ* hydration study of c274\_119.

Phases	C <sub>4</sub> A <sub>3</sub> S	Cs	AFt	AFm	C <sub>2</sub> ASH <sub>8</sub>	CH	C <sub>3</sub> S	ACn+FW
Age (h)								
0	11.4	5.0	-	-	-	-	27.6	55.9
1	10.2	4.6	1.7	-	-	-	27.6	55.9
2	9.5	4.5	2.1	-	-	-	27.6	56.2
3	9.1	4.5	2.4	-	-	-	27.6	56.4
4	8.9	4.5	2.7	-	-	-	27.6	56.3
6	8.4	4.5	2.9	-	-	-	27.6	56.6
8	7.3	4.3	4.1	-	-	-	27.6	56.8
10	3.5	2.9	9.6	-	-	-	27.6	56.4
14	0.3	0.9	15.9	0.2	0.2	-	27.1	55.3
18	-	0.3	18.7	0.3	0.2	-	26.7	53.8
24	-	0.2	19.7	0.3	0.3	0.1	24.5	54.9
38	-	-	19.7	0.3	4.8	0.3	23.0	51.9
47	-	-	19.2	0.3	5.2	0.4	21.9	52.9
168 <sup>a*</sup>	-	-	15.1	5.4	6.7	1.4	14.0	56.7

a. Also 0.6 wt% of hemihydrate.

\*168 h = 7 days of hydration



**Table A7.** RQPA results (wt%) of the *in-situ* hydration study of o274\_059.

Phases Age (h)	C <sub>4</sub> A <sub>3</sub> S	Cs	AFt	AFm	C <sub>2</sub> ASH <sub>8</sub>	C <sub>3</sub> S	ACn+FW
0	13.3	6.6	-	-	-	37.6	42.5
1	13.0	6.5	2.5	-	-	37.6	40.5
2	12.4	6.5	3.1	-	-	37.6	40.4
3	12.2	6.4	3.2	-	-	37.5	40.6
4	12.1	6.4	3.4	-	-	37.5	40.7
7	1.2	4.9	10.6	5.5	-	36.7	41.0
10	0.9	3.3	10.6	6.0	5.6	33.8	40.5
12	-	3.2	10.7	6.7	5.8	33.8	40.2
16	-	3.1	10.8	7.4	6.1	33.0	39.6
24	-	2.5	10.9	8.3	6.5	32.6	39.2
47	-	1.0	13.1	10.8	7.4	27.1	40.6
168*	-	0.3	15.3	14.7	7.1	20.2	42.4

\*168 h = 7 days of hydration

**Table A8.** RQPA results (wt%) of the *in-situ* hydration study of o274\_119.

Phases	C <sub>4</sub> A <sub>3</sub> S	Cs	AFt	AFm	C <sub>2</sub> ASH <sub>8</sub>	C <sub>3</sub> S	ACn+FW
Age (h)							
0	9.7	4.8	-	-	-	27.3	58.2
1.5	8.9	4.6	0.9	-	-	27.3	58.2
3	8.7	4.6	1.1	-	-	27.3	58.3
4	6.6	4.4	1.9	1.6	-	27.3	58.2
5	1.4	3.6	5.4	4.0	-	27.3	58.3
7	-	2.8	6.8	5.2	3.4	26.0	55.8
10	-	2.8	6.8	5.2	4.1	25.1	55.9
12	-	2.8	7.0	5.4	4.6	25.1	55.1
16	-	2.3	8.4	6.0	4.8	25.1	53.3
24	-	2.0	8.8	6.5	5.1	24.3	52.3
47	-	0.6	10.7	8.7	6.0	23.2	50.8
168 <sup>a*</sup>	-	-	8.4	13.1	2.8	1.2	68.9

a. Also 2.0 wt% of hemicarbonates and 3.6 wt% of portlandite.

\*168 h = 7 days of hydration

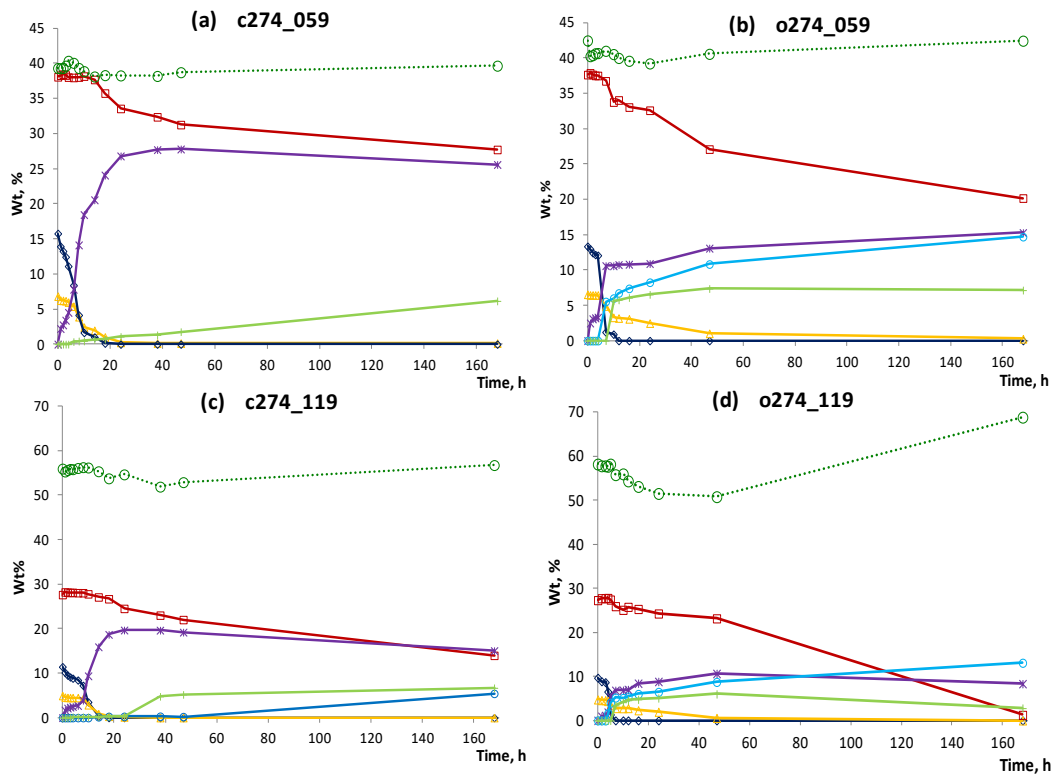


**Figure A2.** Phase assemblage during 168 hours (7 days) of hydration of (a and c) c274 and (b and d) o274. Dark green circle: ACn+FW, blue diamond: C<sub>4</sub>A<sub>3</sub>S, yellow triangle: Cs, red square: C<sub>3</sub>S, purple asterisk: AFt, light blue circle: AFm and green cruise: C<sub>2</sub>ASH<sub>8</sub>.



UNIVERSIDAD  
DE MÁLAGA

**Annex III:**  
***Copyright Agreements.***



Figure Int.1.

6/3/2018 Rightslink® by Copyright Clearance Center

Copyright Clearance Center RightsLink® Home Account Info Help



**Title:** Research review of cement clinker chemistry  
**Author:** Horst-Michael Ludwig, Wensheng Zhang  
**Publication:** Cement and Concrete Research  
**Publisher:** Elsevier  
**Date:** December 2015  
 Copyright © 2015 Elsevier Ltd. All rights reserved.

Logged in as:  
 Diana Londono  
 University of Malaga  
 LOGOUT

**Order Completed**

Thank you for your order.

This Agreement between University of Malaga -- Diana Londono-Zuluaga ("You") and Elsevier ("Elsevier") consists of your license details and the terms and conditions provided by Elsevier and Copyright Clearance Center.

Your confirmation email will contain your order number for future reference.

printable details

License Number	4303011372387
License date	Mar 06, 2018
Licensed Content Publisher	Elsevier
Licensed Content Publication	Cement and Concrete Research
Licensed Content Title	Research review of cement clinker chemistry
Licensed Content Author	Horst-Michael Ludwig, Wensheng Zhang
Licensed Content Date	Dec 1, 2015
Licensed Content Volume	78
Licensed Content Issue	n/a
Licensed Content Pages	14
Type of Use	reuse in a thesis/ dissertation
Portion	figures/tables/illustrations
Number of figures/tables/illustrations	2
Format	both print and electronic
Are you the author of this Elsevier article?	No
Will you be translating?	No
Original figure numbers	Figure 7 and Figure 12
Title of your thesis/ dissertation	Eco-cements containing Belite, Alite and Ye'elimite. Hydration and mechanical properties
Expected completion date	Jul 2018
Estimated size (number of pages)	200
Attachment	
Requestor Location	University of Malaga Inorganic Chemistry Science School  Malaga, Malaga 29071 Spain Attn: University of Malaga
Publisher Tax ID	GB 494 6272 12
Total	0.00 EUR

[ORDER MORE](#)

[CLOSE WINDOW](#)

<https://s100.copyright.com/AppDispatchServlet>

1/2

Figure Int.2.

6/3/2018 Rightslink® by Copyright Clearance Center









**Title:** Trends and developments in green cement and concrete technology  
**Author:** Mohammed S. Imbabi, Collette Carrigan, Sean McKenna  
**Publication:** International Journal of Sustainable Build Environment  
**Publisher:** Elsevier  
**Date:** December 2012  
 Copyright © 2013 Production and hosting by Elsevier B.V.

Logged in as:  
 Diana Londono-Zuluaga  
 University of Malaga  
 Account #: 3001257607  
[LOGOUT](#)

**Creative Commons Attribution-NonCommercial-No Derivatives License (CC BY NC ND)**

This article is published under the terms of the [Creative Commons Attribution-NonCommercial-No Derivatives License \(CC BY NC ND\)](#).

For non-commercial purposes you may copy and distribute the article, use portions or extracts from the article in other works, and text or data mine the article, provided you do not alter or modify the article without permission from Elsevier. You may also create adaptations of the article for your own personal use only, but not distribute these to others. You must give appropriate credit to the original work, together with a link to the formal publication through the relevant DOI, and a link to the Creative Commons user license above. If changes are permitted, you must indicate if any changes are made but not in any way that suggests the licensor endorses you or your use of the work.

Permission is not required for this non-commercial use. For commercial use please continue to request permission via Rightslink.

[BACK](#)
[CLOSE WINDOW](#)

Copyright © 2018 [Copyright Clearance Center, Inc.](#) All Rights Reserved. [Privacy statement](#), [Terms and Conditions](#). Comments? We would like to hear from you. E-mail us at [customer-care@copyright.com](mailto:customer-care@copyright.com)

**Figures 2.3-2.4, 2.7-2.8 and 3.12-3.13 and Tables 2.3, 2.5-2.6 and 3.10.**

6/3/2018 Rightslink® by Copyright Clearance Center




Home Account Info Help 



**Title:** Clinkering and hydration of belite-alite-ye'elimite cement  
**Author:** D. Londono-Zuluaga, J.I. Tobón, M.A.G. Aranda, I. Santacruz, A.G. De la Torre  
**Publication:** Cement and Concrete Composites  
**Publisher:** Elsevier  
**Date:** July 2017  
 © 2017 Elsevier Ltd. All rights reserved.

Logged in as:  
 Diana Londono-Zuluaga  
 University of Malaga  
 Account #: 3001257607  
 LOGOUT

Please note that, as the author of this Elsevier article, you retain the right to include it in a thesis or dissertation, provided it is not published commercially. Permission is not required, but please ensure that you reference the journal as the original source. For more information on this and on your other retained rights, please visit: <https://www.elsevier.com/about/our-business/policies/copyright#Author-rights>

BACK CLOSE WINDOW

Copyright © 2018 Copyright Clearance Center, Inc. All Rights Reserved. [Privacy statement](#), [Terms and Conditions](#).  
 Comments? We would like to hear from you. E-mail us at [customer-care@copyright.com](mailto:customer-care@copyright.com)



## References

- [1] P. Hewlett, Lea's Chemistry of Cement and Concrete, 2004. doi:10.1016/B978-0-7506-6256-7.50031-X.
- [2] L. Barcelo, J. Kline, G. Walenta, E. Gartner, Cement and carbon emissions, *Mater. Struct.* 47 (2014) 1055–1065. doi:10.1617/s11527-013-0114-5.
- [3] E. Gartner, Industrially interesting approaches to “low-CO<sub>2</sub>” cements, *Cem. Concr. Res.* 34 (2004) 1489–1498. doi:10.1016/j.cemconres.2004.01.021.
- [4] H.F.W. Taylor, *Cement chemistry*. 2nd ed., Acad. Press. 20 (1997) 335. doi:10.1016/S0958-9465(98)00023-7.
- [5] I. Odler, *Special Inorganic Cements*, E & FN Spo, New York, 2005.
- [6] G. Habert, C. Billard, P. Rossi, C. Chen, N. Roussel, Cement production technology improvement compared to factor 4 objectives, *Cem. Concr. Res.* 40 (2010) 820–826. doi:10.1016/j.cemconres.2009.09.031.
- [7] J.S. Damtoft, J. Lukasik, D. Herfort, D. Sorrentino, E. Gartner, Sustainable development and climate change initiatives, *Cem. Concr. Res.* 38 (2008) 115–127. doi:10.1016/j.cemconres.2007.09.008.
- [8] C. Shi, A.F. Jiménez, A. Palomo, New cements for the 21st century: The pursuit of an alternative to Portland cement, *Cem. Concr. Res.* 41 (2011) 750–763. doi:10.1016/j.cemconres.2011.03.016.
- [9] (U.S Geological Survey) USGS, *Cement Mineral Resources Program Report*, 2017.
- [10] Cembureau, *The role of cement in the 2050 low-carbon economy*, (2013) 64.
- [11] B.L. Damineli, F.M. Kemeid, P.S. Aguiar, V.M. John, Measuring the eco-efficiency of cement use, *Cem. Concr. Compos.* 32 (2010) 555–562. doi:10.1016/j.cemconcomp.2010.07.009.
- [12] E. Gartner, H. Hirao, A review of alternative approaches to the reduction of CO<sub>2</sub> emissions associated with the manufacture of the binder phase in concrete, *Cem. Concr. Res.* 78 (2015) 126–142. doi:10.1016/j.cemconres.2015.04.012.
- [13] M.C.G. Juenger, R. Siddique, Recent advances in understanding the role of supplementary cementitious materials in concrete, *Cem. Concr. Res.* 78



- (2015) 71–80. doi:10.1016/j.cemconres.2015.03.018.
- [14] K. Scrivener, A. Favier, *Calcined Clays for Sustainable Concrete*, in: RILEM Bookseries, 2015: pp. 1–597. doi:10.1007/978-94-017-9939-3.
- [15] M.C.G. Juenger, F. Winnefeld, J.L. Provis, J.H. Ideker, *Advances in alternative cementitious binders*, *Cem. Concr. Res.* 41 (2011) 1232–1243. doi:10.1016/j.cemconres.2010.11.012.
- [16] E. Gartner, T. Sui, *Alternative cement clinkers*, *Cem. Concr. Res.* (2017). doi:10.1016/j.cemconres.2017.02.002.
- [17] L.F. Cabeza, C. Barreneche, L. Miró, J.M. Morera, E. Bartolí, A. Inés Fernández, *Low carbon and low embodied energy materials in buildings: A review*, *Renew. Sustain. Energy Rev.* 23 (2013) 536–542. doi:10.1016/j.rser.2013.03.017.
- [18] C.D. Popescu, M. Muntean, J.H. Sharp, *Industrial trial production of low energy belite cement*, *Cem. Concr. Compos.* 25 (2003) 689–693. doi:10.1016/S0958-9465(02)00097-5.
- [19] A.J.M. Cuberos, A.G. De la Torre, M.C. Martín-Sedeño, L. Moreno-Real, M. Merlini, L.M. Ordóñez, M.A.G. Aranda, *Phase development in conventional and active belite cement pastes by Rietveld analysis and chemical constraints*, *Cem. Concr. Res.* 39 (2009) 833–842. doi:10.1016/j.cemconres.2009.06.017.
- [20] K. Pimraksa, S. Hanjitsuwan, P. Chindaprasirt, *Synthesis of belite cement from lignite fly ash*, *Ceram. Int.* 35 (2009) 2415–2425. doi:10.1016/j.ceramint.2009.02.006.
- [21] K. Morsli, A.G. De la Torre, M. Zahir, M.A.G. Aranda, *Mineralogical phase analysis of alkali and sulfate bearing belite rich laboratory clinkers*, *Cem. Concr. Res.* 37 (2007) 639–646. doi:10.1016/j.cemconres.2007.01.012.
- [22] I. García-Díaz, J.G. Palomo, F. Puertas, *Belite cements obtained from ceramic wastes and the mineral pair CaF<sub>2</sub>/CaSO<sub>4</sub>*, *Cem. Concr. Compos.* 33 (2011) 1063–1070. doi:10.1016/j.cemconcomp.2011.06.003.
- [23] L. Kacimi, A. Simon-Masseron, S. Salem, A. Ghomari, Z. Derriche, *Synthesis of belite cement clinker of high hydraulic reactivity*, *Cem. Concr. Res.* 39 (2009) 559–565. doi:10.1016/j.cemconres.2009.02.004.
- [24] D.C. Hughes, D. Jaglin, R. Kozłowski, D. Mucha, *Roman cements — Belite cements calcined at low temperature*, *Cem. Concr. Res.* 39 (2009) 77–89. doi:10.1016/j.cemconres.2008.11.010.
- [25] T. Hanein, M.S. Imbabi, F.P. Glasser, M.N. Bannerman, *Production of belite calcium sulfoaluminate cement using sulfur as a fuel and as a source of clinker sulfur trioxide : pilot kiln trial*, 28 (2016).
- [26] M. García-Maté, D. Londono-Zuluaga, A.G. De la Torre, E.R. Losilla, A. Cabeza, M.A.G. Aranda, I. Santacruz, *Tailored setting times with high compressive strengths in bassanite calcium sulfoaluminate eco-cements*, *Cem. Concr. Compos.* 72 (2016) 39–47. doi:10.1016/j.cemconcomp.2016.05.021.
- [27] P. Arjunan, M.R. Silsbee, *Sulfoaluminate-belite cement from low-calcium fly ash and sulfur-rich and other industrial by-products*, *Cem. Concr. Res.* 29 (1999) 1305–1311.

- [28] M.A.G. Aranda, A.G. De la Torre, 18 – Sulfoaluminate cement, in: *Eco-Efficient Concr.*, 2013: pp. 488–522. doi:10.1533/9780857098993.4.488.
- [29] L. Senff, A. Castela, W. Hajjaji, D. Hotza, J.A. Labrincha, Formulations of sulfobelite cement through design of experiments, *Constr. Build. Mater.* 25 (2011) 3410–3416. doi:10.1016/j.conbuildmat.2011.03.032.
- [30] A.K. Chatterjee, High belite cements - present status and future technological options: Part I, *Cem. Concr. Res.* 26 (1996) 1213–1225. doi:10.1016/0008-8846(96)00099-3.
- [31] S. Khare, M.C. Bannerman, F.P. Glasser, T. Hanein, M.S. Imbabi, Pilot scale production of novel calcium sulfoaluminate cement clinkers and development of thermal model, *Chem. Eng. Process. Process Intensif.* 122 (2017) 68–75. doi:10.1016/j.cep.2017.10.006.
- [32] F.P. Glasser, L. Zhang, High-performance cement matrices based on calcium sulfoaluminate – belite compositions, *Cem. Concr. Res.* 31 (2001) 1881–1886.
- [33] Y. Al Horr, A. Elhoweris, E. Elsarrag, The development of a novel process for the production of calcium sulfoaluminate: A review, *Int. J. Sustain. Built Environ.* (2017). doi:10.1016/j.ijbsbe.2017.12.009.
- [34] I. a Chen, M.C.G. Juenger, Synthesis and hydration of calcium sulfoaluminate-belite cements with varied phase compositions, *J. Mater. Sci.* 46 (2011) 2568–2577. doi:10.1007/s10853-010-5109-9.
- [35] F.A. Rodrigues, I. Joekes, Cement industry: Sustainability, challenges and perspectives, *Environ. Chem. Lett.* 9 (2011) 151–166. doi:10.1007/s10311-010-0302-2.
- [36] E.B. Da Costa, E.D. Rodríguez, S.A. Bernal, J.L. Provis, L.A. Gobbo, A.P. Kirchheim, Production and hydration of calcium sulfoaluminate-belite cements derived from aluminium anodising sludge, *Constr. Build. Mater.* 122 (2016) 373–383. doi:10.1016/j.conbuildmat.2016.06.022.
- [37] S. Sahu, J. Majling, Phase compatibility in the system CaO - SiO<sub>2</sub> - Al<sub>2</sub>O<sub>3</sub> - Fe<sub>2</sub>O<sub>3</sub> - SO<sub>3</sub> referred to sulphoaluminate belite cement clinker, *Cem. Concr. Res.* 23 (1993) 1331–1339.
- [38] M.S. Imbabi, C. Carrigan, S. McKenna, Trends and developments in green cement and concrete technology, *Int. J. Sustain. Built Environ.* 1 (2012) 194–216. doi:10.1016/j.ijbsbe.2013.05.001.
- [39] K. Quillin, Performance of belite-sulfoaluminate cements, *Cem. Concr. Res.* 31 (2001) 1341–1349. doi:10.1016/S0008-8846(01)00543-9.
- [40] M. García-Maté, A.G. De la Torre, L. León-Reina, E.R. Losilla, M.A.G. Aranda, I. Santacruz, Effect of calcium sulfate source on the hydration of calcium sulfoaluminate eco-cement, *Cem. Concr. Compos.* 55 (2015) 53–61. doi:10.1016/j.cemconcomp.2014.08.003.
- [41] F. Winnefeld, L.H.J. Martin, C.J. Müller, B. Lothenbach, Using gypsum to control hydration kinetics of CSA cements, *Constr. Build. Mater.* 155 (2017) 154–163. doi:10.1016/j.conbuildmat.2017.07.217.
- [42] C.W. Hargis, A. Telesca, P.J.M. Monteiro, Calcium sulfoaluminate

- (Ye'elimite) hydration in the presence of gypsum, calcite, and vaterite, *Cem. Concr. Res.* 65 (2014) 15–20. doi:10.1016/j.cemconres.2014.07.004.
- [43] M.C. Martín-Sedeño, A.J.M. Cuberos, A.G. De la Torre, G. Alvarez-Pinazo, L.M. Ordóñez, M. Gateshki, M.A.G. Aranda, Aluminum-rich belite sulfoaluminate cements: Clinkering and early age hydration, *Cem. Concr. Res.* 40 (2010) 359–369. doi:10.1016/j.cemconres.2009.11.003.
- [44] A.J.M. Cuberos, A.G. De la Torre, G. Alvarez-Pinazo, M.C. Martín-Sedeño, K. Schollbach, H. Pöllmann, M.A.G. Aranda, Active iron-rich belite sulfoaluminate cements: clinkering and hydration., *Environ. Sci. Technol.* 44 (2010) 6855–6862.
- [45] G.Y. Koga, B. Albert, V. Roche, R.P. Nogueira, A comparative study of mild steel passivation embedded in Belite-Ye'elimite-Ferrite and Portland cement mortars, *Electrochim. Acta.* 261 (2017) 66–77. doi:10.1016/j.electacta.2017.12.128.
- [46] M. Idrissi, a Diouri, D. Damidot, J.M. Greneche, M.A. Talbi, M. Taibi, Characterisation of iron inclusion during the formation of calcium sulfoaluminate phase, *Cem. Concr. Res.* 40 (2010) 2–7. doi:10.1016/j.cemconres.2010.02.009.
- [47] A.J.M. Cuberos, A.G. De Torre, M.C. Martín-sedeño, Iron-rich calcium sulfoaluminate cements: Clinkering and Hydration. SI, Universidad de Málaga, 2011.
- [48] G. Alvarez-Pinazo, I. Santacruz, M.A.G. Aranda, A.G. De la Torre, G. Álvarez-Pinazo, Hydration of belite – ye'elimite – ferrite cements with different calcium sulfate sources, *Adv. Cem. Res.* 28 (2016) 529–543. doi:10.1680/jadcr.16.00030.
- [49] G.S. Li, E. Gartner, WO2006018569A3 - High-belite sulfoaluminate clinker: fabrication process and binder preparation, French patent application 04-51586 (publication 2873366), 2006.
- [50] H.-M.M. Ludwig, W. Zhang, Research review of cement clinker chemistry, *Cem. Concr. Res.* 78 (2015) 24–37. doi:10.1016/j.cemconres.2015.05.018.
- [51] T. Link, F. Bellmann, H.M. Ludwig, M. Ben Haha, Reactivity and phase composition of Ca<sub>2</sub>SiO<sub>4</sub> binders made by annealing of alpha-dicalcium silicate hydrate, *Cem. Concr. Res.* 67 (2015) 131–137. doi:10.1016/j.cemconres.2014.08.009.
- [52] A. Cuesta, E.R. Losilla, M.A.G. Aranda, J. Sanz, A.G. De la Torre, Reactive belite stabilization mechanisms by boron-bearing dopants, *Cem. Concr. Res.* 42 (2012) 598–606. doi:10.1016/j.cemconres.2012.01.006.
- [53] T. Stanek, P. Sulovsky, Active low-energy belite cement, *Cem. Concr. Res.* 68 (2015) 203–210. doi:10.1016/j.cemconres.2014.11.004.
- [54] L. Kacimi, M. Cyr, P. Clastres, Synthesis of alpha'L-C<sub>2</sub>S cement from fly-ash using the hydrothermal method at low temperature and atmospheric pressure., *J. Hazard. Mater.* 181 (2010) 593–601. doi:10.1016/j.jhazmat.2010.05.054.
- [55] Y.M. Kim, S.H. Hong, Influence of minor ions on the stability and hydration rates of  $\beta$ -dicalcium silicate, *J. Am. Ceram. Soc.* 87 (2004) 900–905. doi:10.1111/j.1551-2916.2004.00900.x.

- [56] G. Álvarez-Pinazo, I. Santacruz, L. León-Reina, M.A.G. Aranda, A.G. De la Torre, Hydration reactions and mechanical strength developments of iron-rich sulfobelite eco-cements, *Ind. Eng. Chem. Res.* 52 (2013) 16606–16614. doi:10.1021/ie402484e.
- [57] G. Álvarez-Pinazo, A. Cuesta, M. García-Maté, I. Santacruz, E.R. Losilla, S.G. Sanfélix, F. Fauth, M.A.G. Aranda, A.G. De la Torre, In-situ early-age hydration study of sulfobelite cements by synchrotron powder diffraction, *Cem. Concr. Res.* 56 (2014) 12–19. doi:10.1016/j.cemconres.2013.10.009.
- [58] A.G. De la Torre, A.J.M. Cuberos, G. Alvarez-Pinazo, A. Cuesta, M.A.G. Aranda, In situ powder diffraction study of belite sulfoaluminate clinkering., *J. Synchrotron Radiat.* 18 (2011) 506–514. doi:10.1107/S0909049511005796.
- [59] K. Morsli, A.G. De la Torre, A.J.M. Cuberos, M. Zahir, M.A.G. Aranda, Preparación y caracterización de cementos belíticos blancos activados con dopantes alcalinos, *Mater. Construcción.* 59 (2009) 19–29. doi:10.3989/mc.2009.44307.
- [60] D. Koumpouri, G.N. Angelopoulos, Effect of boron waste and boric acid addition on the production of low energy belite cement, *Cem. Concr. Compos.* 68 (2016) 1–8. doi:10.1016/j.cemconcomp.2015.12.009.
- [61] G. Walenta, C. Comparet, CO<sub>2</sub> - New Cements and Innovative Binder Technologies: AETHER (BCSAF) cements, in: ECRA Conf. "New Cem. Innov. Bind. Technol.", 2011.
- [62] K. Quillin, A. Dunster, C. Tipple, G. Walenta, E. Gartner, B. Albert, Project AETHER Testing the durability of a lower-CO<sub>2</sub> alternative to Portland cement, in: 34th Annu. Cem. Concr. Sci. Conf., 2014.
- [63] F. Bullerjahn, D. Schmitt, M. Ben Haha, Effect of raw mix design and of clinkering process on the formation and mineralogical composition of (ternesite) belite calcium sulfoaluminate ferrite clinker, *Cem. Concr. Res.* 59 (2014) 87–95. doi:10.1016/j.cemconres.2014.02.004.
- [64] Y. Shen, J. Qian, Y. Huang, D. Yang, Synthesis of belite sulfoaluminate-ternesite cements with phosphogypsum, *Cem. Concr. Compos.* 63 (2015) 67–75. doi:10.1016/j.cemconcomp.2015.09.003.
- [65] H. Li, D.K. Agrawal, J. Cheng, M.R. Silsbee, Microwave sintering of sulfoaluminate cement with utility wastes, *Cem. Concr. Res.* 31 (2001) 1257–1261.
- [66] N. Sherman, J. Beretka, L. Santoro, G.L. Valenti, Long-term behavior of hydraulic binders based on Calcium sulfoaluminate and Calcium sulfosilicate, *Cem. Concr. Res.* 25 (1995) 113–126.
- [67] M. Montes, E. Pato, P.M. Carmona-Quiroga, M.T. Blanco-Varela, Can calcium aluminates activate ternesite hydration?, *Cem. Concr. Res.* 103 (2018) 204–215. doi:10.1016/j.cemconres.2017.10.017.
- [68] T. Hanein, I. Galan, F.P. Glasser, S. Skalamprinos, A. Elhoweris, M.S. Imbabi, M.N. Bannerman, Stability of ternesite and the production at scale of ternesite-based clinkers, *Cem. Concr. Res.* 98 (2017) 91–100.

- doi:10.1016/j.cemconres.2017.04.010.
- [69] X.X. Li, X. Shen, M. Tang, X.X. Li, Stability of tricalcium silicate and other primary phases in portland cement clinker, *Ind. Eng. Chem. Res.* 53 (2014) 1954–1964. doi:10.1021/ie4034076.
- [70] F. Puertas, M.T. Blanco-Varela, S. Giménez-Molina, Kinetics of the Thermal decomposition of C4A3s in air, *Cem. Concr. Res.* 25 (1995) 572–580.
- [71] X. Li, Y. Zhang, X. Shen, Q. Wang, Z. Pan, Kinetics of calcium sulfoaluminate formation from tricalcium aluminate, calcium sulfate and calcium oxide, *Cem. Concr. Res.* 55 (2014) 79–87. doi:10.1016/j.cemconres.2013.10.006.
- [72] N. Chitvoranund, B. Lothenbach, F. Winnefeld, C.W. Hargis, Synthesis and hydration of alite-calcium sulfoaluminate cement, *Adv. Cem. Res.* 29 (2017) 101–111.
- [73] T. Duvallet, Y. Zhou, T.L. Robl, R. Andrews, Synthesis and Characterization of High-Iron Alite-Calcium Sulfoaluminate-Ferrite Cements Produced from Industrial By-Products, *Coal Combust. Gasif. Prod.* 6 (2014) 29–34. doi:10.4177/CCGP-D-14-00007.1.
- [74] Y. Hu, S. Ma, W. Li, X. Shen, The Preparation and Composition Analysis of Alite-Ye'Elimite With Industrial Wastes, *Ceram. - Silikaty.* 60 (2016) 1–10. doi:10.13168/cs.2016.0027.
- [75] R. Pérez-Bravo, G. Álvarez-Pinazo, J.M. Compañ, I. Santacruz, E.R. Losilla, S. Bruque, A.G. De la Torre, Alite sulfoaluminate clinker: Rietveld mineralogical and SEM-EDX analysis, *Adv. Cem. Res.* 26 (2014) 10–20. doi:10.1680/adcr.12.00044.
- [76] X. Liu, Y. Li, Effect of MgO on the composition and properties of alite-sulphoaluminate cement, *Cem. Concr. Res.* 35 (2005) 1685–1687. doi:10.1016/j.cemconres.2004.08.008.
- [77] X. Liu, Y. Li, N. Zhang, Influence of MgO on the formation of Ca<sub>3</sub>SiO<sub>5</sub> and 3CaO.3Al<sub>2</sub>O<sub>3</sub>.CaSO<sub>4</sub> minerals in alite – sulphoaluminate cement, *Cem. Concr. Res.* 32 (2002) 1125–1129.
- [78] L. Lu, J. Chang, X. Cheng, H. Liu, R. Yuan, Study on a cementing system taking alite-calcium barium sulphoaluminate as main minerals, *J. Mater. Sci.* 40 (2005) 4035–4038. doi:10.1007/s10853-005-2005-9.
- [79] T. Duvallet, Y. Zhou, K. Henke, T. Andrew, Effects of ferrite concentration on synthesis, hydration and mechanical properties of alite-calcium sulfoaluminate-ferrite cements, *J. Sustain. Cem. Mater.* (2015) 1–26. doi:10.1080/21650373.2015.1077753.
- [80] J.H. Li, H.W. Ma, H.W. Zhao, Preparation of Sulphoaluminate-Alite Composite Mineralogical Phase Cement Clinker from High Alumina Fly Ash, *Key Eng. Mater.* 334–335 (2007) 421–424. doi:10.4028/www.scientific.net/KEM.334-335.421.
- [81] X.C. Liu, B.L. Li, T. Qi, X.L. Liu, Y.J. Li, Effect of TiO<sub>2</sub> on mineral formation and properties of alite-sulphoaluminate cement, *Mater. Res. Innov.* 13 (2009) 92–97. doi:10.1179/143307509X435178.
- [82] R. Lili, L. Xiaocun, Q. Tao, L. Jian, Z. Deli, L. Yanjun, Influence of MnO<sub>2</sub>

- on the Burnability and Mineral Formation of Alite-sulphoaluminate Cement Clinker, *Silic. Ind.* 74 (2009) 183–188.
- [83] L. Yanjun, L. Xiaocun, N. Zhang, Influence of phosphate on the composition and properties of alite-sulphoaluminate cement, *ZKG Int.* 53 (2000) 164–166.
- [84] X. Liu, T. Liu, Y. Wu, W. Wang, Y. Li, Effect of alkalis on the mineral formation and properties of alite-sulphoaluminate cement, *Adv. Cem. Res.* 25 (2013) 98–103. doi:10.1680/adcr.11.00050.
- [85] S. Ma, R. Snellings, X. Li, X. Shen, K.L. Scrivener, Alite-ye'elinite cement: Synthesis and mineralogical analysis, *Cem. Concr. Res.* 45 (2013) 15–20. doi:10.1016/j.cemconres.2012.10.020.
- [86] X. Lu, C. Li, S. Wang, Y. Zhengmao, X. Cheng, Effect of ferrite phase on the formation and coexistence of  $3\text{CaO}\cdot 3\text{Al}_2\text{O}_3\cdot \text{CaSO}_4$  and  $3\text{CaO}\cdot \text{SiO}_2$  minerals, *Ceram. - Silikaty.* 62 (2018) 67–73. doi:10.13168/cs.2017.0046.
- [87] S. Ma, X. Shen, X. Gong, B. Zhong, Influence of CuO on the formation and coexistence of  $3\text{CaO}\cdot \text{SiO}_2$  and  $3\text{CaO}\cdot 3\text{Al}_2\text{O}_3\cdot \text{CaSO}_4$  minerals, *Cem. Concr. Res.* 36 (2006) 1784–1787. doi:10.1016/j.cemconres.2006.05.030.
- [88] J.I. Tobon, M.F. Diaz-Burbano, O.J. Restrepo-Baena, Optimal fluorite / gypsum mineralizer ratio in Portland cement clinkering, *Mater. Constr.* 66 (2016) 1–12. doi:10.3989/mc.2016.05515.
- [89] C. Jun, C. Xin, L. Futian, L. Lingchao, T. Bing, Influence of fluorite on the Ba-bearing sulphoaluminate cement, *Cem. Concr. Res.* 31 (2001) 1999–2002.
- [90] M.T. Blanco-Varela, A. Palomo, F. Puertas, T. Vázquez,  $\text{CaF}_2$  and  $\text{CaSO}_4$  in white cement clinker production, *Adv. Cem. Res.* 9 (1997) 105–113. doi:10.1680/adcr.1997.9.35.105.
- [91] S. Giménez-Molina, M.T. Blanco-Varela, Solid state phases relationship in the  $\text{CaO}\text{-SiO}_2\text{-Al}_2\text{O}_3\text{-CaF}_2\text{-CaSO}_4$  system, *Cem. Concr. Res.* 25 (1995) 870–882. doi:10.1016/0008-8846(95)00078-Q.
- [92] Y.B. Pliego-Cuervo, F.P. Glasser, The role of sulphates in cement clinkering reactions: phase formation in the system  $\text{CaO}\text{-Al}_2\text{O}_3\text{-Fe}_2\text{O}_3\text{-SiO}_2\text{-CaSO}_4\text{-K}_2\text{SO}_4$ , *Cem. Concr. Res.* 9 (1979) 573–581. doi:10.1016/0008-8846(79)90141-8.
- [93] C. Xin, C. Jun, L. Lingchao, L. Futian, T. Bing, Study of Ba-bearing calcium sulphoaluminate minerals and cement, *Cem. Concr. Res.* 30 (2000) 77–81.
- [94] J. Zhao, J. Chang, Kinetic Analysis for Formation Process of Sr-Bearing Ye'elinite, *J. Inorg. Organomet. Polym. Mater.* 27 (2017) 1861–1869. doi:10.1007/s10904-017-0653-2.
- [95] I. Odler, H. Zhang, Investigation on high  $\text{SO}_3$ , portland clinkers and cements. I. Clinker synthesis and cement preparation, *Cem. Concr. Res.* 26 (1996) 1307–1313.
- [96] H. Zhang, I. Odler, Investigations on high  $\text{SO}_3$  Portland clinkers and cements II. Properties of cements, *Cem. Concr. Res.* 26 (1996) 1315–

1324. doi:10.1016/0008-8846(96)00129-9.
- [97] X. Li, X. Shen, J. Xu, X. Li, S. Ma, Hydration properties of the alite – ye'elimite cement clinker synthesized by reformation, *Constr. Build. Mater.* 99 (2015) 254–259. doi:10.1016/j.conbuildmat.2015.09.040.
- [98] A. Cuesta, R.U. Ichikawa, D. Londono-Zuluaga, A.G. De la Torre, I. Santacruz, X. Turrillas, M.A.G. Aranda, Aluminum hydroxide gel characterization within a calcium aluminate cement paste by combined Pair Distribution Function and Rietveld analyses, *Cem. Concr. Res.* 96 (2017) 1–12. doi:10.1016/j.cemconres.2017.02.025.
- [99] F. Song, Z. Yu, F. Yang, Y. Lu, Y. Liu, Microstructure of amorphous aluminum hydroxide in belite-calcium sulfoaluminate cement, *Cem. Concr. Res.* 71 (2015) 1–6. doi:10.1016/j.cemconres.2015.01.013.
- [100] F. Winnefeld, B. Lothenbach, Hydration of calcium sulfoaluminate cements — Experimental findings and thermodynamic modelling, *Cem. Concr. Res.* 40 (2010) 1239–1247. doi:10.1016/j.cemconres.2009.08.014.
- [101] A. Cuesta, G. Álvarez-Pinazo, S.G. Sanfélix, I. Peral, M.A.G. Aranda, A.G. De la Torre, Hydration mechanisms of two polymorphs of synthetic ye'elimite, *Cem. Concr. Res.* 63 (2014) 127–136. doi:10.1016/j.cemconres.2014.05.010.
- [102] F. Winnefeld, S. Barlag, Influence of calcium sulfate and calcium hydroxide on the hydration of calcium sulfoaluminate clinker, *ZKG Int.* (2009) 42–53.
- [103] C.W. Hargis, A.P. Kirchheim, P.J.M. Monteiro, E. Gartner, Early age hydration of calcium sulfoaluminate (synthetic ye'elimite, C4A3s) in the presence of gypsum and varying amounts of calcium hydroxide, *Cem. Concr. Res.* 48 (2013) 105–115. doi:10.1016/j.cemconres.2013.03.001.
- [104] A. Palomo, M.J. Sánchez-Herrero, A. Fernández-Jiménez, C4A3S hydration in different alkaline media, *Cem. Concr. Res.* 46 (2013) 41–49. doi:http://dx.doi.org/10.1016/j.cemconres.2013.01.008.
- [105] R. Trauchessec, J.M. Mechling, A. Lecomte, A. Roux, B. Le Rolland, Hydration of ordinary Portland cement and calcium sulfoaluminate cement blends, *Cem. Concr. Compos.* 56 (2015) 106–114. doi:10.1016/j.cemconcomp.2014.11.005.
- [106] E. L'Hôpital, B. Lothenbach, G. Le Saout, D. Kulik, K. Scrivener, Incorporation of aluminium in calcium-silicate-hydrates, *Cem. Concr. Res.* 75 (2015) 91–103. doi:10.1016/j.cemconres.2015.04.007.
- [107] B.Z. Dilnesa, B. Lothenbach, G. Renaudin, A. Wichser, D. Kulik, Synthesis and characterization of hydrogarnet  $\text{Ca}_3(\text{Al}_x\text{Fe}_{1-x})_2(\text{SiO}_4)_y(\text{OH})_4(3-y)$ , *Cem. Concr. Res.* 59 (2014) 96–111. doi:10.1016/j.cemconres.2014.02.001.
- [108] T.G. Jappy, F.P. Glasser, Synthesis and stability of silica-substituted hydrogarnet  $\text{Ca}_3\text{Al}_2\text{Si}_{3-x}\text{O}_{12-4x}(\text{OH})_{4x}$ , *Adv. Cem. Res.* 4 (1991) 1–8.
- [109] T. Matschei, B. Lothenbach, F.P. Glasser, Thermodynamic properties of Portland cement hydrates in the system  $\text{CaO-Al}_2\text{O}_3\text{-SiO}_2\text{-CaSO}_4\text{-CaCO}_3\text{-H}_2\text{O}$ , *Cem. Concr. Res.* 37 (2007) 1379–1410. doi:10.1016/j.cemconres.2007.06.002.
- [110] S. Hanehara, K. Yamada, Rheology and early age properties of cement



- systems, *Cem. Concr. Res.* 38 (2008) 175–195. doi:10.1016/j.cemconres.2007.09.006.
- [111] O.H. Wallevik, D. Feys, J.E. Wallevik, K.H. Khayat, Avoiding inaccurate interpretations of rheological measurements for cement-based materials, *Cem. Concr. Res.* 78 (2015) 100–109. doi:10.1016/j.cemconres.2015.05.003.
- [112] M. García-Maté, I. Santacruz, A.G. De la Torre, L. León-Reina, M.A.G. Aranda, Rheological and hydration characterization of calcium sulfoaluminate cement pastes, *Cem. Concr. Compos.* 34 (2012) 684–691. doi:10.1016/j.cemconcomp.2012.01.008.
- [113] J.E. Wallevik, Rheological properties of cement paste: Thixotropic behavior and structural breakdown, *Cem. Concr. Res.* 39 (2009) 14–29. doi:10.1016/j.cemconres.2008.10.001.
- [114] P.F.G. Banfill, Additivity effects in the rheology of fresh concrete containing water-reducing admixtures, *Constr. Build. Mater.* 25 (2011) 2955–2960. doi:10.1016/j.conbuildmat.2010.12.001.
- [115] P.F.G. Banfill, Rheological methods for assessing the flow properties of mortar and related materials, *Constr. Build. Mater.* 8 (1994) 43–50. doi:10.1016/0950-0618(94)90007-8.
- [116] B. Ma, M. Ma, X. Shen, X. Li, X. Wu, Compatibility between a polycarboxylate superplasticizer and the belite-rich sulfoaluminate cement: Setting time and the hydration properties, *Constr. Build. Mater.* 51 (2014) 47–54. doi:10.1016/j.conbuildmat.2013.10.028.
- [117] J. Plank, E. Sakai, C.W. Miao, C. Yu, J.X. Hong, Chemical admixtures - Chemistry, applications and their impact on concrete microstructure and durability, *Cem. Concr. Res.* 78 (2015) 81–99. doi:10.1016/j.cemconres.2015.05.016.
- [118] D. Londono-Zuluaga, J.I. Tobon, M.A.G. Aranda, I. Santacruz, A.G. De la Torre, Clinkering and hydration of Belite-Alite-Ye'elimitite cement, *Cem. Concr. Compos.* 80 (2017) 333–341. doi:10.1016/j.cemconcomp.2017.04.002.
- [119] M. García-Maté, A.G. De la Torre, L. León-Reina, M.A.G. Aranda, I. Santacruz, Hydration studies of calcium sulfoaluminate cements blended with fly ash, *Cem. Concr. Res.* 54 (2013) 12–20. doi:10.1016/j.cemconres.2013.07.010.
- [120] A. Cuesta, A.G. De la Torre, E.R. Losilla, I. Santacruz, M.A.G. Aranda, Pseudocubic crystal structure and phase transition in doped ye'elimitite, *Cryst. Growth Des.* 14 (2014) 5158–5163. doi:10.1021/cg501290q.
- [121] A. Cuesta, A.G. De la Torre, E.R. Losilla, V.K. Peterson, P. Rejmak, A. Ayuela, C. Frontera, M.A.G. Aranda, Structure, atomistic simulations, and phase transition of stoichiometric yeelimitite, *Chem. Mater.* 25 (2013) 1680–1687. doi:10.1021/cm400129z.
- [122] A.G. De la Torre, S. Bruque, M.A.G. Aranda, Rietveld quantitative amorphous content analysis, *J. Appl. Crystallogr.* 34 (2001) 196–202.

- doi:10.1107/S0021889801002485.
- [123] L. León-Reina, M. García-Maté, G. Álvarez-Pinazo, I. Santacruz, O. Vallcorba, A.G. De la Torre, M.A.G. Aranda, Accuracy in Rietveld quantitative phase analysis: A comparative study of strictly monochromatic Mo and Cu radiations, *J. Appl. Crystallogr.* 49 (2016) 722–735. doi:10.1107/S1600576716003873.
- [124] F. Fauth, I. Peral, C. Popescu, M. Knapp, The new Material Science Powder Diffraction beamline at ALBA Synchrotron, *Powder Diffr.* 28 (2013) S360–S370. doi:10.1017/S0885715613000900.
- [125] R. Von Dreele, A. Larson, General structure analysis system (GSAS), Los Alamos Natl. Lab. Rep. LAUR. 748 (2004) 86–748.
- [126] P. Thompson, D.E. Cox, J.B. Hastings, Rietveld Refinement of Debye-Scherrer Synchrotron X-ray Data from A1203, *J. Appl. Crystallogr.* 20 (1987) 79–83. doi:10.1107/S0021889887087090.
- [127] L.W. Finger, D.E. Cox, A.P. Jephcoat, Correction for powder diffraction peak asymmetry due to axial divergence, *J. Appl. Crystallogr.* 27 (1994) 892–900. doi:10.1107/S0021889894004218.
- [128] W.A. Dollase, Correction of intensities of preferred orientation in powder diffractometry: application of the march model, *J. Appl. Crystallogr.* 19 (1986) 267–272. doi:10.1107/S0021889886089458.
- [129] W.H. Duda, *Manual Tecnológico del Cemento*, Editores T, Romargraf S.A., Barcelona, Spain, 1977.
- [130] X. Li, W. Xu, S. Wang, M. Tang, X. Shen, Effect of SO<sub>3</sub> and MgO on Portland cement clinker: Formation of clinker phases and alite polymorphism, *Constr. Build. Mater.* 58 (2014) 182–192. doi:10.1016/j.conbuildmat.2014.02.029.
- [131] S. Horkoss, R. Lteif, T. Rizk, Influence of the clinker SO<sub>3</sub> on the cement characteristics, *Cem. Concr. Res.* 41 (2011) 913–919. doi:10.1016/j.cemconres.2011.04.015.
- [132] F. Puertas, M.T. Blanco-Varela, A. Palomo, T. Vázquez, Behaviour of a new white cement fabricated with raw materials containing CaF<sub>2</sub> and CaSO<sub>4</sub>.2H<sub>2</sub>O. Part 1: Hydration process, *ZKG Int.* 50 (1997) 232–239.
- [133] J. Bensted,  $\delta$ -dicalcium silicate and its hydraulicity, *Cem. Concr. Res.* 8 (1978) 73–76. doi:10.1016/0008-8846(78)90059-5.
- [134] I. Pajares, A.G. De la Torre, S. Martínez-Ramírez, F. Puertas, M.T. Blanco-Varela, M.A.G. Aranda, Quantitative analysis of mineralized white Portland clinkers: The structure of Fluorellestadite, *Powder Diffr.* 17 (2002) 281–286. doi:10.1154/1.1505045.
- [135] M.T. Blanco-Varela, T. Vázquez, A. Palomo, A study of a new liquid phase to obtain low-energy cements, *Cem. Concr. Res.* 16 (1986) 97–104. doi:10.1016/0008-8846(86)90073-6.
- [136] D. Londono-Zuluaga, J.I. Tobon, M.A.G. Aranda, I. Santacruz, A.G. De la Torre, Influence of Fly Ash blending on hydration and physical behavior of Belite-Alite-Ye'elimite cement, *Constr. Build. Mater.* (2018). doi:Submitted 13 Oct 2017.
- [137] B. Lothenbach, F. Winnefeld, R. Figi, The influence of superplasticizers on

- the hydration of Portland cement, in: Proc. 12th Int. Congr. Chem. Cem., 2007: pp. 9–12. doi:10.1007/s10973-016-5598-0.
- [138] P.F.G. Banfill, The rheology of fresh mortar: a review, in: VI Simpósio Bras. Tecnol. Argamassas. I Int. Symposium Mortars Technol., Florianópolis, 2005: pp. 73–82.
- [139] M.M. Alonso, M. Palacios, F. Puertas, A.G. De la Torre, M.A.G. Aranda, Influencia de la estructura de aditivos basados en policarboxilato sobre el comportamiento reológico de pastas de cemento, *Mater. Construcción*. 57 (2007) 65–81.
- [140] C. Hoffmann, T. Armbruster, Clinotobermorite,  $\text{Ca}_5[\text{Si}_3\text{O}_8(\text{OH})]_2 \cdot 4 \text{H}_2\text{O} - \text{Ca}_5[\text{Si}_6\text{O}_{17}] \cdot 5\text{H}_2\text{O}$ , a natural C-S-H(I) type cement mineral: Determination of the substructure, *Zeitschrift Fur Krist. - New Cryst. Struct.* 212 (1997) 864–873. doi:10.1524/zkri.1997.212.12.864.
- [141] S. Merlino, E. Bonaccorsi, T. Armbruster, The real structures of clinotobermorite and tobermorite 9 Å: OD character, polytypes, and structural relationships, *Eur. J. Mineral.* 12 (2000) 411–429. doi:10.1127/0935-1221/2000/0012-0411.
- [142] I. Santacruz, A.G. De la Torre, G. Alvarez-Pinazo, A. Cabeza, A. Cuesta, J. Sanz, M.A.G. Aranda, Structure of stratlingite and effect of hydration methodology on microstructure, *Adv. Cem. Res.* 28 (2016) 13–22. doi:10.1680/adcr.14.00104.
- [143] J.I. Tobon, J. Paya, M. V. Borrachero, L. Soriano, O.J. Restrepo, Determination of the optimum parameters in the high resolution thermogravimetric analysis (HRTG) for cementitious materials, *J. Therm. Anal. Calorim.* 107 (2012) 233–239. doi:10.1007/s10973-010-0997-0.
- [144] F. Winnefeld, S. Barlag, Calorimetric and thermogravimetric study on the influence of calcium sulfate on the hydration of ye’elimite, *J. Therm. Anal. Calorim.* 101 (2010) 949–957. doi:10.1007/s10973-009-0582-6.
- [145] L. Rolland, R. Trauchessec, D.L. Institut, J. Lamour, B. Le Rolland, Impact of anhydrite proportion in a calcium sulfoaluminate cement and Portland cement blend, *Adv. Cem. Res.* 26 (2014) 325–333.
- [146] R.T. Chancey, Characterization of crystalline and amorphous phases and respective reactivities in a class F fly ash, University of Texas at Austin, 2008.
- [147] D. Londono-Zuluaga, J.I. Tobon, M.A.G. Aranda, I. Santacruz, A.G. De la Torre, Early-age hydration mechanism between alite-ye’elimite-anhydrite associated with Belite-Alite-Ye’elimite cements, *Mater. Struct.* (n.d.). doi:Manuscript to be submitted soon.
- [148] D. Jansen, A. Spies, J. Neubauer, D. Ectors, F. Goetz-Neunhoeffler, Studies on the early hydration of two modifications of ye’elimite with gypsum, *Cem. Concr. Res.* 91 (2017) 106–116. doi:10.1016/j.cemconres.2016.11.009.
- [149] L. Pelletier-Chaignat, F. Winnefeld, B. Lothenbach, G. Le Saout, C.J. Müller, C. Famy, Influence of the calcium sulphate source on the hydration

- mechanism of Portland cement-calcium sulfoaluminate clinker-calcium sulphate binders, *Cem. Concr. Compos.* 33 (2011) 551–561. doi:10.1016/j.cemconcomp.2011.03.005.
- [150] J. Péra, J. Ambroise, New applications of calcium sulfoaluminate cement, *Cem. Concr. Res.* 34 (2004) 671–676. doi:10.1016/j.cemconres.2003.10.019.
- [151] F. Winnefeld, B. Lothenbach, Phase equilibria in the system  $\text{Ca}_4\text{Al}_6\text{O}_{12}\text{SO}_4 - \text{Ca}_2\text{SiO}_4 - \text{CaSO}_4 - \text{H}_2\text{O}$  referring to the hydration of calcium sulfoaluminate cements, *RILEM Tech. Lett.* 1 (2016) 10–16.
- [152] L.H.J. Martin, F. Winnefeld, E. Tschopp, C.J. Müller, B. Lothenbach, Influence of fly ash on the hydration of calcium sulfoaluminate cement, *Cem. Concr. Res.* 95 (2017) 152–163. doi:10.1016/j.cemconres.2017.02.030.
- [153] X. Gaviria, M. V. Borrachero, J. Paya, J.M. Monzó, J.I. Tobon, Mineralogical evolution of cement pastes at early ages based on thermogravimetric analysis (TG), *J. Therm. Anal. Calorim.* 0 (2017). doi:10.1007/s10973-017-6905-0.
- [154] A. Cuesta, A.G. De la Torre, I. Santacruz, P. Trtik, J.C. da Silva, A. Diaz, M. Holler, M.A.G. Aranda, Chemistry and Mass Density of Aluminum Hydroxide Gel in Eco-Cements by Ptychographic X-ray Computed Tomography, *J. Phys. Chem. C.* 121 (2017) 3044–3054. doi:10.1021/acs.jpcc.6b10048.
- [155] A. V. Soin, L.J.J. Catalan, S.D. Kinrade, A combined QXRD/TG method to quantify the phase composition of hydrated Portland cements, *Cem. Concr. Res.* 48 (2013) 17–24. doi:10.1016/j.cemconres.2013.02.007.
- [156] O. Mendoza, J.I. Tobon, An alternative thermal method for identification of pozzolanic activity in  $\text{Ca}(\text{OH})_2$ /pozzolan pastes, *J. Therm. Anal. Calorim.* 114 (2013) 589–596. doi:10.1007/s10973-013-2973-y.
- [157] I. García-Lodeiro, A. Fernández-Jiménez, I. Sobrados, J. Sanz, A. Palomo, C-S-H gels: Interpretation of  $^{29}\text{Si}$  MAS-NMR spectra, *J. Am. Ceram. Soc.* 95 (2012) 1440–1446. doi:10.1111/j.1551-2916.2012.05091.x.
- [158] A. Mendes, W.P. Gates, J.G. Sanjayan, F. Collins, NMR, XRD, IR and synchrotron NEXAFS spectroscopic studies of OPC and OPC/slag cement paste hydrates, *Mater. Struct.* 44 (2011) 1773–1791. doi:10.1617/s11527-011-9737-6.
- [159] O. Mendoza, C. Giraldo, S.S. Camargo, J.I. Tobon, Structural and nano-mechanical properties of Calcium Silicate Hydrate (C-S-H) formed from alite hydration in the presence of sodium and potassium hydroxide, *Cem. Concr. Res.* 74 (2015) 88–94. doi:10.1016/j.cemconres.2015.04.006.
- [160] D.A. Kulik, Improving the structural consistency of C-S-H solid solution thermodynamic models, *Cem. Concr. Res.* 41 (2011) 477–495. doi:10.1016/j.cemconres.2011.01.012.
- [161] S. Kwan, J. LaRosa, M.W. Grutzeck,  $^{29}\text{Si}$  and  $^{27}\text{Al}$  MASNMR Study of Stratlingite, *J. Am. Ceram. Soc.* 78 (1995) 1921–1926. doi:10.1111/j.1151-2916.1995.tb08910.x.
- [162] E. Pustovgar, R.K. Mishra, M. Palacios, J.B. d’Espinose de Lacaillerie, T.

- Matschei, A.S. Andreev, H. Heinz, R. Verel, R.J. Flatt, Influence of aluminates on the hydration kinetics of tricalcium silicate, *Cem. Concr. Res.* 100 (2017) 245–262. doi:10.1016/j.cemconres.2017.06.006.
- [163] G. Paul, E. Boccaleri, L. Buzzi, F. Canonico, D. Gastaldi, Friedel's salt formation in sulfoaluminate cements: A combined XRD and <sup>27</sup>Al MAS NMR study, *Cem. Concr. Res.* 67 (2015) 93–102. doi:10.1016/j.cemconres.2014.08.004.
- [164] D. Gastaldi, G. Paul, L. Marchese, S. Irico, E. Boccaleri, S. Mutke, L. Buzzi, F. Canonico, Hydration products in sulfoaluminate cements: Evaluation of amorphous phases by XRD/solid-state NMR, *Cem. Concr. Res.* 90 (2016) 162–173. doi:10.1016/j.cemconres.2016.05.014.
- [165] M. Alesiani, I. Pirazzoli, B. Maraviglia, F. Canonico, NMR and XRD study on calcium sulfoaluminate cement, *Appl. Magn. Reson.* 35 (2008) 33–41. doi:10.1007/s00723-008-0152-2.
- [166] J. Skibsted, M.T. Pedersen, J. Holzinger, Resolution of the Two Aluminum Sites in Ettringite by <sup>27</sup>Al MAS and MQMAS NMR at Very High Magnetic Field (22.3 T), *J. Phys. Chem. C.* 121 (2017) 4011–4017. doi:10.1021/acs.jpcc.6b11875.
- [167] S. Allevi, M. Marchi, F. Scotti, S. Bertini, C. Cosentino, Hydration of calcium sulfoaluminate clinker with additions of different calcium sulphate sources, *Mater. Struct.* (2015) 1–14. doi:10.1617/s11527-014-0510-5.
- [168] A.B. Kudryavtev, T.V. Kouznetsova, W. Linert, G. Hunter, On the possibilities on In-situ studies of the hydration of aluminate cement using wide-line <sup>27</sup>Al NMR spectroscopy, *Cem. Concr. Res.* 27 (1997) 501–513.
- [169] A. Rawal, B.J. Smith, G.L. Athens, C.L. Edwards, L. Roberts, V. Gupta, B.F. Chmelka, Molecular silicate and aluminate species in anhydrous and hydrated cements, *J. Am. Chem. Soc.* 132 (2010) 7321–7337. doi:10.1021/ja908146m.
- [170] A. Rungchet, P. Chindaprasirt, C.-S. Poon, K. Pimraksa, Hydration and Physico-mechanical Properties of Blended Calcium Sulfoaluminate-belite Cement Made of Industrial By-products, *King Mongkut's Univ. Technol. North Bangkok Int. J. Appl. Sci. Technol.* 9 (2016) 279–287. doi:10.14416/j.ijast.2016.11.006.
- [171] K. Wesche, ed., *Fly Ash in Concrete. Properties and Performance*, Taylor & Francis e-Library, 2005.
- [172] T. Hemalatha, A. Ramaswamy, A review on fly ash characteristics-Towards promoting high volume utilization in developing sustainable concrete, *J. Clean. Prod.* 147 (2017) 546–559. doi:10.1016/j.jclepro.2017.01.114.
- [173] A. Duran, R. Sirera, M. Pérez-Nicolás, I. Navarro-Blasco, J.M. Fernández, J.I. Alvarez, Study of the early hydration of calcium aluminates in the presence of different metallic salts, *Cem. Concr. Res.* 81 (2016) 1–15. doi:10.1016/j.cemconres.2015.11.013.

- [174] K. Scrivener, R. Snellings, B. Lothenbach, A Practical Guide to Microstructural Analysis of Cementitious Materials, CRC Press, Boca Raton, FL, 2016.